Local Interactions: Determinants of Protein Structure

And

Guides for Structure-Based Drug Design

A Dissertation Presented

by

Raphaël Geney

to

The Graduate School

in Partial fulfillment of the

Requirements

for the Degree of

Doctor of Philosophy

in

Chemistry

Stony Brook University

August 2005

Stony Brook University

The Graduate School

Raphaël Geney

We, the dissertation committee for the above candidate for the
Doctor of Philosophy degree,
hereby recommend acceptance of this dissertation.

_____

Iwao Ojima
Distinguished Professor, Department of Chemistry

_____

Carlos L. Simmerling
Associate Professor, Department of Chemistry

_____

Kathlyn A. Parker
Professor, Department of Chemistry

_____

Nicole S. Sampson
Professor, Department of Chemistry

_____

Robert C. Rizzo
Assistant Professor, Department of Applied Mathematics and Statistics
Stony Brook University

This dissertation is accepted by the Graduate School

_____

Dean of the Graduate School

Abstract of the Dissertation

Local Interactions: Determinants of Protein Structure

And

Guides for Structure-Based Drug Design

by

Raphaël Geney

Doctor of Philosophy

in

Chemistry

Stony Brook University

2005

A new computational docking protocol has been developed and used in combination with conformational information inferred from REDOR solid state NMR experiments on microtubule-bound 2-(p-fluorobenzoyl)paclitaxel to delineate the tubulin-bound structure of paclitaxel. Conformationally constrained macrocyclic taxoids bearing linkers between various positions have been designed and synthesized with a view to enforce this REDOR-Taxol conformation. One of these analogs, SB-T-2053, inhibits the growth of MCF-7 and LCC-6 human breast cancer cells (wild type and drug-resistant strains) on the same order of magnitude as paclitaxel. Moreover, SB-T-2053 induces in vitro tubulin polymerization at least as well as paclitaxel, which directly validates our drug design process.

Improvements in the modeling of solvation effects in molecular simulations have also been addressed. Accurate modeling of these effects is a key undertaking of computational chemistry, as most chemical processes happen in a solvent. Free energy profiles of salt bridge formation between oppositely charged amino acid side chains were calculated both in explicit solvent and in a generalized Born (GB) continuum solvent model to quantify a suspected over-stabilization of protein side chains ion pairs in GB, relative to explicit solvent. Salt bridges are found to be excessively stable in GB by as much as 4 kcal/mol, which is consistent with previous reports describing radically different structural ensembles for proteins with ionizable groups in GB and explicit solvent.

A simple empirical correction is proposed, in which the intrinsic GB radii of hydrogen atoms bound to charged nitrogen atoms are reduced. This effectively increases the desolvation penalty of cationic side chains, while minimally affecting the solvation energy of the rest of the protein. The thermodynamics of salt bridge formation are considerably improved by this correction, which further permitted a close reproduction of the experimental Trp-cage miniprotein temperature melting profile, otherwise distorted by prevalent non-native salt bridges.

In loving memory of Adrien and Thérèse,

Contents

List of Tables

List of Figures

List of Abbreviations

10-DAB III	10-deacetylbaccatin III
2-FB-PT	2-(*p*-fluorobenzoyl)paclitaxel
Boc	butoxycarbonyl
BzDC	benzodihydrocinnamoyl
CD	circular dichroism
CDR	complementarity determining region
CIP	contact ion pair
CSD	chemical shift deviation
DAPI	4'-6-diamidino-2-phenylindole
DMAP	4-dimethylaminopyridine
DMSO	dimethyl sulfoxide
DNA	deoxyribonucleic acid
EC	electron crystallography
EE	1-ethoxyethoxyl
EM	electron microscopy
Fab	fragment antigen binding
FDA	Food and Drug Administration
GB	generalized Born
GBSA	generalized Born/surface area
GDP	guanosine diphosphate
GTP	guanosine triphosphate
Hsps	heat shock proteins
LPS	lipopolysaccharide
MAP	microtubule-associated protein
MAPK	mitogen-activated protein kinase
MC	Monte Carlo
MD	molecular dynamics
MTB	microtubule
MTOC	microtubule-organizing center
NCI	national cancer institute
NMR	nuclear magnetic resonance
PB	Poisson-Boltzmann
PCD	programmed cell death
PDA	pairwise descreening approximation
PDB	protein databank
pf	protofilament
PME	particle-mesh Ewald
PMF	potential of mean force
PTX	paclitaxel
RCM	ring-closing metathesis
REDOR	rotational-echo double resonance
REMD	replica exchange molecular dynamics
RISM	reference interaction site model

RMSD	root mean square deviation
RNA	ribonucleic acid
SAR	structure-activity relationship
SEER	Surveillance Epidemiology and End Results
SSIP	solvent-separated ion pair
TIP3P	transferable intermolecular potential 3 points
TNF-α	tumor necrosis factor-α
US	umbrella sampling
vdW	van der Waals
z-VAD-fmk	benzyloxycarbonyl-Val-Ala-Asp(OMe)-CH_2F

Acknowledgments

First and foremost, I want to thank my two advisors, Prof Iwao Ojima and Prof. Carlos Simmerling for welcoming me in their labs and schedules, supporting me for the last five years, and always keeping my best interest in mind. Each in their own way, their great drive towards scientific excellence has greatly inspired me and will leave a lasting impression I can always look up to. I sincerely feel it is a rare chance to come across such brilliant individuals, let alone two of them at the same time! Thanks to both of them for the flexibility they showed helping me reach my learning objectives and allowing me to achieve my lifelong aspiration to somewhat contribute to the progress of scientific knowledge and its dissemination.

I wish to thank the members of my thesis committee (Profs. Parker, Sampson, Rizzo, and Sieburth) for their time spent assessing my progress, accessibility, and good counsel at the various stages of my graduate life in the Chemistry Department.

I also wish to extend special thanks to Dr. Viktor Hornak for his relentless technical assistance with our computer systems and ample research advice.

Thanks to our many collaborators on the anticancer drug design project: Shujun Xia and Prof. Susan Horwitz at Albert Einstein College of Medicine, Paula Pera and Dr. Ralph Bernacki at Roswell Park Cancer Institute and Dr. Muriel Cuendet of the University of Illinois at Chicago, for performing all of the biological tests described herein and making this research at all possible.

To all Simmerling and Ojima lab members: spending such long hours in the lab together will for sure make us a tightly knit family. Thanks also to all the students of the Chemistry Department and ‘Mega Meeting’ labs for the scientific insights and plain fun they provided through talks and informal discussions. I hope to have provided some in return.

At this time my special thoughts go to Dr. Sylvia Tracz, to whom I most profoundly wish a complete and rapid recovery.

Even after all these years, I will not forget to thank Prof. Anthony Smith and Catherine Ponthus, at the CPE Lyon study abroad office for facilitating my coming to Stony Brook and keeping in touch with me throughout my graduate years. Thanks also to the Rhône-Alpes region for a generous study abroad fellowship, which helped me get settled enormously.

Thanks to all my extended family and friends for always being supportive, providing strong moral support and being present - if only over the phone - in times of need. Special thanks to Jerome Lauret for providing expert assistance in my first years at Stony Brook, mostly in the form of a four-wheeled vehicle.

Thanks to my parents for allowing me to stand here today and, although half-heartedly, letting me pursue a graduate degree 3582 miles away from home.

Finally, my greatest thanks go to Julie who deliberately chose to be by my side throughout this precarious endeavor and the rest of our lives.

Parts of Chapters 2 and 3 of this dissertation contain material reprinted from Geney *et al.* (2005): 'Use of the Tubulin Bound Paclitaxel Conformation for Structure-Based Rational Drug Design.' *Chemistry & Biology* **12**(3): 339-348. Some co-authors listed in the publication directed and supervised the research that forms the basis for this thesis or dissertation. Permission was granted by Cell Press to include this article in the present dissertation, in accord with Cell Press Transfer of Copyright Agreement Version Number: 1/2002, Cell Press rev. 6/2004.

Figure 1.7 is reprinted from *Current Biology*, Vol 14, Gadde, S., Heald, R., 'Mechanisms and molecules of the mitotic spindle', Pages R797-R805, Copyright (2004), with permission from Elsevier.

Figures 1.8 and 1.9 are reprinted from *Organic & Biomolecular Chemistry*, Vol 2, Amos, L. A., 'Microtubule structure and its stabilisation', Pages 2153-2160, Copyright (2004), with permission from The Royal Society of Chemistry.

Chapter 1

Introduction

1.1 Cancer Today

Cancer is a major health concern worldwide, with over 10 million new cases diagnosed and 7 million deaths every year, i.e. 12.5% of deaths worldwide. The number of cases is expected to increase to 15 million new cases per year by 2020, mainly as a consequence of world population ageing, and the spread of the Western lifestyle.[1] In the United States alone, cancer is second only to heart disease as a cause of death (Figure 1.1), but first in terms of person-years lost, with lung cancer as the leading type of malignancy (Figure 1.2). The threat posed by cancer was recognized in 1971, with the legislation of the National Cancer Act, which increased research funding and launched the development of several national research centers, making the conquest of cancer a 'national crusade'.[2]

Considerable progress has been made since then towards the understanding of the mechanism of the disease and its control, both in terms of prevention and therapy. One third of cancers could be avoided by conforming to healthier habits (ceasing tobacco usage, consuming healthy food, avoiding exposure to carcinogens), and fortunately, close to half of the new cases of cancer are now diagnosed at an early stage and an ablative treatment, such as surgery or radiotherapy, can be used to remove the malignant tumor.[1] In the remaining cases, however, the cancer spreads by metastasis and the only chance of survival lies in chemotherapy. Several cancers, such as leukemia, lymphomas, and sarcomas, can be effectively treated by chemotherapy, and long-term survival has improved notably for breast cancer, the most common malignancy in women. The drugs most commonly used in cancer treatment are the *Vinca* alkaloids (vinblastine, vincristine, vindesine, vinorelbine), anthracyclines (daunorubicin, doxorubicin, epirubicin, idarubicin, mitoxantrone), epipodophyllotoxins (etoposide, amsacrine, teniposide), camptothecins (irinotecan, topotecan), cisplatin, and the taxanes: paclitaxel (generic name for Taxol®, licensed to Brystol-Myers Squibb), and docetaxel (generic for Taxotère®, licensed to Sanofi-Aventis).

Despite this pharmacological arsenal, there is still dire need for more effective therapies and palliative care and pain management strategies to reach even the pragmatic goal of turning rapidly fatal cancers into manageable chronic illnesses.

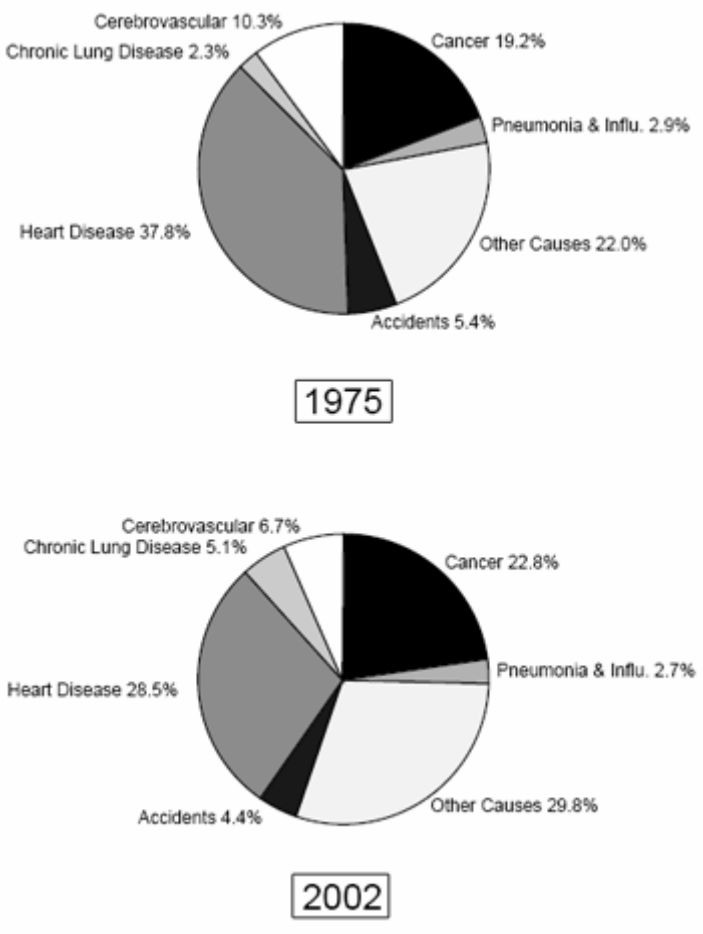

Figure 1.1. Evolution of the leading causes of death in the United States between 1975 and 2002 (Source: NCI, SEER Cancer Statistics Review 1975-2002).

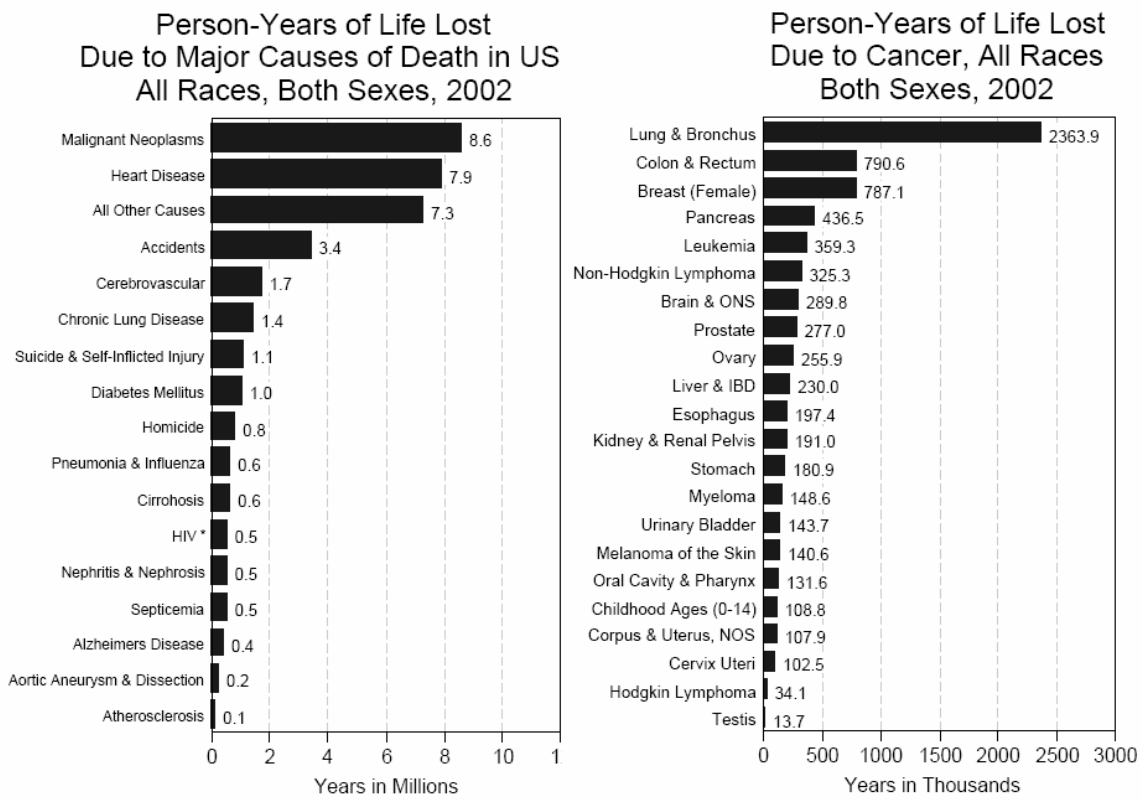

Figure 1.2 Human impact of cancer in relation to other causes of death (left), and leading cancer types (right) in the United States (Source: NCI, SEER Cancer Statistics Review 1975-2002).

1.2 The Taxanes

The taxanes Taxol®[3] (paclitaxel) and Taxotere®[4] (docetaxel, Figure 1.3), currently serve as two leading chemotherapeutic drugs in the clinic.[5-7] Both drugs bind to the β-tubulin subunit of the α,β-tubulin heterodimer and act through an anti-mitotic mechanism of action based on stabilization of microtubules (MTBs), thus disrupting the mitosis of cancer cells and eventually leading to apoptosis, the programmed cell death.[8-11] The following is a more detailed account of their discovery and mechanism of action at the cellular and sub-cellular levels.

1.2.1 From Discovery to the Clinic

The discovery of paclitaxel can be traced back to 1962 in Gifford Pinchot National Forest (WA), where under a U.S. Department of Agriculture plant screening program, the botanist Arthur S. Barclay gathered leaves, twigs and bark from the Pacific yew tree (*Taxus Brevifolia*) for biological pre-screening. Bark extracts rapidly showed high activity in leukemia models. However, the feat of isolating paclitaxel and elucidating its extremely complex novel structure was delayed until 1971 due to supply difficulties and equipment limitations. This was accomplished by Mansukh C. Wani and Monroe E. Wall, working under a Cancer Chemotherapy National Service Center contract from the National Cancer Institute (NCI) at the Research Triangle Institute (NC) using X-ray analysis and published in a 1971 landmark paper.[3] Their findings were stupefying: paclitaxel was composed of a tricyclic taxane core ring system (A, B and C rings) fused to a 4-membered oxetane ring (D ring), with an *N*-benzoylphenylisoserine side chain at the C13 position. The molecule possessed eleven stereocenters (Figure 1.3).

Under a 1989 Cooperative Research & Development Agreement, Bristol-Meyers-Squibb obtained the rights from NCI to further develop and market paclitaxel (Taxol®). However, paclitaxel development had to face two very serious obstacles that definitely hampered the introduction of the drug to the clinic: its extremely poor solubility in common pharmaceutical excipients and the very limited supply available from natural sources.

The solubility issue could be solved by formulating paclitaxel in a vehicle of 50% ethanol and 50% polyethoxylated castor oil (Cremophor EL), a formulation responsible for a high rate of hypersensitivity reactions in patients not preemptively treated with an antihistaminic-corticosteroid combination.[12]

The supply question was even problematic, as harvesting the entire bark of a 40-foot Pacific yew tree, which could easily be more than 200 years old, yields only half a gram of paclitaxel and requires the felling of the tree. This consideration set off a major environmental controversy about the preservation of the old-growth Pacific Northwest forest and its ecosystem.[13] Other methods had to be devised to secure the supply of this promising drug candidate. Fortunately, in 1980, 10-deacetylbaccatin III (10-DAB III), a natural product isolated from the European yew (*Taxus baccata*), was identified as a readily accessible possible starting material for the semisynthesis of anticancer

taxoids.[14,15] This compound comprises the tetracyclic skeleton of paclitaxel without its C13 isoserine side chain (Figure 1.3) and can be isolated from the leaves of the European yew tree, a renewable source, in relatively good yield (1 g / 1 kg of fresh leaves).[16]

With the discovery of 10-DAB III, paclitaxel and its congeners could be prepared through semi-synthesis by attaching the chiral C13 side chain. Different approaches to the side chain have been proposed and investigated.

In 1988, the first semi-synthesis of paclitaxel utilizing 10-DAB III was accomplished by Greene and Potier using a direct esterification of modified 10-DAB III and *N*-benzoyl-(2*R*,3*S*)-phenylisoserine (Figure 1.4a).[17] However, this high temperature coupling process induces significant epimerization at the C2' position of the C13 side chain. An improved process was disclosed by Holton in a 1990 patent application, claiming that (3*R*,4*S*)-*N*-benzoyl-3-*O*-EE-4-phenylazetidin-2-one (EE = 1-ethoxyethoxyl), could be directly coupled with 7-TES-baccatin III in the presence of 4-dimethylaminopyridine (DMAP) and pyridine, to afford the 7-TES-2'-*O*-EE-paclitaxel in 92% yield; subsequent deprotection affording paclitaxel in 90% yield (Figure 1.4b).[18] The limitations of this protocol include the necessity of a large excess of β-lactam (5 equivalents), long reaction times, and the restriction to *N*-benzoyl protected β-lactams.

A more practical and efficient semi-synthesis of paclitaxel was proposed by Ojima which relied on the 'β-Lactam Synthon Method'.[19,20] The optically active β-lactam (3*R*,4*S*)-3-hydroxyl-4-phenylazetidin-2-one could be prepared via a lithium chiral ester enolate-imine cyclocondensation in high yield and enantioselectivity.[21-23] Coupling of the β-lactam with 13-*O*-metalated derivatives of 7-TES-baccatin III was then performed. A variety of bases were examined, and NaHMDS was found to be the best for this ring-opening coupling.[22,23] In this case, the ring-opening coupling proceeds smoothly at -30 ~ 0 ^{o}C using only a slight excess of *N*-acyl-β-lactam to give the coupling product within 30 min in excellent yield (Figure 1.4c). The subsequent deprotection affords paclitaxel with high overall yield.

These semisyntheses and their variants allowed the securing of an inexhaustible supply of paclitaxel from 10-DAB III and also proved pivotal in the definition of an exhaustive structure-activity relationships (SAR) model (Figure 1.5).[24-26] Interestingly enough, though, since 2002, paclitaxel is produced for Bristol-Myers-Squibb entirely by Phyton Biotech, Inc., using *Taxus chinensis* needle cells cultures, following a licensed USDA patent.[27] Paclitaxel is directly obtained from the fermentation broth after chromatography and recrystallization.[28]

Paclitaxel obtained FDA regulatory approval in December 1992 - 30 years after its initial discovery- for the treatment of metastatic carcinoma of the ovary, subsequent to failure of first-line chemotherapy. This indication was augmented to first line treatment in June 2000. A second indication was approved in April 1994: the treatment of breast cancer after failure of anthracycline combination therapy; a third in June 1998, in combination with cisplatin, for the first-line treatment of non-small cell lung cancer in patients who are not candidates for surgery or radiation therapy. Lastly, paclitaxel is also indicated for second-line treatment of AIDS-related Kaposi's sarcoma (approved: August 1997).

Docetaxel, the first semi-synthetic analog of paclitaxel and only other taxane marketed thus far, received FDA approval for second-line treatment of both metastatic breast and non-small cell lung cancers, respectively in May 1996 and December 1999. Approval for first-line treatment of non-small cell lung cancer in combination with cisplatin was granted in November 2002, while a last indication for treatment, in combination with prednisone (a corticosteroid), of metastatic prostate cancer was approved in May 2004 (Source: FDA Center for Drug Evaluation and Research).

The proven clinical efficacy of these two taxanes and the uniqueness of their mechanism of action have resulted in both of these drugs reaching ‘blockbuster’ status, each with worldwide sales well in excess of $1 billion per year.

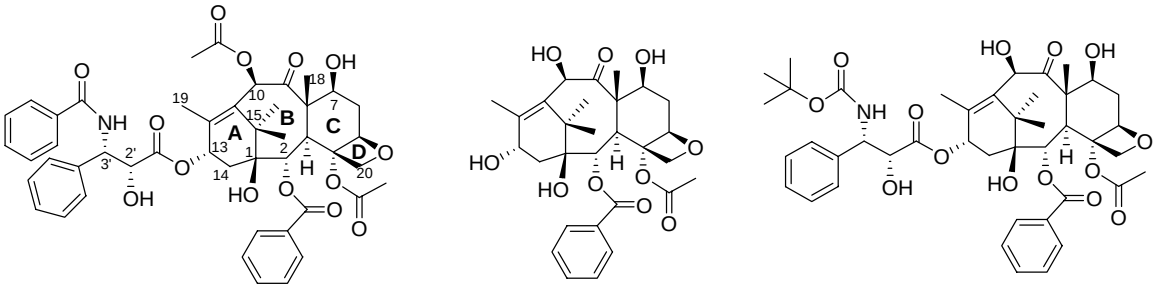

Figure 1.3. Structures of paclitaxel, docetaxel and 10-deacetylbaccatin III (10-DAB III).

(A) Original Greene-Potier semi-synthesis of paclitaxel.

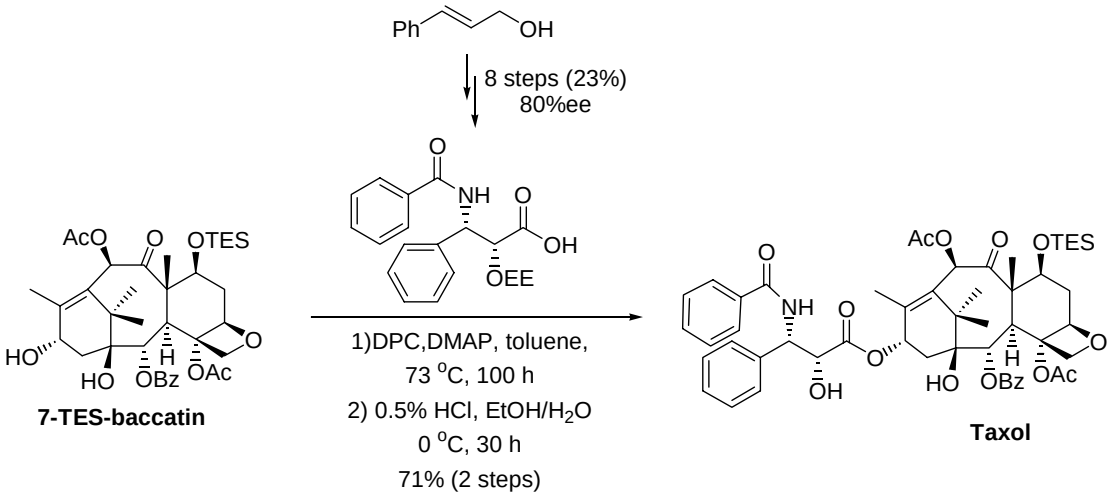

(B) Holton's 1990 semi-synthesis of paclitaxel.

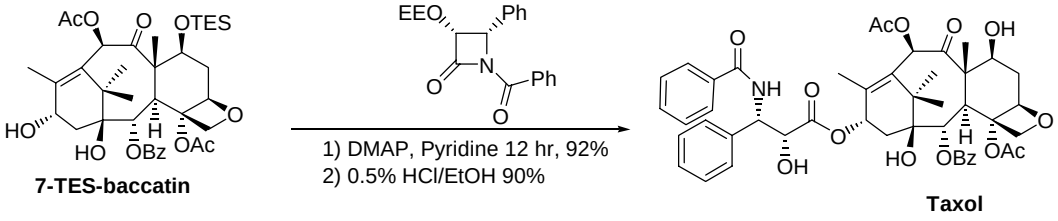

(C) Ojima's β-Lactam Synthon Method semi-synthesis of paclitaxel.

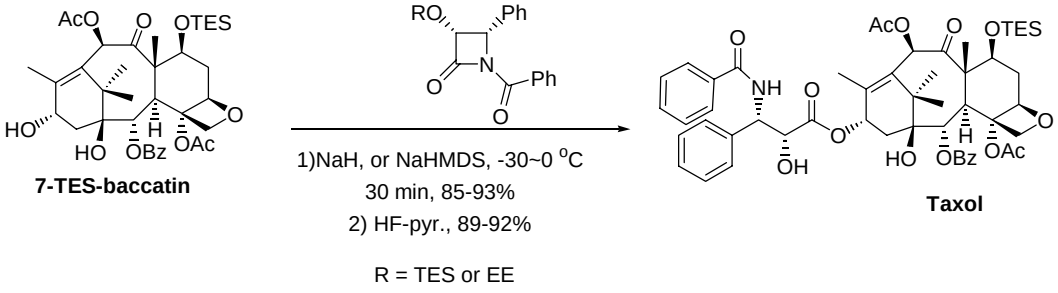

Figure 1.4. Early semisynthetic approaches towards paclitaxel.

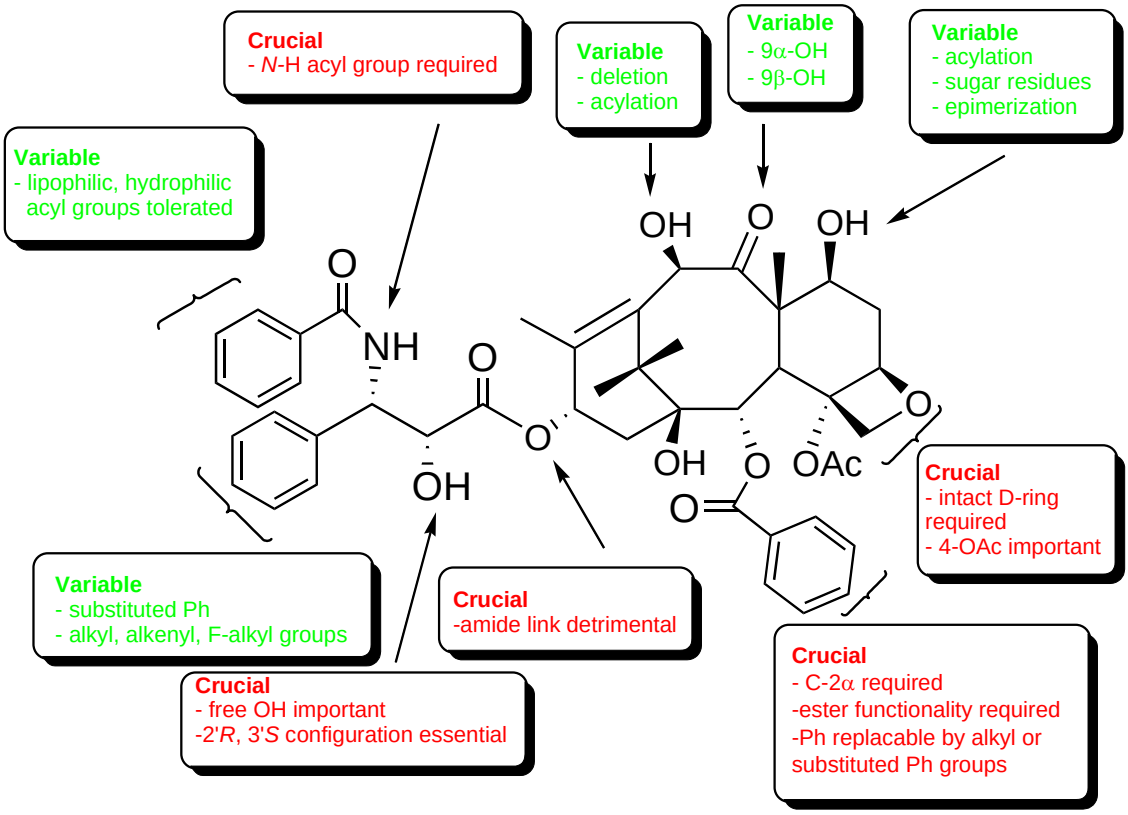

Figure 1.5. Summary of paclitaxel SAR studies.

1.2.2 Mechanism of Action

Paclitaxel was originally believed to be yet another mitotic spindle poison akin to vincristine, vinblastine, colchicines, or podophyllotoxin.[29] These agents act by binding to tubulin, the main protein component of the cytoskeleton, inhibiting its ability to form microtubules, thereby arresting the cell division cycle in metaphase.

Increased impetus in the development of paclitaxel came in 1979, when its unique mechanism of action at the cellular level was unveiled by Dr. Susan B. Horwitz at the Albert Einstein College of Medicine of Yeshiva University, New York City.[8] Indeed, it was found that paclitaxel was actually promoting the assembly of stable microtubules *in vitro*, suggesting that the mechanism of action of paclitaxel could be related to its ability to modulate cellular microtubules. The drug promotes microtubule assembly *in vitro* in the absence of GTP or MAPs and the microtubules assembled by paclitaxel are stable to depolymerization by cold or calcium, which readily depolymerize normal microtubules (Figure 1.6).[8,30,31] Until recently, paclitaxel was unique in its ability to assemble microtubules in the absence of GTP and microtubule-associated proteins (MAPs) that are normally required for microtubule assembly.

Paclitaxel is believed to induce apoptosis in cells through a variety of mechanisms. Cells treated with high concentrations of paclitaxel (μM) exhibit a reorganization of the microtubule cytoskeleton with the formation of microtubule bundles and multiple asters. Such cells have a larger population of their tubulin content in polymeric form, compared to untreated cells and are arrested in the G_2/M phase of the cell cycle.[9,32,33] Normal mitosis is disrupted with a block appearing between the metaphase and anaphase. This leads to the activation of the mitotic checkpoint and eventually brings cells into apoptosis.

Lower concentrations of paclitaxel (30-100 nM), that do not increase the amount of microtubule polymer, are still effective due to their suppression of microtubule dynamics. Indeed in Caov-3 ovarian adenocarcinoma cells and A-498 kidney carcinoma cells incubated with 30 nM paclitaxel, the mean shortening rate of microtubules was reduced by 31% and 26%, respectively. Simultaneously, the average growth rate of microtubules was lowered by 24% in Caov-3 cells and 18% in A-498 cells. This resulted in the dynamicity (the summed gain and loss of tubulin subunits at the microtubule ends and a measure of overall dynamic instability) being significantly reduced in both cell lines: 31% in Caov-3 cells treated with 30 nM paclitaxel and 63% in A-498 cells treated with 100 nM paclitaxel. In each case, cell cycle progress was blocked at the metaphase/anaphase transition which inhibited cell proliferation.[11]

At even lower concentrations of 3-7 nM, paclitaxel induced apoptosis in approximately 30% of A549 lung carcinoma cells, even though these concentrations were not sufficient to induce mitotic arrest.[34] However, alterations were visible in cellular microtubule morphology: partial parallel alignment of microtubules, microtubule bundle formation and multiple asters. Since microtubules are crucial for the transport of

intracellular vesicles, the maintenance of cell shape, the mobility of the cell and other essential cellular functions, it is likely that the impairment of the microtubule network in cells treated with low levels of paclitaxel still triggers the apoptosis process.

Other cellular effects not directly related to the stabilization of microtubules have been reported for paclitaxel. For example, paclitaxel induced the phosphorylation of the anti-apoptotic protein Bcl-2 in leukemia, prostate and ovarian cancer cell lines.[35-39] Screening a library of phage-displayed peptides with a biotinylated derivative of paclitaxel also identified the loop region of Bcl-2 as a paclitaxel-binding peptide.[40] Deletion of this loop region in Bcl-2 blocked the apoptosis-inducing effect of paclitaxel and its phosphorylation of Bcl-2.[41] Bcl-2 derives anti-apoptotic activity from its ability to dimerize with Bax, a pro-apoptotic protein.[42] Serine phosphorylation of Bcl-2 leads to the loss of anti-apoptotic activity due to decreased affinity for Bax.[36]

In the murine macrophage cell line RAW 264.7, paclitaxel mimics the ability of bacterial lipopolysaccharide (LPS) to induce tumor necrosis factor-α (TNF-α) gene expression.[43,44] SAR studies on paclitaxel revealed that its effect on TNF-α gene expression is distinct from its known effects on microtubules.[44] Heat shock proteins (Hsps) of the 70- and 90-kDa families from murine macrophages were identified as binding biotin-labeled paclitaxel .[45] Furthermore, geldanamycin, an inhibitor of the Hsp 90 family, blocked the effect of both paclitaxel and LPS on TNF-α gene expression.[45] Paclitaxel, like LPS, also rapidly induced the tyrosine phosphorylation of mitogen-activated protein kinase (MAPK) in murine macrophages, thereby elevating its enzymatic activity.[46]

It is likely that the cytotoxic effects of paclitaxel all are based on its interaction with microtubules resulting in the activation of various signal transduction pathways in all cells except murine macrophages, which appear to present distinct receptors shared by paclitaxel and LPS.

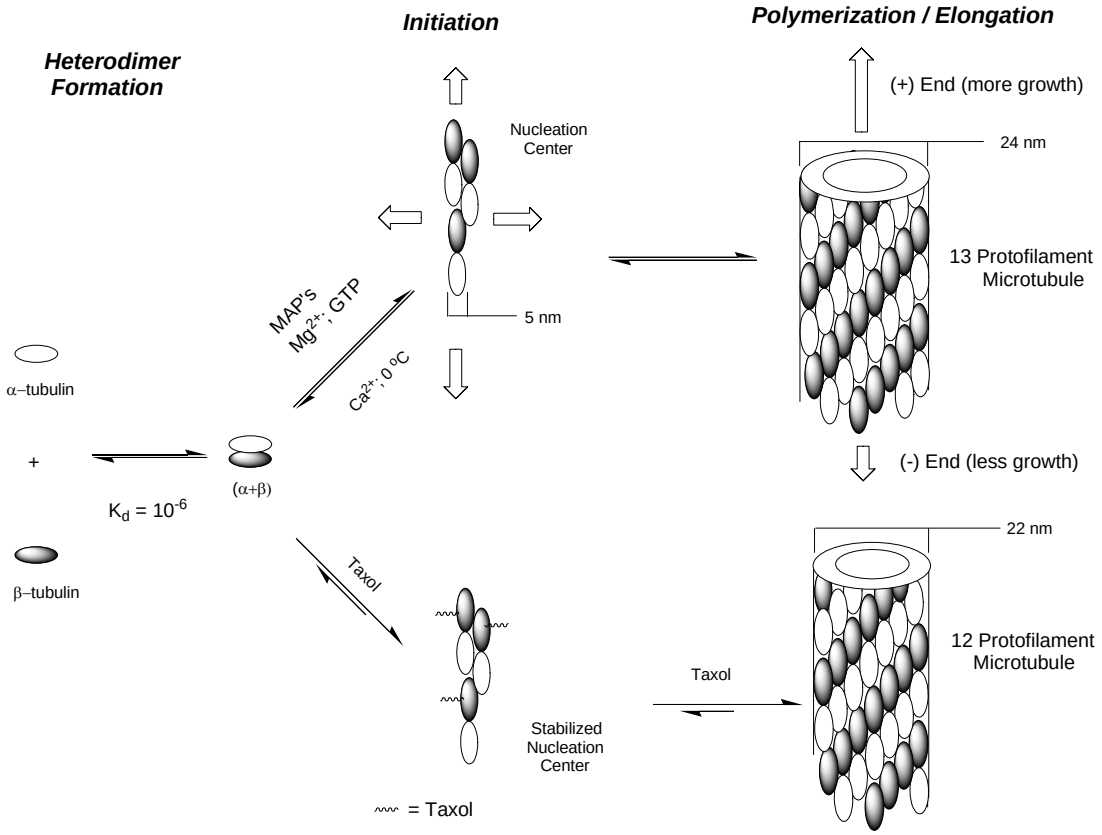

Adapted from: Nicolaou, K.C. et al., Chemistry and Biology of Taxol. *Angew. Chem. Int. Ed. Eng.,* 1994. 33(1): p. 15-44.

Figure 1.6. Compared microtubule formation mechanisms in presence and absence of paclitaxel.

1.3 Tubulin Biochemistry

1.3.1 Microtubule Function

Microtubules are fundamental structural component of all eukaryotic cells and play a crucial role in the cell cycle. Throughout interphase (Figure 1.7b), microtubules help maintaining the shape of the cell and serve as a scaffold for the localization of the organelles and for the transport of vesicles and granules.[47,48] Microtubules act to provide a network for microtubule motor proteins, such as kinesin and dyneins and to transport 'cargo' in a polarized manner throughout the cell.[49-51] Microtubules are also involved in the formation of cilia, centrioles and flagella in eukaryotes.[52-54] However, the most important function of microtubules is their involvement in the formation of microtubule spindles that are needed to partition and move duplicated chromosomes into daughter cells during the mitotic phase of the cell cycle (Figure 1.7b).[55-57]

When eukaryotic cells enter mitosis, their microtubule network undergoes major reorganizations. In early prophase, the centrosome replicates, with each new one becoming a microtubule-organizing center (MTOC). The microtubule minus ends remain associated with the centrosome, the location of the γ-tubulin ring complex, and the plus ends move outward toward the cell membrane. The duplicate centrosomes move to opposite poles of the cell with microtubules forming a bipolar spindle (Figure 1.7a). During metaphase, microtubule spindles interact with the kinetochore regions of the chromosomes.[55] In anaphase, microtubules attached to kinetochores depolymerize and drag the chromosomes towards each pole.[56] At telophase, the nuclear membrane reassembles and microtubule spindles reorganize into typical interphase microtubule arrays. The growth rate of microtubules increases 20- to 100-fold during mitosis relative to interphase. These rapid dynamics make mitotic spindles highly sensitive to microtubule-targeting drugs, such as taxanes, colchicines and vinca alkaloids.[58]

Microtubule polymerization is initiated at the MTOC and α,β-tubulin subunits are added to assemble the microtubule polymer. In 1989, Oakley *et al.* discovered that the centrosome is composed of γ-tubulin forming ring structures of 10 to 13 units. These rings serve as templates for microtubule polymerization with the minus end of the microtubule remaining bound to the MTOC while α,β-tubulin heterodimers are added.[59,60]

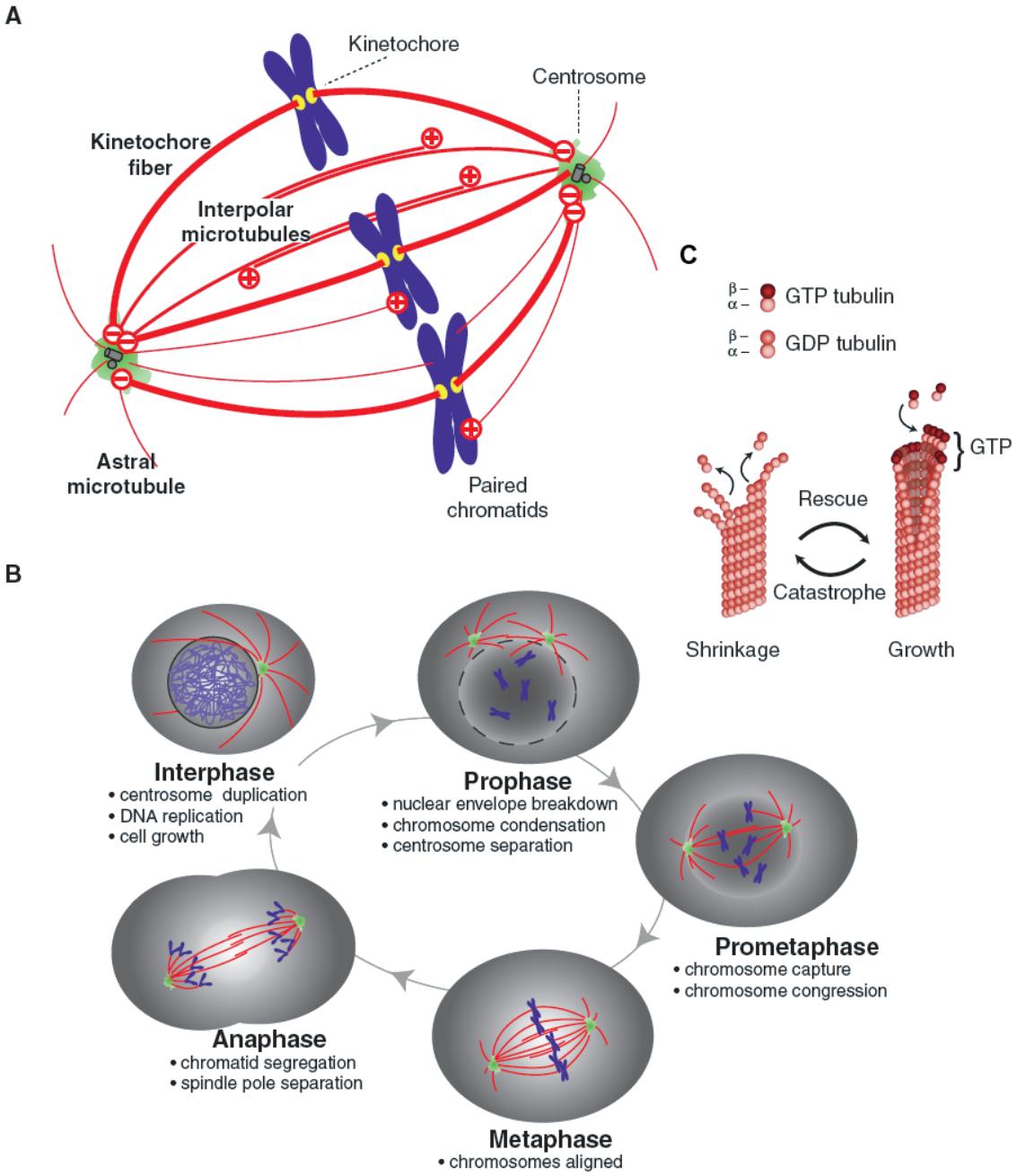

Figure 1.7. (A) Schematic features of the metaphase mitotic spindle. (B) Chromosome translocation by microtubules during the different stages of mitosis. (C) Microtubule dynamic instability. Adapted from Ref. 57.

1.3.2 Dynamic Instability

The rapid reorganization of the microtubule network required for mitosis is made possible by the 'dynamic instability' of microtubules (Figure 1.7c). Indeed, microtubule ends have the ability to alternate between persistent phases of growth and shortening.[61] The abrupt transition from rapid growth to shortening is termed *catastrophe* while the switch back to growth is called a *rescue*.[62]

Microtubule assembly and disassembly are regulated through GTP hydrolysis at the β-tubulin subunit.[63,64] In the polymerization phase, GTP-bound tubulin subunits are added to the ends of microtubules. The GTP on β-tubulin is rapidly hydrolyzed to GDP and phosphate (Pi) during polymerization, while GTP bound to α-tubulin is non-exchangeable and is not hydrolyzed.[65] The plus end of microtubules are stabilized by a circle of GTP bound tubulin, the 'GTP cap', maintaining the more curved GDP bound subunits into a linear arrangement (Figure 1.7c).[66,67] Upon depolymerization, GTP, bound to the last ring of α,β-tubulin heterodimer, is hydrolyzed. Without this 'GTP cap', α,β-tubulin heterodimers dissociate from the ends of microtubules, forming ring-like structures.[68]

Microtubule dynamics are regulated by a variety of endogenous factors. Microtubule-associated proteins (MAPs) such as MAP4[69] and tau[70] are known to promote the assembly of microtubules and stabilize polymerized microtubule arrays. There are also proteins that destabilize microtubules (*catastrophins*): stathmin[71] and XKCM1,[72] for example. Microtubule dynamics are also regulated by various natural products evolved by plants, fungi, or sponges that do not wish to be eaten by eukaryotes.[58] Colchicine and vinca alkaloids inhibit the assembly of microtubules by binding to the tubulin heterodimer and favoring a bent conformation similar to the GDP bound dimer, which results in the depolymerization of microtubules.[73,74] On the other hand, paclitaxel and the recently discovered epothilones,[75] discodermolide,[76] eleutherobin,[77,78] and sarcodictins[78] all promote the assembly and stability of microtubules.[79] However, at low concentrations, both paclitaxel and vinblastine suppress microtubule dynamics. At 3-64 nM, vinblastine suppressed the rate of microtubule growth and shortening in interphase BS-C-1 cells.[80] At 32 nM, vinblastine decreased the overall dynamic activity of microtubules by 75%. Substoechiometric levels of paclitaxel, between 0.001 to 0.01 mol of paclitaxel/mol of α,β-tubulin potently and selectively suppressed the rate and extent of shortening at the plus ends of microtubules in an *in vitro* assay using bovine brain microtubules.[81]

1.3.3 Microtubule and Tubulin Structure

Structurally, microtubules are composed of linear polymers, protofilaments, formed by α,β-tubulin heterodimers.[82] Within each protofilament, α,β-tubulin heterodimers are arranged with the β-tubulin subunit pointing toward the plus end of the microtubule and the α-tubulin subunit at the minus end.[83] Microtubules are hollow tubes approximately 24 nm in diameter and several μm in length. Typically, they are assembled from 13 protofilaments arranged parallel to a cylindrical axis (Figure 1.8). However, depending on the conditions, the number of protofilaments present in the microtubule can vary from 9 to 13. For example, the majority of microtubules formed with paclitaxel consist of only 12 protofilaments.[84] Lateral contacts occur between like tubulin subunits, that is, α-α or β-β, corresponding to a B-lattice.[85] Microtubules composed of 13 or 14 protofilaments can only close with a 'seam' where each α-tubulin monomer makes lateral contact with a β-tubulin subunit (Figure 1.8).

α,β-Tubulin

The tubulin heterodimer is composed of globular α- and β-tubulin. These monomers are approximately 40% identical in amino-acid sequence and each has a molecular weight of approximately 50 kDa (~440 residues). Each tubulin monomer can incorporate a GTP molecule. Upon polymerization, the GTP bound to β-tubulin is hydrolyzed by the incoming α-tubulin subunit. GTP bound to α-tubulin is buried in the interface between α- and β-tubulin and therefore is not hydrolyzed. Each of the tubulin subunits is highly conserved among species.[86]

In 1998, Nogales and Downing generated a 3.7 Å resolution model for the α,β-tubulin heterodimer by electron crystallography of two-dimensional zinc-induced tubulin sheets.[87] This structural model was later refined to 3.5 Å resolution by reprocessing with a more complete dataset.[88] Docking this high resolution model in a 20 Å resolution cryo-electron microscopy (cryo-EM) map of frozen-hydrated microtubules, allowed to reconstitute an approximate structural model for the α,β-tubulin heterodimer in the microtubule arrangement.[89] This microtubule model was later improved to 8 Å resolution, a level of detail sufficient to resolve secondary structure elements.[90] The α- and β-tubulin monomers are ellipsoids approximately 46 x 40 x 65 Å in size. These models provide deep insight into lumenal, outside, longitudinal and lateral surfaces of α- and β-tubulin subunits (Figure 1.9).

The N-terminal 1-205 amino-acid residues form the nucleotide binding domain, the center section of the β-tubulin sequence contains the paclitaxel binding site and the C-terminal tail is exposed on the outside surface of microtubules to make contact with MAPs. These three domains are close to each other on the three dimensional structure and coordinate to regulate the conformation of the tubulin subunit. The majority of the outside (external) surface of the microtubule is composed of C-terminal helices H11 and

H12 and the loop between H10 and β-strand S9. The inside (lumenal) surface of the microtubule is formed by several loops: H1-S2 loop, H2-S3 loop and S9-S10 loop (L loop, Figure 1.9).[89,90]

Two types of longitudinal interactions occur along the protofilament axis: interdimer interactions and intradimer interactions. The intradimer interaction is stronger than the interdimer interaction as the α- and β-tubulin subunits normally bind tightly together to form a functional unit. The nucleotide (GTP/GDP) binding site is located in the center of the interdimer and intradimer interfaces. When a tubulin heterodimer is added to the plus end of the microtubule, contact is made between the α-tubulin of the incoming heterodimer and the β-tubulin exposed at the former plus end. The minus end of α-tubulin is assumed to then contribute an essential residue to the catalytic site of β-tubulin.[91] The α subunit minus end thus serves as a GTPase activating protein for β-tubulin of the adjacent dimer in a protofilament. The GTP bound to the final incoming β-tubulin subunit remains unhydrolyzed and forms a circle of GTP bound β-tubulin, the so-called 'GTP cap' (Figure 1.7c). Unpolymerized tubulin dimers with GDP bound have a curved conformation. However, the GDP bound dimers along the microtubule are constrained to form straight protofilaments by contact with neighbouring subunits of the lattice. In microtubules, nucleotide hydrolysis causes a 2-4 % reduction in the length of the tubulin dimer.[92] The conformational energy stored in the lattice is then released during depolymerization.[93]

The S7-H9 loop (M loop, Figure 1.9) is the central element involved in lateral interactions between tubulin subunits of neighboring protofilaments. The M loop comprises the most divergent peptide segment between α- and β-tubulin sequences: AEKAYHEQ in α-tubulin compared to RGSQQYRA in β-tubulin. In the structural models, it makes close contact with the H3 helix, the C-terminal part of the H2-S3 loop and part of the H1-S2 loop of the adjacent tubulin monomer.[89] The interaction of the M loop with H3 had been suggested by early biochemical studies.[94,95] The M loop points away from the tubulin surface, which allows the required conformational flexibility necessary to accommodate microtubules of as few as 9 or as many as 18 protofilaments. The loop preceding the H3 helix, the T3 loop (Figure 1.9), is near the binding site for the γ-phosphate of GTP and is probably influenced by the hydrolysis of GTP in β-tubulin, by analogy to what is observed in FtsZ, the bacterial homolog of tubulin.[96] The current hypothesis is that hydrolysis of GTP in β-tubulin induces a conformational change in H3 mediated by T3 and therefore the interaction between neighboring protofilaments is weakened.

In their initial α,β-tubulin dimer model,[87] Nogales *et al.* placed docetaxel as a placeholder in the region of the density map attributable to paclitaxel, which was actually used to stabilize the 2D tubulin zinc sheets. As this region falls near the M loop of β-tubulin (Figure 1.9), paclitaxel is proposed to stabilize microtubules by interacting with the M loop, effectively overriding the structural effect of GTP hydrolysis and thereby enhancing lateral interactions between protofilaments.

Interestingly, in α-tubulin, the S9-S10 loop (L loop, Figure 1.9) is 8 residues longer because of a conserved TVVPGGDL insert, which extends into the paclitaxel binding

site.[87] It is therefore assumed that this loop is responsible for the permanent stabilization of the α-tubulin conformation, in addition to the absence of GTP hydrolysis in this subunit, making the dynamics of the two ends of the tubulin dimer more dissimilar to induce polarity. The highly conserved paclitaxel site has also been suggested to be the interaction site for select MAPs, such as neuronal proteins MAP2 and tau.[74] Tau, in particular includes a THVPGGN repeat similar to the α-tubulin L loop extension, and was shown to bind competitively with paclitaxel.[97]

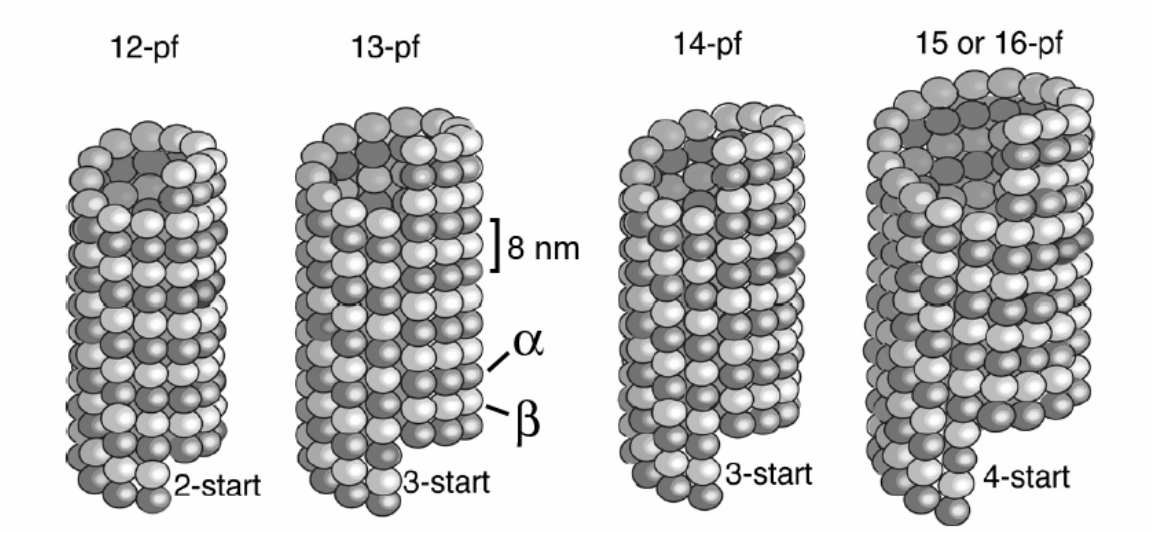

Figure 1.8. Microtubules of various protofilament (pf) counts. 13-pf microtubules can only close with a 'seam' wherein unlike tubulin monomers are in lateral contact. Adapted from Ref. 74.

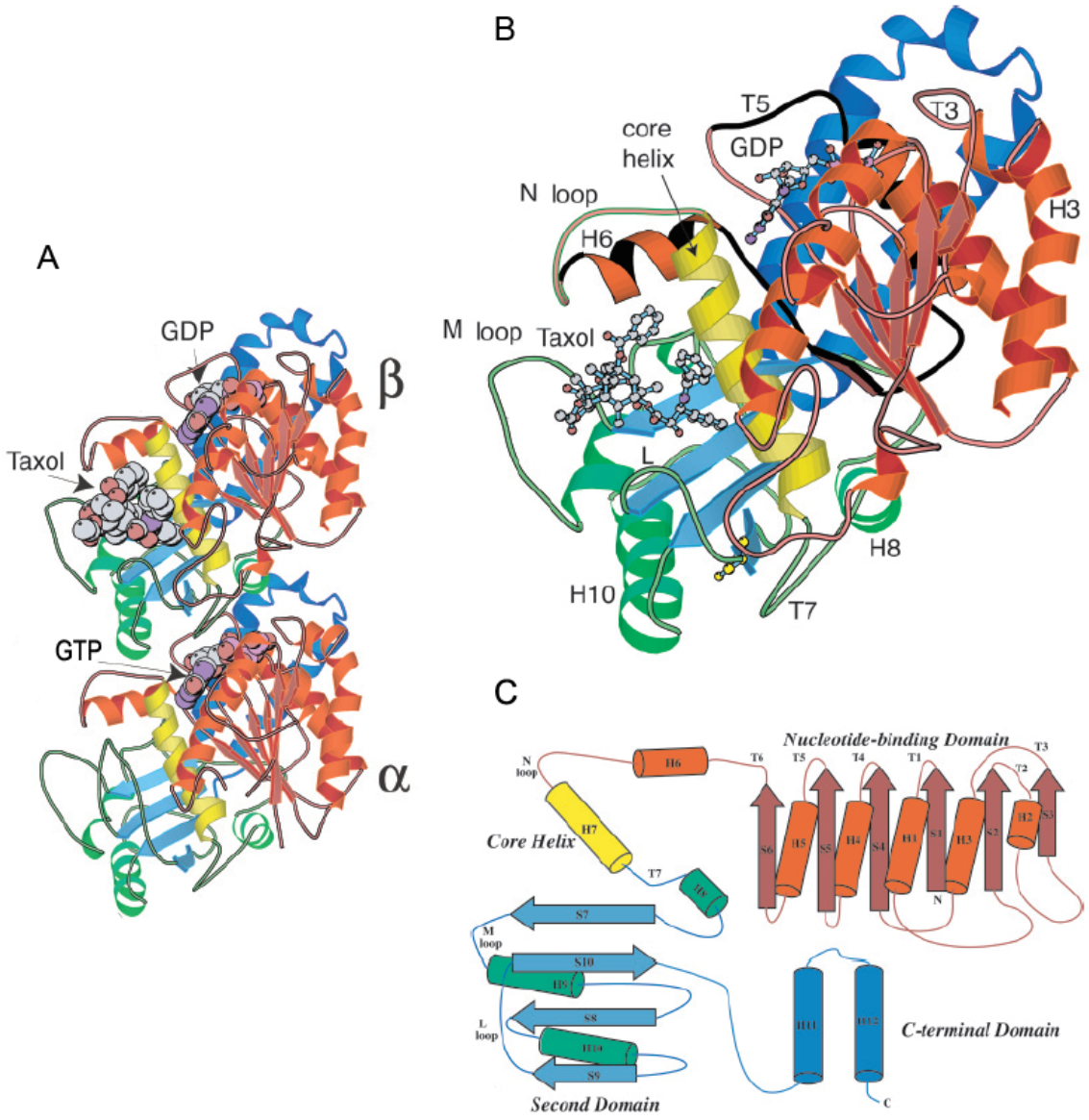

Figure 1.9. (A) Structural view of the α-β tubulin dimer[87] from the inside of the microtubule. (B) Details of the β tubulin subunit with key structural elements indicated. The putative colchicine binding site encompasses Cys354,[98] shown as a yellow ball-and-stick model, near the interface with α-tubulin in the heterodimer. (C) Diagrammatic primary sequence topology of β-tubulin. Adapted from Ref. 74.

1.4 Molecular Mechanics Background

Molecular simulations of biological systems permit the study of the interplay between structure, dynamics and function down to the atomic level. Since many of the problems that one would like to address in biological systems involve large numbers of atoms, it is not yet practical to treat these systems using a quantum mechanical description. This is particularly true of the tubulin-paclitaxel interaction we planned to study, as β-tubulin itself incorporates nearly 3400 atoms.

In molecular mechanics, instead of solving the full Schrödinger equation for the molecule, the focus is on nuclear motions, in accordance with the Born-Oppenheimer approximation. Indeed, nucleons have masses nearly 2000 times larger than that of an electron, which means the electrons can adjust almost instantaneously to a change in position of the nucleus. Molecular mechanics methods cannot therefore calculate properties that depend on the electronic configuration of the molecule: bonding pattern, reactivity, excited states, *et cetera*. However, molecular mechanics is the only practical choice to simulate large systems, such as biological macromolecules, and with appropriate parameterization is able to predict some experimental properties as accurately as quantum methods. The great computational speed of molecular mechanics also allows for its use in the simulation of whole thermodynamic ensembles, conformational searches, and docking, that require large numbers of energy evaluations.

The two essential components of molecular mechanics are (i) an energy function parameterized from empirical data that implicitly incorporate all the relativistic and quantum effects, and (ii) a simulation algorithm capable of efficiently integrating the classical laws of motion.

1.4.1 Force field

Central to the concept of molecular mechanics is the definition of a potential energy function used to describe the relationship of the structure, $\mathbf{r}$ to the energy, V, of the system of interest. Towards this end, potential energy penalties are associated with the deviation of bonds and angles in the simulated molecule from their reference equilibrium values, obtained either from experiment or high precision quantum calculations (Eq. 1.1). The potential function also contains terms to describe long range non-bonded interactions. This partition of the energy function according to the different internal coordinates makes it convenient to parameterize the corresponding energy terms independently. The functional form of the potential energy expression and the entire set of parameters needed to fit the potential energy surface constitute the *force field*.[99]

The following equation describes the functional form of the widely used AMBER force field,[100] however, it remains largely valid for other pairwise additive force fields, including CVFF[101] used in InsightII:

$$
\begin{aligned}
V(\mathbf{r}) = & \sum_{bonds} K_r \left(r - r_{eq} \right)^2 \\
& + \sum_{angles} K_\theta \left(\theta - \theta_{eq} \right)^2 \\
& + \sum_{dihedrals} \frac{V_n}{2} [1 + \cos(n\Phi - \gamma)] \\
& + \sum_{\substack{nonbonded \\ pairs}} [\frac{A_{ij}}{R_{ij}^{12}} - \frac{B_{ij}}{R_{ij}^{6}} + \frac{q_i q_j}{\varepsilon R_{ij}}]
\end{aligned}
\tag{1.1}
$$

The first three summations in Eq. 1.1 are performed over bonds, angles and torsions. The torsion terms also include 'improper' terms, calculated for groups of 4 atoms not sequentially bonded. The main usage of these improper terms is to maintain planarity around sp^2 hybridized atoms. The final summation refers to non-bonded interactions, which include electrostatic and van der Waals (vdW) components. The 1,2 (between neighbors) and 1,3 (between second neighbors) interactions are excluded from the non-bonded term summation while 1,4 electrostatic and vdW interactions are usually scaled by separate empirical factors.[100] The vdW term is commonly calculated by a 6-12 Lennard-Jones potential, empirically accounting for London dispersion forces at long internuclear distances R_{ij} and enforcing the Pauli Exclusion Principle by a steep energy term at small values of R_{ij}.

The electrostatic interactions are most commonly computed by a pairwise Coulombic potential between fixed atomic point charges (Eq. 1.1). Such an additive model does not explicitly treat electronic polarizability. Instead, polarizability is incorporated implicitly by deliberately assigning atomic charges that overestimate molecular dipoles.[102,103] This overestimation is designed to approximate electrostatic interactions that occur in the aqueous environment common to biomolecules. Fast-paced development in the explicit treatment of polarizability has been ongoing over the past decade or so, and have recently been reviewed.[104,105] However, due to their added computational cost, polarizable force fields have not yet gained popularity for biomolecular simulations.

The focus of force field improvement efforts has recently been shifted to the refitting of torsion parameters.[106] Traditionally, torsion parameters were dealt with at the last stage of the fitting process and were the least rationally justified of the force field terms. A variety of approaches have been proposed to assess and correct these terms[107-114], most of which attempt to reproduce high precision dihedral maps of the alanine dipeptide obtained via *ab initio* quantum mechanics.[115] The efforts toward this direction have resulted in several promising applications such as the correct prediction of peptide structures[116,117] or side chain rotamer libraries.[118]

1.4.2 Energy Minimization

In computational chemistry, one is particularly interested in the geometry of stable and transition states of our systems, which correspond to minima and saddle points of the energy surface, respectively. However, except for the simplest of molecular systems, the potential energy is a complex, multidimensional function of the atomic coordinates. So in order to identify these geometries, computational chemists have employed or adapted some of the many optimization algorithms long devised by mathematicians.

For a system of potential energy $V(x_1,...,x_N)$, with N degrees of freedom of coordinate x_i, a minimum point of the potential energy is located when for all *i*,

$$\frac{\partial V(x_1,...,x_N)}{\partial x_i} = 0 \text{ and } \frac{\partial^2 V(x_1,...,x_N)}{\partial^2 x_i} > 0 \qquad (1.2)$$

The two most frequently used minimization techniques in molecular mechanics are the *steepest descent* and *conjugate gradient* methods described below. In both methods, the atomic coordinates of the system are iteratively changed ($\mathbf{x}_k \rightarrow \mathbf{x}_{k+1}$) as the system progressively approaches the minimum location.

Steepest descent

In the steepest descent algorithm, the system is moved in the direction of the net force acting on the system, opposite to the energy gradient $\mathbf{g}_k = \nabla V(\mathbf{x}_k)$. In a real-life geographical analogy, this would correspond to walking straight downhill along the direction of steepest slope. How far to go on the direction of the net force is decided by either locating a minimum along this direction - a computationally demanding approach - or by taking steps of arbitrary length.

The exclusive reliance of steepest descents on gradients is both its weakness and its strength as convergence is slow near the minimum because the gradient approaches zero, but the method is extremely robust. It is the method most likely to generate a lower-energy structure regardless of the nature of the energy function or initial starting position. Therefore, the steepest descent method is often used when the gradients are large and the configurations are far from the minimum. This is commonly the case for initial relaxation of poorly refined experimental data or for manually built models. As a result, more refined minimization algorithms often begin with a small series of steepest descents steps.

Conjugate gradients

In the steepest descent method, both the gradients and search directions of successive steps are orthogonal, leading to oscillations as the path persistently overcorrects for poor choices of directions in earlier steps.

In the original conjugate gradient method of Fletcher and Reeves,[119] the search direction vector $\mathbf{s}_k$ from $\mathbf{x}_k$ is computed from the gradient at that point and the previous search vector $\mathbf{s}_{k-1}$:

$$\mathbf{s}_k = -\mathbf{g}_k + \gamma_k \mathbf{s}_{k-1} \tag{1.3}$$

with the scalar γ_k given by:

$$\gamma_k = \frac{\mathbf{g}_k \cdot \mathbf{g}_k}{\mathbf{g}_{k-1} \cdot \mathbf{g}_{k-1}} \tag{1.4}$$

A line search is then conducted along this new direction, rather than in the gradient direction, as was the case in steepest descent. This particular construction has the remarkable property that the next gradient, $\mathbf{g}_{k+1}$, is orthogonal to all previous gradients, $\mathbf{g}_0,...,\mathbf{g}_k$ and that the next direction, $\mathbf{s}_{k+1}$, is conjugate to all previous directions, $\mathbf{s}_0,...,\mathbf{s}_k$, i.e. $\mathbf{s}_i \cdot \mathbf{V}'' \cdot \mathbf{s}_j = 0,\ i \neq j$, where $\mathbf{V}''_{ij} = \frac{\partial^2 V}{\partial x_i \partial x_j}$ is a positive-definite matrix. The attribute *'conjugate'* is thus somewhat misplaced, and the algorithm should rather be called the *conjugate directions* method. The method converges in approximately *N* steps, for a system of *N* degrees of freedom.

1.4.3 Phase Space Sampling Algorithms

The central goals of molecular simulations are to generate thermodynamic ensemble averages and observe configurational transitions. Following Boltzmann's ergodic hypothesis, which states that due to thermal motion, a single system runs through all states of the thermodynamic ensemble in the limit of infinite time, we take the assumption that a sufficiently long time average derived from a single molecular simulation is equivalent to the statistical ensemble average. Molecular systems have to exhaustively sample phase space, in order to adequately approximate this condition of infinite time, and therefore efficient sampling schemes such as those described below have been developed to allow the calculation of statistical ensemble averages on computationally tractable time scales.

Molecular Dynamics

Following the Born-Oppenheimer approximation, we assume that a molecular system of N particles of masses m_i can be described by classical mechanics. For each particle, Newton's equation of motion is given by:

$$F_i = m_i a_i \tag{1.5}$$

where F_i is the force exerted on particle *i*, and a_i its acceleration. As the force derives from the gradient of the potential energy,

$$-\frac{\partial V(r_1,...,r_N)}{\partial r_i} = m_i \frac{\partial^2 r_i}{\partial t^2} \tag{1.6}$$

Several finite difference integrating methods can be used to iteratively solve this differential system, which can only be solved analytically for the simplest of molecular systems. Variants of the Verlet algorithm[120] of integrating the equations of motion (Eq. 1.5) are perhaps the most widely used method in molecular dynamics. The advantages of Verlet integrators is that these methods require only one energy evaluation per step, require only modest memory, and also allow a relatively large timestep to be used. The Verlet leap-frog algorithm[121] employed in both AMBER and InsightII functions as follows:

- the velocities, $\mathbf{v}(t+\frac{1}{2}\delta t)$, are first calculated from the velocities at $t-\frac{1}{2}\delta t$ and the acceleration at time *t*:

$$\mathbf{v}(t+\frac{1}{2}\delta t) = \mathbf{v}(t-\frac{1}{2}\delta t) + \delta t.\mathbf{a}(t) \tag{1.7}$$

- updated positions, $\mathbf{r}(t+\delta t)$, are then deduced from the new velocities and current positions, and the new acceleration calculated from the forces:

$$\mathbf{r}(t+\delta t) = \mathbf{r}(t) + \delta t.\mathbf{v}(t+\frac{1}{2}\delta t) \tag{1.8}$$

$$\mathbf{a}(t+\delta t) = \frac{\mathbf{F}(t+\delta t)}{\mathbf{m}} \tag{1.9}$$

- the system is then iterated to the next δt. But as the positions literally 'leapfrogged' past the velocities, it is necessary to take an average in order to synchronize the velocities (kinetic energy) and positions (potential energy):

$$\mathbf{v}(t) = \frac{1}{2}\left(\mathbf{v}(t+\frac{1}{2}\delta t) + \mathbf{v}(t-\frac{1}{2}\delta t) \right) \tag{1.10}$$

The time step of integration δt must be chosen small enough so that even the fastest atomic motions get sampled adequately, to avoid instabilities and allow conservation of the energy. As a C-H bond vibrates with a frequency on the order of 10 fs, all-atom molecular simulations are limited to time steps of about 1 fs. As bond vibrations are of little interest in non-spectroscopic studies, holonomic restraints are usually applied to bond lengths[122-125] to rigidify them and therefore extend the time step to ~2 fs.

The first application of molecular dynamics to a biological macromolecule dates back to 1977, when McCammon and Karplus simulated the bovine pancreatic trypsin inhibitor protein in the gas phase for 9.2 picoseconds.[126] Since then, owing to the considerable progress in computer power, molecular dynamics simulations have become a routine tool for understanding the structure and motion of biological systems. In comparison to the early BPTI studies, current state of the art simulations now involve tens of thousands of atoms for tens of nanoseconds[127] or hundreds of atoms for microseconds.[128]

Monte Carlo Sampling

In contrast to molecular dynamics, Monte Carlo simulations directly generate configurations for a system by making successive random changes to the positions of its components. The Monte Carlo method thus samples a 3N-dimensional space for a system of N particles, and does not require momentum information. In the Metropolis implementation[129] popular in the statistical thermodynamics field, the energy is calculated at every step, and the random move is automatically accepted if the new configuration is lower in energy. If the energy increases, the Boltzmann factor for the move at the simulation temperature, $\exp(-\Delta V/k_B T)$, is compared to a random number taken from a uniform distribution between 0 and 1. If the Boltzmann factor is larger than the random number, the move is accepted. If not, the move is rejected and the initial configuration is retained for the next random move.

More concisely written, each random move is accepted with the following probability:

$$p_{acc} = \min\left(1, \exp\left(-\frac{1}{k_B T}\Delta V\left(r_1,...,r_N\right)\right)\right) \tag{1.11}$$

Iterations are performed until the configurational space has been sufficiently sampled to generate ensemble averages with satisfying statistics. This particular Monte Carlo scheme effectively performs an 'importance sampling' by focusing on the generation of the high probability, low energy configurations that dominate the mean properties of the ensemble. However, in contrast to molecular dynamics, there is no physical time connection between the sampled configurations, which precludes the direct derivation of kinetic information.

The sampling efficiency of the Monte Carlo algorithm depends primarily on the choice of random displacement. Usage of the Monte Carlo sampling scheme in all-atom molecular simulations has been so far limited to small conformational moves, as the ruggedness of the potential energy surface (in the form of steric clashes) leads to very few moves being accepted in large systems such as proteins, with excessive computational time wasted on the energy evaluation of rejected moves.

Replica Exchange Molecular Dynamics

Complex biomolecular systems with many degrees of freedom may become trapped in low-energy regions of the thermally accessible space, using MD or MC simulations at constant temperature.[130-132] Such simulations may display all attributes of a converged simulation, while producing erroneous results because of this sampling bias. Such simulations are known to suffer from the *quasi-ergodicity* problem. A variety of methods have been proposed to tackle this problem,[133] with one of them, the replica exchange method[134] (also referred to as parallel tempering[135]) quickly gaining popularity in the molecular dynamics simulation community.[136-143]

In replica exchange molecular dynamics (REMD), a generalized ensemble is constructed from N non interacting copies of the system of configurations $\mathbf{x}_i$, $i = 1,...,N$, each at a different temperature T_i. The state of this generalized ensemble is

denoted $X = \{\mathbf{x}_1, ..., \mathbf{x}_N\}$. Because the replicas are fully independent, the weight factor of the generalized state is simply the product of all replica Boltzmann factors:

$$W_{REM}(X) = \exp\left(-\sum_{i=1}^{N} \beta_i H(\mathbf{r}_i, \mathbf{p}_i)\right) \tag{1.12}$$

where $\beta_i = \frac{1}{k_B T_i}$ is the inverse temperature, and $\mathbf{p}_i$ and $\mathbf{r}_i$ are the replica momentum and position vectors. Replica temperature exchanges are allowed to take place within the generalized ensemble, altering the state of the system. In the case of an $i \leftrightarrow j$ permutation the state goes from X to X':

$$X = \{..., \mathbf{x}_{i,T_i}, ..., \mathbf{x}_{j,T_j}, ...\} \rightarrow X' = \{..., \mathbf{x}_{i,T_j}, ..., \mathbf{x}_{j,T_i}, ...\} \tag{1.13}$$

To maintain detailed balance in this equilibrium ensemble, microscopic reversibility has to be satisfied:

$$W_{REM}(X).\rho(X \rightarrow X') = W_{REM}(X').\rho(X' \rightarrow X) \tag{1.14}$$

with $\rho(X \rightarrow X')$ denoting the probability of a transition from X to X'. Using the following momenta scaling condition introduced by Sugita and Okamoto for molecular dynamics applications of the replica exchange method:[134]

$$\begin{cases} p_{i,T_j} = \sqrt{\frac{T_j}{T_i}} p_{i,T_i} \\ p_{j,T_i} = \sqrt{\frac{T_i}{T_j}} p_{j,T_j} \end{cases} \tag{1.15}$$

the exchange probability is expressed by:

$$\rho(X \rightleftharpoons X') = \frac{\rho(X \rightarrow X')}{\rho(X' \rightarrow X)} = \exp(-\Delta) \tag{1.16}$$

where

$$\Delta = (\beta_i - \beta_j)(V_{j,T_j} - V_{i,T_i}) \tag{1.17}$$

and V_{i,T_i} is the potential energy of replica *i* at its original temperature T_i.

As in the Monte Carlo sampling algorithm, the preceding probability can be enforced by a Metropolis criterion[129] :

$$\rho(X \rightleftharpoons X') = \min\left(1, \exp\left(-\Delta\right)\right) \tag{1.18}$$

In practice, replicas are simulated simultaneously and independently for a certain number of MD steps. Then, pairs of replicas at neighboring temperatures are tested for exchange with a probability calculated by Eq. 1.18. If the exchange is accepted, the temperatures of the two replicas are swapped, and the velocities scaled accordingly (Eq. 1.15). Otherwise, if the exchange is rejected, each replica will proceed with its own trajectory. This algorithm is particularly well suited for calculations on clusters of poorly communicating processors, as the temperatures are the only information exchanged, and rather infrequently.

A comparison of this algorithm with constant temperature molecular dynamics applied to a peptide at room temperature showed that this algorithm decreased the

sampling time by a factor of 20 or more and sampled a 5 times larger conformational space for an identical number of iterations.[139,144]

Chapter 2

Determining the Bioactive Conformation of Taxol®

2.1 Introduction

Over the last two decades, various biological and pharmacological activity data as well as structure-activity relationships have been reported for paclitaxel and its congeners (taxoids).[145-147] Structural biology investigations into the paclitaxel-tubulin interactions has so far culminated in the determination of the electron crystallographic (EC) structure of the α,β-tubulin heterodimer bound to paclitaxel at 3.7 Å resolution and its subsequent refinement to 3.5 Å resolution.[87,88] Although representing a seminal achievement, this EC structure lacks the atomic resolution necessary to ascertain the structure of paclitaxel in the β-tubulin binding pocket and the intermolecular interactions responsible for the stabilizing effect of the drug on microtubules.

Solution[148] and solid phase[149,150] NMR studies, photolabeling studies[151-153] as well as computational modeling[154-156] have provided additional information regarding the binding structure and location of paclitaxel. The set of computational protocols described below has been developed in order to unify these highly valuable pieces of information into a more detailed description of the tubulin-binding mode of paclitaxel and its analogs.

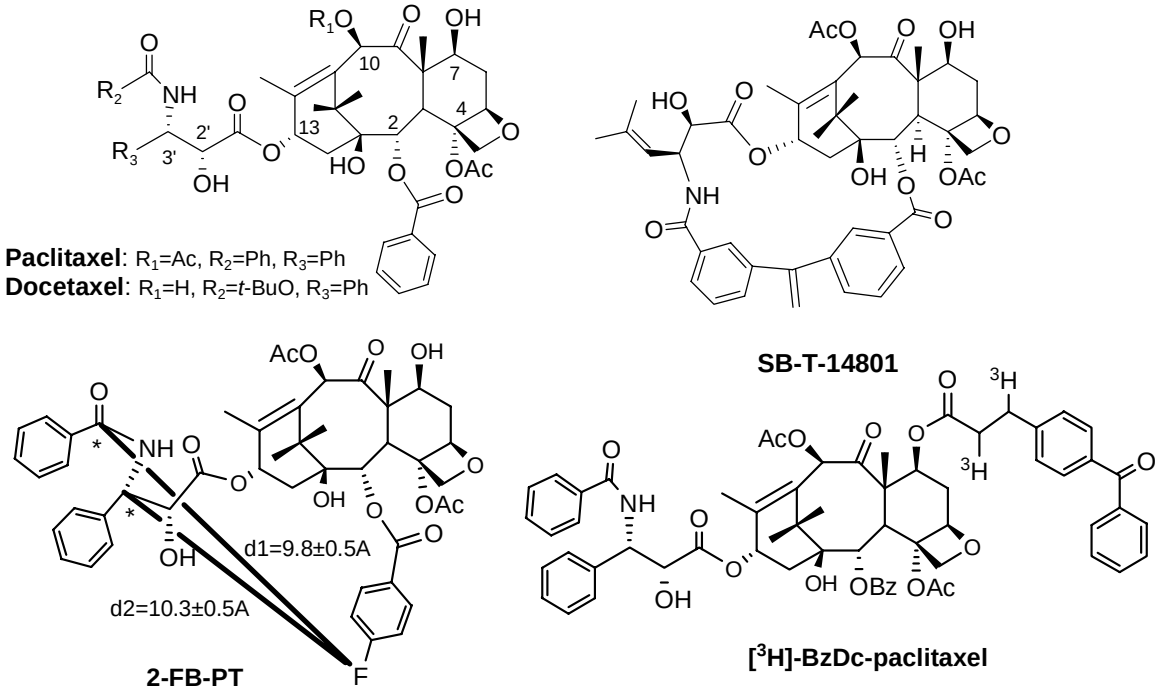

Figure 2.1. Structures of paclitaxel, docetaxel, photoaffinity probe [^{3}H]7-BzDc-paclitaxel,[153] conformationally constrained taxoid SB-T-14801. 2-FB-PT[150] is also shown, with intramolecular REDOR-NMR distances indicated.

2.2 Computational Protocol

To determine the bound conformation of paclitaxel in β-tubulin, 2-(*p*-Fluorobenzoyl)paclitaxel (2-FB-PT) was modeled from the X-ray structure of paclitaxel[157] in Macromodel 6.5 (Schrödinger Inc.) by substituting an F atom at the *para* position of the C2 benzoate group. Monte-Carlo conformational searching was conducted with energy minimization on the isolated 2-FB-PT molecule in the gas phase using the Monte Carlo Multiple Minimum (MCMM) procedure[158,159] (4000 MC steps, minimization for 1000 steps with Polak-Ribiere conjugate gradients) and MM3* force field,[160-163] well suited for the conformational analysis of small molecules. All side chain rotatable bonds were allowed to vary. 1371 structures were found within 50 kJ/mol which complied with both REDOR NMR distances. These conformers were clustered according to their C13 and C2 side chains dihedral angles using the Xcluster facility packaged with Macromodel 6.1. 16 clusters were obtained at the 1356 clustering level, comprising 124, 250, 76, 236, 1, 129, 243, 220, 69, 1, 1, 1, 2, 1, 1 and 16 members, respectively. A representative structure for each cluster was selected as the structure with minimal root mean square distance to the centroid of all cluster members, regardless of its energy relative to the global minimum of the conformational search.

All 16 representative conformations of paclitaxel (Figure 2.2) were then manually docked into the paclitaxel binding site of β-tubulin, following the same procedure: their taxane skeleton (carbon atoms of the A, B and C rings) was overlaid with that of docetaxel present in the deposited β-tubulin EC structure (PDB ID: 1TUB). The benzodihydrocinnamoyl (BzDc) linker was modeled and attached to C7 of paclitaxel in InsightII 2000 (Accelrys Inc.). Finally, the linker was attached to the Cα of Arg282 by merging the two fragments, thus creating an elongated C-C bond (Figure 2.3).

The docked molecular complex was allowed to minimize for 1000 steps, with the conjugate gradients method, CVFF force field and distance dependent dielectric. The BzDc linker was then erased and H atoms were added to reconstitute the free paclitaxel ligand and the protein after a binding domain comprising all residues within 10 Å of the bound 7-BzDc-PTX has been defined. A second minimization is then conducted on the non-covalent complex of paclitaxel with this 10 Å binding domain (same conditions as first minimization). The approach was identical for all the taxoids docked.

2.3 Results and Discussion

2.3.1 Conformation of Paclitaxel in β-Tubulin

Solution [148,164-166] NMR spectroscopy and X-ray crystallography[4,157] of paclitaxel and its analogs have provided rich information about the various conformations paclitaxel can adopt in the unbound state. This information is only of limited use since ligands commonly undergo large conformational changes upon binding to their targets.[167]

Recently, a fluorinated paclitaxel analog, 2-FB-PT, was used bound to microtubules in solid state $^{13}C\{^{15}N$ or $^{19}F\}$-double-REDOR-NMR experiments.[150] After three months of data acquisition, Schaefer and his collaborators were able to determine two ^{13}C-^{19}F intramolecular distances for 2-FB-PT in the bound state (d1 and d2 in Figure 2.1).

Molecular Dynamics (MD) simulations were initially conducted on 2-FB-PT *in vacuo* at increasing temperatures from 300K to 500K (InsightII 2000, Accelrys, CVFF force field). Unfortunately, some side chain bonds (e.g. C2'-C3') of the molecule present a high-energy barrier to rotation, impeding adequate sampling. For this reason, we switched to a Monte-Carlo (MC) conformational search.[158] The two intramolecular distances determined were then used as constraints in an extensive MC conformational search on 2-FB-PT *in vacuo*. Conformational diversity in the set of resultant minimized structures was assessed by performing a cluster analysis on the 1371 retained conformations with energies within 50 kJ/mol of the global minimum. Sixteen clusters were formed according to the values of 10 dihedral angles of the C13 and C2 side chains. A representative structure for each cluster is shown in Figure 2.2. Remarkably, most of these structures have their C3' benzamido moiety pointing in the same direction as the C2 fluorobenzoate group, as seen for docetaxel in its X-ray structure[4]. Also, to accommodate the REDOR-NMR geometric requirements, the entire C13 side chain has to move away from the C2 fluorobenzoate, unlike in the 'hydrophobic collapse' conformation observed for the free drug in polar solvents.[164-166]

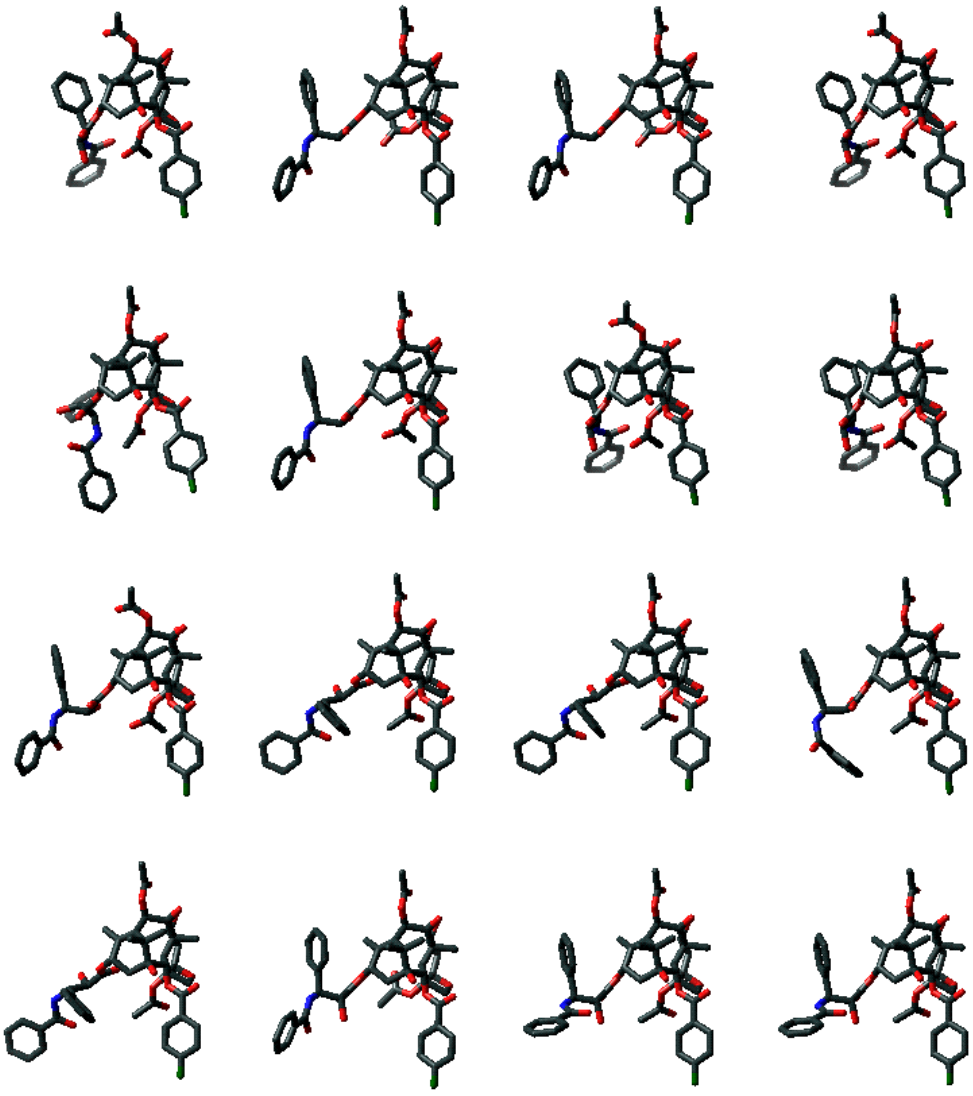

Figure 2.2. REDOR-NMR constrained Monte Carlo conformational search on 2-FB-PT: representative structures of the 16 conformational clusters.

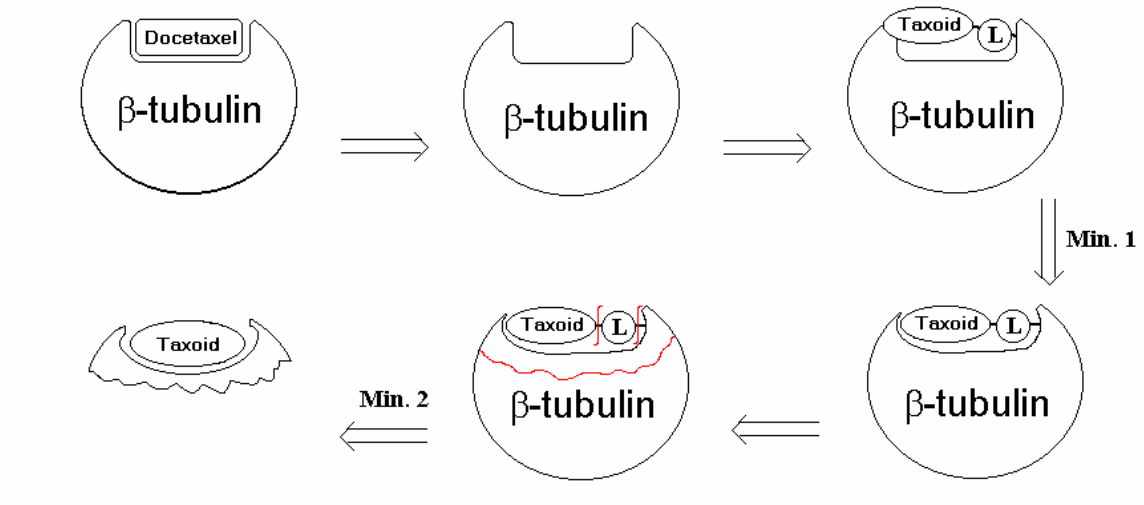

Figure 2.3. Guided docking protocol diagram (L=BzDc linker).

2.3.2 Guided Docking of Taxoids in β-Tubulin

The exact orientation of paclitaxel in β-tubulin has been much debated.[150,153] Some agreement was nevertheless found between the electron crystallographic density and three photoaffinity labeling experiments.[151-153,168] It is worth mentioning that a C7-benzodihydrocinnamoyl (C7-BzDC) derivative of paclitaxel (Figure 2.1) labeled exclusively the Arg282 residue in the M loop of β-tubulin. This specificity prompted us to model this covalent complex. This way, translational and rotational motions of the ligand are hampered, while the ligand evolves in its most likely position. A two-step procedure was then adopted in order to get a refined binding site model. First, the complex formed by β-tubulin and the bound C7-BzDc paclitaxel in the possible bioactive conformation inferred from the Monte-Carlo conformational search were modeled and minimized. The carbonyl carbon of the benzophenone moiety (i.e., as α-hydroxy radical) was connected to the α-carbon of Arg282, since the excited state of the benzophenone moiety would selectively abstract hydrogen from the α-position of an amino acid residue because of the capto-dative stabilization of the resulting radical species.[169] The peptide backbone atoms of the protein were kept fixed at all times during the minimizations, while side chain atoms were free to move, allowing the reorganization of side chains upon binding of modified taxoids (partial induced-fit). After cleavage of the BzDc linker, a free ligand-binding site complex, comprising only residues within 10 Å of any ligand or linker atom is minimized again under the same conditions.

The procedure was applied to paclitaxel, starting from all 16 conformations retained from the Monte-Carlo conformational search of 2-FB-PT. The REDOR-NMR distances were verified after docking and used as a filter to determine the tubulin-bound paclitaxel conformation. However, none of the representative structures could strictly maintain both distances in the allowed REDOR-NMR ranges after docking. Two factors could contribute to that: (i) the availability of large empty spaces in the binding site, and (ii) the fact that the REDOR distances were derived from microtubules (MTBs) while the EC structure corresponds to the Zn-sheet form of tubulin, which might present some structural differences to the MTB form. The structure deviating the least from the two REDOR-NMR restraints (i.e., d_1 = 9.38 Å, d_2 = 9.97 Å) was selected as our tubulin-bound paclitaxel structure, and denominated 'REDOR-Taxol' (Figure 2.4).

A significant asset of this guided docking protocol is the total flexibility of the protein side chains during the minimization stages. This allows docking of heavily modified or bulky taxoids, under the assumption that their baccatin skeleton remains in the vicinity of paclitaxel in the binding pocket. Figure 2.5 shows an example of a tubulin-bound macrocyclic paclitaxel analog, SB-T-14801, a surprisingly active analog in its series (IC_{50} 71 nM against the LCC6 lung cancer cell line).[170] The protein shows extensive rearrangements induced by the connection of the C2 and C13 taxoid side chains: in particular, the His227 side chain has to rotate, and face the C2 benzoyl group of the taxoid, confirming that even partial flexibility of the protein allows the binding site to accommodate bulkier analogs.

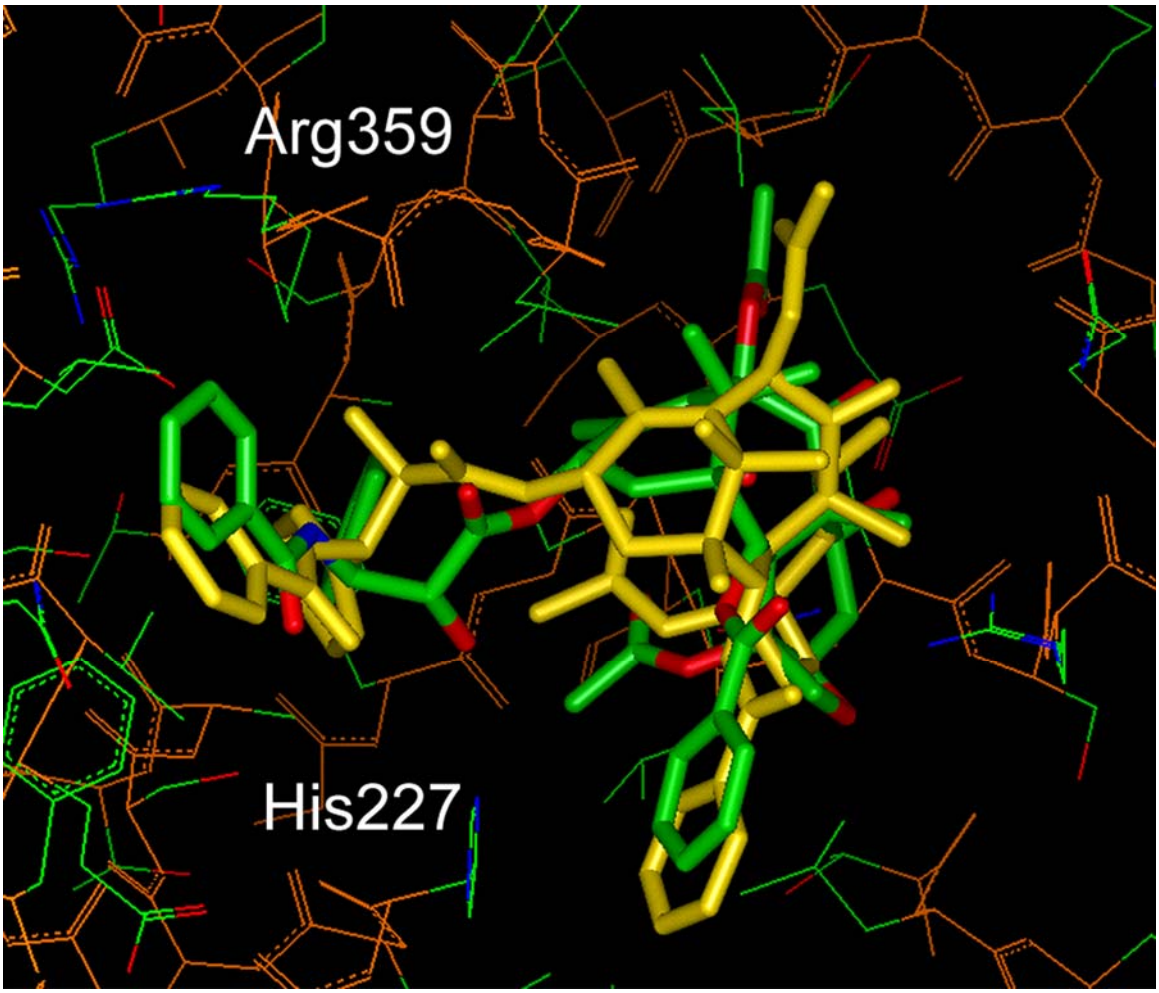

Figure 2.4. Proposed β-tubulin-binding models of paclitaxel. Overlay of the docked REDOR-Taxol (green) and T-Taxol (yellow) structures. The overlay is performed by matching the protein backbone, which is kept fixed throughout the docking process.

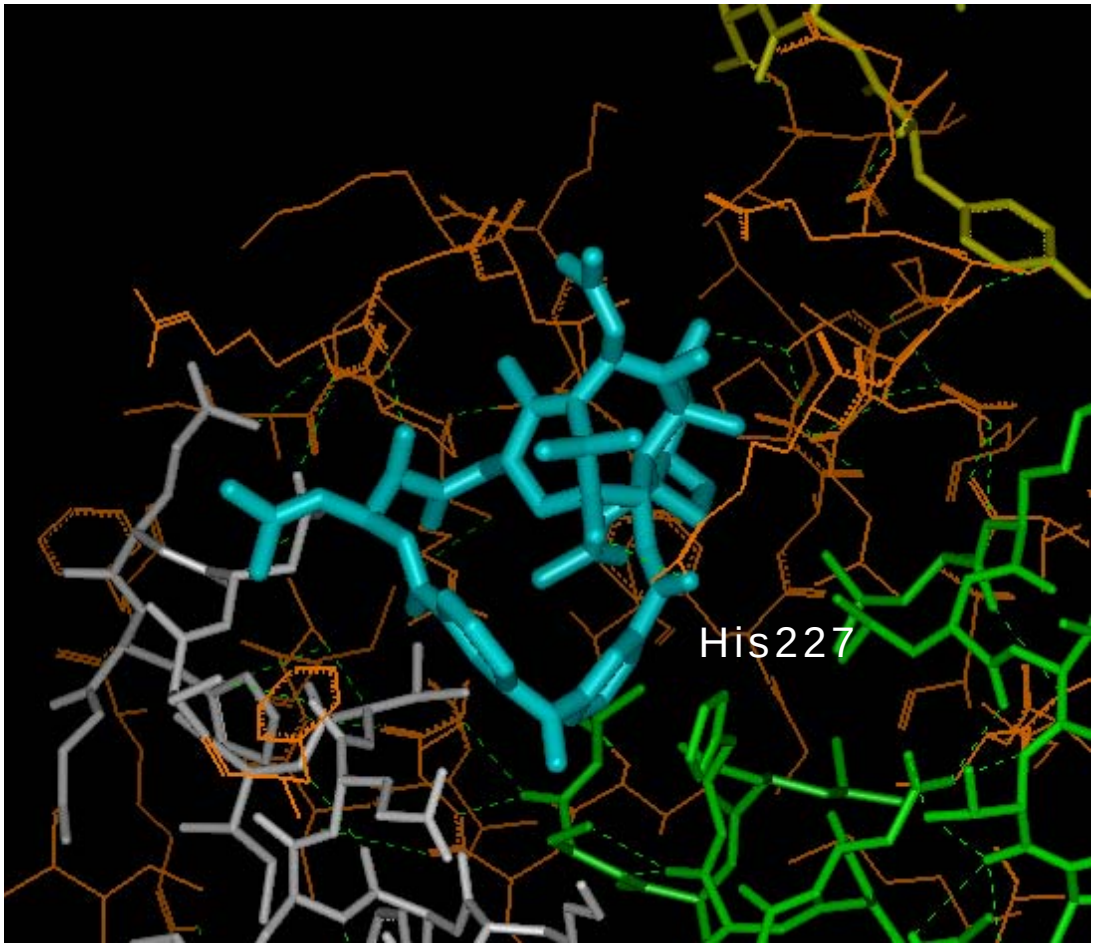

Figure 2.5. Docked complex of SB-T-14801.

2.3.3 Analysis of Paclitaxel Binding Site Models

While preliminary results of this work were obtained, producing the REDOR-Taxol structure, Snyder *et al.* reported a binding site model for paclitaxel by docking 26 experimentally observed unbound paclitaxel conformers into the Zn-sheets EC density map.[155] Although this approach also resulted in an extended bioactive conformation for paclitaxel, 'T-Taxol', the resolution of the EC map appears insufficient for unequivocal selection of the optimal binding conformation of paclitaxel. It is worth pointing out that T-Taxol does not comply with the REDOR-NMR distances, with values of 9.32 Å and 8.11 Å for d_1 and d_2, respectively (measured on 2-FB-PT in the T-Taxol conformation), denoting that in T-Taxol, the C2 and C3' side chains are more collapsed than those deduced by the REDOR-NMR experiment.

The main difference between Snyder's T-Taxol and our REDOR-Taxol is the conformation of the C13 side chain. In order to fairly compare REDOR-Taxol to T-Taxol, we docked the T-Taxol structure into the β-tubulin binding site using our guided docking protocol. This procedure caused a small but significant realignment of the T-Taxol conformation and an overlay of the resulting pose with REDOR-Taxol is shown in Figure 2.4. The two models locate their C3' phenyl rings in nearly identical loci. However, the C2'-hydroxyl group which usually forms an intramolecular H-bond with the C1'-carbonyl oxygen in the free drug is pointed towards His227 in the REDOR-Taxol structure, forming a very buried H-bond of increased strength. This makes a sharp contrast to the more solvent exposed H-bond between the C2'-hydroxyl and the backbone carbonyl oxygen of Arg359 in the T-Taxol binding pose.

Additionally, the internal energy of the 'unbound' form of paclitaxel detached from tubulin *in vacuo* is ~10 kcal/mol lower in the REDOR-Taxol conformation than in the T-Taxol conformation (CVFF force field, InsightII). This energy difference mostly arises from torsional terms, and suggests that the REDOR-Taxol structure is a less strained conformation requiring less stabilizing interaction with the protein to make the overall association favorable.

However, due to the low resolution of the tubulin EC density map, direct experimental evidence is lacking to confirm or rule out one of these two conformations as the bioactive form, assuming it is unique.

2.4 Conclusions

A bioactive structure of paclitaxel, REDOR-Taxol, has been proposed on the basis of detailed computational analysis of the combined data from the REDOR-NMR, the electron crystallography and photoaffinity labeling experiments. Although the REDOR-Taxol structure shares similar features to Snyder's T-Taxol,[155] the REDOR-Taxol structure allows strong H-bonding between the C2' hydroxyl group of paclitaxel and the His227 residue in contrast to T-Taxol having H-bonding between the C2'-OH and Arg359 in the β-tubulin S9-S10 loop.

Chapter 3

Design and Biological Evaluation of Conformationally Constrained Taxol® Analogs

In order to confirm the proposed REDOR-Taxol conformation identified in Chapter 2, a typical synthetic approach is to construct conformationally constrained analogs which retain potencies similar to that of the lead compound, paclitaxel. The inclusion of protruding cyclic restraints at various positions also helps delineate the essential intermolecular contact areas of the binding site and further refine the pharmacophore model. This chapter briefly reviews previous approaches towards bioactive conformationally constrained analogs of paclitaxel and presents our successful design of potent restrained paclitaxel analogs based on the REDOR-Taxol bound conformation.

3.1 Previous Designs

3.1.1 C2 Benzoyl to C3' Phenyl Tethering: 'C-Linked' Taxoids

Following up on their discovery of the 'hydrophobic collapse' conformation of taxoids in polar solvent,[166,171,172] the Georg group was the first to attempt the connection of paclitaxel pharmacophoric elements in order to mimic this biologically relevant conformation. To enforce the short C2-benzoate to C3'-phenyl distance observed in the DMSO-d_6/$D_2$0 NOESY experiments, they synthesized a series of taxoids bearing various 2 atom linkers between these positions (Figure 3.1). Heck cyclization provided olefins **3.1** and **3.2**, with subsequent hydrogenation yielding the saturated analog **3.3**. A separate synthetic approach provided lactone **3.4**.[173] None of these four compounds demonstrated any measurable activity *in vitro* in the microtubule polymerization assay, nor did they compete with paclitaxel for tubulin binding. These adverse results strongly suggested that the polar conformation was not the bioactive one and that conformational rearrangements occurred in the binding process.

A similar approach to a tethered polar conformation was taken in the Ojima lab, starting from a 2D NOESY NMR study of nonataxel (**3.5**, Figure 3.1), a highly bioactive C10-acetyl docetaxel derivative with isobutenyl groups in place of the C2 and C3' phenyl moieties.[154] Similarly to paclitaxel, in a polar DMSO-d_6/D_2O mixture, nonataxel adopted the hydrophobic collapse conformation, with strong NOE signals between the C2 and C3' isobutenyl groups. The modeled nonataxel structure derived from simulated annealing incorporating NOE restraints then served as a template for generating conformations of paclitaxel and other MT-stabilizing agents (epothilone B, discodermolide and eleutherobin, Figure 3.2) compatible with a common pharmacophore hypothesis based on SAR information. The resulting 3D pharmacophore inspired the design and synthesis of paclitaxel-epothilone hybrid SB-TE-1120, (**3.6**, Figure 3.1) bearing a macrocycle

connecting the C2 and C3' positions. Interestingly, the C2 phenyl tether is branching from the *ortho* position rather than *meta* in the first series of inactive C-linked compounds by Georg *et al.* (**3.1**-**3.4**). SB-TE-1120 was the first macrocyclic restrained taxoid to represent a viable lead, as it maintained 37% of the tubulin polymerization activity of paclitaxel and substantial activity against the LCC6-WT human breast cancer cell line (IC_{50} = 0.39 μM; i.e. two orders of magnitude larger than paclitaxel).[154]

An entire series of related macrocyclic taxoids was prepared using ring-closing metathesis (RCM), by connecting the C2 and C3' positions with tethers of varied length and composition (**3.7**, Figure 3.1).[174] The cell growth inhibition effect of these compounds was variable, with IC_{50} against the LCC6-WT cell line ranging from over 10 μM to sub-micromolar for two compounds (**3.8** and **3.9**, Figure 3.1), comparably to SB-TE-1120. Two other compounds in this series, with 2.33 and 4.1 μM IC_{50} against the LCC6-WT cell line, were also assayed for their tubulin polymerization ability. It was found that their activity in this test was 19% and 21% that of paclitaxel in the same assay, correlating well with the 3 orders of magnitude decrease observed in cytotoxic activity.

In spite of the increased mobility of the C2-C3' tether employed in compounds of this series, relative to the compounds of the Georg *et al.* study, their diminished bioactivity possibly indicated that they too were unable to adopt the tubulin-bound conformations of paclitaxel and nonataxel. Another explanation to this loss of bioactivity could be that the binding of paclitaxel to β-tubulin is a stepwise process requiring conformational rearrangements not possible in those restrained analogs. Alternatively, the molecule could adopt the appropriate conformer, but the bulk of the added tether might generate unfavorable steric contacts with the protein.

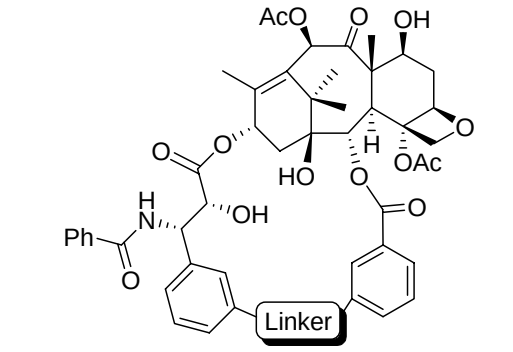

Linker: 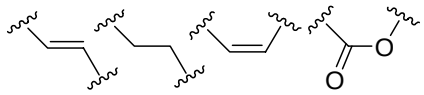

3.2 **3.3** **3.1** **3.4**

Georg *et al.* macrocyclic constructs

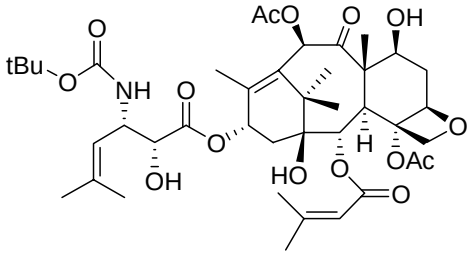

3.5 Nonataxel

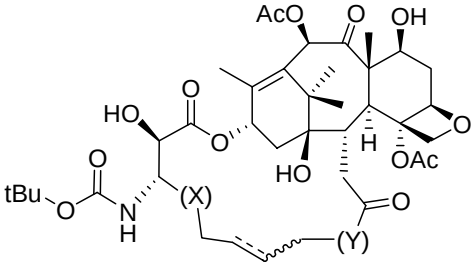

3.7 Template for C-linked macrocycles

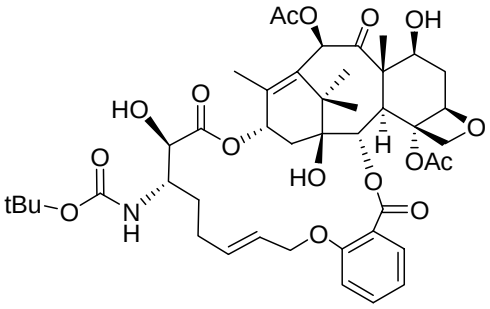

3.6 SB-TE-1120

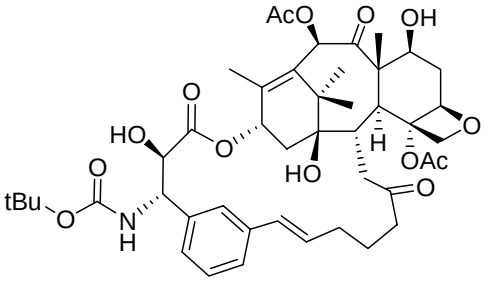

3.8

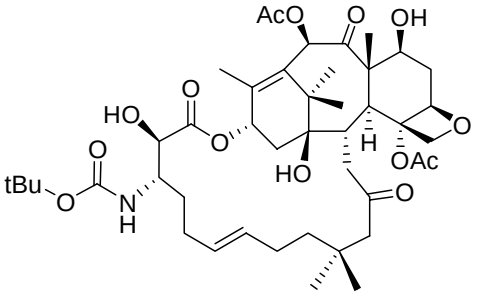

3.9

Figure 3.1. 'C-linked' macrocyclic taxoids.

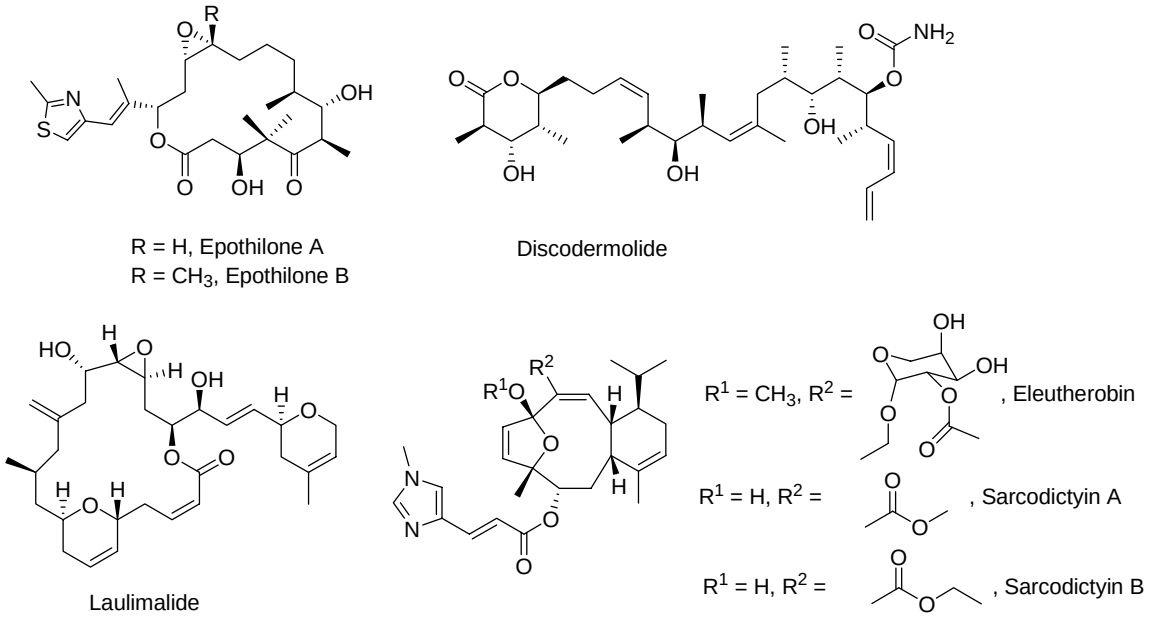

Figure 3.2. Structures of non-taxane microtubule stabilizing agents.

3.1.2 C2 Benzoyl to C3' Benzamido Tethering: 'N-Linked' Taxoids

As it became apparent from the cryo-EM studies of Nogales et al.[87,155] that the bound conformation of paclitaxel in β-tubulin was not the collapsed one observed in polar solvents, but rather an extended structure similar to that of docetaxel in the solid phase,[4] our group became interested in studying a new series of macrocyclic taxoids wherein a tether links the C2 carboxylate and C3'N acyl positions (**3.10**, Figure 3.3).[175]

All compounds in this series exhibited some level of growth inhibition against the LCC6-WT cell line. Seven out of twelve compounds exhibited single digit micromolar IC_{50} values, while the remaining five compounds were sub-micromolar with IC_{50} between 0.09 and 0.70 μM, the most active being **3.11** (Figure 3.3). While an IC_{50} of 0.09 μM represents a 30-fold reduction in cytotoxic activity, relative to paclitaxel, it nevertheless shows a 4-fold improvement from the lead C-linked taxoid. Interestingly, the same growth inhibition assay conducted on the multi-drug resistant variant of the cell line (LCC6-MDR) demonstrated a 1.4 to 33 resistance index for compounds in the N-linked series, as opposed to 112 for paclitaxel, suggesting that the P-glycoprotein might not recognize these macrocyclic analogs as well as the parent drug.

A second synthetic approach towards N-linked macrocyclic paclitaxel analogs was also explored, wherein a highly regioselective Heck macrocyclization is employed to close the macrocyclic ring.[170] In spite of their higher structural rigidity, *exo* isomers were found to be more cytotoxic than their *endo* counterparts. Indeed, against the LCC6-WT breast cancer cell line, the IC_{50} values of **3.12**-*exo* and **3.13**-*exo* (Figure 3.3) were 0.067 and 0.071 μM, respectively, while that of **3.12**-*endo* was 0.530 μM, showing an 8-fold reduction in activity. Although slightly better than that of the best N-linked compound obtained by RCM,[154,174] the bioactivity of these *exo* isomers was still 15 times inferior to that of paclitaxel in the same assay.

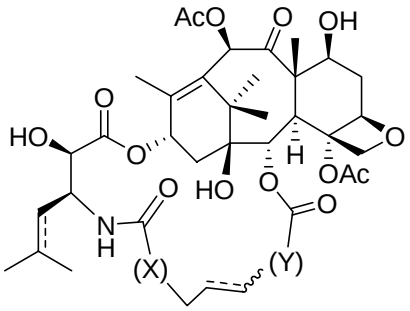

3.10 Template for N-linked macrocycles via RCM

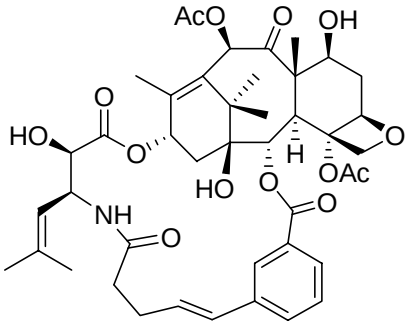

3.11

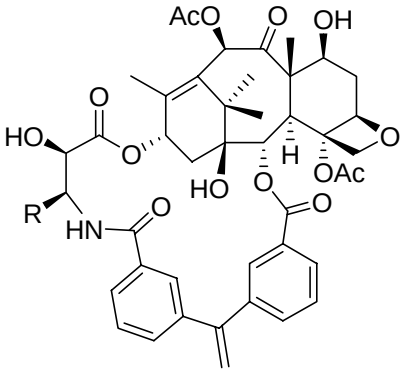

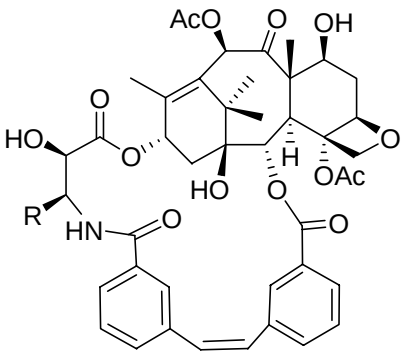

3.12-*exo*: R=Ph
3.13-*exo*: R=CHC(Me)$_2$

3.12-*endo*: R=Ph
3.13-*endo*: R=CHC(Me)$_2$

Figure 3.3. 'N-linked' macrocyclic taxoids.

3.2 Early Design Attempts

Visualizing the paclitaxel binding model, we noticed that space was left unoccupied around the paclitaxel structure. We therefore set off to introduce conformationally restraining groups that would fill these empty volumes and lower the entropy loss upon binding, while causing minimal disruption to the binding interactions and possibly adding further stabilizing interactions via the restraining moieties.

The REDOR-Taxol conformation of paclitaxel suggested that the C4 acetyl and C13 side chains were in close proximity in the bioactive conformation. Furthermore, the β-tubulin binding site of paclitaxel is a deep crevice of which paclitaxel only occupies the most superficial region. This incited us to insert a linking moiety connecting the C4 acetyl and C2' positions in restrained taxoid **3.14** (Figure 3.4). The binding model also opens the possibility of inserting linking moieties in the vast hydrophobic cluster formed by the C3'N and C2 benzoyl groups and the imidazole of His227. Accordingly, we designed C14-C3'N linked taxoid **3.15** (Figure 3.4) in which a short (four C atoms) linker should lock the C13 side chain in an unequivocal conformation close to the bioactive with minimum impact on the original binding interactions of the taxoid by avoiding steric clash with His227 of the core β-tubulin helix, H7.

Compounds **3.14** and **3.15** were also selected as our targets because our laboratory had greater experience in the synthesis of isobutenyl β-lactams, which enabled increased bioactivities relative to paclitaxel when incorporated in taxoids of the 2nd generation.[176,177] In particular, **3.14** was chosen as a target because β-lactam chemistry readily allows modification at the C2' position and the SAR studies of paclitaxel showed that longer side chains at the C4 position enhanced the activity slightly.[24]

3.2.1 Synthetic and Analytical Methods

The synthesis of the designed C14 to C3' and C4 to C2' restrained taxoids was performed by Dr. Xudong Geng of the Ojima laboratory. RCM[178] was used as the key reaction based on the previous successful applications of this protocol in constructing C2-C3'[154,174] and C2-C3'N[175] linked macrocyclic taxoids. The precursors of RCM, i.e., dienes, were synthesized through our highly efficient β-lactam-baccatin ring-opening coupling protocol.[20,179,180]

The syntheses of C4-C2' linked taxoids require a C4 modified baccatin **3.16**. This baccatin was synthesized using a reported protocol by Kingston *et al.*[181] with modifications. As shown in Figure 3.5, baccatin **3.16** was coupled with β-lactam **3.17**,[182] which bears an allyl group, to afford diene **3.18** in 60% yield. A certain amount (22%) of C13 Boc baccatin **3.19** side product was isolated, presumably because the 13-oxygen anion of baccatin **3.16** might attack the Boc carbonyl group due to the steric hindrance of the C2 carbonyl group in β-lactam **3.17**.

Diene **3.18** was then subjected to RCM reaction using 'Grubbs's catalyst'[178] to afford macrocyclic taxoid **3.20** in 70% yield. Desilylation using HF-pyridine gave C4-C2' linked taxoid **3.14** in 60% yield. Interestingly, only the *Z*-isomer of **3.14** was obtained.

Hydrogenation of **3.14** using palladium on carbon as catalyst afforded saturated macrocyclic taxoid **3.14(H)** in quantitative yield.

The C13 side chain precursor for C14-C3'N linked taxoids, β-lactam **3.21**, was prepared as shown in Figure 3.6. *N*-H β-lactam[183] **3.22** was treated with 2-allylbenzoyl chloride[184] to give β-lactam **3.21** in 80% yield.

In order to synthesize the C14-C3'N linked taxoids, it is necessary to introduce an olefin moiety at the C14 position of baccatin. This was realized by allylation of the 14-OH of the derivative of a naturally occurring baccatin, 14β-OH-10-DAB.[185] As shown in Figure 3.6, 14-OH-10-DAB was first treated with excess amount of TESCl and imidazole to afford 7,10-di-TES-14β-OH-10-DAB **3.23** in 70% yield. Then, 10-acetylation of **3.23** using LiHMDS and AcCl at -40 ^{o}C provided baccatin **3.24** in 93% yield. The silyl groups of **3.24** were removed using HF-pyridine and selective TES protection of the C7 OH of baccatin **3.25** using TESCl and imidazole gave 7-TES-14-OH-baccatin **3.26** in good yield. Finally, in the presence of NaHMDS, **3.26** was treated with allyl iodide to afford **3.27** with an allyl ether moiety attached to the C14 position.

As shown in Figure 3.6, coupling of baccatin **3.27** and β-lactam **3.21** gave diene **3.28** in 80% conversion yield. RCM reaction gave the desired macrocycle taxoid **3.29** in 80% yield. The silyl groups were then removed with HF-pyridine to afford **3.15** (*E*-isomer only). Finally, hydrogenation of **3.15** using Pd on carbon as catalyst gave **3.15(H**) in 80% yield.

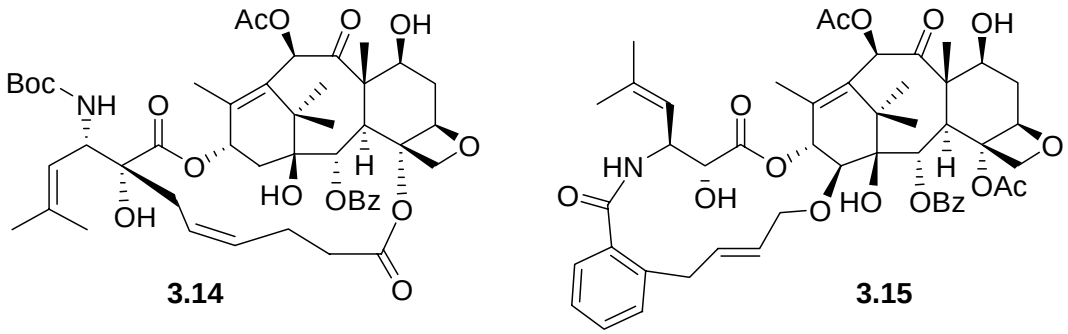

Figure 3.4. Target restrained macrocyclic taxoids.

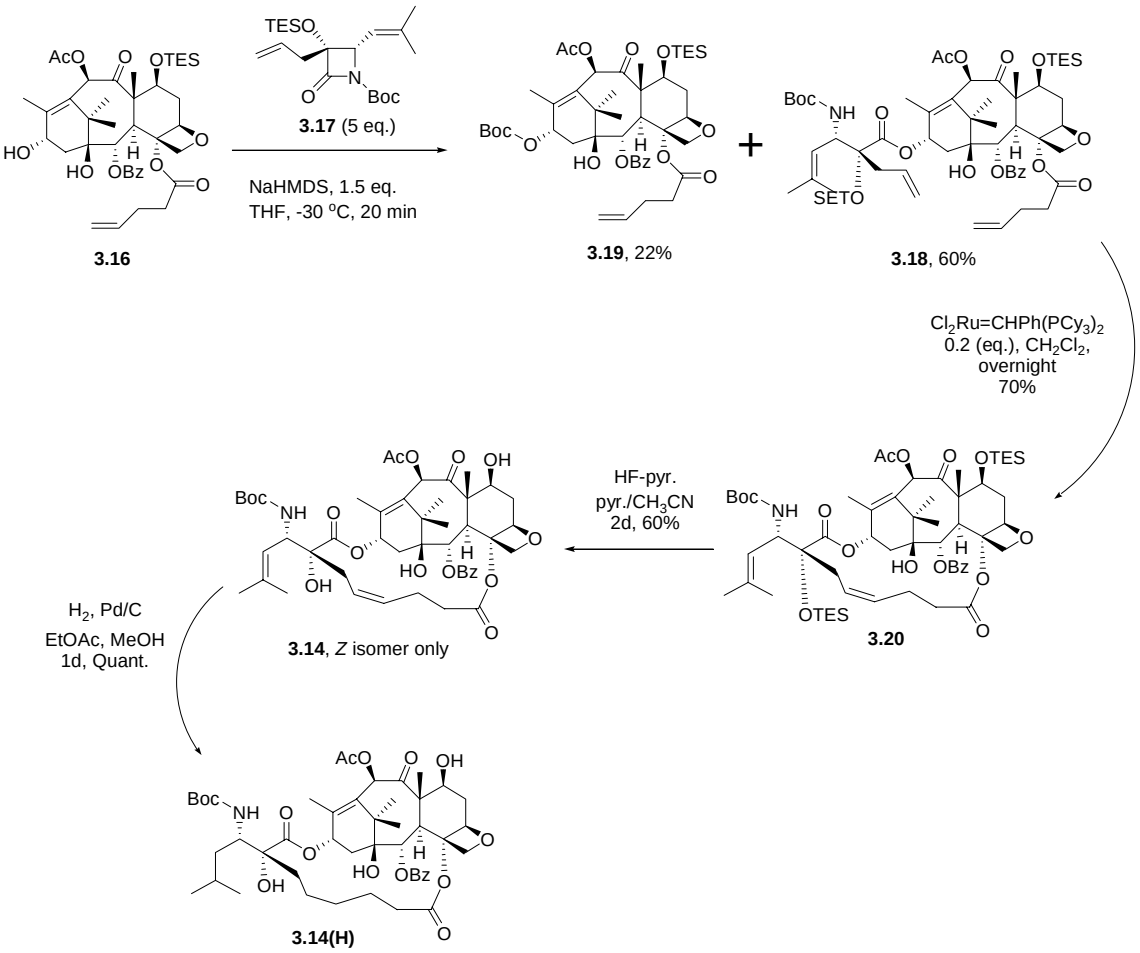

Figure 3.5. Synthesis of C4-C2' linked taxoids 3.14 and 3.14(H).

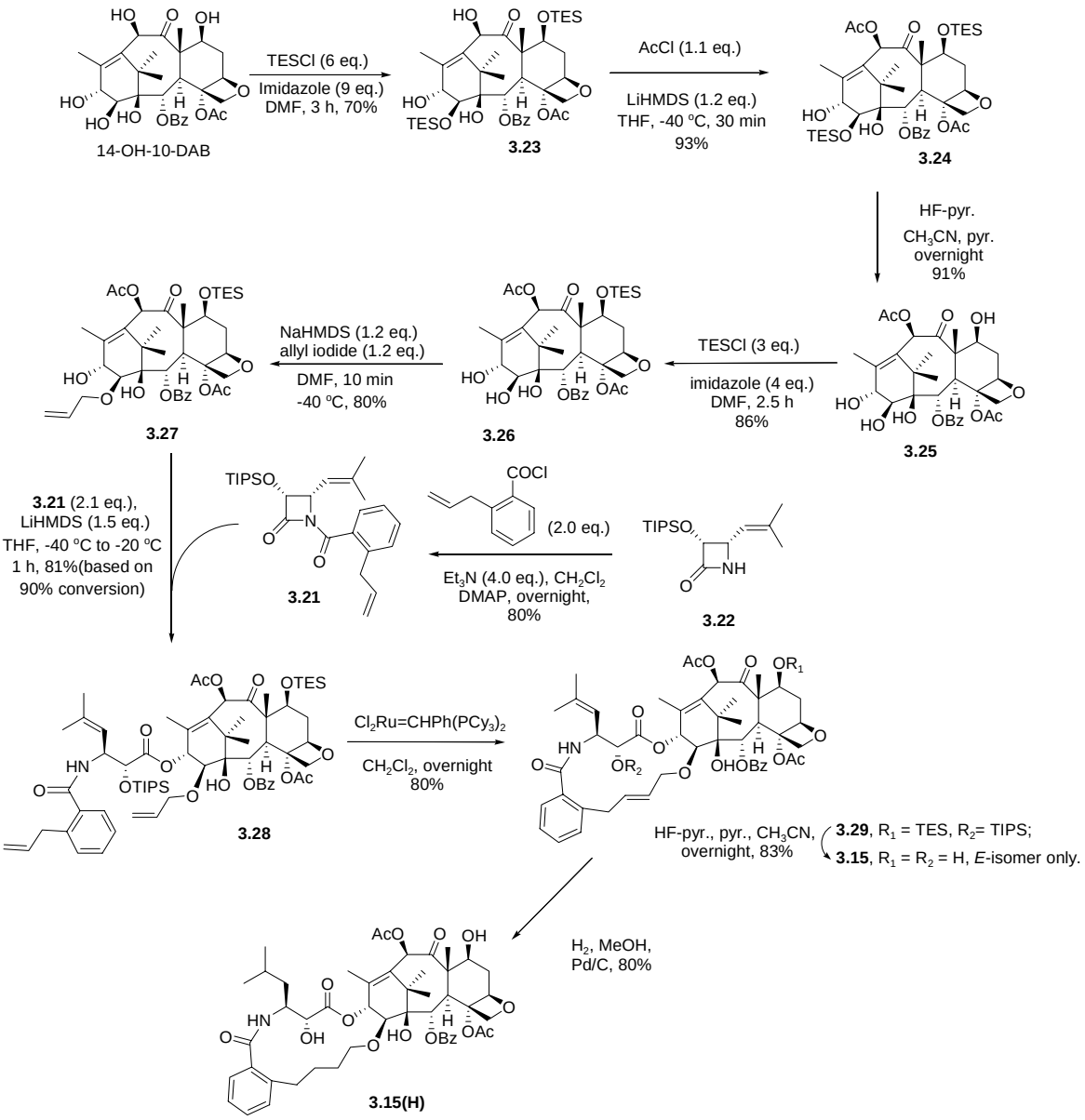

Figure 3.6. Synthesis of C14-C3'N linked taxoids 3.15 and 3.15(H).

3.2.2 Biological Activity

The synthesized macrocyclic taxoid **3.14**, **3.14(H)**, **3.15**, and **3.15(H)** were tested for their cytotoxicities and tubulin binding activities. The tubulin polymerization assays were performed in the laboratory of Prof. Susan Horwitz at the Department Molecular Pharmacology of the Albert Einstein College of Medicine. Cell growth inhibition assays were conducted by Paula Pera in the laboratory of Dr. Ralph Bernacki at Roswell Park Cancer Institute. The assay results are summarized in Table 1.

Table 3.1. *In vitro* cytotoxicities (IC_{50}, nM[a]) and tubulin-polymerization assays of C4-C2' and C14-C3'N linked macrocyclic taxoids **3.14** and **3.15**.

Taxoid	LCC6-WT[b]	LCC6-MDR[c]	MCF7-S[d]	MCF7-R[e]	Tubulin pol.
Paclitaxel	4.0±0.15	379±7.0	2.2±0.18	1185±40	100%
3.14	91±2.8	230±23	35±1.9	365±32	9%
3.14(H)	283±30	629±46	105±7.3	904±19	NT
3.15	213±17	2130±97	463±33	>3000	60%
3.15(H)	461±35	1933±163	764±45	2818±138	NT

[a]The concentration of compound which inhibits 50% of the growth of human tumor cell line after 72 h drug exposure; [b]LCC6-WT: human breast carcinoma; [c]LCC6-MDR: MDR1 transduced line; [d]MCF7-S: human breast carcinoma; [e]MCF7-R: MDR phenotype human breast carcinoma; NT: not tested.

The C4-C2' linked taxoid **3.14** exhibits strong potency against LCC6-WT and MCF-7 human breast cancer cell lines with IC_{50} values of 0.091 and 0.035 μM, respectively. These cytotoxicities are 16-20 times less potent than paclitaxel against the same cell lines. However, taxoid **3.14** is 1.5-3 times more potent than paclitaxel against drug-resistant cancer cell lines (LCC6-MDR and MCF7-R), suggesting that the introduction of a macrocycle linking the C4 and the C2' positions might disrupt the binding of P-glycoprotein to this taxoid and thus offset the effect of this 'efflux pump', believed to be responsible for multi-drug resistance.[186-188] The hydrogenated taxoid, **3.14(H)**, was approximately 3 times less potent than **3.14**, although it still exhibited more potent cytotoxicity than paclitaxel against MCF7-R breast cancer cells.

Macrocyclic taxoid **3.15**, which bears a tether connecting the C14 and the C3'N positions, exhibited cytotoxicities 2-10 times weaker than that of **3.14** and its potency was significantly lower than that of paclitaxel in all tested cancer cell lines (5-250 times less active). The hydrogenation of **3.15** resulted in analog **3.15(H)** with further loss of

activity (2 times less active) against drug-sensitive cell lines (LCC6-WT and MCF7-S) but seemed to slightly increase the potency against drug-resistant cell lines (LCC6-MDR and MCF7-R).

Intriguingly, taxoid **3.14**, which is 3 to 10 times more cytotoxic than taxoid **3.15**, exhibits only 9% of the binding ability of paclitaxel while **3.15** possesses 60%. The fact that the more cytotoxic taxoid exhibited less tubulin polymerization ability suggested a poor ability for compound 2 to cross the cancer cell membrane, resulting in insufficient concentrations of the agent in the cytoplasm. Alternatively, compounds **3.14** and **3.14(H)** might be taking advantage of the other mechanisms that taxoids operate by to kill cancer cells.

As paclitaxel has been shown to induce apoptosis in HeLa[189] and prostate cancer cells,[36] our collaborator, Dr. Muriel Cuendet at the Department of Medicinal Chemistry and Pharmacognosy of the University of Illinois at Chicago, investigated the apoptosis-inducing abilities of novel taxoids **3.14** and **3.15** in KB cells. 4'-6-Diamidino-2-phenylindole (DAPI, a fluorescent DNA dye) staining of KB cells treated with taxoids **3.14** and **3.15** evidenced the formation of apoptotic bodies with IC_{50} values of 289 nM (**3.14**) and 795 nM (**3.15**), compared to 12.3 nM for paclitaxel in the same assay. In order to further elucidate the mechanism underlying the pro-apoptotic effects of the taxoids, their effect on the activities of various caspases was studied. Apoptosis induced by **3.14** and **3.15** was only marginally reduced by the addition of Z-VAD-fmk (Z-Val-Ala-Asp(OMe)-CH_2F), a caspase-1,-3,-4,-7 inhibitor. This suggests that **3.14** and **3.15** induce apoptosis via a caspase-independent mechanism, identically to paclitaxel, and in contrast to most DNA-damaging agents.[190,191]

3.2.3 Summary

Although the project goal to match or exceed the *in vitro* biological effects of paclitaxel was not achieved by the compounds in this series, the tubulin polymerization assay still ranked **3.15** as the best macrocyclic taxoid ever tested in our lab, with an activity 60% that of paclitaxel. The *in vitro* tubulin polymerization assay provides the clearer test of our restrained analog design process, as it is not affected by cellular permeation or active transport issues. On the other hand, compound **3.14** fared honorably in the cellular growth inhibition assay with a 91 nM IC_{50} against the LCC6-WT cell line ranking it among our top macrocyclic compounds.

Apoptosis probing assays confirmed that these macrocyclic taxanes, like paclitaxel, induce a caspase-independent pathway to programmed cell death (PCD), especially **3.14** which is otherwise a weak tubulin polymerization inducer. This shows that strong tubulin polymerization ability is not a requirement for induction of PCD and underlines the fact that cellular permeability is of utmost importance when designing taxoid anticancer drugs, as **3.15** could not translate its significant *in vitro* polymerization ability into an effective cell growth inhibition activity.

3.3 SB-T-2053

After the relative setback of our first series of restrained taxoids, the idea came to us to revert to conformationally restrained analogs of first generation taxanes, as Kingston *et al.* were experiencing some success with C4 acetyl to C3' phenyl restrained compounds in that series.[181,192] Also, direct comparison to the REDOR-Taxol conformation and the paclitaxel biochemical data would be facilitated and could provide an accurate measure of the perturbation introduced by the conformational restraint.

Synthesis of these 1st generation-based restrained analogs once again made use of the RCM reaction[178] and was performed by Liang Sun in the Ojima laboratory. The isobutenyl moieties of β-lactams **3.14** and **3.15** were replaced by phenyl groups, and conformationally restrained paclitaxel analogs **3.30** and **3.31** could be obtained by following protocols very similar to those of our earlier approach (Figures 3.7 and 3.8).

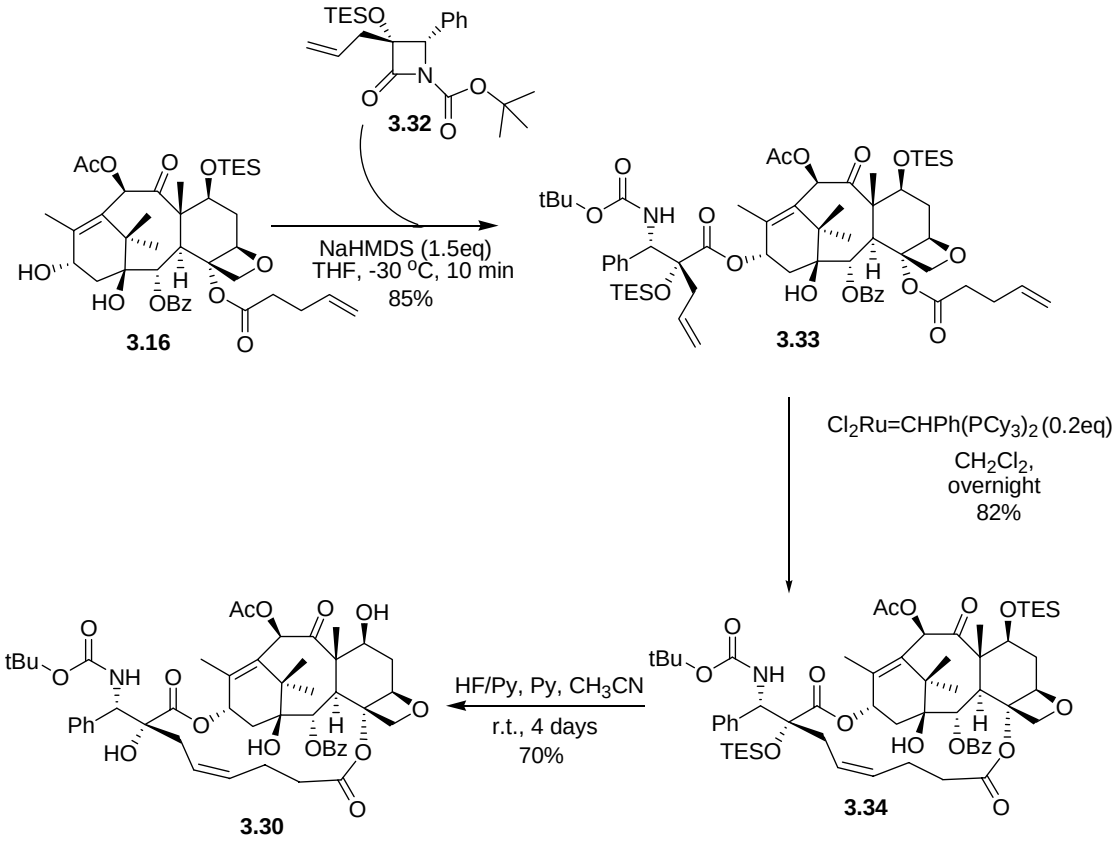

Figure 3.7. Synthesis of C4-C2' linked taxoid 3.30.

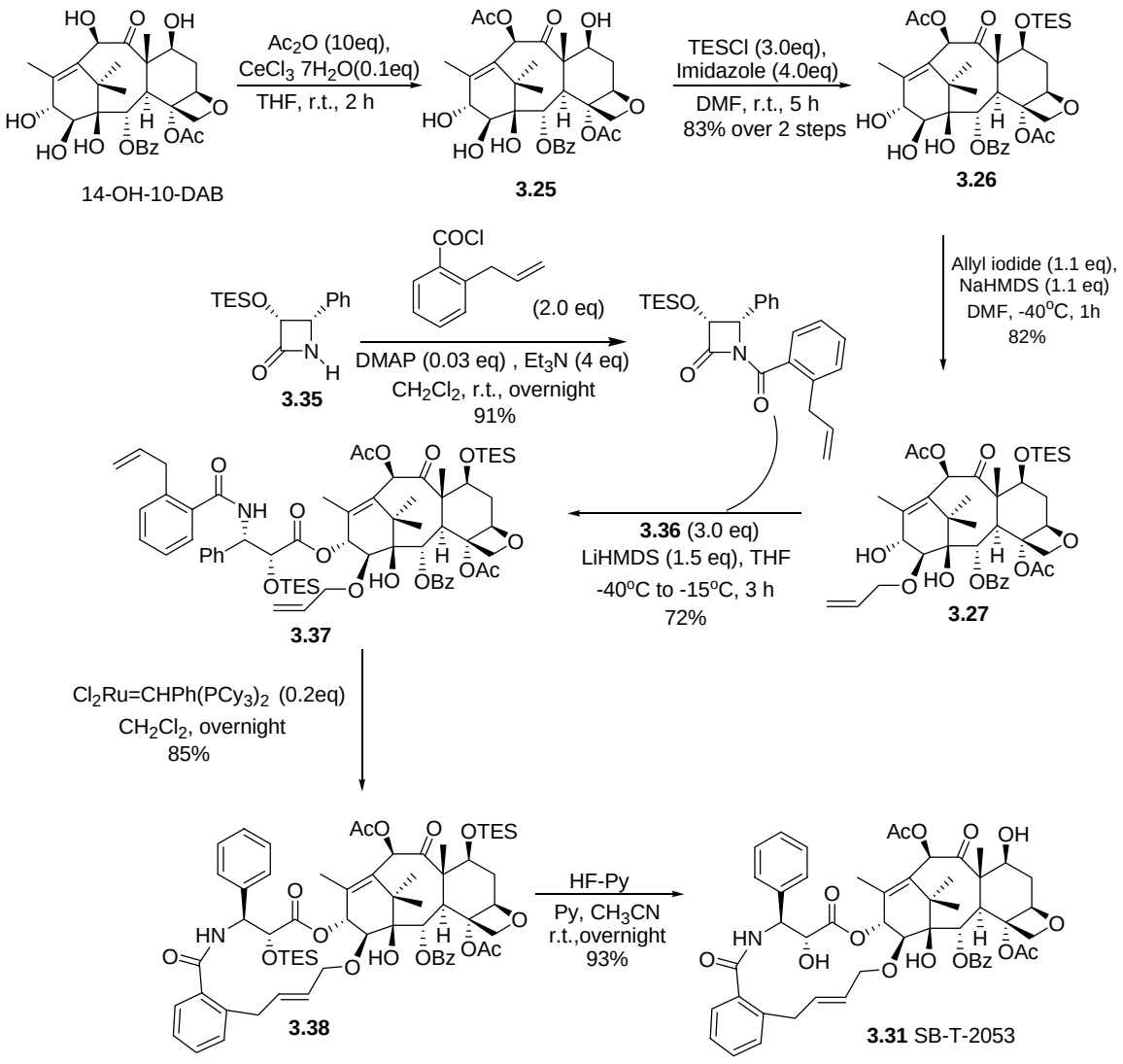

Figure 3.8. Synthesis of C14-C3'N linked taxoid SB-T-2053 (3.31).

3.3.1 Biological Activity

The activities of **3.30** and **3.31** were compared to those of paclitaxel in the *in vitro* tubulin polymerization assay and against human mammary and lung cancer cell lines. The results, compiled in Table 3.2, show that neither of the two compounds could match the cytotoxic activity of paclitaxel on the cell lines studied. In particular, **3.30** was surprisingly inactive against all strains of LCC6 and MCF7 cancer cells and was not tested for *in vitro* tubulin polymerization. Compound **3.31** (SB-T-2053), on the other hand, achieved the highest cytotoxicity levels ever encountered for a restrained macrocyclic taxoid in our group. IC_{50} values were 15 and 42 nM against the LCC6-WT and MCF7 cell lines, respectively, corresponding to only 3.3- and 14-fold reductions in activity relative to paclitaxel. These ratios were even improved in the resistant variants of these two cell lines (1.4 and 2, respectively), as SB-T-2053 appeared to be slightly less subject to MDR than paclitaxel.

Table 3.2. *In vitro* cytotoxicities (IC_{50}, nM[a]) and tubulin-polymerization assays of C4-C2' and C14-C3'N linked macrocyclic taxoids **3.30** and **3.31**.

Taxoid	LCC6-WT[b]	LCC6-MDR[c]	MCF7-S[d]	MCF7-R[e]	Tubulin pol.
Paclitaxel	4.5±0.8	323±23	3.0±0.3	518±71	100%
3.30	>10000	>10000	5636±214	>10000	NT
3.31	15±1.6	455±38	42±2.3	1066±59	100%

[a]The concentration of compound which inhibits 50% of the growth of human tumor cell line after 72 h drug exposure; [b]LCC6-WT: human breast carcinoma; [c]LCC6-MDR: MDR1 transduced line; [d]MCF7-S: human breast carcinoma; [e]MCF7-R: MDR phenotype human breast carcinoma; NT: not tested.

Above all, and directly validating our design approach, SB-T-2053 showed a level of *in vitro* tubulin polymerization activity comparable to that of paclitaxel. SB-T-2053, like paclitaxel, induces tubulin polymerization in the absence of GTP that is normally required for microtubule assembly. Furthermore, the microtubules formed in the presence of SB-T-2053 and paclitaxel were both stable against calcium-induced depolymerization (Figure 3.9). The calculated critical concentration of protein required to achieve assembly is approximately 0.08 mg tubulin/ml for both drugs.

Furthermore, a competitive binding assay indicated that both paclitaxel and SB-T-2053 effectively displace [^{3}H]paclitaxel from microtubules (Figure 3.10). This result provides strong supporting evidence that SB-T-2053 binds to the paclitaxel-binding site on the microtubule *in vitro*.

In an attempt to evidence possible differences between the dose-dependent microtubule stabilization effects of SB-T-2053 and paclitaxel that could explain the lower toxicity of the former on cancer cells, the microtubule polymerization assay was repeated

at a series of drug to tubulin concentration ratios (Figure 3.11). At all drug/tubulin ratios, the polymerization profiles were nearly indistinguishable, once again stressing the similarity in the biological profiles of SB-T-2053 and its parent drug paclitaxel, *in vitro*.

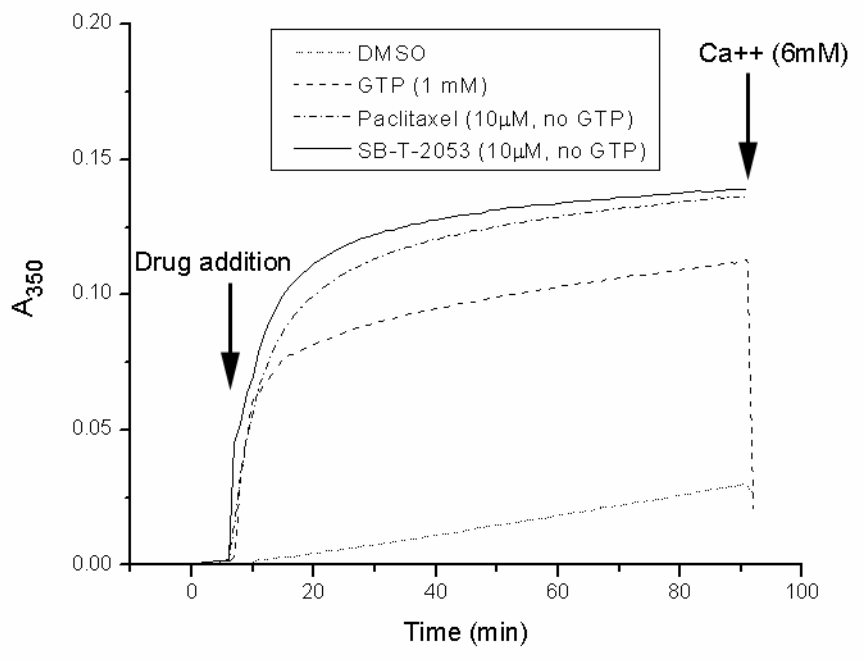

Figure 3.9. Effect of calcium on microtubules polymerized by paclitaxel and SB-T-2053 (3.31).

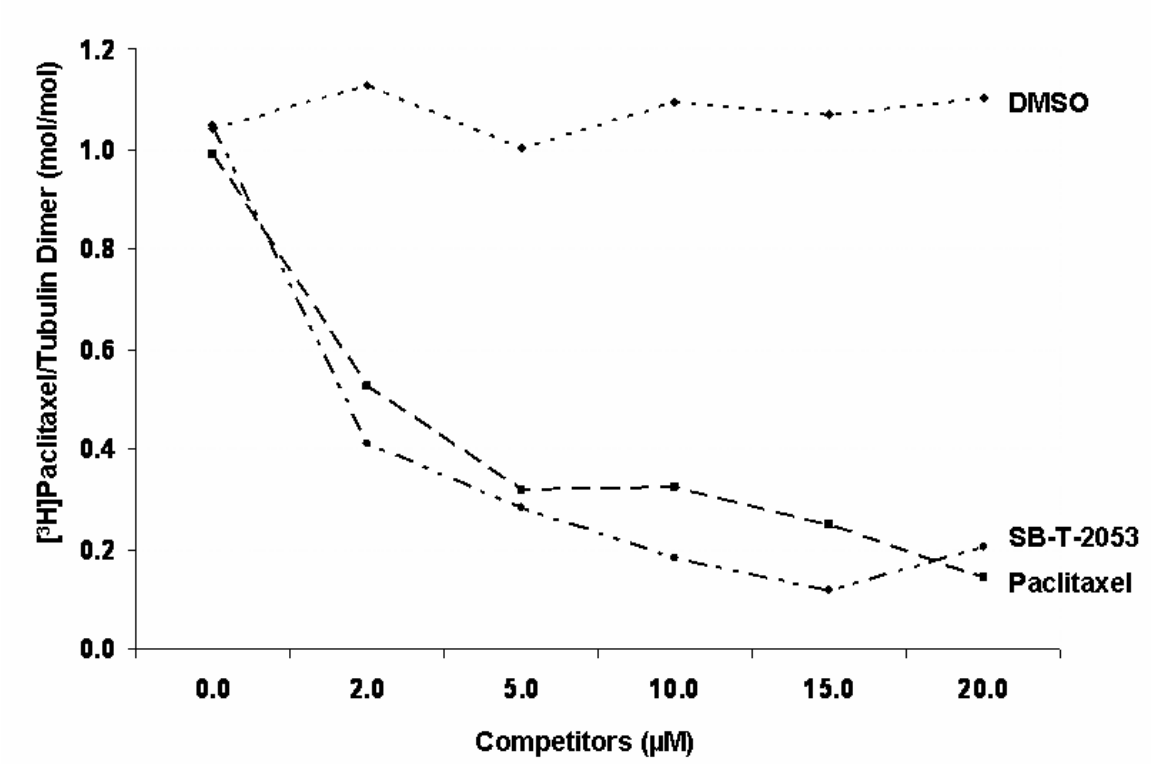

Figure 3.10. SB-T-2053 competitively inhibits [^{3}H]paclitaxel binding to microtubules as potently as paclitaxel.

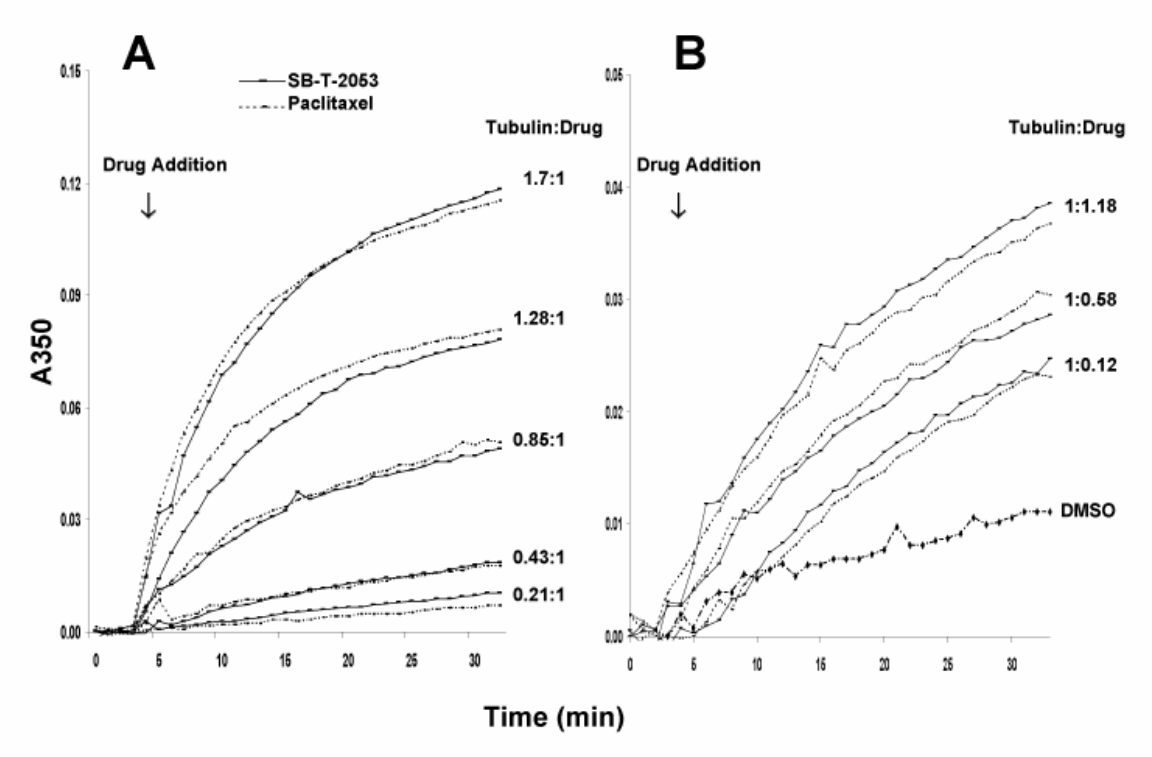

Figure 3.11. Tubulin polymerization and microtubule stabilization assay for 5 µM paclitaxel or SB-T-2053 (3.31) and various concentrations of tubulin (A), or 5 mg/mL tubulin and various concentrations of drug (B).

3.3.2 Conformational Restriction to the Binding Conformation

In order to measure the level of conformational restriction imposed by the C14-C3'N linker, we conducted a Monte Carlo conformational search on SB-T-2053 in a simulated aqueous environment (GBSA[193]) using Macromodel 6.5 (Schrödinger, Inc.). Performing the same calculation on paclitaxel provided a reference state from which the perturbation can be assessed. Our attention focused on the C13 side chain dihedral angles since they should be the ones most affected by the introduction of the constraint. Figure 3.12 shows the dihedral angle distributions for both SB-T-2053 and paclitaxel and compares those to the reference values of the REDOR-Taxol and T-Taxol conformations.

The C13-O13 torsion angle remains quite distributed in SB-T-2053, covering the same range as paclitaxel, with surprisingly low propensity for the -105° and -150° peaks seen for paclitaxel. The next torsion angle, around O13-C1', is for the ester linkage and mostly centered on 0°. However, paclitaxel in solution also adopts the reversed conformation (i.e., 180°) in lesser extent, contrary to SB-T-2053. The last two dihedral angles, around C1'-C2' and C2'-C3' are where the most flexibility is observed in paclitaxel. Indeed, except for the 90° to 150° region, the O13-C1'-C2'-O2' dihedral angle can adopt every value, with peaks at 10°, -30°, -75°, -120° and -165°. In sharp contrast, SB-T-2053, does not show any density between 0 and 90°. In the 50 kJ/mol energy range scrutinized, no SB-T-2053 structure was detected that matched REDOR-Taxol or T-Taxol. However, a peak of the probability density exists near each of the two reference conformations at -15° and -150°. In addition, the T-Taxol value should be quite unfavorable since it corresponds to a fully eclipsed conformation.

The O2'-C2'-C3'-N3' dihedral angle distribution shows the most striking effects of the conformational constraint: while paclitaxel exists in 4 major conformations, SB-T-2053 is restricted to only two, each of them reproducing the value observed in either REDOR-Taxol (176°) or T-Taxol (-67°). Therefore, we conclude that the constraint introduced is quite effective in restricting conformational diversity while enriching the solution ensemble in bioactive conformations.

Additionally, very little reorganization of protein side chains is observed after docking of SB-T-2053, as compared to REDOR-Taxol (Figure 3.13), confirming the benign nature of our perturbation on intermolecular interactions.

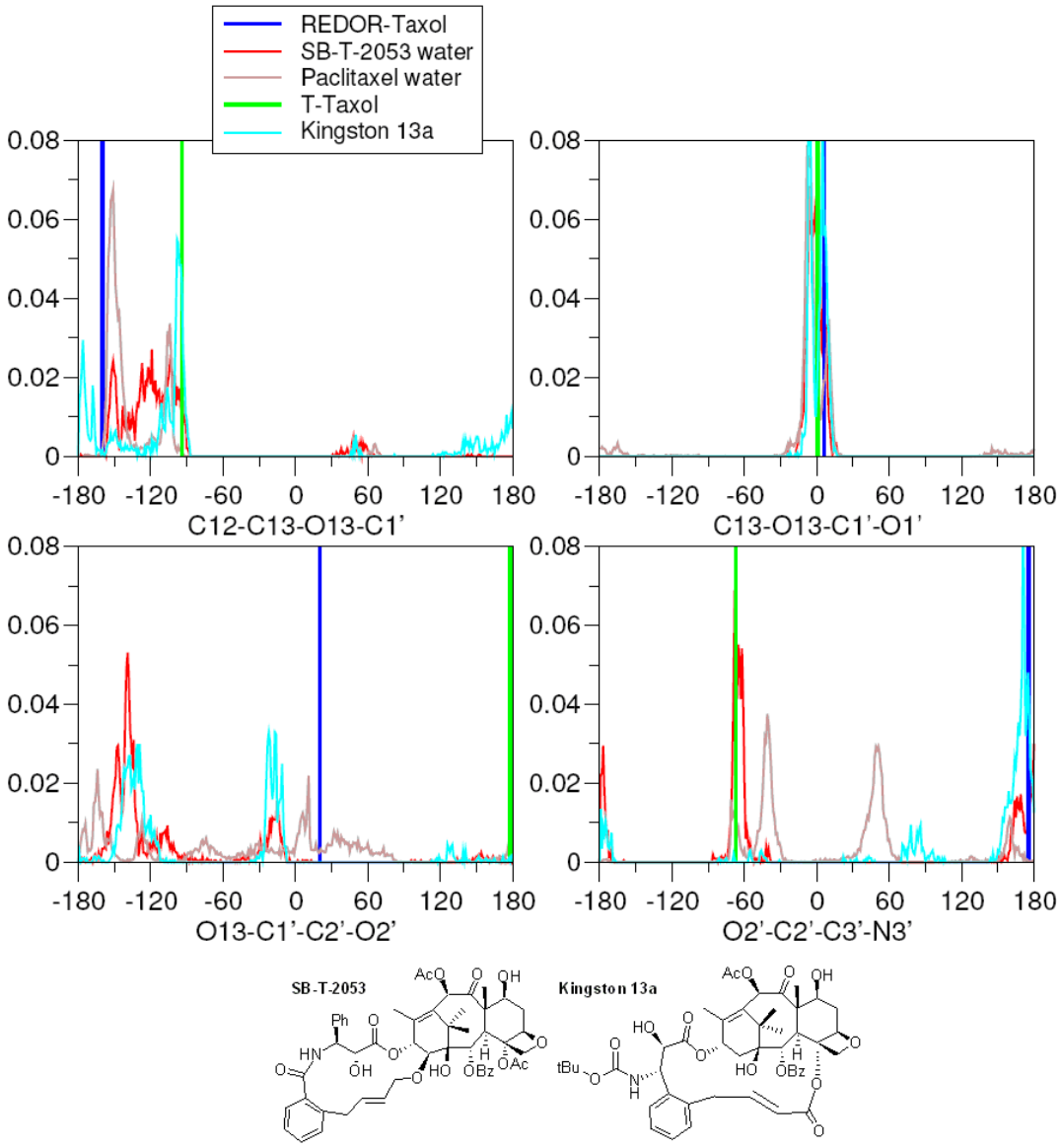

Figure 3.12. Conformational diversity in constrained taxoid SB-T-2053: comparison of the C13 side chain dihedral angle distributions for paclitaxel (brown) , SB-T-2053 (red) and Kingston et al. compound 13a of Ref. 192 (cyan) in water. The reference values for REDOR-Taxol (blue) and T-Taxol (green) are indicated by vertical lines.

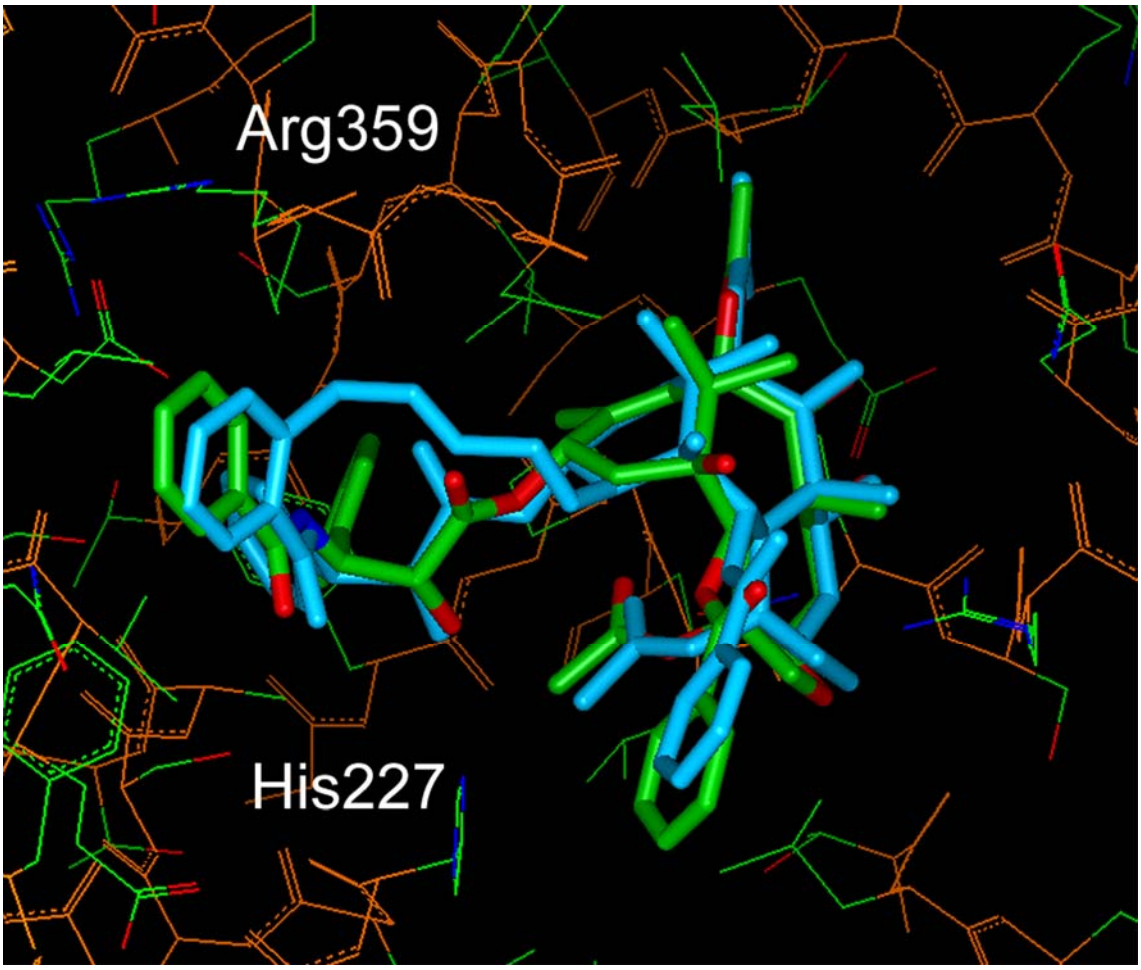

Figure 3.13. Overlay of REDOR-Taxol (green) with SB-T-2053 (blue). The overlay is performed by matching the protein backbone, which is kept fixed during docking.

3.3.3 Summary

The C4-C2' restrained paclitaxel analog **3.30** showed surprisingly weak activity against cancer cells suggesting that the C4-C2' linker might be too bulky to be accommodated in the β-tubulin paclitaxel binding site. Analogs with smaller C4-C2' linker length might be able to perform considerably better, as the groups of Kingston and Snyder have shown that a reduction in a similar C4-C3' linker could have dramatic improvements in the biological activities of macrocyclic taxoids. In particular, compound 13a in Ref. 192 (Figure 3.12), with a 2-atom linker between the C4 acetate methyl and the *ortho* position of the C3' phenyl group showed 186 times higher activity than the equivalent 5-atom linked compound.[192] The conformational restriction imposed by the 2 atom C4-C3' linker of this compound is compared to that of SB-T-2053 in Figure 3.12. Although this drug was designed to adopt the T-Taxol conformation, it appears to more closely mimic our REDOR-Taxol conformation.

On the other hand, the biological activities of the C14-C3'N restrained analog were enhanced to levels comparable with paclitaxel by substituting the C3' isobutenyl, typical of 2nd generation taxoids,[176,177] with the original phenyl group of paclitaxel and docetaxel.

Considering that SB-T-2053 is comparable to paclitaxel in the induction of microtubule polymerization, the small differences in IC_{50} values between paclitaxel and SB-T-2053 could be due to cell permeability and solubility factors. The same observation was made in the case of the isobutenyl analog **3.15** which retained 60% of the tubulin polymerization ability of paclitaxel but was only 50 times less active than paclitaxel in cancer cell growth inhibition (Table 3.1). A number of factors could specifically account for this phenomenon. Firstly, these compounds could suffer from low permeation into cells because their structures are fixed in an extended conformation, similar to the one observed in non-polar solvent NMR of paclitaxel or the in the crystalline environment, which could hinder their partitioning into the aqueous cellular interior and lead to an accumulation of the drug in the cell membrane. As the cellular interior is a complex milieu, there is also the possibility that these drugs bind to an unrelated protein or other entity, thus thwarting their binding to cellular tubulin. Alternatively, because of the C14-C3'N conformational restriction, these compounds may not be able to access the β-tubulin binding site as well in live MAP-decorated microtubules as in the purified microtubules of the *in vitro* test. Indeed, the paclitaxel binding site lies on the lumenal side of the microtubule,[89,90] which would suggest that paclitaxel has to diffuse through the microtubule wall at great speed in order to keep up with the fast growth of the tubule.[194]

3.4 Conclusions

3.4.1 Advantages of Structure-Based Design Approaches

Prior to the release of the tubulin dimer structure, scientists relied on 'ligand-based' approaches, referring to the vast SAR available for paclitaxel to identify positions that could be linked to produce more potent cytostatic agents by restriction of binding entropy loss. This resulted in more or less a hit-or-miss approach, as reflected by the few compounds that retained a level of activity similar to paclitaxel in the early macrocyclic taxoids series. By including structural data at the core of our design process, we were able to identify two good MTB-stabilizing compounds in a set of just six synthesized designs, one of which is as potent as paclitaxel in the growth inhibition of cancer cell lines. Underlining the value and sensitivity of binding site information. Out of the six synthesized analogs, five showed submicromolar activities against mammary and lung cancer cell lines, showing the remarkable improvement in the quality of synthetic candidates made possible by a precise 3D binding site modeling.

3.4.2 Drug Design Possibilities Opened

This study sanctions the viability of drug design and discovery of new generation taxoids and new microtubule-stabilizing agents based on the refined structural information of drug-protein complexes following the typical medicinal chemistry approach of generating constrained analogs of the bioactive conformation. In just two synthetic rounds, a lead compound with tubulin polymerization activity at least as potent as paclitaxel could be isolated.

Following the example of Kingston and Snyder,[195] we now suggest that varying the linker length could produce refined mimics of the REDOR-Taxol conformation and generate stronger binders of β-tubulin. The synthesis of such a series of analogs, with either one less or one more atom in the C14-C3'N linker is currently underway in the Ojima laboratory (Figure 3.14).

Another exciting recent development in the chemical biology of microtubule stabilizing agents was the production of a α,β-tubulin dimer structure with epothilone A (Figure 3.2) bound at the paclitaxel binding site.[195] With such a model at hand, we propose to overhaul the original common pharmacophore hypothesis with the 3D information from these epothilone A cryo-EM studies. Indeed, cross information from the epothilone A and paclitaxel bound tubulin dimer structures opens the way to understand drug-protein interactions at this binding site and delineate a diminutive epothilone-paclitaxel structure maintaining the key drug-tubulin interactions.

Along these lines, new hybrid designs have been proposed to answer persisting questions about the importance of the C13 side chain of paclitaxel, and how it is replaced in the epothilone familly. In these designs, we propose to attach the epothilone thiazole side chain either at the C1 or C14 positions of the baccatin scaffold, with and without a

C13 phenyl isoserine side chain (Figure 3.15). This proposition originates from the comparative observation of the overlaid epothilone A and paclitaxel structures in their respective zinc sheet tubulin dimer environment, and detection of a near-perfect overlap between the C1 of paclitaxel and the thiazole side chain bearing C15 of epothilone A. While functionalization of the baccatin C1 position might be an insurmountable task, due to the low reactivity of its shielded tertiary alcohol, the C14 position of 14β-hydroxybaccatin should provide a close surrogate and is readily amenable to chemical modification.

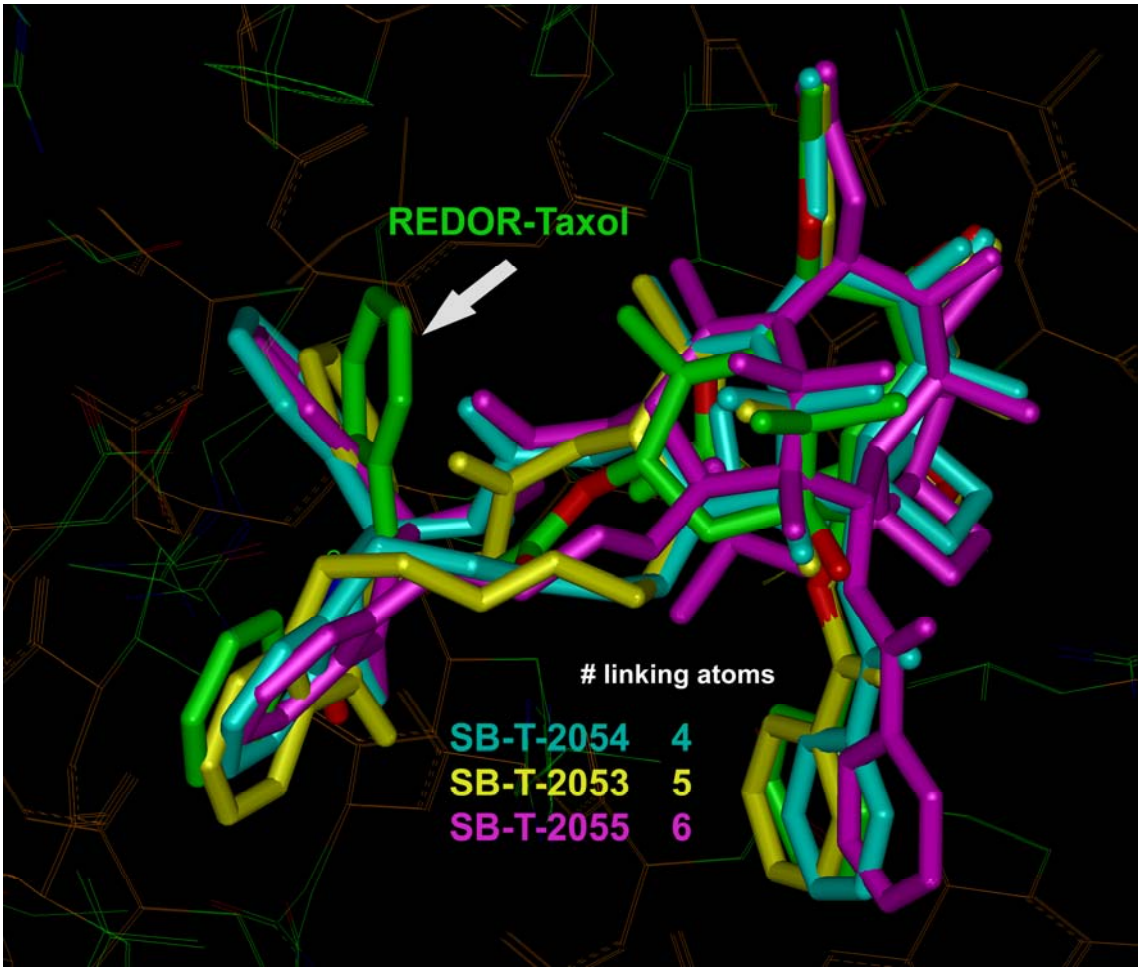

Figure 3.14. Overlaid structures of paclitaxel in the REDOR-Taxol conformation and C14-C3'N linked macrocyclic taxoids of variable linker length.

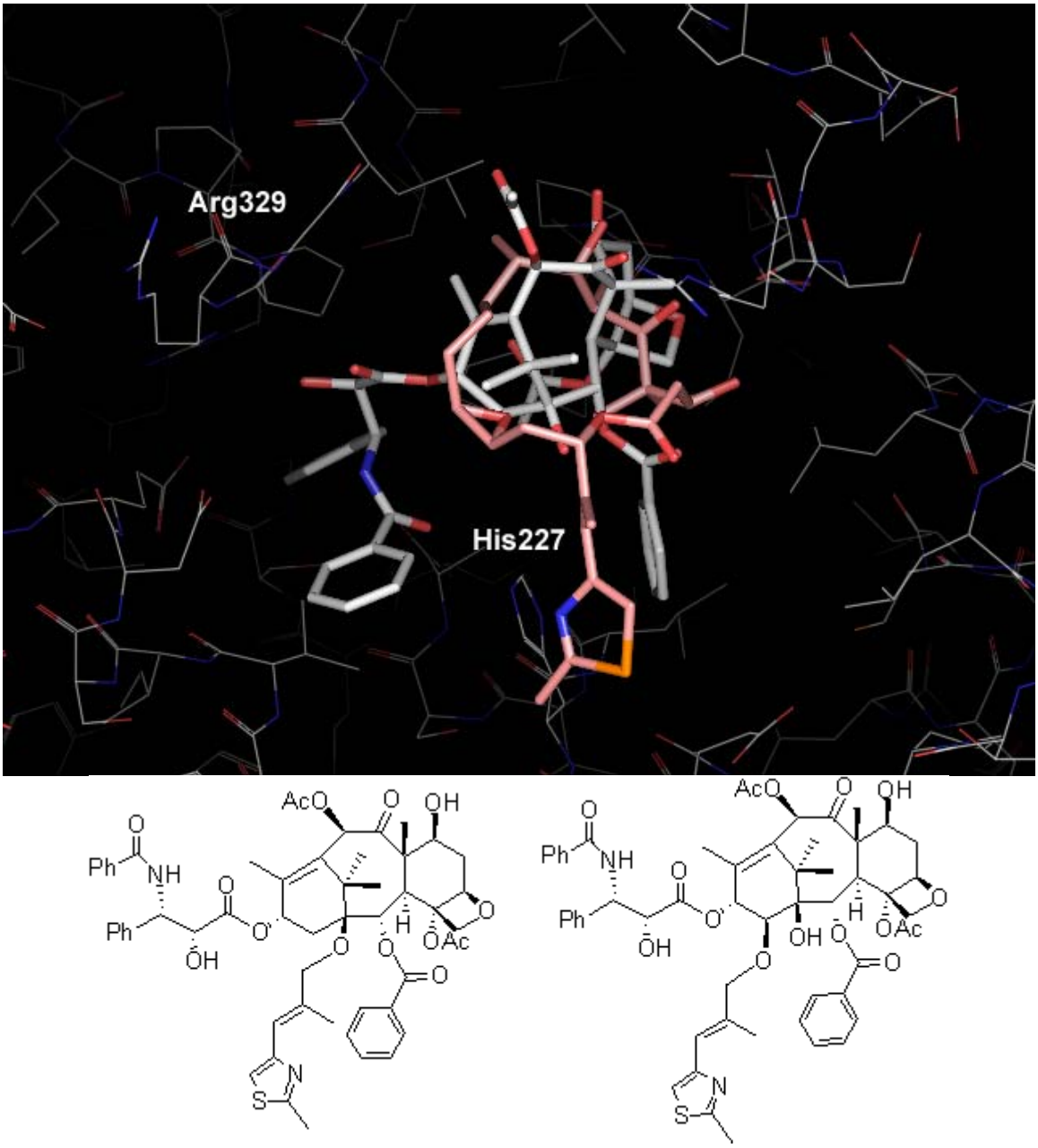

Figure 3.15. Top: Direct overlay of the paclitaxel (white sticks) and epothilone A (pink sticks) bound conformations in the β-tubulin binding site (shown as lines) from PDB entries 1JFF[155] and 1VTK.[195] Bottom: Proposed C1 (left) and C14 (right) paclitaxel-epothilone hybrid constructs.

Chapter 4

Investigation of Salt-bridge Stability in the Generalized Born Model

4.1 Introduction

One of the greatest challenges in the application of computation techniques to biological systems is the accurate determination of protein and RNA three-dimensional structures. The native structure of proteins is maintained at the edge of thermodynamic stability, the free energy of unfolding being in the range of a few kcal/mol. A dominant contributor to stability is the hydrophobic effect, but other important stabilizing factors include van der Waals interactions, hydrogen bonds, and electrostatic interactions, notably salt bridges.[196-198] However, the stability of salt bridges, i.e., the net balance of favorable Coulombic interactions between opposite charges and their costly desolvation, as well as the extent of their involvement in native state stabilization remain ambiguous.[199-204] Nevertheless , salt bridges have been linked to the thermal stability of hyperthermophilic proteins.[196,205-210]

Molecular simulations have proven to be valuable tools for probing the various interactions that define the protein native state and characterize possible folding pathways towards it.[211] Recently, continuum solvent simulations[212-217] have become popular alternatives to their more computationally demanding explicit solvent counterparts, as their lack of solvent friction increases conformational transition rates significantly,[218-226] allowing for faster sampling of the configurational space. Furthermore, because continuum solvent models implicitly average over the water and counterion distributions, this averaging does not need to be done by the simulation itself which leads to considerable simplification when calculating thermodynamic properties.[227] Lastly, some macroscopic solvent properties, such as dielectric effects, are difficult to reproduce accurately with explicit solvation.[228] The ability to build these into implicit solvent descriptions may actually give them some advantage for certain kinds of simulations.

Due to its computational efficiency, the generalized Born (GB) implicit solvent model[193,229,230] has become a popular choice to accelerate molecular dynamics (MD) simulations and to study large scale conformational transitions. However, this model lacks structural water features and has been reported to yield higher fluctuations than explicit solvent simulations.[231] To some extent, this might be a consequence of the improved conformational sampling, which lets the simulation more quickly find non-native structures that are energetically favored by the particular force field. But it also seems likely that the current generation of GB models do not have as good a balance between protein-protein and protein-solvent interactions as do the more widely tested explicit solvent models. More particularly, we[116] and others[140,142,232,233] have observed

that salt bridges were frequently too stable in the GB implicit water model, causing salt bridged conformations to be oversampled in MD simulations, thus altering the thermodynamics and kinetics of folding for small peptides. A clear illustration was given by Zhou and Berne,[140] who sampled the C-terminal β-hairpin of protein G (GB1) with both a surface-GB (SGB)[234] continuum model and explicit solvent using a replica-exchange molecular dynamics (REMD)[134] protocol. The lowest free energy state with SGB was significantly different from the lowest free energy state in explicit solvent, with incorrect salt bridges formed at the core of the peptide, in place of hydrophobic contacts. Zhou extended this study on GB1 by examining several force field–GB model combinations,[232] with all GB models showing erroneous salt-bridges. Nevertheless, as the MD simulation community envisions characterizing entire folding landscapes and pathways, implicit solvent models like GB could be beneficial in supplementing the more slowly-converging explicit models, but should be devoid of structural bias in order to maintain comparable levels of accuracy.

In this study, the Potential of Mean Force (PMF) of salt bridge formation is calculated for two residues in a solvated protein environment. Masunov and Lazaridis[235] performed similar calculations on isolated side chain pairs in coplanar monodirectional approaches and concluded that CHARMM GB[236] matches the explicit solvent contact minimum energy to within 1kcal/mol for both the $Arg^{+}\cdots Glu^{-}$ and $Lys^{+}\cdots Glu^{-}$ pairs. In our case, comparisons between the GB models implemented in the AMBER package (GB^{HCT} [237-240], GB^{OBC} [241,242]) and TIP3P explicit water salt bridge PMFs confirm the excessive strength of salt bridges in the AMBER GB models, at least, and offer a way to assess their parameterization. A simple empirical change in the assignment of GB atomic radii for hydrogen atoms of charged protein groups is investigated and shown to significantly improve the GB PMF of our test salt bridge system. This parameter change is further examined on a range of control systems by comparison to explicit solvent and experimental data.

4.2 Methods

All calculations were performed using the AMBER suite of programs[243], versions 7 and 8, with the ff99 force field[107] modified to improve agreement with ab initio relative energies of alanine tetrapeptide conformations (frcmod.mod_phipsi.1).[115,116] The Trp-cage simulations employed an optimized version of this force field, refit to also capture *ab initio* relative energies of the glycine tetrapepide.[244]

Bonds involving hydrogen atoms were constrained using the SHAKE algorithm,[122] and a 2 fs integration time step was adopted. Explicit solvent simulations were performed with the TIP3P water model,[245] widely popular for its computational simplicity and near-experimental bulk permittivity.[228,246-248] The Fab 17/9 (PDB ID:1HIL[249]) H3 loop fragment and the small helical peptides were placed in truncated octahedral boxes with respectively 5 or 6 Å minimum buffer clearance from the solute.

The Particle Mesh Ewald[250-253] (PME) treatment of long-range electrostatics was used with a direct space cutoff of 8 Å in constant pressure simulations at 1 bar. Implicit

solvent runs employed the GB^{HCT} [237,239,240] or GB^{OBC} [242] models with no cutoff and modified Bondi radii.[254] Radii reductions in GB^{HCT} were further applied to hydrogen atoms bonded to nitrogens of N2 and N3 AMBER types,[100] as in Arg, Lys and charged N-terminal groups.

In the PMF calculations, the varied reaction coordinate was the distance between the carbonyl carbon of the acidic side chain (Cγ in Asp, Cδ in Glu) and either Nζ of Lys or Cζ of Arg, the geometric center of the ionized guanido group. In all cases, the backbone atoms were positionally restrained with sufficient force to prevent significant conformational changes (1 kcal/mol.Å^2 force constant for the Fab 17/9 H3 loop, 10 kcal/mol.Å^2 for the test helical peptides). All PMFs were calculated using Umbrella Sampling (US)[255] with the reaction coordinate constrained to a narrow range by application of a harmonic biasing potential $V(r) = k_{umb}(r - r_0)^2$. US windows were centered every 0.5 Å of the coordinate range (3 to 11.5 Å) and a 1 ns MD run was performed for each. Umbrella potentials with k_{umb} = 10 kcal/Å^2 were applied in all windows, to enforce continuous sampling of high-energy regions. The biased frequency distributions were converted to free energies using the WHAM method,[256] as implemented by Roux.[257] Additional windows were placed at 3.25, 3.75, 4.25, 4.75, 5.25, 5.75 Å for TIP3P simulations, in order to improve sampling of the barrier region. Data from the first 200 ps of each US window were discarded and only the last 800 ps were analyzed.

To extensively explore the conformational space of the TC5b miniprotein (NLYIQWLKDGGPSSGRPPPS) in the GB^{HCT} solvent model, we employed replica-exchange molecular dynamics simulations (REMD[134,135]) using REMD as implemented in AMBER 8. TC5b was modeled in its zwitterionic form, with ionizable residues in their expected ionization state at pH=7, for a total of 304 atoms. The 267-715.7 K temperature range was covered using 16 replicas (267.0, 285.1, 304.5, 325.2, 347.3, 370.9, 396.1, 423.0, 451.8, 482.4, 515.2, 550.2, 587.6, 627.5, 670.2, 715.7 K), resulting in average exchange acceptance probabilities in the 22-32% range. Starting from arbitrary pre-equilibrated initial structures with 1.8 to 6.4 Å backbone RMSD to model 1 of the NMR set[258] for residues 3 to 18, exchanges were attempted and replica conformations recorded every 500 MD steps (1 ps). The Berendsen temperature coupling scheme[259] was applied with a 0.1 ps heat bath coupling constant for all replicas (1ps for non-REMD simulations). After a 9 ns thermal equilibration period, data was accumulated for 50 ns for each temperature. In GB^{HCT} with standard H^{N+} radii (1.3 Å), REMD runs were extended to 92 ns in an effort to improve the convergence of the ensembles.

Lower bound estimates of the sampling uncertainty and convergence of our simulation protocols were derived by splitting datasets in half and comparing individual half-length averages to the full-length values.

4.3 Results and Discussion

4.3.1 Unstable Behavior of the 17/9 Anti-Influenza Fab H3 Loop in GB Simulations

In the course of our research on loop structure modeling[260,261], our attention focused on the H3 CDR loop of the 17/9 anti-influenza antibody.[249] In preliminary GB^{HCT} MD simulations, its experimentally determined native structure appeared highly unstable, with backbone transitions of nearly 1 Å RMSD magnitude occurring within a few ns (Figure 4.1a). This seems unlikely to be attributable to a poorly refined experimental structure, since the 1HIL structure was solved at a reasonable 2.0 Å resolution, and the H3 loop under study is rather well defined, with maximum backbone and side-chain atomic B-factors of 22.08 and 44.82 Å^2, respectively. Nevertheless, this loop incorporates intrinsic flexibility as revealed by crystallography studies that indicate substantial loop rearrangement occurs upon binding to a nonapeptide antigen.[249]

The H3 loop and its surroundings incorporate numerous charged residues, and during simulation, the flexible Arg97 side chain (the Kabat antibody sequence numbering convention[262] is followed throughout this paper) associates with Glu100, thereby irreversibly shifting the backbone in a bent non-native conformation (Figure 4.2). This transformation happens through an intermediate where Tyr98 and Asp99, at the tip of the loop, have simultaneously undergone backbone conformational transitions (Figure 4. 2), yet maintaining the hydrogen bond observed between the Arg97 and Tyr98 side-chains in the native state. Rapidly following, the last step of this transformation is the conversion of Arg97 from a polyproline II to a left-handed α-helix conformation, simultaneous to salt bridge formation (Figure 4.2). This last step generates a ~14 kcal/mol drop in potential energy, which effectively locks the loop in the non-native conformation (Figure 4.1).

Artificially neutralizing both the Arg97 and Glu100 side chains prevented this behavior (Figure 4.1b), clearly suggesting the electrostatic nature of the phenomenon, and in particular an imbalance between GB desolvation energy and Coulombic attraction. This control run also evidenced that backbone parameters alone are not responsible for the observed conformational transition.

Additionally, a TIP3P/PME explicit solvent simulation initiated from the salt-bridged structure saw several openings of the Arg97···Glu100 ion pair (Figure 4.1c). However, this was not accompanied by rearrangement of the backbone back to the X-ray conformation during the 10 ns, a process assumed to be slow in explicit solvent. The native loop conformation was also stable throughout a 10 ns TIP3P/PME run started from the X-ray structure, with no salt bridge formation observed (Figure 4.1d).

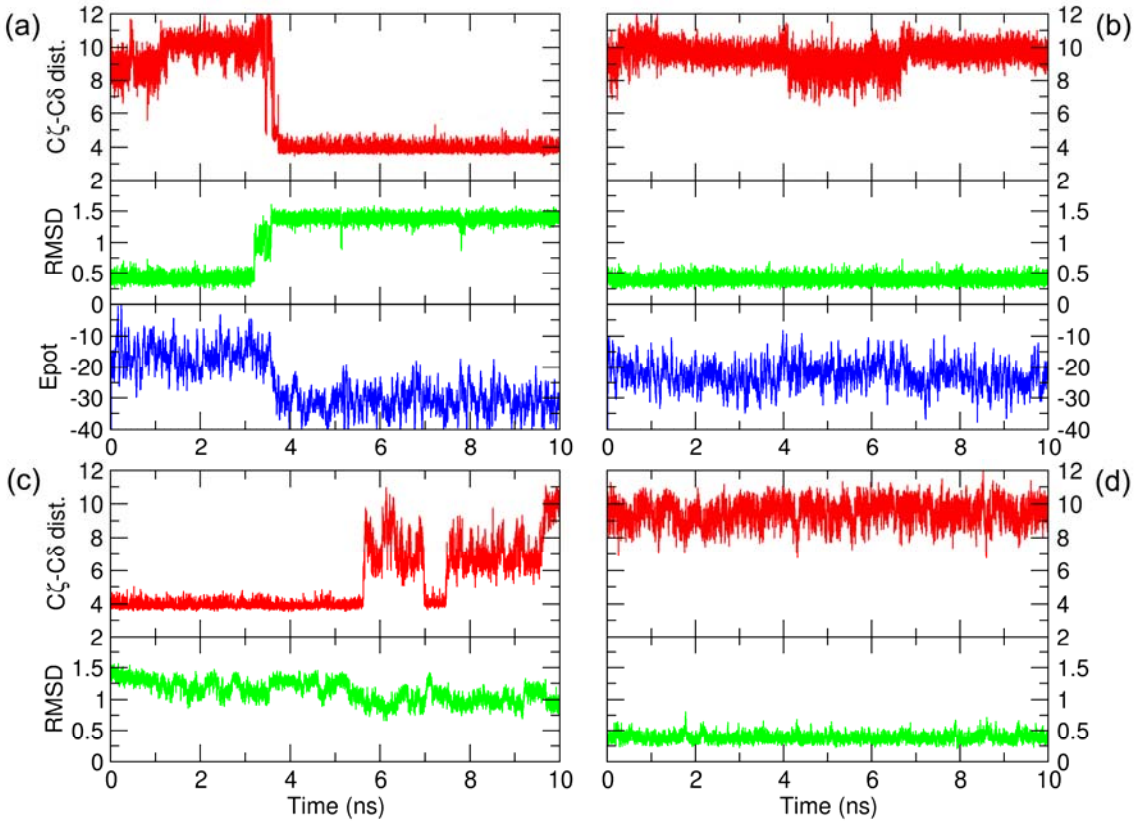

Figure 4.1. Root-mean-square deviation (RMSD, Å) of Fab 17/9 H3 loop backbone heavy atoms, and salt bridge distance (Arg97 Cζ - Glu100 Cδ, Å) as a function of simulation time, in different conditions at 300K: (a) GB^{HCT} from native, (b) GB^{HCT} with uncharged Arg97 and Glu100 side-chains from native, (c) TIP3P explicit solvent simulation from salt bridge conformation, (d) TIP3P from native. The RMSD fit to the X-ray conformation is performed over the restrained, non-loop atoms of the fragment. Relative potential energy values, window averaged over 25ps, are also reported for implicit solvent simulations in kcal/mol. The backbone transition and concomitant salt bridge formation in GB^{HCT}, not observed with neutralized side chains or explicit solvent, induce a 14 kcal/mol reduction in potential energy.

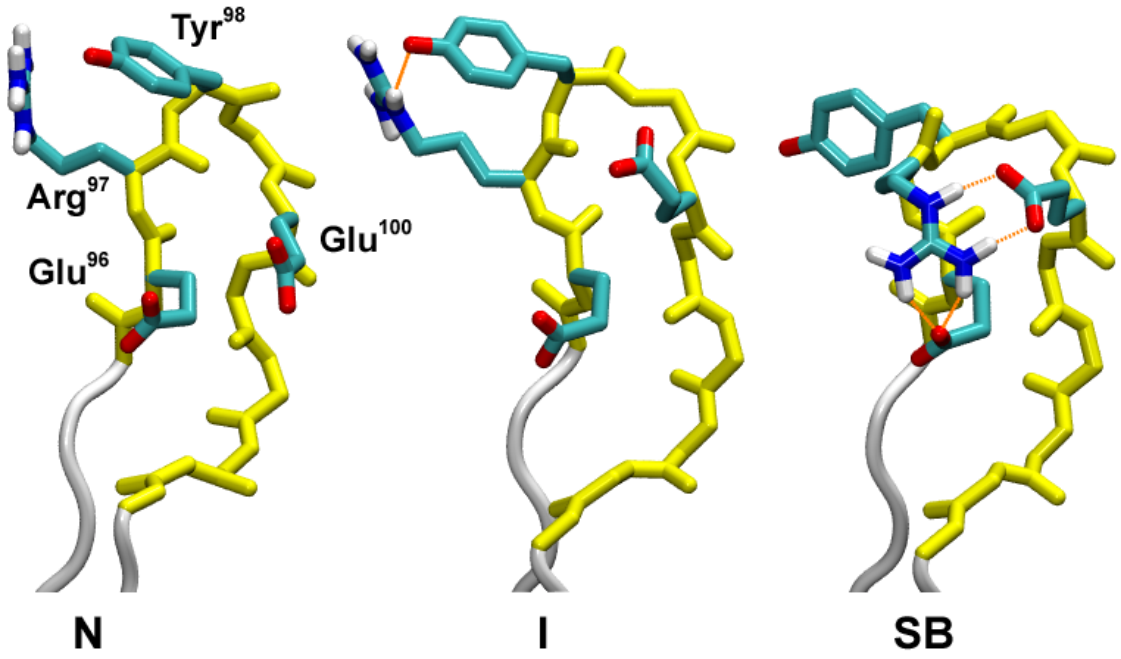

Figure 4.2. Fab 17/9 H3 loop in native conformation (N), transient intermediate state with inverted Tyr98 ψ and Asp99 ϕ dihedral angles (I), and stable salt bridged conformation with bidentate H-bond (SB), taken from a standard GB^{HCT} simulation. Loop backbone heavy atoms are colored yellow while interacting charged side chains are colored by element. H-bonds are indicated by dashed orange lines.

4.3.2 Potentials of Mean Force as Measures of GB Deviation from Explicit Solvent Behavior

Owing to the difficulty of directly comparing simulations with experimental salt bridge stability data, mostly of mutational origin, explicit water simulations with the simple TIP3P model[245] were chosen as our reference for evaluating the PMF profile of the Fab 17/9 H3 loop Arg97···Glu100 salt bridge in GB. As no computationally tractable model - especially not the rigid non-polarizable TIP3P model - is presently able to correctly reproduce all experimental properties of water,[228] we cannot claim to accurately reproduce experimental ion pair behaviour. However, the inclusion of solvent discreteness provides a significantly less crude approach than the ad hoc GB model, and is used here for consistency with previously published ion pair solvation studies.[235,263-268]

PMFs were obtained in GB^{HCT} and TIP3P explicit solvent using umbrella sampling[255] along the intersidechain distance, with the loop backbone restrained in the SB conformation (Figure 4.2). The resulting TIP3P profile (Figure 4.3) consists of a series of well-defined minima: the contact ion pair (CIP) at 3.9 Å, corresponding to the free energy minimum, is accompanied by two solvent-separated ion pair (SSIP) minima at 6.4 Å and 8.2 Å, corresponding to the insertion of one or two TIP3P molecules in the intersidechain volume.[264,269] Qualitatively, the overall shape of the PMF is in good agreement with that reported by Lazaridis for an isolated Arg^{+}···Glu^{-} pair in a coplanar monodirectional approach.[235] Quantitatively, however, our method yields a barrier height of 6 kcal/mol for going from the CIP to the first SSIP in TIP3P, while the PMF they reported for the isolated Arg^{+}···Glu^{-} ion pair in the coplanar, double H-bonded approach presents a 7.7 kcal/mol barrier to escape the contact minimum.[235] This slight difference is readily justified by the different solvent exposure levels, approach geometries (cf. Figures 4a,b of Ref. 235) and presence of a very polar environment around the Fab 17/9 ion pair, with the possibility for Arg97 to also interact with Glu96. Gruia *et al.* similarly calculated the potential of mean force of the Arg105···Glu135 salt bridge on the surface of truncated Staphylococcal nuclease, after observing in explicit water molecular dynamics simulations that breaking this salt bridge was the rate limiting step of the early unfolding transition.[270,271] Using umbrella sampling, they measured a ~7 kcal/mol transition barrier height for breaking the contact minimum of the two charged side chains.

In contrast to the TIP3P profile, the GB^{HCT} salt bridge PMF shows no depiction of the various SSIPs and grossly overestimates the TIP3P CIP-SSIP energy difference by 3.8 kcal/mol. The activation energy barrier to breaking the salt bridge is also overestimated by almost 2 kcal/mol, providing clear direct evidence for our hypothesis that salt bridges were too stable in this GB model.

The manifestly insufficient desolvation penalty experienced by the salt bridge in GB^{HCT} prompted us to reexamine the parameterization of this GB solvent model, and in particular its handling of cationic protein side chains.

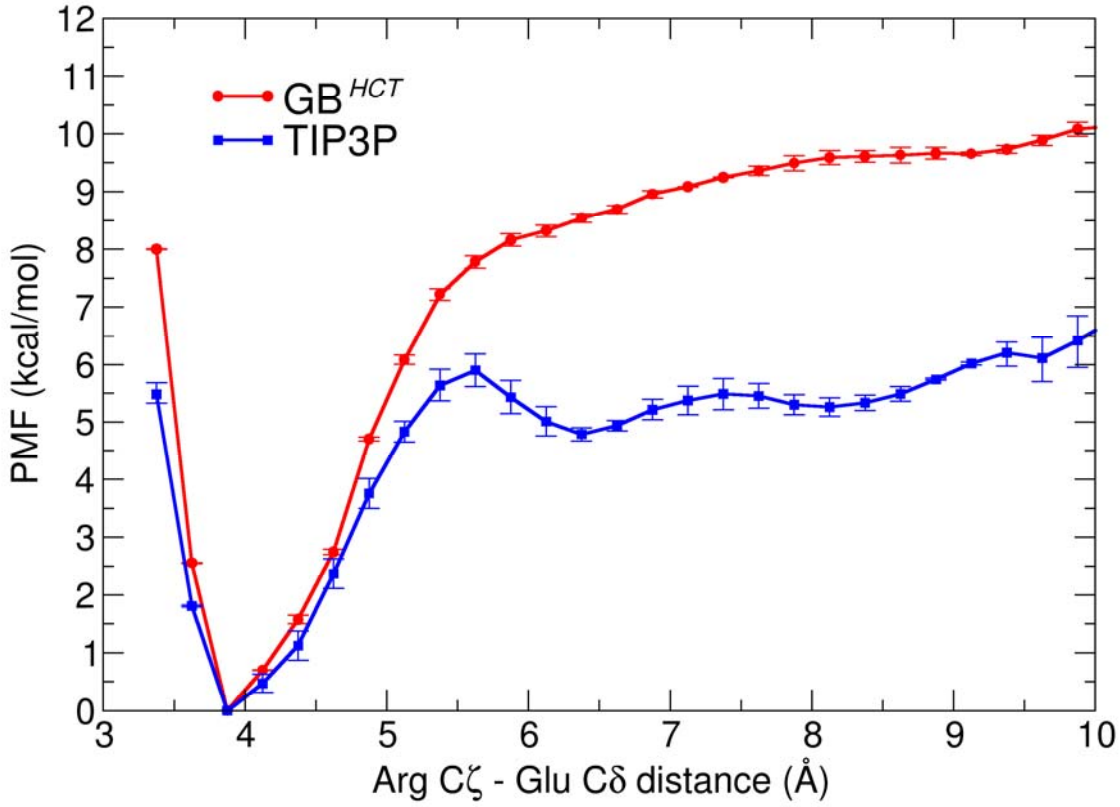

Figure 4.3. Fab 17/9 antibody Arg97···Glu100 ion pair PMF as a function of the inter-charged groups distance (Arg97 Cζ - Glu100 Cδ), at 300K. The GB^{HCT} PMF overestimates the contact ion pair stability by as much as ~4 kcal/mol. The loop backbone conformation is restrained in the SB state (Figure 4.2). Error bars on both curves estimate the sampling error and were derived by separately considering the first or the second half of the dataset.

4.3.3 GB Model Parameterization and Rationale for Reduced H^{N+} Radii.

The original Born model computes the electrostatic reversible work required to move a charged sphere from a vacuum environment into a continuous high dielectric region. The result is proportional to the square of the charge, and inversely proportional to the size of the ion.[272] These ideas were extended to the case of non-spherical solutes in the generalized Born theory[193,229], which evaluates the electrostatic component of the solvation free energy in the following way:

$$\Delta G_{elec} = -\frac{1}{2}\sum_i \sum_j \frac{q_i q_j}{f_{GB}}\left(1-\frac{1}{\varepsilon_{out}}\right) \tag{4.1}$$

f_{GB} is designed to interpolate between an effective Born radius α_i at short interatomic distance r_{ij}, and r_{ij} itself at long distances. Various functional forms are possible for f_{GB}, but AMBER employs the analytically differentiable one originally proposed by Still et al.[193]:

$$f_{GB}(r_{ij},\alpha_i,\alpha_j) = \left[r_{ij}^2 + \alpha_i \alpha_j \exp\left(-\frac{r_{ij}^2}{4\alpha_i \alpha_j} \right) \right]^{\frac{1}{2}} \tag{4.2}$$

The effective Born radius α_i corresponds to the radius that would return the electrostatic energy of the system using the original Born equation if all atoms $j \neq i$ in the solute were uncharged. Therefore, α_i reflects the degree of burial of atomic charge q_i from the solute-solvent dielectric boundary. The computation of effective radii in the particular AMBER GB model discussed here (GB^{HCT})[239,240] follows the pairwise descreening approximation (PDA) of Hawkins et al.,[237,238] wherein the molecule is described as a set of atomic spheres of radii ρ_i (Eq. 4.3). The corresponding volume integrals can be calculated analytically even when spheres i and j overlap, following Equation 13 in Hawkins et al.[237] An additional atom-dependent screening parameter S_i is required in order to avoid over-counting overlap volume between two or more neighboring spheres j, leading to Eq. 4.4.

$$\alpha_i^{-1} = \rho_i^{-1} - \frac{1}{4\pi}\sum_{j\neq i} \int_{sphere_j} \frac{1}{r^4} dV \tag{4.3}$$

$$\text{with } \rho_i = S_i(R_i + b_{offset}) \tag{4.4}$$

Although many combinations of S_i, R_i and b_{offset} could be used, the GB^{HCT} model of AMBER employs screening parameters from the TINKER molecular modeling package[273] and Bondi radii[254] slightly modified for hydrogen atoms, to reflect their bonding environment (Table 1).[239,240] The original b_{offset} value of -0.09 Å, suggested by Still et al.[193] is employed for GB simulations of proteins in AMBER.

Table 4.1. Parameter sets used in AMBER GB implementations. The superscript on H atoms indicates the heavy atom to which it is bound. The H^N R_i value was increased in AMBER7 to stabilize Watson-Crick hydrogen bonds in a 10-base pair DNA duplex.[240]

Atom	R_i (Å), GB^{HCT} AMBER6[239]	R_i (Å), GB^{HCT} AMBER7,8[240]	R_i (Å) GB^{OBC} [242]	S_i[273]
H^C	**1.3**	**1.3**	**1.2**	0.85
H^N	**1.2**	**1.3**	**1.3**	0.85
H^O	**0.8**	**0.8**	**1.2**	0.85
H^S	**0.8**	**0.8**	**1.2**	0.85
C	1.7	1.7	1.7	0.72
N	1.55	1.55	1.55	0.79
O	1.5	1.5	1.5	0.85
F	1.5	1.5	1.5	0.88
P	1.85	1.85	1.85	0.86
S	1.8	1.8	1.8	0.96

4.3.4 Reparameterization of GB^{HCT} for Improved Handling of Ionic Interactions.

In order to correct the stability of the native Fab 17/9 H3 loop conformation, we reasoned that smaller effective GB radii for atoms involved in the salt bridge would increase their desolvation penalty, thus balancing an otherwise dominating Coulombic attraction. Intuitively, formally charged nitrogens can be seen as having increased electronegativity relative to uncharged nitrogens. This should translate in hydrogen atoms bonded to them (H^{N+} atoms) being assigned smaller dielectric radii than H^{N} atoms, following the suggestion by Tsui and Case that hydrogen GB radii should decrease with increasing electronegativity of their bonding partner.[239] This reasoning is further substantiated by the lower electron density around H atoms in the ammonium ion, relative to ammonia (14% decrease, based on HF/6-31+G* calculations performed with the GAMESS program[274]). Radii reductions were applied only to hydrogens bonded to nitrogens of N2 and N3 AMBER types,[100] as found in Arg, Lys, and charged N-terminal residues. His protons were not considered, thus far, as their involvement in ionic pairs is less frequent[275,276] and generally weak.[235] Reducing only the radii of H^{N+} atoms also does not greatly affect the overall protein solvation energy (<8 % in preliminary tests), while specifically weakening the ion pair. Interestingly, similar ad hoc corrections have been recently proposed by both the Levy and Honig groups, in which additional dielectric screening is applied to oxygen and nitrogen atoms of formally charged groups either through Eq. 4.2[233] or Eq. 4.4.[277]

The GB^{HCT} salt bridge PMF profiles are very sensitive to the choice of H^{N+} radii applied, as a 0.1 Å decrease in radius can produce up to a 3 kcal/mol decrease in stability (Figure 4.4). Both 1.3 Å and 1.2 Å H^{N+} radii (the standard values in AMBER 7[240] and 6[239] GB^{HCT},) overestimate the TIP3P salt bridge stability by as much as 3.8 and 2.4 kcal/mol, respectively. A 3.8 kcal/mol free energy error by itself is on the same order of magnitude as the folding free energies at room temperature[197] and can have profound consequences on the stability of the ion pair and the structural arrangement of residues around it. In comparison, the 1.1 Å profile adequately captures the energy difference between CIP and SSIP, while the intermediate 1.15 Å H^{N+} radii profile comes close to reproducing the CIP$\rightarrow$SSIP barrier height, barely underestimating it by 0.5 kcal/mol. All GB PMFs lack the solvent-separated minima observed with explicit solvent models, resulting in an absence of barrier to salt bridge formation. This limitation of GB, typical of continuum solvent models,[235] stems from the omission of solvent molecularity and is only addressed in more computationally intensive implicit models such as the RISM formalism,[278-281] molecular surface area-based solvent models[282,283], or specifically parameterized PB models.[284,285]

Employing the recently developed GB^{OBC} model of Onufriev, Bashford and Case (model II in Ref. 242) with their suggested Bondi radii[254] modified only for H^{N} atoms

(1.3 Å instead of 1.2 Å) also produced an improved salt bridge profile relative to standard GB^{HCT}, with the PMF just slightly underestimating the CIP→SSIP barrier height by 0.5 kcal/mol and the stabilities of the SSIPs by 0.8 kcal/mol. As a simple PDA-based GB model with no depiction of solvent discreteness cannot capture both the barrier height and the CIP-SSIP energy difference, it is reasonable to prioritize the correct reproduction of the CIP-SSIP energy gap over the barrier height, since in absence of solvent discreteness, salt bridge formation is a barrierless downhill process and accurate kinetic behavior cannot be reproduced.

Dynamics were then run on the Fab 17/9 H3 loop with H^{N+} radii set to 1.1 Å (Figure 4.5a), and while the native state could be maintained for an extended period of time (>8ns), the conversion of the native X-ray structure (N) to the salt bridged conformation (SB, Figure 4.2) observed in standard GB^{HCT} still occurs. Because of computational limitations, we could not run a significantly longer or several independent simulations on this system, which would be necessary to fully characterize its kinetic behavior. Yet, a simulation initiated from the SB conformation showed repeated openings of the ion pair, but those events were too transient (<0.5 ns) to allow the loop backbone to relax back to the native conformation (Figure 4.5c). In contrast, simulations of the SB conformation conducted with the standard radii showed no reopening of the salt bridge. Also encouraging was the reduced 10 kcal/mol energy drop accompanying the N→SB transition, down from 14 kcal/mol in standard GB^{HCT} (Figure 4.1a). This energy difference matches the 4 to 5 kcal/mol free energy correction visible in the GB^{HCT} 1.1 salt bridge PMF, relative to standard GB^{HCT}, and suggests that additional factors are also responsible for the excessive stability of Fab 17/9 H3 loop non-native conformations. We then took a more systematic approach that is less dependent on a correct backbone parameterization in order to characterize the influence of H^{N+} GB radii reductions on native state stability.

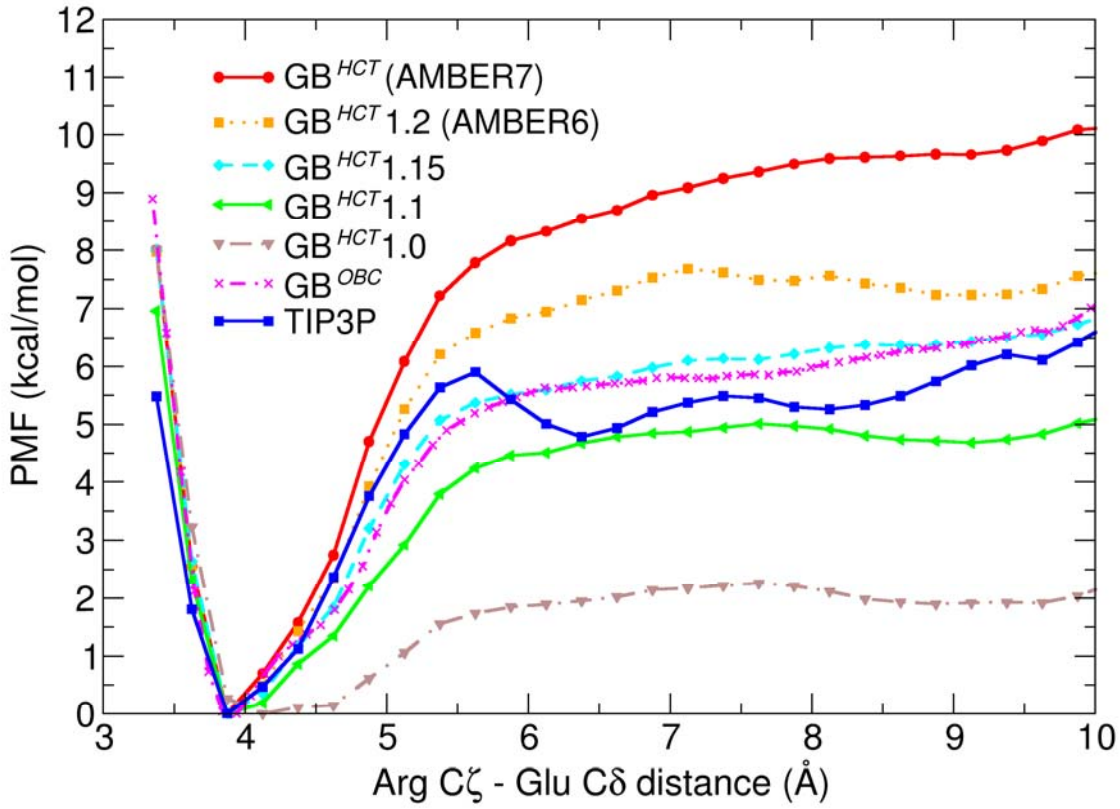

Figure 4.4. Potentials of mean force for the Fab 17/9 H3 loop Arg97···Glu100 ion pair in different solvent models, at 300K. The distance coordinate is measured between Cζ of Arg97 and Cδ of Glu100. See Table 4.1 for the full list of atomic radii used in GB^{HCT} and GB^{OBC}.

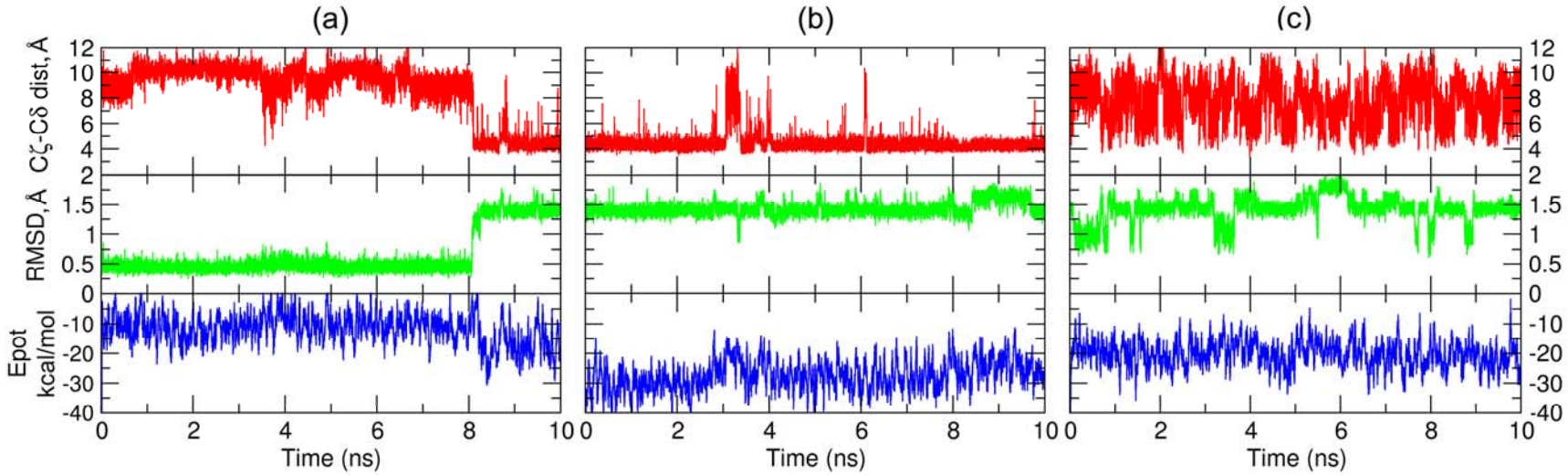

Figure 4.5. GB^{HCT} simulations of the Fab 17/9 H3 loop with 1.1 Å H^{N+} radii at 300K, initiated from the native X-ray (a), or SB conformations (b). Even with reduced H^{N+} radii, the X-ray loop conformation converts to SB with a 10 kcal/mol decrease in potential energy. The salt bridge, however, reopens transiently in the SB simulation. (c) Simulation from the SB state with neutralized Arg97 and Glu100 side chains and 1.1 Å H^{N+} radii. Uncharging the salt bridging side chains effectively breaks the salt bridge, but the backbone does not relax back to the native conformation.

4.3.5 Validation of Radii Modifications on Test Peptides

To assess the relevance of our radii reduction to other systems, including lysine side chains, we studied the PMFs of side chain ion pairs in small Ala-rich hexapeptides restrained in α-helical conformations. Oppositely charged side chains were spaced one α-helix turn apart (i,i+4) to create favorable salt-bridge orientations (Figure 4.6).[286,287] For these simple systems, a stronger positional restraint (10 kcal/mol force constant) was necessary to maintain the backbone in a fully helical conformation.

These exposed salt bridges (Figure 4.6) displayed markedly reduced stabilities, compared to the Fab 17/9 H3 loop ion pair, due to the absence of a second interacting anionic side chain and the large conformational entropy of the opened state.[288] In particular, the (i+4) Glu,Arg ion pair, directly comparable to the Fab 17/9 H3 loop ion pair, shows only a 1.2 kcal/mol barrier in TIP3P explicit solvent. This is accompanied by a ~4 kcal/mol decrease in the CIP-SSIP relative stability from the corresponding pair in Fab 17/9. The same qualitative trend is followed by the GB PMFs, with standard GB^{HCT} still overestimating the stability of the CIP by 2 to 2.5 kcal/mol, while GB^{HCT} 1.1 falls in close agreement with the TIP3P profile. This improvement suggests that the H^{N+} radii reduction empirically parameterized on the Fab 17/9 salt bridge can be advantageously transferred to other $Arg^{+}\cdots Glu^{-}$ ion pair geometries.

As observed by Masunov and Lazaridis,[235] the $Lys^{+}\cdots Glu^{-}$ PMFs tend to be less pronounced, with GB PMFs following, if not accentuating this trend. The discrepancy in interaction energy between GB^{HCT} and TIP3P only fluctuates between 0.7 and 1.6 kcal/mol here, while GB^{HCT} 1.1 falls within 0.5 kcal/mol of the explicit solvent result. These PMF profiles suggest that the GB radii adjustment, while not as crucial as in the stronger $Arg^{+}\cdots Glu^{-}$ pair, still has the potential to improve the energetics of the $Lys^{+}\cdots Glu^{-}$ pair appreciably.

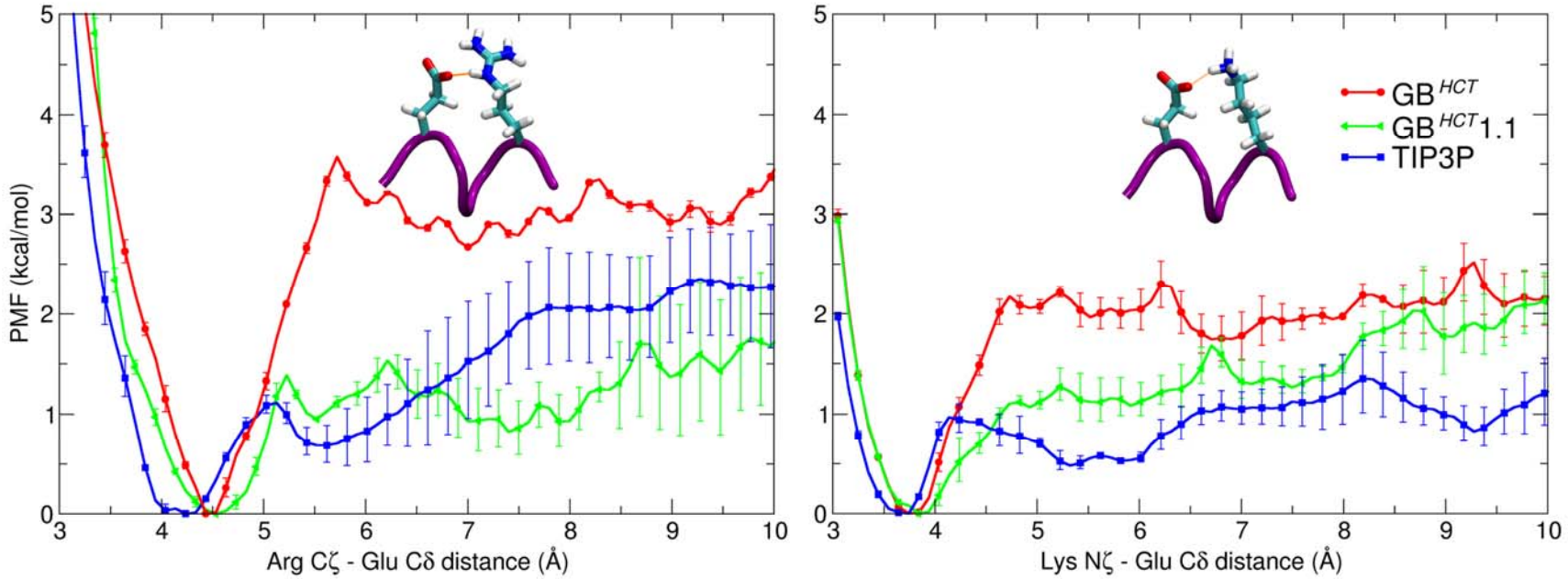

Figure 4.6. Potentials of mean force of salt bridge formation for the Ac-AEAAARA-NH_2 (left) and Ac-AEAAAKA-NH_2 (right) helical peptides in various solvent models at 300K. Error bars correspond to separately considering the first or the second half of the dataset.

4.3.6 Thermodynamical Behavior of the Trp-Cage Miniprotein.

As the Fab 17/9 H3 loop native conformation instability appeared to be a coupled salt bridge/backbone problem, we focused our validation effort on Trp-cage TC5b, a miniprotein whose fold has been successfully predicted using long molecular dynamics simulations in implicit solvent,[116] and for which experimental thermodynamic data is available.[258] Even with long MD simulations, there is no assurance that the thermodynamical behavior of protein chains has been sampled to convergence, as some conformational barriers are simply too high to cross on computationally accessible time scales at room temperature. Therefore, we turned ourselves to generalized ensemble techniques to evaluate the effect of our GB correction on the thermal stability of charged residue-bearing proteins. However, even generalized ensemble methods such as REMD[134] can require long simulation times to converge, that is why we focused our attention on the TC5b miniprotein construct, a small model (304 atoms), with protein-like features: a stable fold including tertiary structure and well-defined two state folding kinetics.[258,289] The TC5b construct features an $Arg^{+}\cdots Asp^{-}$ i/i+7 ion pair purposely introduced during the original protein design to generate a stabilizing salt bridge between these positions[258] (Figure 4.7a). A Glu5Gln mutation was further introduced to avoid forming an unfavorable Glu-X-X-X-Asp like-charge interaction in the α-helical N-terminal segment of the construct.

Although we and others have performed folding simulations of TC5b to near NMR conformations and submitted close to experimental folding rate values,[116,117,290] because of sampling and potential energy accuracy issues, it has proven more challenging to reproduce its full thermodynamic characteristics and in particular experimental melting profiles. The free energy landscape of folding for TC5b has been previously explored by all-atom REMD simulations both in explicit solvent with OPLS-AA[291] by Zhou[143] and implicit solvent using GB^{HCT} and the AMBER ff94[100] force field by Pitera and Swope.[142] Both of these studies predicted significantly higher melting temperatures than the experimental value of 315K (440K in TIP3P, ~400K in the GB study), raising legitimate doubt about the ability of these force-field/solvation model combinations, parameterized for near-room temperatures, to model temperature-dependent behavior. Additionally, in the implicit solvent study, distorted hydrogen-bonding patterns in solvent-exposed regions of the miniprotein were found to cause the largest deviations from the experimental NMR restraints.[142]

Two REMD simulations were performed on the TC5b construct: one in GB^{HCT} with the standard radii of AMBER8 (modified Bondi[240]), and another with H^{N+} radii set to 1.1 Å, as found optimal for the reproduction of the TIP3P salt bridge PMF in the 17/9 antibody H3 loop study. The simulations covered an extensive temperature range (267K - 715.7K) to ensure that high energy barriers did not prevent exhaustive conformational sampling.

Figure 4.8 shows the TC5b free energy landscapes at various temperatures projected on 2D contour maps using as reaction coordinates the RMSD of backbone heavy atoms in residues 3 to 18 (corresponding to the well-defined region of the 1L2Y PDB NMR

ensemble, with model #1 as reference) and the Asp9 Cδ - Arg16 Cζ salt bridge distance, to highlight the importance of this ion pair in determining the overall structure of the miniprotein. The lowest free energy basin in standard GB^{HCT} at 267 K (the replica temperature nearest to 0°C, where experimentally the folded fraction is maximal[258]) comprises only non-native conformations, with a global minimum at 2.8 Å 3-18 backbone RMSD (Figure 4.7c) and an almost equiprobable (ΔG~0.13 kcal/mol) other minimum at 3.7 Å (Figure 4.7d). Cluster analysis on the structures comprising this unfolded basin reveals dominant, enthalpically favored ionic networks involving nearly all formally charged moieties of the miniprotein (C-terminal carboxylate, Lys8, Asp9) clustering around Arg16 (Figure 4.7c,d). Again, these formations underline the insufficient desolvation penalty incurred by charged groups in the standard GB^{HCT} model, as the NMR ensemble shows only one such ionic interaction: the Asp9···Arg16 salt bridge. In addition, the Arg16 side chain is not well resolved by the NMR assignment,[116] suggesting ample conformational freedom, incompatible with the rigid and thermodynamically stable ionic networks observed in Figure 4.7c,d.

At 267K, while the folded region (RMSD < 2.5 Å) is 1 kcal/mol higher in free energy than the global minimum in standard GB^{HCT}, it is the lowest free energy basin in GB^{HCT} 1.1, with a free energy minimum at 1.8 Å RMSD, and 4.5 Å salt bridge distance. Structures in this basin still display most of the features of the TC5b native fold: a 2-8 helix (mainly α-helical, according to DSSP[292]) and a second helical segment between residues 11 and 14, with equal proportions of 3_{10}- and α-helical conformations. As a representative structure of the GB^{HCT} 1.1 267K free energy minimum ensemble shows (Figure 4.7b), the largest deviation from the NMR reference conformation (Figure 4.7a) occurs between the 3_{10}-helix and the C-terminal polyproline II segment at Ser14 and the flexible Gly15, inducing a slight shift in the location of the polyproline II helix. Nevertheless, the key hydrophobic cage motif remains well preserved, with Tyr3, Trp6, Pro12, Pro18, and Pro19 clustering nearly as well as in the NMR models. As in the NMR models, the Asp9···Arg16 salt bridge is present while the Lys8 side chain is fully solvent exposed and does not take part in intramolecular ionic interactions.

Interestingly, in standard GB^{HCT}, the salt bridge distance distribution is shifted towards longer distances by almost 0.5 Å in the low RMSD ensemble, reflecting the preferential formation of a monodentate H-bond in the near-NMR ensemble ion pair (Figure 4.7b), while in distorted low free energy structures, a bidentate interaction is favored by the recruitment of Lys8 in the ionic network (Figure 4.7c,d). The relative stability of these distorted low energy structures quickly decreases with temperature, since already at 304.5K, the folded ensemble is more stable by 0.08 kcal/mol. However, the most striking difference between the two GB parameter sets lies in the composition of their respective non-native ensembles, as in the GB^{HCT} 1.1 simulation, the unfolded state shows a nearly random distribution of ion pair distances with little residual salt bridge formed, while in standard GB^{HCT}, almost all structures have the ion pair formed (Figure 4.8).

Salt bridge formation PMFs were calculated at 304.5K from the GB1.3 and GB1.1 REMD populations and compared to one derived from a short (26 ns) REMD in TIP3P explicit solvent started from the NMR-derived conformation (Figure 4.9a). This simulation time is sufficient to effectively sample salt bridge distances in the folded state. More details on this explicit solvent REMD simulation will be published elsewhere. The

GB^{HCT} 1.1 salt bridge PMF for the native ensemble shows much improved agreement with its TIP3P counterpart, only overestimating the SSIP stability by ~0.7 kcal/mol, while standard GB^{HCT} overestimates it by as much as ~2.7 kcal/mol.

To follow the influence of ion pair strength on the overall stability of the TC5b miniprotein, we calculated the stability contribution of the salt bridge to the folding free energy, $\Delta\Delta G_F$, defined as the difference in free energy of folding of the protein with and without the salt bridge (Eq. 4.5).[293] This quantity corresponds to the free energy difference between forming the salt bridge in the folded and unfolded states:

$$\begin{aligned}\Delta\Delta G_F &= \Delta G_F^{sb} - \Delta G_F^{nosb} \\ &= (G_F^{sb} - G_U^{sb}) - (G_F^{nosb} - G_U^{nosb}) \\ &= (G_U^{nosb} - G_U^{sb}) - (G_F^{nosb} - G_F^{sb})\end{aligned} \tag{4.5}$$

Therefore, assuming REMD generates a converged thermodynamic ensemble at each of the replica temperatures, $\Delta\Delta G_F$ was calculated for all REMD temperatures by:

$$\Delta\Delta G_F = -RT \ln\left(\frac{p_U^{nosb} \cdot p_F^{sb}}{p_U^{sb} \cdot p_F^{nosb}}\right) \tag{4.6}$$

where p_U and p_F stand for the unfolded and folded fractions in the absence or presence of the Asp9···Arg16 salt bridge (*nosb* and *sb* superscripts, respectively). An RMSD cutoff of 2.5 Å was adopted to define the folded state as it clearly corresponds to the peak of the barrier between native and non-native basins in the 2D PMFs (Figure 4.8). We defined salt bridged states as having an Asp9 Cγ - Arg16 Cζ distance ≤ 5.5 Å. This value corresponds approximately to the peak of the CIP→SSIP transition barrier in the explicit solvent salt bridge PMF (Figure 4.9a).

Figure 4.9b simultaneously shows $\Delta\Delta G_F$ and the overall folding free energy, ΔG_F, for both the standard GB^{HCT} and GB^{HCT} 1.1 REMD simulations. At 304.5K, the salt bridge stabilization of the folded state is ~1.4 kcal/mol in GB^{HCT} and ~1.8 kcal/mol in GB^{HCT} 1.1, well within the range of experimentally observed values.[294]

At low temperatures, the Asp9···Arg16 salt bridge in standard GB^{HCT}, although intrinsically stronger (Figure 4.9a), actually stabilizes the native state less than in GB^{HCT} 1.1. This phenomenon stems from the almost equally strong stabilization of non-native conformations by the salt bridge, as observed in the two compact 267K GB^{HCT} free energy minima (Figure 4.7c,d). On the contrary, past 340K, the salt bridge contributes more strongly to folded state stability in standard GB^{HCT} than in GB^{HCT} 1.1, at least partly accounting for the increased high-T stability of TC5b in standard GB^{HCT}.

Interestingly, in both GB^{HCT} and the improved GB^{HCT} 1.1 solvent models, salt bridge stabilization decreases much more slowly than the overall protein stability with increasing temperature, and remains stabilizing at elevated temperatures, providing a rationale for the increased number of ionic pairs observed in proteins from hyperthermophilic organisms.[196,205,207-210] In addition, the GB^{HCT} model used here, with its constant water dielectric of 78.5, is expected to provide only an underestimation of salt bridge stability at high temperature, as experimentally the dielectric constant of water continuously decreases with temperature, to reach only ~55 at 100°C and 1 atm,[295] thus favoring Coulombic interactions even more at high temperatures.[296]

Finally, still using a folding criterion of 3-18 backbone RMSD ≤ 2.5 Å, it is possible to generate melting curves for TC5b in each of the GB models and compare them to

experiment (Figure 4.10). The standard GB^{HCT} yields a melting profile shifted upwards by ~30K relative to the NMR and CD experimental profiles, as reported by Pitera and Swope.[142] In addition, the prevalence of enthalpically stabilized non-native structures is responsible for the drop in folded fraction at low temperature seen in the GB^{HCT} profile and even prevents reaching the melting transition midpoint (Figure 4.10). In sharp contrast, the melting temperature measured by cubic spline interpolation of the melting profile in GB^{HCT} 1.1 (314K) is in excellent agreement with the experimental value of 315 K.[258] Furthermore, the entire simulated melting profile falls in very good overall agreement with experiment, only departing noticeably (~10% of fraction folded) from the experimental curves at extremes of the temperature range. We therefore concur with the earlier conclusions by Zhou[143] and Pitera[142] that current force fields are most accurate around room temperature, where they were parameterized. This is especially true of the GB component of the energy function, which most commonly fails to include the temperature dependence of the dielectric constant. However, current force fields are expected to predict near-room temperature melting temperatures and we show here that in GB^{HCT}, this ability was only obscured by incorrectly treated ionic interactions.

As it was not necessary to parameterize the potential function against variable temperature data to capture the most important features of the melting profile and a correct T_m value, we believe that the large overapproximations of T_m by earlier REMD studies[142,143] might originate from insufficient sampling caused by overwhelming salt bridges in GB or solvent friction in TIP3P, preventing reaching ergodicity in either case. In the Pitera and Swope study, the mostly helical TC5b native structure might also have drawn stability from the helical bias of the AMBER ff94 force field[297] that they employed. Although Pitera and Swope employed an energy function very similar to ours (AMBER ff94/GB^{HCT}), they did not report observing the distorted structures with ionic networks we encountered in GB^{HCT}. Possible reasons for this discrepancy could be the small number of replica exchanges attempted in their protocol (400) hampering the sampling of remote regions of the folding landscape by low temperature replicas, or the excessive stability of helices in ff94 preventing formation of non-native conformations.

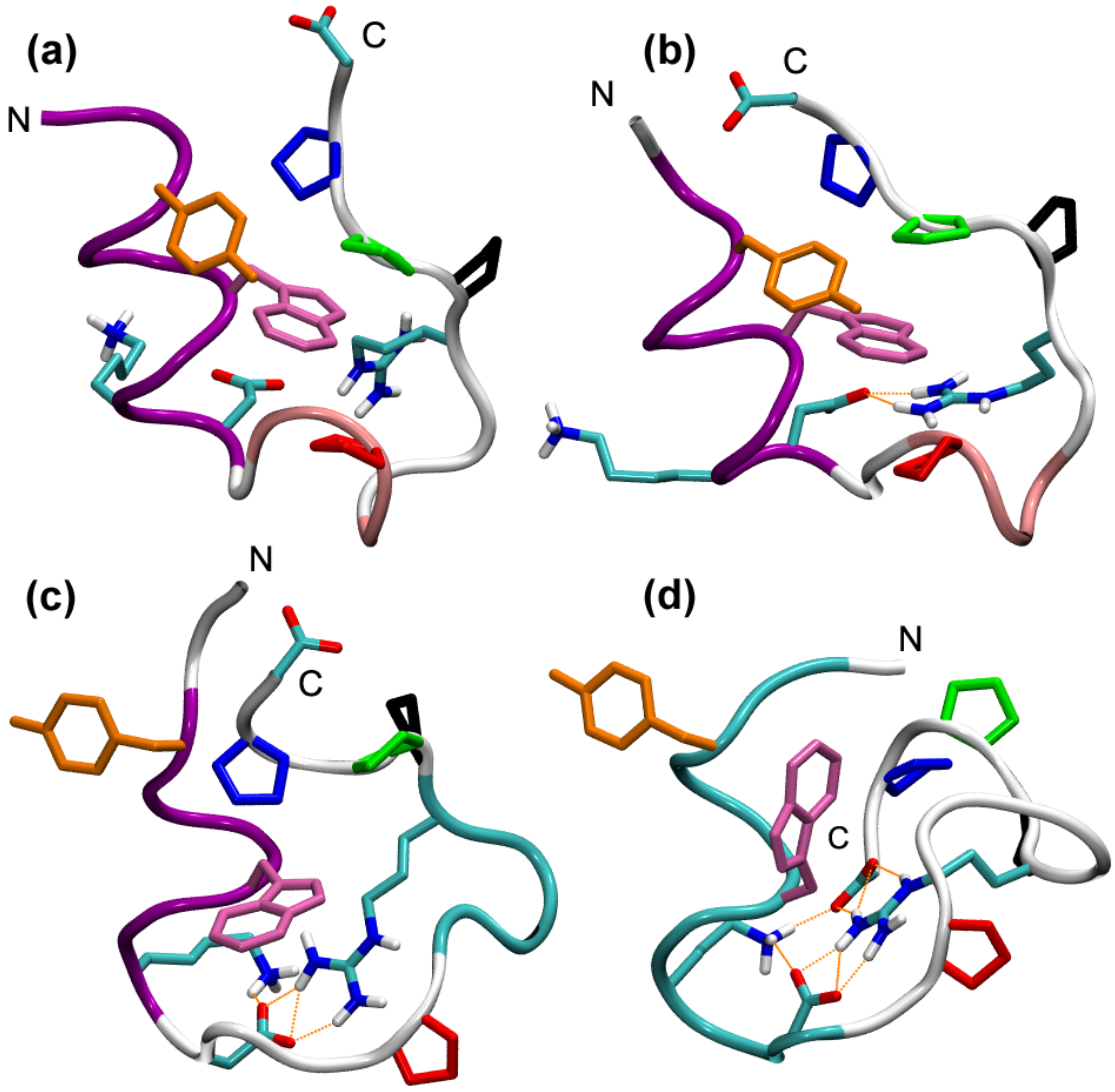

Figure 4.7. Trp-cage TC5b. (a) Reference NMR structure (model 1 of PDB entry 1L2Y). (b) 267K GB^{HCT} 1.1 REMD global free energy minimum, exhibiting most native like features (1.8 Å 3-18 RMSD). (c) 267K standard GB^{HCT} REMD global minimum and (d) second-lowest free energy minimum, both adopting distorted conformations (2.8 and 3.7 Å 3-18 RMSD, respectively) with multiple salt bridges, not seen in the NMR set. The protein backbone is shown in tube representation colored by secondary structure type (α: purple, 3_{10}: pink, turn: cyan, coil: white) while Trp-cage motif residue side chains are colored as in Ref. 258: Tyr3 (orange), Trp6 (magenta), Pro12 (red), Pro17 (black), Pro18 (green), Pro19 (blue). Salt bridge forming side chains are colored by atom. H-bonds between ionized side chains are indicated by orange dotted line.

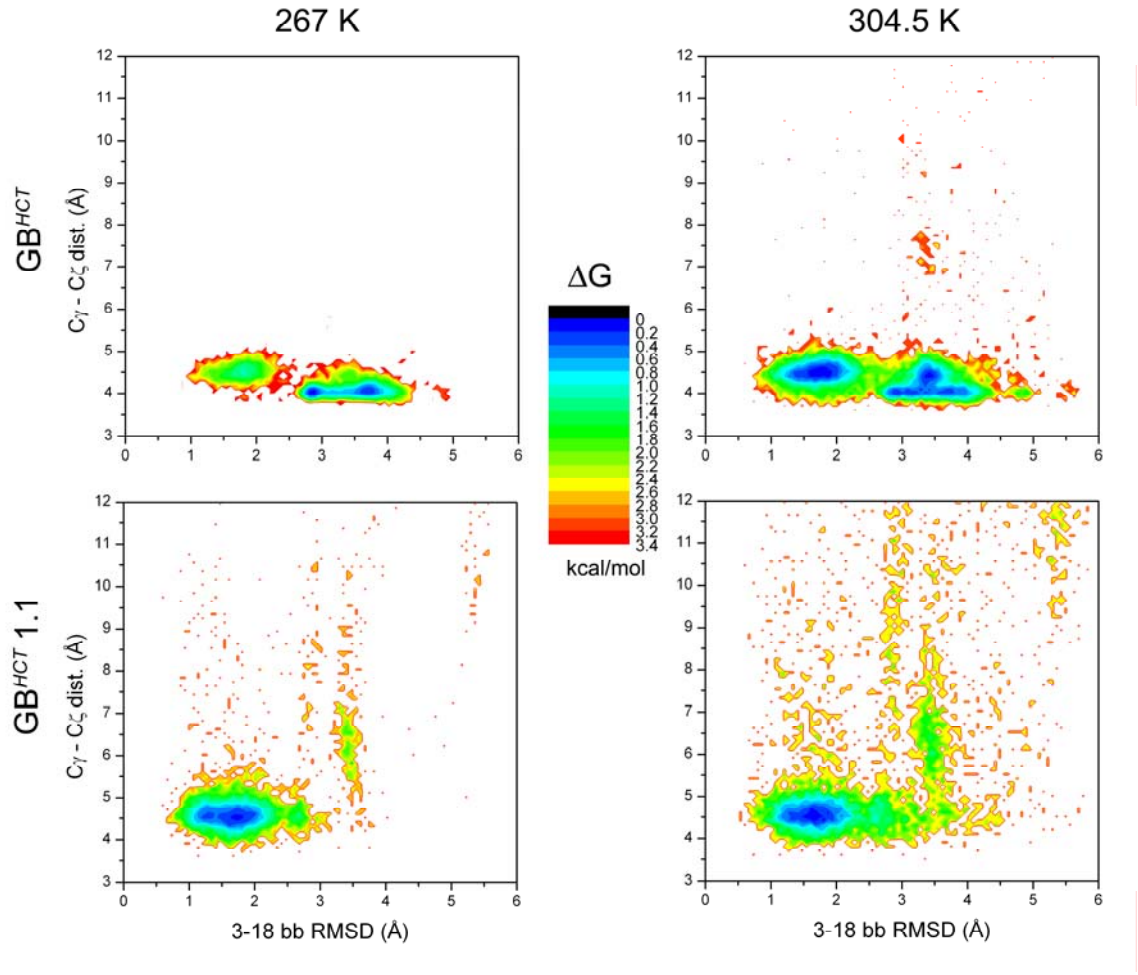

Figure 4.8. Two dimensional free energy maps in kcal/mol from REMD data. Top row: GB^{HCT} replicas at 267 K (left) and 304.5 K (right). Bottom row: GB^{HCT} 1.1 replicas at corresponding temperatures. The Asp9···Arg16 salt bridge is present in nearly all GB^{HCT} conformations, while it is observed to break more frequently in GB^{HCT} 1.1, particularly for non-native conformations. The average salt bridge distance is shorter in the non-native conformations favored by GB^{HCT}. The folded ensemble, which is not the lowest energy basin at 267K, becomes progressively more stable with rising temperature in GB^{HCT}.

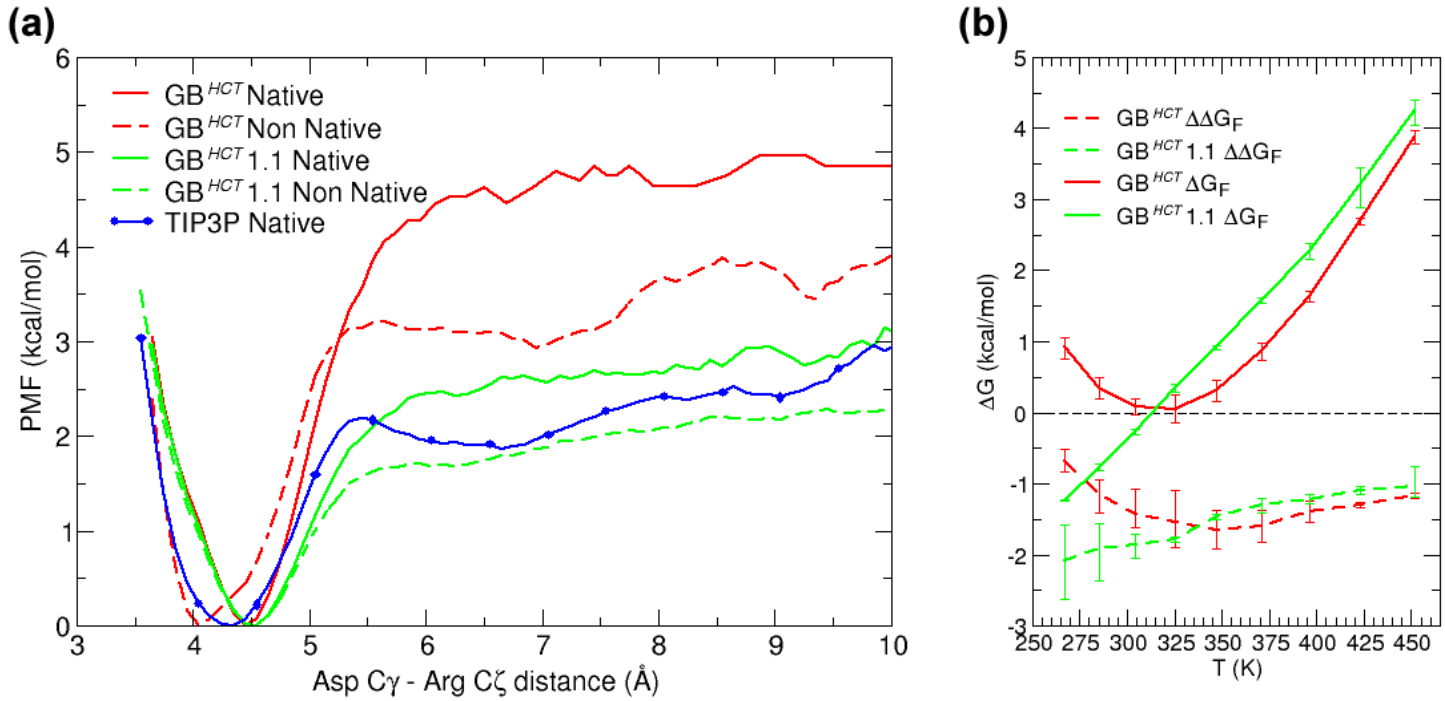

Figure 4.9. (a) Salt bridge formation PMFs along the Asp9 Cγ – Arg16 Cζ distance coordinate for native and non-native ensembles at 304.5K from REMDs in GB with different radii sets or TIP3P water at 306K. All curves were smoothed by taking 4-point moving window averages. (b) Native state stabilization by salt bridge, $\Delta\Delta G_F$, as calculated from Eq. 4.5 (dashed lines), and folding free energy, ΔG_F (solid lines), in GB^{HCT} with 1.3 Å (red) and 1.1 Å (green) H^{N+} radii. Error bars correspond to separately considering the first or second half of the dataset.

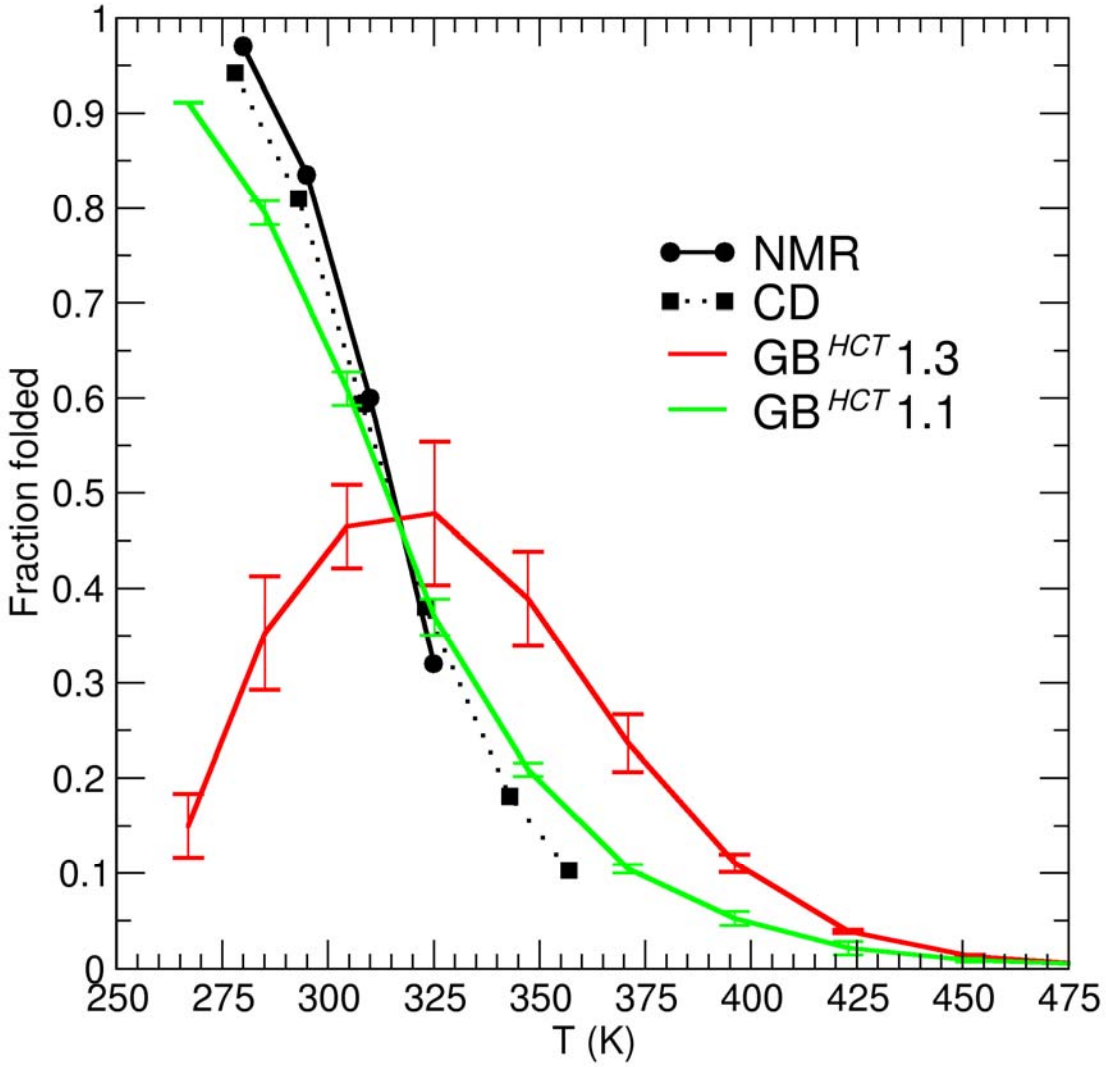

Figure 4.10. Experimental (CD, NMR CSD)[258] and simulated melting curves for the TC5b miniprotein. Error bars estimating the sampling uncertainty were determined by considering separately the first and second halves of the data set, each 45 ns in GB^{HCT}, and 25 ns in GB^{HCT} 1.1.

4.4 Conclusions

Simple GB models based on the pairwise descreening approximation are a popular choice for molecular simulations as they allow significant computational speedup over more accurate GB implementations or PB equation-based implicit solvent models.[298] It is therefore important to ensure that they can achieve an adequate level of accuracy.

Using potentials of mean force, we were able to quantify the problematic over-stabilization of ionic pairs observed in the standard GB^{HCT} implementation of the AMBER package. A simple empirical reduction of the GB radii of H^{N+} atoms from 1.3 to 1.1 Å allows a close reproduction of explicit solvent CIP-SSIP relative energies in both the Fab 17/9 H3 loop Arg97···Glu100 ion pair, and test model helical peptide systems. However, in the absence of solvent discreteness, salt bridge formation remains a kinetically downhill process and therefore GB models cannot be expected to accurately reproduce the kinetics of conformational transitions. This shortcoming has started to be addressed,[216,217] notably by explicitly including the first solvation shell around solutes in mixed explicit/implicit solvent models.[299-305]

From our preliminary results, the recent GB^{OBC} model represents a sizeable improvement in the depiction of ion pair interactions, as its PMF of the Fab 17/9 H3 loop salt bridge nearly reproduces the barrier height and CIP-SSIP relative stabilities. However, GB^{HCT} 1.1 more closely captures the TIP3P CIP-SSIP relative energy for ion pairs, at least in the peptides and small proteins that we studied. It is likely that a similar fitting of intrinsic radii could result in improved fit for GB^{OBC} as well.

By comparing experimental thermal denaturation data to REMD simulations of the Trp-cage miniprotein TC5b, we confirmed that charge-charge interactions clearly outweigh the desolvation penalty incurred by ionized side chains upon salt bridge formation in the standard GB^{HCT} model of AMBER. In sharp contrast, the same GB model with only reduced H^{N+} Born radii closely captures the thermodynamics of the Asp9···Arg16 salt bridge and for the first time allowed the generation of a near-experimental melting profile for TC5b. The GB^{HCT} 1.1 T_m value of 314 K falls in remarkable agreement with the experimental value of 315 K, while the standard GB^{HCT} profile barely approaches the melting transition midpoint and shows a majority of non-native structures at low temperature. While the GB model is expected to be capable of correctly predicting thermodynamical observables at or around room temperature, we acknowledge that our reproduction of the TC5b melting profile might be fortunate, as GB^{HCT} was not parameterized to reproduce the temperature dependence of water solvation. This study also provides further indication that strong electrostatic interactions are not predominant factors in protein native state stability, as they can stabilize non-native states by similar or even greater amounts, depending on the unfolded state topology.[204,294] Nevertheless, from our corrected GB REMD simulation of the TC5b miniprotein, it appears that native state stabilization by ionic interactions decreases at a

slower rate than the overall protein stability with increasing temperature, providing a rationale for the observed preponderance of charged amino acid residues in the proteins of thermophilic organisms.[196,205,207-210]

Bibliography

(1) Stewart, B. W.; Kleihues, P. *World Cancer Report*; WHO: Geneva, **2003**.

(2) Retting, R. A. *Cancer Crusade: The Story of the National Cancer Act of 1971*; Joseph Henry Press: Washington, **1977**.

(3) Wani, M. C.; Taylor, H. L.; Wall, M. E.; Coggon, P.; McPhail, A. T. Plant Antitumor Agents .6. Isolation and Structure of Taxol, a Novel Antileukemic and Antitumor Agent from Taxus-Brevifolia. *J. Am. Chem. Soc.* **1971**, *93*, 2325-2327.

(4) Gueritte-Voegelein, F.; Guenard, D.; Mangatal, L.; Potier, P.; Guilhem, J.; Cesario, M.; Pascard, C. Structure of a Synthetic Taxol Precursor - N-Tert-Butoxycarbonyl-10-Deacetyl-N-Debenzoyltaxol. *Acta Crystallogr. Sect. C-Cryst. Struct. Commun.* **1990**, *46*, 781-784.

(5) Crown, J.; O'Leary, M.; Ooi, W. S. Docetaxel and Paclitaxel in the Treatment of Breast Cancer: A Review of Clinical Experience. *Oncologist* **2004**, *9*, 24-32.

(6) Crown, J.; O'Leary, M. The Taxanes: An Update. *Lancet* **2000**, *355*, 1176-1178.

(7) Rowinsky, E. K. The Development and Clinical Utility of the Taxane Class of Antimicrotubule Chemotherapy Agents. *Annu. Rev. Med.* **1997**, *48*, 353-374.

(8) Schiff, P. B.; Fant, J.; Horwitz, S. B. Promotion of Microtubule Assembly In Vitro by Taxol. *Nature* **1979**, *277*, 665-667.

(9) Schiff, P. B.; Horwitz, S. B. Taxol Stabilizes Microtubules in Mouse Fibroblast Cells. *Proc. Natl. Acad. Sci. USA* **1980**, *77*, 1561-1565.

(10) Horwitz, S. B. Mechanism of Action of Taxol. *Trends Pharmacol. Sci.* **1992**, *13*, 134-136.

(11) Yvon, A. M. C.; Wadsworth, P.; Jordan, M. A. Taxol Suppresses Dynamics of Individual Microtubules in Living Human Tumor Cells. *Mol. Biol. Cell* **1999**, *10*, 947-959.

(12) Hardman, J. G.; Limbird, L. E.; Gilman, A. G. *Goodman & Gilman's the Pharmacological Basis of Therapeutics*; Tenth ed.; McGraw-Hill Professional: New York, **2001**.

(13) Anonymous. Demand for Yew Tree Concerns Environmentalists. *The New York Times*, Late City Final Edition, New York, May 3 **1987**, p 29.

(14) Chauviere, G.; Guenard, D.; Picot, F.; Senilh, V.; Potier, P. Structural-Analysis and Biochemical Study of Isolated Products of the Yew Taxus-Baccata L (Taxaceae). *Comptes Rendus De L' Academie Des Sciences Serie II* **1981**, *293*, 501-503.

(15) Gueritte-Voegelein, F.; Senilh, V.; David, B.; Guenard, D.; Potier, P. Chemical Studies of 10-Deacetyl Baccatin .3. Hemisynthesis of Taxol Derivatives. *Tetrahedron* **1986**, *42*, 4451-4460.

(16) Senilh, V.; Blechert, S.; Colin, M.; Guenard, D.; Picot, F.; Potier, P.; Varenne, P. Evidence of New Taxol Derivatives Extracted from Taxus-Baccata. *J. Nat. Prod.* **1984**, *47*, 131-137.

(17) Denis, J. N.; Greene, A. E.; Guenard, D.; Gueritte-Voegelein, F.; Mangatal, L.; Potier, P. A Highly Efficient, Practical Approach to Natural Taxol. *J. Am. Chem. Soc.* **1988**, *110*, 5917-5919.

(18) Holton, R. A. *Method for Preparation of Taxol*; European Patent Office, **1990**; EP0400971

(19) Ojima, I. *The Organic Chemistry of ß-Lactam Antibiotics*; Georg, G. I., Ed.; VCH Publishers: New York, **1992**, pp 197-255.

(20) Ojima, I. Recent Advances in the Beta-Lactam Synthon Method. *Acc. Chem. Res.* **1995**, *28*, 383-389.

(21) Ojima, I.; Park, Y. H.; Sun, C. M.; Brigaud, T.; Zhao, M. Z. New and Efficient Routes to Norstatine and Its Analogs with High Enantiomeric Purity by Beta-Lactam Synthon Method. *Tetrahedron Lett.* **1992**, *33*, 5737-5740.

(22) Ojima, I.; Sun, C. M.; Zucco, M.; Park, Y. H.; Duclos, O.; Kuduk, S. A Highly Efficient Route to Taxotere by the Beta-Lactam Synthon Method. *Tetrahedron Lett.* **1993**, *34*, 4149-4152.

(23) Ojima, I.; Zucco, M.; Duclos, O.; Kuduk, S. D.; Sun, C. M.; Park, Y. H. N-Acyl-3-Hydroxy-Beta-Lactams as Key Intermediates for Taxotere and Its Analogs. *Bioorg. Med. Chem. Lett.* **1993**, *3*, 2479-2482.

(24) Nicolaou, K. C.; Dai, W. M.; Guy, R. K. Chemistry and Biology of Taxol. *Angew. Chem.-Int. Edit. Engl.* **1994**, *33*, 15-44.

(25) Georg, G. I.; Chen, T. T.; Ojima, I.; Vyas, D. M. *Taxane Anticancer Agents: Basic Science and Current Status*; American Chemical Society: Washington D.C., **1995**; Vol. 583.

(26) Suffness, M. *Taxol: Science and Applications*; CRC Press: New York, **1995**.

(27) Christen, A. A.; M., G. D.; Bland, J. *Production of Taxol or Taxol-Like Compounds in Cell Culture*; United States Patent Office, USA, **1991**; 5,019,504

(28) Ritter, S. K. In *Chemical & Engineering News*: Washington, **2004**; Vol. 82, pp 25-30.

(29) Fuchs, D. A.; Johnson, R. K. Cytologic Evidence That Taxol, an Anti-Neoplastic Agent from Taxus-Brevifolia, Acts as a Mitotic Spindle Poison. *Cancer Treatment Reports* **1978**, *62*, 1219-1222.

(30) Hamel, E.; Delcampo, A. A.; Lowe, M. C.; Lin, C. M. Interactions of Taxol, Microtubule-Associated Proteins, and Guanine-Nucleotides in Tubulin Polymerization. *J. Biol. Chem.* **1981**, *256*, 1887-1894.

(31) Schiff, P. B.; Horwitz, S. B. Taxol Assembles Tubulin in the Absence of Exogenous Guanosine 5'-Triphosphate or Microtubule-Associated Proteins. *Biochemistry* **1981**, *20*, 3247-3252.

(32) Herman, B.; Langevin, M. A.; Albertini, D. F. The Effects of Taxol on the Organization of the Cytoskeleton in Cultured Ovarian Granulosa-Cells. *Eur. J. Cell Biol.* **1983**, *31*, 34-45.

(33) Rowinsky, E. K.; Donehower, R. C.; Jones, R. J.; Tucker, R. W. Microtubule Changes and Cyto-Toxicity in Leukemic Cell Lines Treated with Taxol. *Cancer Res.* **1988**, *48*, 4093-4100.

(34) Torres, K.; Horwitz, S. B. Mechanisms of Taxol-Induced Cell Death Are Concentration Dependent. *Cancer Res.* **1998**, *58*, 3620-3626.

(35) Haldar, S.; Jena, N.; Croce, C. M. Inactivation of Bcl-2 by Phosphorylation. *Proc. Natl. Acad. Sci. USA* **1995**, *92*, 4507-4511.

(36) Haldar, S.; Chintapalli, J.; Croce, C. M. Taxol Induces Bcl-2 Phosphorylation and Death of Prostate Cancer Cells. *Cancer Res.* **1996**, *56*, 1253-1255.

(37) Haldar, S.; Basu, A.; Croce, C. M. Bcl2 Is the Guardian of Microtubule Integrity. *Cancer Res.* **1997**, *57*, 229-233.

(38) Haldar, S.; Basu, A.; Croce, C. M. Serine-70 Is One of the Critical Sites for Drug-Induced Bcl2 Phosphorylation in Cancer Cells. *Cancer Res.* **1998**, *58*, 1609-1615.

(39) Makhija, S.; Taylor, D. D.; Gibb, R. K.; Gercel-Taylor, C. Taxol-Induced Bcl-2 Phosphorylation in Ovarian Cancer Cell Monolayer and Spheroids. *Int. J. Oncol.* **1999**, *14*, 515-521.

(40) Rodi, D. J.; Janes, R. W.; Sanganee, H. J.; Holton, R. A.; Wallace, B. A.; Makowski, L. Screening of a Library of Phage-Displayed Peptides Identifies Human Bcl-2 as a Taxol Binding Protein. *J. Mol. Biol.* **1999**, *285*, 197-203.

(41) Srivastava, R. K.; Mi, Q. S.; Hardwick, J. M.; Longo, D. L. Deletion of the Loop Region of Bcl-2 Completely Blocks Paclitaxel-Induced Apoptosis. *Proc. Natl. Acad. Sci. USA* **1999**, *96*, 3775-3780.

(42) Sato, T.; Hanada, M.; Bodrug, S.; Irie, S. J.; Iwama, N.; Boise, L. H.; Thompson, C. B.; Golemis, E.; Fong, L.; Wang, H. G.; Reed, J. C. Interactions among Members of the Bcl-2 Protein Family Analyzed with a Yeast 2-Hybrid System. *Proc. Natl. Acad. Sci. USA* **1994**, *91*, 9238-9242.

(43) Ding, A. H.; Porteu, F.; Sanchez, E.; Nathan, C. F. Shared Actions of Endotoxin and Taxol on TNF Receptors and TNF Release *Science* **1990**, *248*, 370-372.

(44) Burkhart, C. A.; Berman, J. W.; Swindell, C. S.; Horwitz, S. B. Relationship between the Structure of Taxol and Other Taxanes on Induction of Tumor-Necrosis-Factor-Alpha Gene-Expression and Cytotoxicity. *Cancer Res.* **1994**, *54*, 5779-5782.

(45) Byrd, C. A.; Bornmann, W.; Erdjument-Bromage, H.; Tempst, P.; Pavletich, N.; Rosen, N.; Nathan, C. F.; Ding, A. Heat Shock Protein 90 Mediates Macrophage Activation by Taxol and Bacterial Lipopolysaccharide. *Proc. Natl. Acad. Sci. USA* **1999**, *96*, 5645-5650.

(46) Ding, A.; Sanchez, E.; Nathan, C. F. Taxol Shares the Ability of Bacterial Lipopolysaccharide to Induce Tyrosine Phosphorylation of Microtubule-Associated Protein-Kinase. *J. Immunol.* **1993**, *151*, 5596-5602.

(47) Ball, E. H.; Singer, S. J. Mitochondria Are Associated with Microtubules and Not with Intermediate Filaments in Cultured Fibroblasts. *Proc. Natl. Acad. Sci. USA* **1982**, *79*, 123-126.

(48) Cooper, M. S.; Cornellbell, A. H.; Chernjavsky, A.; Dani, J. W.; Smith, S. J. Tubulovesicular Processes Emerge from Trans-Golgi Cisternae, Extend Along

Microtubules, and Interlink Adjacent Trans-Golgi Elements into a Reticulum. *Cell* **1990**, *61*, 135-145.

(49) Scholey, J. M.; Porter, M. E.; Grissom, P. M.; McIntosh, J. R. Identification of Kinesin in Sea-Urchin Eggs, and Evidence for Its Localization in the Mitotic Spindle. *Nature* **1985**, *318*, 483-486.

(50) Porter, M. E.; Johnson, K. A. Dynein Structure and Function. *Annu. Rev. Cell Biol.* **1989**, *5*, 119-151.

(51) Welte, M. A. Bidirectional Transport Along Microtubules. *Curr. Biol.* **2004**, *14*, R525-R537.

(52) Haimo, L. T.; Rosenbaum, J. L. Dynein Binding to Microtubules Containing Microtubule-Associated Proteins. *Cell Motil. Cytoskeleton* **1981**, *1*, 499-516.

(53) Joshi, H. C. Gamma-Tubulin - the Hub of Cellular Microtubule Assemblies. *Bioessays* **1993**, *15*, 637-643.

(54) Song, Y. H.; Mandelkow, E. The Anatomy of Flagellar Microtubules - Polarity, Seam, Junctions, and Lattice. *J. Cell Biol.* **1995**, *128*, 81-94.

(55) McIntosh, J. R.; Pfarr, C. M. Mitotic Motors. *J. Cell Biol.* **1991**, *115*, 577-585.

(56) Gorbsky, G. J. Chromosome Motion in Mitosis. *Bioessays* **1992**, *14*, 73-80.

(57) Gadde, S.; Heald, R. Mechanisms and Molecules of the Mitotic Spindle. *Curr. Biol.* **2004**, *14*, R797-R805.

(58) Hamel, E. Antimitotic Natural Products and Their Interactions with Tubulin. *Med. Res. Rev.* **1996**, *16*, 207-231.

(59) Oakley, C. E.; Oakley, B. R. Identification of Gamma-Tubulin, a New Member of the Tubulin Superfamily Encoded by mipA Gene of Aspergillus-Nidulans. *Nature* **1989**, *338*, 662-664.

(60) Schiebel, E. Gamma-Tubulin Complexes: Binding to the Centrosome, Regulation and Microtubule Nucleation. *Curr. Opin. Cell Biol.* **2000**, *12*, 113-118.

(61) Mitchison, T.; Kirschner, M. Dynamic Instability of Microtubule Growth. *Nature* **1984**, *312*, 237-242.

(62) Walker, R. A.; Inoue, S.; Salmon, E. D. Asymmetric Behavior of Severed Microtubule Ends after Ultraviolet Microbeam Irradiation of Individual Microtubules In Vitro. *J. Cell Biol.* **1989**, *108*, 931-937.

(63) Weisenberg, R. C.; Deery, W. J. Role of Nucleotide Hydrolysis in Microtubule Assembly. *Nature* **1976**, *263*, 792-793.

(64) David-Pfeuty, T.; Erickson, H. P.; Pantaloni, D. GTPase Activity of Tubulin Associated with Microtubule Assembly. *J. Cell Biol.* **1977**, *75*, A273-A273.

(65) Spiegelman, B. M.; Penningroth, S. M.; Kirschner, M. W. Turnover of Tubulin and N Site GTP in Chinese-Hamster Ovary Cells. *Cell* **1977**, *12*, 587-600.

(66) Caplow, M.; Ruhlen, R.; Shanks, J.; Walker, R. A.; Salmon, E. D. Stabilization of Microtubules by Tubulin GDP-Pi Subunits. *Biochemistry* **1989**, *28*, 8136-8141.

(67) Mandelkow, E. M.; Mandelkow, E.; Milligan, R. A. Microtubule Dynamics and Microtubule Caps - a Time-Resolved Cryoelectron Microscopy Study. *J. Cell Biol.* **1991**, *114*, 977-991.

(68) Wang, H. W.; Nogales, E. Nucleotide-Dependent Bending Flexibility of Tubulin Regulates Microtubule Assembly. *Nature* **2005**, *435*, 911-915.

(69) Parysek, L. M.; Wolosewick, J. J.; Olmsted, J. B. MAP-4 - a Microtubule-Associated Protein Specific for a Subset of Tissue Microtubules. *J. Cell Biol.* **1984**, *99*, 2287-2296.

(70) Panda, D.; Goode, B. L.; Feinstein, S. C.; Wilson, L. Kinetic Stabilization of Microtubule Dynamics at Steady-State by Tau and Microtubule-Binding Domains of Tau. *Biochemistry* **1995**, *34*, 11117-11127.

(71) Belmont, L. D.; Mitchison, T. J. Identification of a Protein That Interacts with Tubulin Dimers and Increases the Catastrophe Rate of Microtubules. *Cell* **1996**, *84*, 623-631.

(72) Walczak, C. E.; Mitchison, T. J.; Desai, A. XKCM1: A Xenopus Kinesin-Related Protein That Regulates Microtubule Dynamics During Mitotic Spindle Assembly. *Cell* **1996**, *84*, 37-47.

(73) Venier, P.; Maggs, A. C.; Carlier, M. F.; Pantaloni, D. Analysis of Microtubule Rigidity Using Hydrodynamic Flow and Thermal Fluctuations. *J. Biol. Chem.* **1994**, *269*, 13353-13360.

(74) Amos, L. A. Microtubule Structure and Its Stabilisation. *Org. Biomol. Chem.* **2004**, *2*, 2153-2160.

(75) Bollag, D. M.; McQueney, P. A.; Zhu, J.; Hensens, O.; Koupal, L.; Liesch, J.; Goetz, M.; Lazarides, E.; Woods, C. M. Epothilones, a New Class of Microtubule-Stabilizing Agents with a Taxol-Like Mechanism of Action. *Cancer Res.* **1995**, *55*, 2325-2333.

(76) Haar, E.; Kowalski, R.; Hamel, E.; C., L.; Longley, R. E.; Gunnasekera, S. P.; Rosenkranz, H. S.; Day, B. W. Discodermolide, a Cytotoxic Marine Agent That Stabilizes Microtubules More Potently Than Taxol. *Biochemistry* **1996**, *35*, 243-250.

(77) Long, B. H.; Carboni, J. M.; Wasserman, A. J.; Cornell, L. A.; Casazza, A. M.; Jensen, P. R.; Lindel, T.; Fenical, W.; Fairchild, C. R. Eleutherobin, a Novel Cytotoxic Agent That Induces Tubulin Polymerization, Is Similar to Paclitaxel. *Cancer Res.* **1998**, *58*, 1111-1115.

(78) Hamel, E.; Sackett, D. L.; Vourloumis, D.; Nicolaou, K. C. The Coral-Derived Natural Products Eleutherobin and Sarcodictyins a and B: Effects on the Assembly of Purified Tubulin with and without Microtubule-Associated Proteins and Binding at the Polymer Taxoid Site. *Biochemistry* **1999**, *38*, 3490-3498.

(79) Altmann, K. H. Microtubule-Stabilizing Agents: A Growing Class of Important Anticancer Drugs. *Curr. Opin. Chem. Biol.* **2001**, *5*, 424-431.

(80) Dhamodharan, R.; Jordan, M. A.; Thrower, D.; Wilson, L.; Wadsworth, P. Vinblastine Suppresses Dynamics of Individual Microtubules in Living Interphase Cells. *Mol. Biol. Cell* **1995**, *6*, 1215-1229.

(81) Derry, W. B.; Wilson, L.; Jordan, M. A. Substoichiometric Binding of Taxol Suppresses Microtubule Dynamics. *Biochemistry* **1995**, *34*, 2203-2211.

(82) Tilney, L. G.; Bryan, J.; Bush, D. J.; Fujiwara, K.; Mooseker, M. S.; Murphy, D. B.; Snyder, D. H. Microtubules - Evidence for 13 Protofilaments. *J. Cell Biol.* **1973**, *59*, 267-275.

(83) Wade, R. H.; Hyman, A. A. Microtubule Structure and Dynamics. *Curr. Opin. Cell Biol.* **1997**, *9*, 12-17.

(84) Andreu, J. M.; Diaz, J. F.; Gil, R.; Depereda, J. M.; Delacoba, M. G.; Peyrot, V.; Briand, C.; Townsandrews, E.; Bordas, J. Solution Structure of Taxotere-Induced

Microtubules to 3 nm Resolution - the Change in Protofilament Number Is Linked to the Binding of the Taxol Side-Chain. *J. Biol. Chem.* **1994**, *269*, 31785-31792.

(85) Mandelkow, E. M.; Schultheiss, R.; Rapp, R.; Muller, M.; Mandelkow, E. On the Surface Lattice of Microtubules - Helix Starts, Protofilament Number, Seam, and Handedness. *J. Cell Biol.* **1986**, *102*, 1067-1073.

(86) Burns, R. G. Alpha-Tubulin, Beta-Tubulin, and Gamma-Tubulins - Sequence Comparisons and Structural Constraints. *Cell Motil. Cytoskeleton* **1991**, *20*, 181-189.

(87) Nogales, E.; Wolf, S. G.; Downing, K. H. Structure of the αβ Tubulin Dimer by Electron Crystallography. *Nature* **1998**, *391*, 199-203.

(88) Loewe, J.; Li, H.; Downing, K. H.; Nogales, E. Refined Structure of αβ-Tubulin at 3.5 Å Resolution. *J. Mol. Biol.* **2001**, *313*, 1045-1057.

(89) Nogales, E.; Whittaker, M.; Milligan, R. A.; Downing, K. H. High-Resolution Model of the Microtubule. *Cell* **1999**, *96*, 79-88.

(90) Li, H. L.; De Rosier, D. J.; Nicholson, W. V.; Nogales, E.; Downing, K. H. Microtubule Structure at 8 Å Resolution. *Structure* **2002**, *10*, 1317-1328.

(91) Sage, C. R.; Dougherty, C. A.; Davis, A. S.; Burns, R. G.; Wilson, L.; Farrell, K. W. Site-Directed Mutagenesis of Putative GTP-Binding Sites of Yeast Beta-Tubulin - Evidence That Alpha-Tubulins, Beta-Tubulins, and Gamma-Tubulins Are Atypical GTPases. *Biochemistry* **1995**, *34*, 7409-7419.

(92) Hyman, A. A.; Chretien, D.; Arnal, I.; Wade, R. H. Structural-Changes Accompanying GTP Hydrolysis in Microtubules - Information from a Slowly Hydrolyzable Analog Guanylyl-(Alpha,Beta)-Methylene-Diphosphonate. *J. Cell Biol.* **1995**, *128*, 117-125.

(93) Caplow, M.; Ruhlen, R. L.; Shanks, J. The Free-Energy for Hydrolysis of a Microtubule-Bound Nucleotide Triphosphate Is near Zero - All of the Free-Energy for Hydrolysis Is Stored in the Microtubule Lattice. *J. Cell Biol.* **1994**, *127*, 779-788.

(94) Reijo, R. A.; Cooper, E. M.; Beagle, G. J.; Huffaker, T. C. Systematic Mutational Analysis of the Yeast Beta-Tubulin Gene. *Mol. Biol. Cell* **1994**, *5*, 29-43.

(95) dePereda, J. M.; Andreu, J. M. Mapping Surface Sequences of the Tubulin Dimer and Taxol-Induced Microtubules with Limited Proteolysis. *Biochemistry* **1996**, *35*, 14184-14202.

(96) Dai, K.; Mukherjee, A.; Xu, Y. F.; Lutkenhaus, J. Mutations in FtsZ That Confer Resistance to SulA Affect the Interaction of FtsZ with GTP. *J. Bacteriol.* **1994**, *176*, 130-136.

(97) Kar, S.; Fan, J.; Smith, M. J.; Goedert, M.; Amos, L. A. Repeat Motifs of Tau Bind to the Insides of Microtubules in the Absence of Taxol. *Embo J.* **2003**, *22*, 70-77.

(98) Bai, R. L.; Covell, D. G.; Pei, X. F.; Ewell, J. B.; Nguyen, N. Y.; Brossi, A.; Hamel, E. Mapping the Binding Site of Colchicinoids on Beta-Tubulin - 2-Chloroacetyl-2-Demethylthiocolchicine Covalently Reacts Predominantly with Cysteine 239 and Secondarily with Cysteine 354. *J. Biol. Chem.* **2000**, *275*, 40443-40452.

(99) Ermer, O. Calculation of Molecular Properties Using Force Fields. Applications in Organic Chemistry. *Structure and Bonding* **1976**, *27*, 161-211.

(100) Cornell, W. D.; Cieplak, P.; Bayly, C. I.; Gould, I. R.; Merz, K. M.; Ferguson, D. M.; Spellmeyer, D. C.; Fox, T.; Caldwell, J. W.; Kollman, P. A. A 2nd Generation Force-Field for the Simulation of Proteins, Nucleic-Acids, and Organic-Molecules. *J. Am. Chem. Soc.* **1995**, *117*, 5179-5197.

(101) Dauber-Osguthorpe, P.; Roberts, V. A.; Osguthorpe, D. J.; Wolff, J.; Genest, M.; Hagler, A. T. Structure and Energetics of Ligand-Binding to Proteins - Escherichia-Coli Dihydrofolate Reductase Trimethoprim, a Drug-Receptor System. *Proteins* **1988**, *4*, 31-47.

(102) Bayly, C. I.; Cieplak, P.; Cornell, W. D.; Kollman, P. A. A Well-Behaved Electrostatic Potential Based Method Using Charge Restraints for Deriving Atomic Charges - the RESP Model. *J. Phys. Chem.* **1993**, *97*, 10269-10280.

(103) Cornell, W. D.; Cieplak, P.; Bayly, C. I.; Kollman, P. A. Application of RESP Charges to Calculate Conformational Energies, Hydrogen-Bond Energies, and Free-Energies of Solvation. *J. Am. Chem. Soc.* **1993**, *115*, 9620-9631.

(104) Halgren, T. A.; Damm, W. Polarizable Force Fields. *Curr. Opin. Struct. Biol.* **2001**, *11*, 236-242.

(105) Ponder, J. W.; Case, D. A. Force Fields for Protein Simulations. In *Advances in Protein Chemistry, Protein Simulations*, **2003**; Vol. 66, pp 27-85.

(106) Mackerell, A. D. Empirical Force Fields for Biological Macromolecules: Overview and Issues. *J. Comput. Chem.* **2004**, *25*, 1584-1604.

(107) Wang, J. M.; Cieplak, P.; Kollman, P. A. How Well Does a Restrained Electrostatic Potential (RESP) Model Perform in Calculating Conformational Energies of Organic and Biological Molecules? *J. Comput. Chem.* **2000**, *21*, 1049-1074.

(108) Garcia, A. E.; Sanbonmatsu, K. Y. Alpha-Helical Stabilization by Side Chain Shielding of Backbone Hydrogen Bonds. *Proc. Natl. Acad. Sci. U. S. A.* **2002**, *99*, 2782-2787.

(109) Okur, A.; Strockbine, B.; Hornak, V.; Simmerling, C. Using PC Clusters to Evaluate the Transferability of Molecular Mechanics Force Fields for Proteins. *J. Comput. Chem.* **2003**, *24*, 21-31.

(110) Duan, Y.; Wu, C.; Chowdhury, S.; Lee, M. C.; Xiong, G. M.; Zhang, W.; Yang, R.; Cieplak, P.; Luo, R.; Lee, T.; Caldwell, J.; Wang, J. M.; Kollman, P. A Point-Charge Force Field for Molecular Mechanics Simulations of Proteins Based on Condensed-Phase Quantum Mechanical Calculations. *J. Comput. Chem.* **2003**, *24*, 1999-2012.

(111) Yoda, T.; Sugita, Y.; Okamoto, Y. Secondary-Structure Preferences of Force Fields for Proteins Evaluated by Generalized-Ensemble Simulations. *Chem. Phys.* **2004**, *307*, 269-283.

(112) Sakae, Y.; Okamoto, Y. Protein Force-Field Parameters Optimized with the Protein Data Bank. I. Force-Field Optimizations. *J. Theor. Comput. Chem.* **2004**, *3*, 339-358.

(113) Sakae, Y.; Okamoto, Y. Protein Force-Field Parameters Optimized with the Protein Data Bank. II. Comparisons of Force Fields by Folding Simulations of Short Peptides. *J. Theor. Comput. Chem.* **2004**, *3*, 359-378.

(114) Sorin, E. J.; Pande, V. S. Empirical Force-Field Assessment: The Interplay between Backbone Torsions and Noncovalent Term Scaling. *J. Comput. Chem.* **2005**, *26*, 682-690.

(115) Beachy, M. D.; Chasman, D.; Murphy, R. B.; Halgren, T. A.; Friesner, R. A. Accurate Ab Initio Quantum Chemical Determination of the Relative Energetics

of Peptide Conformations and Assessment of Empirical Force Fields. *J. Am. Chem. Soc.* **1997**, *119*, 5908-5920.

(116) Simmerling, C.; Strockbine, B.; Roitberg, A. E. All-Atom Structure Prediction and Folding Simulations of a Stable Protein. *J. Am. Chem. Soc.* **2002**, *124*, 11258-11259.

(117) Chowdhury, S.; Lee, M. C.; Xiong, G. M.; Duan, Y. Ab Initio Folding Simulation of the Trp-Cage Mini-Protein Approaches NMR Resolution. *J. Mol. Biol.* **2003**, *327*, 711-717.

(118) Jacobson, M. P.; Kaminski, G. A.; Friesner, R. A.; Rapp, C. S. Force Field Validation Using Protein Side Chain Prediction. *J. Phys. Chem. B* **2002**, *106*, 11673-11680.

(119) Fletcher, R.; Reeves, C. M. Function Minimization by Conjugate Gradients. *Comput. J.* **1964**, *7*, 149-&.

(120) Verlet, L. Computer Experiments on Classical Fluids .I. Thermodynamical Properties of Lennard-Jones Molecules. *Physical Review* **1967**, *159*, 98-103.

(121) Hokney, R. W. The Potential Calculation and Some Applications. *Method. Comput. Phys.* **1970**, *9*, 136-211.

(122) Ryckaert, J. P.; Ciccotti, G.; Berendsen, H. J. C. Numerical-Integration of Cartesian Equations of Motion of a System with Constraints - Molecular-Dynamics of N-Alkanes. *J. Comput. Phys.* **1977**, *23*, 327-341.

(123) Andersen, H. C. Rattle - a Velocity Version of the Shake Algorithm for Molecular-Dynamics Calculations. *J. Comput. Phys.* **1983**, *52*, 24-34.

(124) Miyamoto, S.; Kollman, P. A. Settle - an Analytical Version of the Shake and Rattle Algorithm for Rigid Water Models. *J. Comput. Chem.* **1992**, *13*, 952-962.

(125) Hess, B.; Bekker, H.; Berendsen, H. J. C.; Fraaije, J. Lincs: A Linear Constraint Solver for Molecular Simulations. *J. Comput. Chem.* **1997**, *18*, 1463-1472.

(126) McCammon, J. A.; Gelin, B. R.; Karplus, M. Dynamics of Folded Proteins. *Nature* **1977**, *267*, 585-590.

(127) Pitman, M. C.; Grossfield, A.; Suits, F.; Feller, S. E. Role of Cholesterol and Polyunsaturated Chains in Lipid-Protein Interactions: Molecular Dynamics

Simulation of Rhodopsin in a Realistic Membrane Environment. *J. Am. Chem. Soc.* **2005**, *127*, 4576-4577.

(128) Duan, Y.; Kollman, P. A. Pathways to a Protein Folding Intermediate Observed in a 1-Microsecond Simulation in Aqueous Solution. *Science* **1998**, *282*, 740-744.

(129) Metropolis, N.; Rosenbluth, A. W.; Rosenbluth, M. N.; Teller, A. H.; Teller, E. Equation of State Calculations by Fast Computing Machines. *J. Chem. Phys.* **1953**, *21*, 1087-1092.

(130) Straub, J. E.; Rashkin, A. B.; Thirumalai, D. Dynamics in Rugged Energy Landscapes with Applications to the S-Peptide and Ribonuclease-A. *J. Am. Chem. Soc.* **1994**, *116*, 2049-2063.

(131) Wolynes, P. G.; Onuchic, J. N.; Thirumalai, D. Navigating the Folding Routes. *Science* **1995**, *267*, 1619-1620.

(132) Berne, B. J.; Straub, J. E. Novel Methods of Sampling Phase Space in the Simulation of Biological Systems. *Curr. Opin. Struct. Biol.* **1997**, *7*, 181-189.

(133) Okamoto, Y. Generalized-Ensemble Algorithms: Enhanced Sampling Techniques for Monte Carlo and Molecular Dynamics Simulations. *J. Mol. Graph.* **2004**, *22*, 425-439.

(134) Sugita, Y.; Okamoto, Y. Replica-Exchange Molecular Dynamics Method for Protein Folding. *Chem. Phys. Lett.* **1999**, *314*, 141-151.

(135) Hansmann, U. H. E. Parallel Tempering Algorithm for Conformational Studies of Biological Molecules. *Chem. Phys. Lett.* **1997**, *281*, 140-150.

(136) Irback, A.; Sandelin, E. Monte Carlo Study of the Phase Structure of Compact Polymer Chains. *J. Chem. Phys.* **1999**, *110*, 12256-12262.

(137) Garcia, A. E.; Sanbonmatsu, K. Y. Exploring the Energy Landscape of a Beta Hairpin in Explicit Solvent. *Proteins* **2001**, *42*, 345-354.

(138) Zhou, R. H.; Berne, B. J.; Germain, R. The Free Energy Landscape for Beta Hairpin Folding in Explicit Water. *Proc. Natl. Acad. Sci. U. S. A.* **2001**, *98*, 14931-14936.

(139) Sanbonmatsu, K. Y.; Garcia, A. E. Structure of Met-Enkephalin in Explicit Aqueous Solution Using Replica Exchange Molecular Dynamics. *Proteins* **2002**, *46*, 225-234.

(140) Zhou, R. H.; Berne, B. J. Can a Continuum Solvent Model Reproduce the Free Energy Landscape of a Beta-Hairpin Folding in Water? *Proc. Natl. Acad. Sci. U. S. A.* **2002**, *99*, 12777-12782.

(141) Bratko, D.; Blanch, H. W. Effect of Secondary Structure on Protein Aggregation: A Replica Exchange Simulation Study. *J. Chem. Phys.* **2003**, *118*, 5185-5194.

(142) Pitera, J. W.; Swope, W. Understanding Folding and Design: Replica-Exchange Simulations of "Trp-Cage" Miniproteins. *Proc. Natl. Acad. Sci. U. S. A.* **2003**, *100*, 7587-7592.

(143) Zhou, R. H. Trp-Cage: Folding Free Energy Landscape in Explicit Water. *Proc. Natl. Acad. Sci. U. S. A.* **2003**, *100*, 13280-13285.

(144) Nymeyer, H.; Gnanakaran, S.; Garcia, A. E. Atomic Simulations of Protein Folding, Using the Replica Exchange Algorithm. In *Methods in Enzymology Numerical Computer Methods, Pt D*, **2004**; Vol. 383, pp 119-149.

(145) Lin, S.; Ojima, I. Recent Strategies in the Development of Taxane Anticancer Drugs. *Expert Opin. Ther. Patents* **2000**, *10*, 869-889.

(146) Gueritte, F. General and Recent Aspects of the Chemistry and Structure-Activity Relationships of Taxoids. *Curr. Pharm. Design* **2001**, *7*, 1229-1249.

(147) Dubois, J.; Guenard, D.; Gueritte, F. Recent Developments in Antitumour Taxoids. *Expert Opin. Ther. Patents* **2003**, *13*, 1809-1823.

(148) Ojima, I.; Kuduk, S. D.; Chakravarty, S.; Ourevitch, M.; Begue, J. P. A Novel Approach to the Study of Solution Structures and Dynamic Behavior of Paclitaxel and Docetaxel Using Fluorine- Containing Analogs as Probes. *J. Am. Chem. Soc.* **1997**, *119*, 5519-5527.

(149) Ojima, I.; Inoue, T.; Chakravarty, S. Enantiopure Fluorine-Containing Taxoids: Potent Anticancer Agents and Versatile Probes for Biomedical Problems. *J. Fluor. Chem.* **1999**, *97*, 3-10.

(150) Li, Y. K.; Poliks, B.; Cegelski, L.; Poliks, M.; Gryczynski, Z.; Piszczek, G.; Jagtap, P. G.; Studelska, D. R.; Kingston, D. G. I.; Schaefer, J.; Bane, S. Conformation of Microtubule-Bound Paclitaxel Determined by Fluorescence Spectroscopy and REDOR NMR. *Biochemistry* **2000**, *39*, 281-291.

(151) Rao, S.; Krauss, N. E.; Heerding, J. M.; Swindell, C. S.; Ringel, I.; Orr, G. A.; Horwitz, S. B. 3'-(p-Azidobenzamido)Taxol Photolabels the N-Terminal 31 Amino- Acids of Beta-Tubulin. *J. Biol. Chem.* **1994**, *269*, 3132-3134.

(152) Rao, S.; Orr, G. A.; Chaudhary, A. G.; Kingston, D. G. I.; Horwitz, S. B. Characterization of the Taxol Binding-Site on the Microtubule - 2-(m-Azidobenzoyl)Taxol Photolabels a Peptide (Amino-Acids 217- 231) of Beta-Tubulin. *J. Biol. Chem.* **1995**, *270*, 20235-20238.

(153) Rao, S.; He, L. F.; Chakravarty, S.; Ojima, I.; Orr, G. A.; Horwitz, S. B. Characterization of the Taxol Binding Site on the Microtubule - Identification of Arg(282) in Beta-Tubulin as the Site of Photoincorporation of a 7-Benzophenone Analogue of Taxol. *J. Biol. Chem.* **1999**, *274*, 37990-37994.

(154) Ojima, I.; Chakravarty, S.; Inoue, T.; Lin, S. N.; He, L. F.; Horwitz, S. B.; Kuduk, S. D.; Danishefsky, S. J. A Common Pharmacophore for Cytotoxic Natural Products That Stabilize Microtubules. *Proc. Natl. Acad. Sci. USA* **1999**, *96*, 4256-4261.

(155) Snyder, J. P.; Nettles, J.; Cornett, B.; Downing, K. H.; Nogales, E. The Binding Conformation of Taxol in Beta-Tubulin: A Model Based on Electron Crystallographic Density. *Proc. Natl. Acad. Sci. USA* **2001**, *98*, 5312-5316.

(156) Giannakakou, P.; Gussio, R.; Nogales, E.; Downing, K. H.; Zaharevitz, D.; Bollbuck, B.; Poy, G.; Sackett, D.; Nicolaou, K. C.; Fojo, T. A Common Pharmacophore for Epothilone and Taxanes: Molecular Basis for Drug Resistance Conferred by Tubulin Mutations in Human Cancer Cells. *Proc. Natl. Acad. Sci. USA* **2000**, *97*, 2904-2909.

(157) Mastropaolo, D.; Camerman, A.; Luo, Y. G.; Brayer, G. D.; Camerman, N. Crystal and Molecular-Structure of Paclitaxel (Taxol). *Proc. Natl. Acad. Sci. USA* **1995**, *92*, 6920-6924.

(158) Chang, G.; Guida, W. C.; Still, W. C. An Internal Coordinate Monte-Carlo Method for Searching Conformational Space. *J. Am. Chem. Soc.* **1989**, *111*, 4379-4386.

(159) Saunders, M.; Houk, K. N.; Wu, Y. D.; Still, W. C.; Lipton, M.; Chang, G.; Guida, W. C. Conformations of Cycloheptadecane - a Comparison of Methods for Conformational Searching. *J. Am. Chem. Soc.* **1990**, *112*, 1419-1427.

(160) Mohamadi, F.; Richards, N. G. J.; Guida, W. C.; Liskamp, R.; Lipton, M.; Caufield, C.; Chang, G.; Hendrickson, T.; Still, W. C. Macromodel - an Integrated

Software System for Modeling Organic and Bioorganic Molecules Using Molecular Mechanics. *J. Comput. Chem.* **1990**, *11*, 440-467.

(161) Allinger, N. L.; Yuh, Y. H.; Lii, J. H. Molecular Mechanics - the MM3 Force-Field for Hydrocarbons .1. *J. Am. Chem. Soc.* **1989**, *111*, 8551-8566.

(162) Lii, J. H.; Allinger, N. L. Molecular Mechanics - the MM3 Force-Field for Hydrocarbons .2. Vibrational Frequencies and Thermodynamics. *J. Am. Chem. Soc.* **1989**, *111*, 8566-8575.

(163) Lii, J. H.; Allinger, N. L. Molecular Mechanics - the MM3 Force-Field for Hydrocarbons .3. The van der Waals Potentials and Crystal Data for Aliphatic and Aromatic-Hydrocarbons. *J. Am. Chem. Soc.* **1989**, *111*, 8576-8582.

(164) Williams, H. J.; Scott, A. I.; Dieden, R. A.; Swindell, C. S.; Chirlian, L. E.; Francl, M. M.; Heerding, J. M.; Krauss, N. E. NMR and Molecular Modeling Study of the Conformations of Taxol and of Its Side-Chain Methylester in Aqueous and Nonaqueous Solution. *Tetrahedron* **1993**, *49*, 6545-6560.

(165) Dubois, J.; Guenard, D.; Gueritte-Voegelein, F.; Guedira, N.; Potier, P.; Gillet, B.; Beloeil, J. C. Conformation of Taxotere(R) and Analogs Determined by NMR Spectroscopy and Molecular Modeling Studies. *Tetrahedron* **1993**, *49*, 6533-6544.

(166) Vandervelde, D. G.; Georg, G. I.; Grunewald, G. L.; Gunn, G. W.; Mitscher, L. A. Hydrophobic Collapse of Taxol and Taxotere Solution Conformations in Mixtures of Water and Organic-Solvent. *J. Am. Chem. Soc.* **1993**, *115*, 11650-11651.

(167) Nicklaus, M. C.; Wang, S. M.; Driscoll, J. S.; Milne, G. W. A. Conformational Changes of Small Molecules Binding to Proteins. *Bioorg. Med. Chem.* **1995**, *3*, 411-428.

(168) Rao, S.; Horwitz, S. B.; Ringel, I. Direct Photoaffinity-Labeling of Tubulin with Taxol. *J. Natl Cancer Inst.* **1992**, *84*, 785-788.

(169) Dorman, G.; Prestwich, G. D. Benzophenone Photophores in Biochemistry. *Biochemistry* **1994**, *33*, 5661-5673.

(170) Geng, X.; Miller, M. L.; Lin, S.; Ojima, I. Synthesis of Novel C2-C3'N-Linked Macrocyclic Taxoids by Means of Highly Regioselective Heck Macrocyclization. *Org. Lett.* **2003**, *5*, 3733-3736.

(171) Boge, T. C.; Himes, R. H.; Vandervelde, D. G.; Georg, G. I. The Effect of the Aromatic Rings of Taxol on Biological Activity and Solution Conformation Synthesis and Evaluation of Saturated Taxol and Taxotere Analogs. *J. Med. Chem.* **1994**, *37*, 3337-3343.

(172) Georg, G. I.; Harriman, G. C. B.; Hepperle, M.; Clowers, J. S.; VanderVelde, D. G.; Himes, R. H. Synthesis, Conformational Analysis, and Biological Evaluation of Heteroaromatic Taxanes. *J. Org. Chem.* **1996**, *61*, 2664-2676.

(173) Boge, T. C.; Wu, Z. J.; Himes, R. H.; Vander Velde, D. G.; Georg, G. I. Conformationally Restricted Paclitaxel Analogues: Macrocyclic Mimics of the "Hydrophobic Collapse" Conformation. *Bioorg. Med. Chem. Lett.* **1999**, *9*, 3047-3052.

(174) Ojima, I.; Lin, S.; Inoue, T.; Miller, M. L.; Borella, C. P.; Geng, X.; Walsh, J. J. Macrocycle Formation by Ring-Closing Metathesis. Application to the Syntheses of Novel Macrocyclic Taxoids. *J. Am. Chem. Soc.* **2000**, *122*, 5343-5353.

(175) Ojima, I.; Geng, X.; Lin, S.; Pera, P.; Bernacki, R. J. Design, Synthesis and Biological Activity of Novel C2-C3' N-Linked Macrocyclic Taxoids. *Bioorg. Med. Chem. Lett.* **2002**, *12*, 349-352.

(176) Ojima, I.; Slater, J. C.; Michaud, E.; Kuduk, S. D.; Bounaud, P. Y.; Vrignaud, P.; Bissery, M. C.; Veith, J. M.; Pera, P.; Bernacki, R. J. Syntheses and Structure-Activity Relationships of the Second-Generation Antitumor Taxoids: Exceptional Activity against Drug-Resistant Cancer Cells. *J. Med. Chem.* **1996**, *39*, 3889-3896.

(177) Ojima, I.; Wang, T.; Miller, M. L.; Lin, S. N.; Borella, C. P.; Geng, X. D.; Pera, P.; Bernacki, R. J. Synthesis and Structure-Activity Relationships of New Second-Generation Taxoids. *Bioorg. Med. Chem. Lett.* **1999**, *9*, 3423-3428.

(178) Grubbs, R. H.; Chang, S. Recent Advances in Olefin Metathesis and Its Application in Organic Synthesis. *Tetrahedron* **1998**, *54*, 4413-4450.

(179) Ojima, I.; Habus, I.; Zhao, M.; Zucco, M.; Park, Y. H.; Sun, C. M.; Brigaud, T. New and Efficient Approaches to the Semisynthesis of Taxol and Its C-13 Side-Chain Analogs by Means of Beta-Lactam Synthon Method. *Tetrahedron* **1992**, *48*, 6985-7012.

(180) Ojima, I.; Kuduk, S. D.; Chakravarty, S. *Advances in Medicinal Chemistry*; Maryanoff, B. E., Reitz, A. B., Eds.; JAI Press: Greenwich, CT, **1998**; Vol. 4, pp 69-124.

(181) Metaferia, B. B.; Hoch, J.; Glass, T. E.; Bane, S. L.; Chatterjee, S. K.; Snyder, J. P.; Lakdawala, A.; Cornett, B.; Kingston, D. G. I. Synthesis and Biological Evaluation of Novel Macrocyclic Paclitaxel Analogues. *Org. Lett.* **2001**, *3*, 2461-2464.

(182) Ojima, I.; Wang, T.; Delaloge, F. Extremely Stereoselective Alkylation of 3-Siloxy-Beta-Lactams and Its Applications to the Asymmetric Syntheses of Novel 2-Alkylisoserines, Their Dipeptides, and Taxoids. *Tetrahedron Lett.* **1998**, *39*, 3663-3666.

(183) Ojima, I.; Slater, J. C.; Kuduk, S. D.; Takeuchi, C. S.; Gimi, R. H.; Sun, C. M.; Park, Y. H.; Pera, P.; Veith, J. M.; Bernacki, R. J. Syntheses and Structure-Activity Relationships of Taxoids Derived from 14-Beta-Hydroxy-10-Deacetylbaccatin III. *J. Med. Chem.* **1997**, *40*, 267-278.

(184) Crich, D.; Yao, Q. Generation of Acyl Radicals from Thiolesters by Intramolecular Homolytic Substitution at Sulfur. *J. Org. Chem.* **1996**, *61*, 3566-3570.

(185) Appendino, G.; Gariboldi, P.; Gabetta, B.; Pace, R.; Bombardelli, E.; Viterbo, D. 14-Beta-Hydroxy-10-Deacetylbaccatin-III, a New Taxane from Himalayan Yew (Taxus-Wallichiana Zucc). *J. Chem. Soc. Perkin Trans. 1* **1992**, 2925-2929.

(186) Ford, J. M.; Hait, W. N. Pharmacology of Drugs That Alter Multidrug Resistance in Cancer. *Pharmacol. Rev.* **1990**, *42*, 155-199.

(187) Gottesman, M. M.; Pastan, I. Biochemistry of Multidrug Resistance Mediated by the Multidrug Transporter. *Annu. Rev. Biochem.* **1993**, *62*, 385-427.

(188) Gottesman, M. M.; Fojo, T.; Bates, S. E. Multidrug Resistance in Cancer: Role of ATP-Dependent Transporters. *Nat. Rev. Cancer.* **2002**, *2*, 48-58.

(189) Arbuck, S. G. Paclitaxel: Current Developmental Approaches of the National Cancer Institute. *Semin Oncol* **1995**, *22*, 55-63.

(190) Huisman, C.; Ferreira, C. G.; Broker, L. E.; Rodriguez, J. A.; Smit, E. F.; Postmus, P. E.; Kruyt, F. A. E.; Giaccone, G. Paclitaxel Triggers Cell Death Primarily Via Caspase-Independent Routes in the Non-Small Cell Lung Cancer Cell Line NCI-H460. *Clin Cancer Res* **2002**, *8*, 596-606.

(191) Ofir, R.; Seidman, R.; Rabinski, T.; Krup, M.; Yavelsky, V.; Weinstein, Y.; Wolfson, M. Taxol-Induced Apoptosis in Human SKOV3 Ovarian and MCF7

Breast Carcinoma Cells Is Caspase-3 and Caspase-9 Independent. *Cell Death Differ.* **2002**, *9*, 636-642.

(192) Ganesh, T.; Guza, R. C.; Bane, S.; Ravindra, S.; Shanker, N.; Lakdawala, A. S.; Snyder, J. P.; Kingston, D. G. I. The Bioactive Taxol Conformation on Beta-Tubulin: Experimental Evidence from Highly Active Constrained Analogs. *Proc. Natl. Acad. Sci. USA* **2004**, *101*, 10006-10011.

(193) Still, W. C.; Tempczyk, A.; Hawley, R. C.; Hendrickson, T. Semianalytical Treatment of Solvation for Molecular Mechanics and Dynamics. *J. Am. Chem. Soc.* **1990**, *112*, 6127-6129.

(194) Diaz, J. F.; Barasoain, I.; Andreu, J. M. Fast Kinetics of Taxol Binding to Microtubules - Effects of Solution Variables and Microtubule-Associated Proteins. *J. Biol. Chem.* **2003**, *278*, 8407-8419.

(195) Nettles, J. H.; Li, H. L.; Cornett, B.; Krahn, J. M.; Snyder, J. P.; Downing, K. H. The Binding Mode of Epothilone A on α,β-Tubulin by Electron Crystallography. *Science* **2004**, *305*, 866-869.

(196) Perutz, M. F. Electrostatic Effects in Proteins. *Science* **1978**, *201*, 1187-1191.

(197) Dill, K. A. Dominant Forces in Protein Folding. *Biochemistry* **1990**, *29*, 7133-7155.

(198) Honig, B.; Yang, A. S. In *Advances in Protein Chemistry, Advances in Protein Chemistry*, **1995**; Vol. 46, pp 27-58.

(199) Honig, B. H.; Hubbell, W. L. Stability of Salt Bridges in Membrane-Proteins. *Proc. Natl. Acad. Sci. U. S. A.* **1984**, *81*, 5412-5416.

(200) Daopin, S.; Soderlind, E.; Baase, W. A.; Wozniak, J. A.; Sauer, U.; Matthews, B. W. Cumulative Site-Directed Charge-Change Replacements in Bacteriophage-T4 Lysozyme Suggest That Long-Range Electrostatic Interactions Contribute Little to Protein Stability. *J. Mol. Biol.* **1991**, *221*, 873-887.

(201) Hendsch, Z. S.; Tidor, B. Do Salt Bridges Stabilize Proteins - a Continuum Electrostatic Analysis. *Protein Sci.* **1994**, *3*, 211-226.

(202) Waldburger, C. D.; Schildbach, J. F.; Sauer, R. T. Are Buried Salt Bridges Important for Protein Stability and Conformational Specificity. *Nat. Struct. Biol.* **1995**, *2*, 122-128.

(203) Waldburger, C. D.; Jonsson, T.; Sauer, R. T. Barriers to Protein Folding: Formation of Buried Polar Interactions Is a Slow Step in Acquisition of Structure. *Proc. Natl. Acad. Sci. U. S. A.* **1996**, *93*, 2629-2634.

(204) Dong, F.; Zhou, H. X. Electrostatic Contributions to T4 Lysozyme Stability: Solvent-Exposed Charges Versus Semi-Buried Salt Bridges. *Biophys. J.* **2002**, *83*, 1341-1347.

(205) Elcock, A. H. The Stability of Salt Bridges at High Temperatures: Implications for Hyperthermophilic Proteins. *J. Mol. Biol.* **1998**, *284*, 489-502.

(206) Xiao, L.; Honig, B. Electrostatic Contributions to the Stability of Hyperthermophilic Proteins. *J. Mol. Biol.* **1999**, *289*, 1435-1444.

(207) Vieille, C.; Zeikus, G. J. Hyperthermophilic Enzymes: Sources, Uses, and Molecular Mechanisms for Thermostability. *Microbiol. Mol. Biol. Rev.* **2001**, *65*, 1-43.

(208) Zhou, H. X. Toward the Physical Basis of Thermophilic Proteins: Linking of Enriched Polar Interactions and Reduced Heat Capacity of Unfolding. *Biophys. J.* **2002**, *83*, 3126-3133.

(209) Dominy, B. N.; Minoux, H.; Brooks, C. L. An Electrostatic Basis for the Stability of Thermophilic Proteins. *Proteins* **2004**, *57*, 128-141.

(210) Thomas, A. S.; Elcock, A. H. Molecular Simulations Suggest Protein Salt Bridges Are Uniquely Suited to Life at High Temperatures. *J. Am. Chem. Soc.* **2004**, *126*, 2208-2214.

(211) Karplus, M.; McCammon, J. A. Molecular Dynamics Simulations of Biomolecules. *Nat. Struct. Biol.* **2002**, *9*, 646-652.

(212) Cramer, C. J.; Truhlar, D. G. Implicit Solvation Models: Equilibria, Structure, Spectra, and Dynamics. *Chem. Rev.* **1999**, *99*, 2161-2200.

(213) Roux, B.; Simonson, T. Implicit Solvent Models. *Biophys. Chem.* **1999**, *78*, 1-20.

(214) Simonson, T. Macromolecular Electrostatics: Continuum Models and Their Growing Pains. *Curr. Opin. Struct. Biol.* **2001**, *11*, 243-252.

(215) Simonson, T. Electrostatics and Dynamics of Proteins. *Rep. Prog. Phys.* **2003**, *66*, 737-787.

(216) Feig, M.; Brooks, C. L. Recent Advances in the Development and Application of Implicit Solvent Models in Biomolecule Simulations. *Curr. Opin. Struct. Biol.* **2004**, *14*, 217-224.

(217) Baker, N. A. Improving Implicit Solvent Simulations: A Poisson-Centric View. *Curr. Opin. Struct. Biol.* **2005**, *15*, 137-143.

(218) Kramers, H. A. Brownian Motion in a Field of Force and the Diffusion Model of Chemical Reactions. *Physica* **1940**, *7*, 284-304.

(219) Weiner, J. H.; Pear, M. R. Computer Simulation of Conformational Transitions in an Idealized Polymer Model. *Macromolecules* **1977**, *10*, 317-325.

(220) Chandler, D. Statistical Mechanics of Isomerization Dynamics in Liquids and Transition-State Approximation. *J. Chem. Phys.* **1978**, *68*, 2959-2970.

(221) Helfand, E. Brownian Dynamics Simulation of Systems with Transitions, Particularly Conformational Transitions in Chain Molecules. *Physica A* **1983**, *118*, 123-135.

(222) Ansari, A.; Jones, C. M.; Henry, E. R.; Hofrichter, J.; Eaton, W. A. The Role of Solvent Viscosity in the Dynamics of Protein Conformational Changes. *Science* **1992**, *256*, 1796-1798.

(223) Haran, G.; Haas, E.; Rapaport, D. C. Molecular Dynamics Simulations of Simple Peptide Models - Solvent Effects and Comparison with Experiment. *J. Phys. Chem.* **1994**, *98*, 10294-10302.

(224) Takano, M.; Yamato, T.; Higo, J.; Suyama, A.; Nagayama, K. Molecular Dynamics of a 15-Residue Poly(L-Alanine) in Water: Helix Formation and Energetics. *J. Am. Chem. Soc.* **1999**, *121*, 605-612.

(225) Karplus, M. Aspects of Protein Reaction Dynamics: Deviations from Simple Behavior. *J. Phys. Chem. B* **2000**, *104*, 11-27.

(226) Zagrovic, B.; Pande, V. Solvent Viscosity Dependence of the Folding Rate of a Small Protein: Distributed Computing Study. *J. Comput. Chem.* **2003**, *24*, 1432-1436.

(227) Srinivasan, J.; Cheatham, T. E.; Cieplak, P.; Kollman, P. A.; Case, D. A. Continuum Solvent Studies of the Stability of DNA, RNA, and Phosphoramidate - DNA Helices. *J. Am. Chem. Soc.* **1998**, *120*, 9401-9409.

(228) Guillot, B. A Reappraisal of What We Have Learnt During Three Decades of Computer Simulations on Water. *J. Mol. Liq.* **2002**, *101*, 219-260.

(229) Constanciel, R.; Contreras, R. Self-Consistent Field-Theory of Solvent Effects Representation by Continuum Models - Introduction of Desolvation Contribution. *Theoretica Chimica Acta* **1984**, *65*, 1-11.

(230) Qiu, D.; Shenkin, P. S.; Hollinger, F. P.; Still, W. C. The GB/SA Continuum Model for Solvation. A Fast Analytical Method for the Calculation of Approximate Born Radii. *J. Phys. Chem. A* **1997**, *101*, 3005-3014.

(231) Cornell, W.; Abseher, R.; Nilges, M.; Case, D. A. Continuum Solvent Molecular Dynamics Study of Flexibility in Interleukin-8. *J. Mol. Graph.* **2001**, *19*, 136-145.

(232) Zhou, R. H. Free Energy Landscape of Protein Folding in Water: Explicit vs. Implicit Solvent. *Proteins* **2003**, *53*, 148-161.

(233) Felts, A. K.; Harano, Y.; Gallicchio, E.; Levy, R. M. Free Energy Surfaces of Beta-Hairpin and Alpha-Helical Peptides Generated by Replica Exchange Molecular Dynamics with the AGBNP Implicit Solvent Model. *Proteins* **2004**, *56*, 310-321.

(234) Ghosh, A.; Rapp, C. S.; Friesner, R. A. Generalized Born Model Based on a Surface Integral Formulation. *J. Phys. Chem. B* **1998**, *102*, 10983-10990.

(235) Masunov, A.; Lazaridis, T. Potentials of Mean Force Between Ionizable Amino Acid Side Chains in Water. *J. Am. Chem. Soc.* **2003**, *125*, 1722-1730.

(236) Dominy, B. N.; Brooks, C. L. Development of a Generalized Born Model Parametrization for Proteins and Nucleic Acids. *J. Phys. Chem. B* **1999**, *103*, 3765-3773.

(237) Hawkins, G. D.; Cramer, C. J.; Truhlar, D. G. Pairwise Solute Descreening of Solute Charges from a Dielectric Medium. *Chem. Phys. Lett.* **1995**, *246*, 122-129.

(238) Hawkins, G. D.; Cramer, C. J.; Truhlar, D. G. Parametrized Models of Aqueous Free Energies of Solvation Based on Pairwise Descreening of Solute Atomic Charges from a Dielectric Medium. *J. Phys. Chem.* **1996**, *100*, 19824-19839.

(239) Tsui, V.; Case, D. A. Molecular Dynamics Simulations of Nucleic Acids with a Generalized Born Solvation Model. *J. Am. Chem. Soc.* **2000**, *122*, 2489-2498.

(240) Tsui, V.; Case, D. A. Theory and Applications of the Generalized Born Solvation Model in Macromolecular Simulations. *Biopolymers* **2001**, *56*, 275-291.

(241) Onufriev, A.; Bashford, D.; Case, D. A. Modification of the Generalized Born Model Suitable for Macromolecules. *J. Phys. Chem. B* **2000**, *104*, 3712-3720.

(242) Onufriev, A.; Bashford, D.; Case, D. A. Exploring Protein Native States and Large-Scale Conformational Changes with a Modified Generalized Born Model. *Proteins* **2004**, *55*, 383-394.

(243) Case, D. A.; Darden, T. A.; Cheatham, T. E.; Simmerling, C. L.; Wang, J.; Duke, R. E.; Luo, R.; Merz, K. M.; Wang, B.; Pearlman, D. A.; Crowley, M.; Brozell, S.; Tsui, V.; Gohlke, H.; Mongan, J.; Hornak, V.; Cui, G.; Beroza, P.; Schafmeister, C.; Caldwell, J. W.; Ross, W. S.; Kollman, P. A. *Amber*; ver. 8; University of California: San Francisco, **2004**.

(244) Hornak, V.; Roitberg, A. E.; Simmerling, C. *in preparation*.

(245) Jorgensen, W. L.; Chandrasekhar, J.; Madura, J. D.; Impey, R. W.; Klein, M. L. Comparison of Simple Potential Functions for Simulating Liquid Water. *J. Chem. Phys.* **1983**, *79*, 926-935.

(246) Essex, J. W. The Application of the Reaction-Field Method to the Calculation of Dielectric Constants. *Mol. Simul.* **1998**, *20*, 159-178.

(247) Hochtl, P.; Boresch, S.; Bitomsky, W.; Steinhauser, O. Rationalization of the Dielectric Properties of Common Three-Site Water Models in Terms of Their Force Field Parameters. *J. Chem. Phys.* **1998**, *109*, 4927-4937.

(248) Richardi, J.; Fries, P. H.; Millot, C. Fast Hybrid Methods for the Simulation of Dielectric Constants of Liquids. *J. Mol. Liq.* **2005**, *117*, 3-16.

(249) Rini, J. M.; Schulze-Gahmen, U.; Wilson, I. A. Structural Evidence for Induced Fit as a Mechanism for Antibody-Antigen Recognition. *Science* **1992**, *255*, 959-965.

(250) Darden, T.; York, D.; Pedersen, L. Particle Mesh Ewald - an N.Log(N) Method for Ewald Sums in Large Systems. *J. Chem. Phys.* **1993**, *98*, 10089-10092.

(251) Essmann, U.; Perera, L.; Berkowitz, M. L.; Darden, T.; Lee, H.; Pedersen, L. G. A Smooth Particle Mesh Ewald Method. *J. Chem. Phys.* **1995**, *103*, 8577-8593.

(252) Crowley, M. F.; Darden, T. A.; Cheatham, T. E.; Deerfield, D. W. Adventures in Improving the Scaling and Accuracy of a Parallel Molecular Dynamics Program. *J. Supercomput.* **1997**, *11*, 255-278.

(253) Toukmaji, A.; Sagui, C.; Board, J.; Darden, T. Efficient Particle-Mesh Ewald Based Approach to Fixed and Induced Dipolar Interactions. *J. Chem. Phys.* **2000**, *113*, 10913-10927.

(254) Bondi, A. Van der Waals Volumes and Radii. *J. Phys. Chem.* **1964**, *68*, 441-&.

(255) Torrie, G. M.; Valleau, J. P. Non-Physical Sampling Distributions in Monte-Carlo Free-Energy Estimation - Umbrella Sampling. *J. Comput. Phys.* **1977**, *23*, 187-199.

(256) Kumar, S.; Bouzida, D.; Swendsen, R. H.; Kollman, P. A.; Rosenberg, J. M. The Weighted Histogram Analysis Method for Free-Energy Calculations on Biomolecules .1. The Method. *J. Comput. Chem.* **1992**, *13*, 1011-1021.

(257) Roux, B. The Calculation of the Potential of Mean Force Using Computer-Simulations. *Comput. Phys. Commun.* **1995**, *91*, 275-282.

(258) Neidigh, J. W.; Fesinmeyer, R. M.; Andersen, N. H. Designing a 20-Residue Protein. *Nat. Struct. Biol.* **2002**, *9*, 425-430.

(259) Berendsen, H. J. C.; Postma, J. P. M.; vanGunsteren, W. F.; Dinola, A.; Haak, J. R. Molecular-Dynamics with Coupling to an External Bath. *J. Chem. Phys.* **1984**, *81*, 3684-3690.

(260) Hornak, V.; Simmerling, C. Development of Softcore Potential Functions for Overcoming Steric Barriers in Molecular Dynamics Simulations. *J. Mol. Graph.* **2004**, *22*, 405-413.

(261) Hornak, V.; Simmerling, C. Generation of Accurate Protein Loop Conformations through Low-Barrier Molecular Dynamics. *Proteins* **2003**, *51*, 577-590.

(262) Kabat, E. A.; Wu, T. T.; Perry, H. M.; Gottesman, K. S.; C., F. *Sequences of Proteins of Immunological Interest*; Diane Books Publishing Company, **1991**.

(263) Bader, J. S.; Chandler, D. Computer-Simulation Study of the Mean Forces between Ferrous and Ferric Ions in Water. *J. Phys. Chem.* **1992**, *96*, 6423-6427.

(264) Rey, R.; Guardia, E. Dynamic Aspects of the Na+-Cl- Ion-Pair Association in Water. *J. Phys. Chem.* **1992**, *96*, 4712-4718.

(265) Friedman, R. A.; Mezei, M. The Potentials of Mean Force of Sodium-Chloride and Sodium Dimethylphosphate in Water - an Application of Adaptive Umbrella Sampling. *J. Chem. Phys.* **1995**, *102*, 419-426.

(266) Resat, H.; Mezei, M.; McCammon, J. A. Use of the Grand Canonical Ensemble in Potential of Mean Force Calculations. *J. Phys. Chem.* **1996**, *100*, 1426-1433.

(267) Martorana, V.; La Fata, L.; Bulone, D.; San Biagio, P. L. Potential of Mean Force between Two Ions in a Sucrose Rich Aqueous Solution. *Chem. Phys. Lett.* **2000**, *329*, 221-227.

(268) Rozanska, X.; Chipot, C. Modeling Ion-Ion Interaction in Proteins: A Molecular Dynamics Free Energy Calculation of the Guanidinium-Acetate Association. *J. Chem. Phys.* **2000**, *112*, 9691-9694.

(269) Belch, A. C.; Berkowitz, M.; McCammon, J. A. Solvation Structure of a Sodium-Chloride Ion-Pair in Water. *J. Am. Chem. Soc.* **1986**, *108*, 1755-1761.

(270) Gruia, A. D.; Fischer, S.; Smith, J. C. Molecular Dynamics Simulation Reveals a Surface Salt Bridge Forming a Kinetic Trap in Unfolding of Truncated Staphylococcal Nuclease. *Proteins* **2003**, *50*, 507-515.

(271) Gruia, A. D.; Fischer, S.; Smith, J. C. Kinetics of Breaking a Salt-Bridge Critical in Protein Unfolding. *Chem. Phys. Lett.* **2004**, *385*, 337-340.

(272) Born, M. *Z. Phys.* **1920**, *1*, 45-48.

(273) Dudek, M. J.; Ponder, J. W. Accurate Modeling of the Intramolecular Electrostatic Energy of Proteins. *J. Comput. Chem.* **1995**, *16*, 791-816.

(274) Schmidt, M. W.; Baldridge, K. K.; Boatz, J. A.; Elbert, S. T.; Gordon, M. S.; Jensen, J. H.; Koseki, S.; Matsunaga, N.; Nguyen, K. A.; Su, S. J.; Windus, T. L.; Dupuis, M.; Montgomery, J. A. General Atomic and Molecular Electronic-Structure System. *J. Comput. Chem.* **1993**, *14*, 1347-1363.

(275) Barlow, D. J.; Thornton, J. M. Ion-Pairs in Proteins. *J. Mol. Biol.* **1983**, *168*, 867-885.

(276) Kumar, S.; Nussinov, R. Salt Bridge Stability in Monomeric Proteins. *J. Mol. Biol.* **1999**, *293*, 1241-1255.

(277) Zhu, J.; Alexov, E.; Honig, B. Comparative Study of Generalized Born Models: Born Radii and Peptide Folding. *J. Phys. Chem. B* **2005**, *109*, 3008-3022.

(278) Chandler, D. Structures of Molecular Liquids. *Annu. Rev. Phys. Chem.* **1978**, *29*, 441-471.

(279) Hirata, F.; Rossky, P. J. An Extended RISM Equation for Molecular Polar Fluids. *Chem. Phys. Lett.* **1981**, *83*, 329-334.

(280) Hirata, F.; Rossky, P. J.; Pettitt, B. M. The Interionic Potential of Mean Force in a Molecular Polar-Solvent from an Extended RISM Equation. *J. Chem. Phys.* **1983**, *78*, 4133-4144.

(281) Pettitt, B. M.; Rossky, P. J. Alkali-Halides in Water - Ion Solvent Correlations and Ion Ion Potentials of Mean Force at Infinite Dilution. *J. Chem. Phys.* **1986**, *84*, 5836-5844.

(282) Fukunishi, Y.; Suzuki, M. Reproduction of the Potential of Mean Force by a Modified Solvent-Accessible Surface Method. *J. Phys. Chem.* **1996**, *100*, 5634-5636.

(283) Fukunishi, Y.; Suzuki, M. Potential of Mean Force Calculation of Solute Molecules in Water by a Modified Solvent-Accessible Surface Method. *J. Comput. Chem.* **1997**, *18*, 1656-1663.

(284) Rashin, A. A. Electrostatics of Ion Ion Interactions in Solution. *J. Phys. Chem.* **1989**, *93*, 4664-4669.

(285) Pratt, L. R.; Hummer, G.; Garcia, A. E. Ion-Pair Potentials-of-Mean-Force in Water. *Biophys. Chem.* **1994**, *51*, 147-165.

(286) Marqusee, S.; Baldwin, R. L. Helix Stabilization by Glu-...Lys+ Salt Bridges in Short Peptides of De Novo Design. *Proc. Natl. Acad. Sci. U. S. A.* **1987**, *84*, 8898-8902.

(287) Perutz, M. F.; Fermi, G. Stereochemistry of Salt-Bridge Formation in Alpha-Helices and Beta-Strands. *Proteins* **1988**, *4*, 294-295.

(288) Luo, R.; David, L.; Hung, H.; Devaney, J.; Gilson, M. K. Strength of Solvent-Exposed Salt-Bridges. *J. Phys. Chem. B* **1999**, *103*, 727-736.

(289) Qiu, L. L.; Pabit, S. A.; Roitberg, A. E.; Hagen, S. J. Smaller and Faster: The 20-Residue Trp-Cage Protein Folds in 4 μs. *J. Am. Chem. Soc.* **2002**, *124*, 12952-12953.

(290) Snow, C. D.; Zagrovic, B.; Pande, V. S. The Trp Cage: Folding Kinetics and Unfolded State Topology Via Molecular Dynamics Simulations. *J. Am. Chem. Soc.* **2002**, *124*, 14548-14549.

(291) Jorgensen, W. L.; Maxwell, D. S.; Tirado-Rives, J. Development and Testing of the OPLS All-Atom Force Field on Conformational Energetics and Properties of Organic Liquids. *J. Am. Chem. Soc.* **1996**, *118*, 11225-11236.

(292) Kabsch, W.; Sander, C. Dictionary of Protein Secondary Structure - Pattern-Recognition of Hydrogen-Bonded and Geometrical Features. *Biopolymers* **1983**, *22*, 2577-2637.

(293) Bosshard, H. R.; Marti, D. N.; Jelesarov, I. Protein Stabilization by Salt Bridges: Concepts, Experimental Approaches and Clarification of Some Misunderstandings. *J. Mol. Recognit.* **2004**, *17*, 1-16.

(294) Pace, C. N.; Alston, R. W.; Shaw, K. L. Charge-Charge Interactions Influence the Denatured State Ensemble and Contribute to Protein Stability. *Protein Sci.* **2000**, *9*, 1395-1398.

(295) Fernandez, D. P.; Goodwin, A. R. H.; Lemmon, E. W.; Sengers, J.; Williams, R. C. A Formulation for the Static Permittivity of Water and Steam at Temperatures from 238 K to 873 K at Pressures up to 1200 Mpa, Including Derivatives and Debye-Huckel Coefficients. *J. Phys. Chem. Ref. Data* **1997**, *26*, 1125-1166.

(296) Elcock, A. H.; McCammon, J. A. Continuum Solvation Model for Studying Protein Hydration Thermodynamics at High Temperatures. *J. Phys. Chem. B* **1997**, *101*, 9624-9634.

(297) Cornell, W. D.; Caldwell, J. W.; Kollman, P. A. Calculation of the Phi-Psi Maps for Alanyl and Glycyl Dipeptides with Different Additive and Non-Additive Molecular Mechanical Models. *J. Chim. Phys.-Chim. Biol.* **1997**, *94*, 1417-1435.

(298) Feig, M.; Onufriev, A.; Lee, M. S.; Im, W.; Case, D. A.; Brooks, C. L. Performance Comparison of Generalized Born and Poisson Methods in the Calculation of Electrostatic Solvation Energies for Protein Structures. *J. Comput. Chem.* **2004**, *25*, 265-284.

(299) Beglov, D.; Roux, B. Finite Representation of an Infinite Bulk System - Solvent Boundary Potential for Computer-Simulations. *J. Chem. Phys.* **1994**, *100*, 9050-9063.

(300) Lounnas, V.; Ludemann, S. K.; Wade, R. C. Towards Molecular Dynamics Simulation of Large Proteins with a Hydration Shell at Constant Pressure. *Biophys. Chem.* **1999**, *78*, 157-182.

(301) Topol, I. A.; Tawa, G. J.; Burt, S. K.; Rashin, A. A. On the Structure and Thermodynamics of Solvated Monoatomic Ions Using a Hybrid Solvation Model. *J. Chem. Phys.* **1999**, *111*, 10998-11014.

(302) Rosenhouse-Dantsker, A.; Osman, R. Application of the Primary Hydration Shell Approach to Locally Enhanced Sampling Simulated Annealing: Computer Simulation of Thyrotropin-Releasing Hormone in Water. *Biophys. J.* **2000**, *79*, 66-79.

(303) Lee, M. S.; Salsbury, F. R.; Olson, M. A. An Efficient Hybrid Explicit/Implicit Solvent Method for Biomolecular Simulations. *J. Comput. Chem.* **2004**, *25*, 1967-1978.

(304) Kentsis, A.; Mezei, M.; Osman, R. MC-PHS: A Monte Carlo Implementation of the Primary Hydration Shell for Protein Folding and Design. *Biophys. J.* **2003**, *84*, 805-815.

(305) Yu, Z. Y.; Jacobson, M. P.; Josovitz, J.; Rapp, C. S.; Friesner, R. A. First-Shell Solvation of Ion Pairs: Correction of Systematic Errors in Implicit Solvent Models. *J. Phys. Chem. B* **2004**, *108*, 6643-6654.

Appendices

Appendix A: REDOR-Taxol in β-Tubulin Binding Site (PDB File Format, Version 2.0)

```
REMARK   4
REMARK   4 COMPLIES WITH FORMAT V. 2.0,  7-AUG-2005
ATOM      1  O1  UNK     1       4.359  12.244  -7.211  0.00  0.00           O
ATOM      2  O2  UNK     1       5.767  10.182  -8.788  0.00  0.00           O
ATOM      3  O3  UNK     1       8.287   9.054  -9.342  0.00  0.00           O
ATOM      4  O4  UNK     1       7.687   6.456  -7.747  0.00  0.00           O
ATOM      5  O5  UNK     1       9.456   8.346  -3.972  0.00  0.00           O
ATOM      6  O6  UNK     1       8.138  10.577  -3.323  0.00  0.00           O
ATOM      7  O7  UNK     1       8.859  13.104  -3.877  0.00  0.00           O
ATOM      8  O8  UNK     1       8.241  13.348  -9.823  0.00  0.00           O
ATOM      9  O9  UNK     1       3.482  10.263  -8.543  0.00  0.00           O
ATOM     10  O10 UNK     1      10.346   9.940  -8.680  0.00  0.00           O
ATOM     11  O11 UNK     1       6.889  14.949 -10.866  0.00  0.00           O
ATOM     12  O12 UNK     1       8.890  12.263 -12.164  0.00  0.00           O
ATOM     13  O13 UNK     1       7.478  15.279 -14.878  0.00  0.00           O
ATOM     14  N14 UNK     1       8.797  15.901 -13.175  0.00  0.00           N
ATOM     15  C15 UNK     1       5.788  12.143  -7.235  0.00  0.00           C
ATOM     16  C16 UNK     1       6.099  10.563  -7.402  0.00  0.00           C
ATOM     17  C17 UNK     1       7.506   9.839  -7.034  0.00  0.00           C
ATOM     18  C18 UNK     1       7.871   8.614  -8.006  0.00  0.00           C
ATOM     19  C19 UNK     1       8.739   7.405  -7.533  0.00  0.00           C
ATOM     20  C20 UNK     1       9.217   7.336  -6.078  0.00  0.00           C
ATOM     21  C21 UNK     1       9.182   8.678  -5.339  0.00  0.00           C
ATOM     22  C22 UNK     1       7.854   9.533  -5.486  0.00  0.00           C
ATOM     23  C23 UNK     1       8.203  10.767  -4.547  0.00  0.00           C
ATOM     24  C24 UNK     1       8.745  12.157  -4.986  0.00  0.00           C
ATOM     25  C25 UNK     1       7.924  12.820  -6.109  0.00  0.00           C
ATOM     26  C26 UNK     1       8.509  13.207  -7.291  0.00  0.00           C
ATOM     27  C27 UNK     1       7.640  13.604  -8.515  0.00  0.00           C
ATOM     28  C28 UNK     1       6.201  12.976  -8.502  0.00  0.00           C
ATOM     29  C29 UNK     1       6.356  12.921  -5.957  0.00  0.00           C
ATOM     30  C30 UNK     1       5.987  14.446  -5.832  0.00  0.00           C
ATOM     31  C31 UNK     1       5.663  12.415  -4.647  0.00  0.00           C
ATOM     32  C32 UNK     1       6.815   7.498  -8.185  0.00  0.00           C
ATOM     33  C33 UNK     1       6.663   8.734  -4.858  0.00  0.00           C
ATOM     34  C34 UNK     1      10.008  13.272  -7.568  0.00  0.00           C
ATOM     35  C35 UNK     1       4.466   9.930  -9.217  0.00  0.00           C
ATOM     36  C36 UNK     1       9.563   9.571  -9.554  0.00  0.00           C
ATOM     37  C37 UNK     1       9.935   9.562 -11.020  0.00  0.00           C
ATOM     38  C38 UNK     1       7.733  14.050 -10.920  0.00  0.00           C
ATOM     39  C39 UNK     1       8.327  13.573 -12.262  0.00  0.00           C
ATOM     40  C40 UNK     1       9.357  14.534 -12.942  0.00  0.00           C
ATOM     41  C41 UNK     1       7.864  16.174 -14.119  0.00  0.00           C
ATOM     42  C75 UNK     1      10.000  13.079  -3.080  0.00  0.00           C
ATOM     43  O76 UNK     1      10.956  12.311  -3.210  0.00  0.00           O
ATOM     44  C77 UNK     1       9.954  14.141  -1.999  0.00  0.00           C
ATOM     45  C81 UNK     1       4.274   9.215 -10.531  0.00  0.00           C
ATOM     46  C82 UNK     1       5.381   8.889 -11.332  0.00  0.00           C
ATOM     47  C83 UNK     1       5.219   8.162 -12.508  0.00  0.00           C
ATOM     48  C84 UNK     1       3.947   7.781 -12.919  0.00  0.00           C
ATOM     49  C85 UNK     1       2.835   8.118 -12.154  0.00  0.00           C
ATOM     50  C86 UNK     1       2.996   8.832 -10.969  0.00  0.00           C
ATOM     51  C92 UNK     1      10.745  14.513 -12.232  0.00  0.00           C
ATOM     52  C93 UNK     1      11.809  13.795 -12.799  0.00  0.00           C
ATOM     53  C94 UNK     1      13.020  13.667 -12.121  0.00  0.00           C
ATOM     54  C95 UNK     1      13.172  14.237 -10.860  0.00  0.00           C
```

```
ATOM     55  C96 UNK     1      12.123  14.945 -10.283  0.00  0.00           C
ATOM     56  C97 UNK     1      10.925  15.097 -10.969  0.00  0.00           C
ATOM     57 C103 UNK     1       7.306  17.585 -14.234  0.00  0.00           C
ATOM     58 C104 UNK     1       6.558  17.908 -15.382  0.00  0.00           C
ATOM     59 C105 UNK     1       6.048  19.189 -15.572  0.00  0.00           C
ATOM     60 C106 UNK     1       6.240  20.161 -14.599  0.00  0.00           C
ATOM     61 C107 UNK     1       6.945  19.858 -13.441  0.00  0.00           C
ATOM     62 C108 UNK     1       7.483  18.589 -13.262  0.00  0.00           C
ATOM     63  H5  UNK     1       9.123   9.086  -3.444  1.00  0.00           H
ATOM     64  H12 UNK     1       9.631  12.327 -11.552  0.00  0.00           H
ATOM     65  H14 UNK     1       9.076  16.700 -12.598  0.00  0.00           H
ATOM     66  H16 UNK     1       5.357  10.063  -6.756  0.00  0.00           H
ATOM     67  H17 UNK     1       8.273  10.561  -7.343  0.00  0.00           H
ATOM     68  H19 UNK     1       9.578   7.200  -8.224  0.00  0.00           H
ATOM     69 1H20 UNK     1      10.240   6.919  -6.035  0.00  0.00           H
ATOM     70 2H20 UNK     1       8.605   6.605  -5.530  0.00  0.00           H
ATOM     71  H21 UNK     1      10.037   9.270  -5.729  0.00  0.00           H
ATOM     72  H24 UNK     1       9.753  11.910  -5.364  0.00  0.00           H
ATOM     73  H27 UNK     1       7.537  14.703  -8.411  0.00  0.00           H
ATOM     74 1H28 UNK     1       5.496  13.823  -8.612  0.00  0.00           H
ATOM     75 2H28 UNK     1       6.022  12.413  -9.433  0.00  0.00           H
ATOM     76 1H30 UNK     1       6.383  15.076  -6.642  0.00  0.00           H
ATOM     77 2H30 UNK     1       4.894  14.615  -5.842  0.00  0.00           H
ATOM     78 3H30 UNK     1       6.384  14.898  -4.902  0.00  0.00           H
ATOM     79 1H31 UNK     1       5.650  11.326  -4.555  0.00  0.00           H
ATOM     80 2H31 UNK     1       6.144  12.806  -3.730  0.00  0.00           H
ATOM     81 3H31 UNK     1       4.593  12.695  -4.593  0.00  0.00           H
ATOM     82 1H32 UNK     1       5.925   7.593  -7.538  0.00  0.00           H
ATOM     83 2H32 UNK     1       6.494   7.338  -9.231  0.00  0.00           H
ATOM     84 1H33 UNK     1       5.700   9.264  -4.844  0.00  0.00           H
ATOM     85 2H33 UNK     1       6.483   7.791  -5.397  0.00  0.00           H
ATOM     86 3H33 UNK     1       6.852   8.470  -3.800  0.00  0.00           H
ATOM     87 1H34 UNK     1      10.627  13.371  -6.659  0.00  0.00           H
ATOM     88 2H34 UNK     1      10.363  12.380  -8.112  0.00  0.00           H
ATOM     89 3H34 UNK     1      10.262  14.153  -8.184  0.00  0.00           H
ATOM     90 1H37 UNK     1       9.053   9.748 -11.656  0.00  0.00           H
ATOM     91 2H37 UNK     1      10.694  10.331 -11.241  0.00  0.00           H
ATOM     92 3H37 UNK     1      10.355   8.580 -11.301  0.00  0.00           H
ATOM     93  H39 UNK     1       7.460  13.491 -12.945  0.00  0.00           H
ATOM     94  H40 UNK     1       9.517  14.094 -13.949  0.00  0.00           H
ATOM     95  H1  UNK     1       4.019  11.538  -7.794  0.00  0.00           H
ATOM     96 1H77 UNK     1       9.261  13.845  -1.193  0.00  0.00           H
ATOM     97 2H77 UNK     1      10.955  14.291  -1.557  0.00  0.00           H
ATOM     98 3H77 UNK     1       9.619  15.108  -2.414  0.00  0.00           H
ATOM     99  H84 UNK     1       3.823   7.227 -13.839  1.00  0.00           H
ATOM    100  H82 UNK     1       6.380   9.188 -11.051  0.00  0.00           H
ATOM    101  H83 UNK     1       6.082   7.907 -13.109  0.00  0.00           H
ATOM    102  H85 UNK     1       1.847   7.822 -12.478  0.00  0.00           H
ATOM    103  H86 UNK     1       2.119   9.071 -10.383  0.00  0.00           H
ATOM    104  H93 UNK     1      11.699  13.314 -13.762  0.00  0.00           H
ATOM    105  H94 UNK     1      13.833  13.112 -12.569  0.00  0.00           H
ATOM    106  H95 UNK     1      14.104  14.122 -10.326  0.00  0.00           H
ATOM    107  H96 UNK     1      12.215  15.361  -9.291  0.00  0.00           H
ATOM    108  H97 UNK     1      10.116  15.634 -10.496  0.00  0.00           H
ATOM    109 H104 UNK     1       6.387  17.169 -16.153  0.00  0.00           H
ATOM    110 H105 UNK     1       5.507  19.428 -16.475  0.00  0.00           H
ATOM    111 H106 UNK     1       5.846  21.156 -14.743  0.00  0.00           H
ATOM    112 H107 UNK     1       7.075  20.609 -12.680  0.00  0.00           H
ATOM    113 H108 UNK     1       8.026  18.390 -12.350  0.00  0.00           H
ATOM    114  N   ALA B  18       9.659  12.580 -25.704  1.00 20.00           N
ATOM    115  CA  ALA B  18       8.461  12.700 -24.999  1.00 20.00           C
ATOM    116  C   ALA B  18       8.692  12.750 -23.534  1.00 20.00           C
ATOM    117  O   ALA B  18       8.016  13.486 -22.831  1.00 20.00           O
```

```
ATOM    118  CB  ALA B  18       7.513  11.565 -25.441  1.00 20.00           C
ATOM    119 1H   ALA B  18       9.468  12.487 -26.708  1.00  0.00           H
ATOM    120 2H   ALA B  18      10.220  13.434 -25.611  1.00  0.00           H
ATOM    121  HA  ALA B  18       7.992  13.661 -25.288  1.00  0.00           H
ATOM    122 1HB  ALA B  18       6.532  11.642 -24.936  1.00  0.00           H
ATOM    123 2HB  ALA B  18       7.310  11.592 -26.528  1.00  0.00           H
ATOM    124 3HB  ALA B  18       7.918  10.561 -25.209  1.00  0.00           H
ATOM    125  N   LYS B  19       9.645  11.981 -23.045  1.00 20.00           N
ATOM    126  CA  LYS B  19       9.807  11.922 -21.625  1.00 20.00           C
ATOM    127  C   LYS B  19      10.918  12.800 -21.054  1.00 20.00           C
ATOM    128  O   LYS B  19      10.976  13.058 -19.887  1.00 20.00           O
ATOM    129  CB  LYS B  19       8.958  11.027 -20.650  1.00 20.00           C
ATOM    130  CG  LYS B  19       7.679  10.343 -21.186  1.00 20.00           C
ATOM    131  CD  LYS B  19       6.865   9.706 -20.040  1.00 20.00           C
ATOM    132  CE  LYS B  19       5.594   8.996 -20.524  1.00 20.00           C
ATOM    133  NZ  LYS B  19       4.885   8.425 -19.362  1.00 20.00           N
ATOM    134  H   LYS B  19      10.071  11.343 -23.728  1.00  0.00           H
ATOM    135  HA  LYS B  19       9.198  12.760 -21.237  1.00  0.00           H
ATOM    136 1HB  LYS B  19       8.623  11.631 -19.773  1.00  0.00           H
ATOM    137 2HB  LYS B  19       9.605  10.345 -20.092  1.00  0.00           H
ATOM    138 1HG  LYS B  19       7.937   9.593 -21.957  1.00  0.00           H
ATOM    139 2HG  LYS B  19       7.049  11.093 -21.701  1.00  0.00           H
ATOM    140 1HD  LYS B  19       6.586  10.494 -19.311  1.00  0.00           H
ATOM    141 2HD  LYS B  19       7.505   9.001 -19.475  1.00  0.00           H
ATOM    142 1HE  LYS B  19       5.844   8.201 -21.253  1.00  0.00           H
ATOM    143 2HE  LYS B  19       4.932   9.709 -21.054  1.00  0.00           H
ATOM    144 1HZ  LYS B  19       4.053   7.894 -19.647  1.00  0.00           H
ATOM    145 2HZ  LYS B  19       5.490   7.770 -18.854  1.00  0.00           H
ATOM    146  N   PHE B  20      11.796  13.271 -21.836  1.00 20.00           N
ATOM    147  CA  PHE B  20      12.844  14.192 -21.361  1.00 20.00           C
ATOM    148  C   PHE B  20      12.181  15.530 -21.231  1.00 20.00           C
ATOM    149  O   PHE B  20      11.968  16.072 -20.156  1.00 20.00           O
ATOM    150  CB  PHE B  20      14.166  14.061 -22.196  1.00 20.00           C
ATOM    151  CG  PHE B  20      15.173  15.232 -22.074  1.00 20.00           C
ATOM    152  CD1 PHE B  20      15.660  15.846 -23.234  1.00 20.00           C
ATOM    153  CD2 PHE B  20      15.543  15.748 -20.824  1.00 20.00           C
ATOM    154  CE1 PHE B  20      16.493  16.959 -23.147  1.00 20.00           C
ATOM    155  CE2 PHE B  20      16.371  16.865 -20.739  1.00 20.00           C
ATOM    156  CZ  PHE B  20      16.846  17.467 -21.901  1.00 20.00           C
ATOM    157  H   PHE B  20      11.673  12.980 -22.811  1.00  0.00           H
ATOM    158  HA  PHE B  20      13.154  13.922 -20.329  1.00  0.00           H
ATOM    159 1HB  PHE B  20      13.908  13.906 -23.262  1.00  0.00           H
ATOM    160 2HB  PHE B  20      14.678  13.123 -21.911  1.00  0.00           H
ATOM    161  HD1 PHE B  20      15.383  15.478 -24.211  1.00  0.00           H
ATOM    162  HD2 PHE B  20      15.170  15.304 -19.913  1.00  0.00           H
ATOM    163  HE1 PHE B  20      16.856  17.435 -24.047  1.00  0.00           H
ATOM    164  HE2 PHE B  20      16.642  17.265 -19.773  1.00  0.00           H
ATOM    165  HZ  PHE B  20      17.480  18.339 -21.835  1.00  0.00           H
ATOM    166  N   TRP B  21      11.882  15.988 -22.347  1.00 20.00           N
ATOM    167  CA  TRP B  21      11.152  17.168 -22.447  1.00 20.00           C
ATOM    168  C   TRP B  21       9.935  17.009 -21.620  1.00 20.00           C
ATOM    169  O   TRP B  21       9.246  17.936 -21.193  1.00 20.00           O
ATOM    170  CB  TRP B  21      10.842  17.502 -23.935  1.00 20.00           C
ATOM    171  CG  TRP B  21      11.996  18.220 -24.652  1.00 20.00           C
ATOM    172  CD1 TRP B  21      13.073  17.604 -25.324  1.00 20.00           C
ATOM    173  CD2 TRP B  21      12.269  19.578 -24.676  1.00 20.00           C
ATOM    174  NE1 TRP B  21      14.025  18.547 -25.759  1.00 20.00           N
ATOM    175  CE2 TRP B  21      13.510  19.762 -25.337  1.00 20.00           C
ATOM    176  CE3 TRP B  21      11.580  20.688 -24.118  1.00 20.00           C
ATOM    177  CZ2 TRP B  21      14.076  21.055 -25.435  1.00 20.00           C
ATOM    178  CZ3 TRP B  21      12.155  21.955 -24.237  1.00 20.00           C
ATOM    179  CH2 TRP B  21      13.385  22.136 -24.882  1.00 20.00           C
ATOM    180  H   TRP B  21      12.162  15.416 -23.148  1.00  0.00           H
```

```
ATOM    181  HA  TRP B  21      11.711  18.014 -22.019  1.00  0.00           H
ATOM    182 1HB  TRP B  21       9.957  18.165 -23.994  1.00  0.00           H
ATOM    183 2HB  TRP B  21      10.533  16.601 -24.502  1.00  0.00           H
ATOM    184  HD1 TRP B  21      13.180  16.535 -25.448  1.00  0.00           H
ATOM    185  HE1 TRP B  21      14.907  18.382 -26.257  1.00  0.00           H
ATOM    186  HE3 TRP B  21      10.643  20.559 -23.596  1.00  0.00           H
ATOM    187  HZ2 TRP B  21      15.028  21.202 -25.923  1.00  0.00           H
ATOM    188  HZ3 TRP B  21      11.646  22.811 -23.816  1.00  0.00           H
ATOM    189  HH2 TRP B  21      13.808  23.129 -24.950  1.00  0.00           H
ATOM    190  N   GLU B  22       9.261  16.086 -21.084  1.00 20.00           N
ATOM    191  CA  GLU B  22       8.173  16.812 -20.466  1.00 20.00           C
ATOM    192  C   GLU B  22       8.510  17.150 -19.056  1.00 20.00           C
ATOM    193  O   GLU B  22       7.758  17.709 -18.249  1.00 20.00           O
ATOM    194  CB  GLU B  22       7.191  15.563 -20.214  1.00 20.00           C
ATOM    195  CG  GLU B  22       6.188  15.181 -21.328  1.00 20.00           C
ATOM    196  CD  GLU B  22       5.497  13.820 -21.188  1.00 20.00           C
ATOM    197  OE1 GLU B  22       5.561  13.095 -20.199  1.00 20.00           O
ATOM    198  OE2 GLU B  22       4.784  13.500 -22.302  1.00 20.00           O
ATOM    199  H   GLU B  22       9.188  15.198 -21.594  1.00  0.00           H
ATOM    200  HA  GLU B  22       7.318  17.391 -20.966  1.00  0.00           H
ATOM    201 1HB  GLU B  22       6.514  15.755 -19.350  1.00  0.00           H
ATOM    202 2HB  GLU B  22       7.726  14.648 -19.867  1.00  0.00           H
ATOM    203 1HG  GLU B  22       6.637  15.282 -22.329  1.00  0.00           H
ATOM    204 2HG  GLU B  22       5.397  15.927 -21.320  1.00  0.00           H
ATOM    205  HE2 GLU B  22       4.375  12.646 -22.160  1.00  0.00           H
ATOM    206  N   VAL B  23       9.488  16.848 -18.745  1.00 20.00           N
ATOM    207  CA  VAL B  23      10.018  17.057 -17.427  1.00 20.00           C
ATOM    208  C   VAL B  23      10.596  18.445 -17.290  1.00 20.00           C
ATOM    209  O   VAL B  23      11.150  18.828 -16.336  1.00 20.00           O
ATOM    210  CB  VAL B  23      10.947  15.844 -17.028  1.00 20.00           C
ATOM    211  CG1 VAL B  23      11.685  15.997 -15.676  1.00 20.00           C
ATOM    212  CG2 VAL B  23      10.161  14.506 -16.960  1.00 20.00           C
ATOM    213  H   VAL B  23       9.980  16.323 -19.489  1.00  0.00           H
ATOM    214  HA  VAL B  23       9.233  17.024 -16.638  1.00  0.00           H
ATOM    215  HB  VAL B  23      11.735  15.733 -17.795  1.00  0.00           H
ATOM    216 1HG1 VAL B  23      12.235  15.084 -15.381  1.00  0.00           H
ATOM    217 2HG1 VAL B  23      12.441  16.802 -15.708  1.00  0.00           H
ATOM    218 3HG1 VAL B  23      10.993  16.242 -14.851  1.00  0.00           H
ATOM    219 1HG2 VAL B  23      10.769  13.653 -16.617  1.00  0.00           H
ATOM    220 2HG2 VAL B  23       9.299  14.566 -16.276  1.00  0.00           H
ATOM    221 3HG2 VAL B  23       9.755  14.219 -17.947  1.00  0.00           H
ATOM    222  N   ILE B  24      10.259  19.080 -18.343  1.00 20.00           N
ATOM    223  CA  ILE B  24      10.780  20.409 -18.505  1.00 20.00           C
ATOM    224  C   ILE B  24       9.689  21.464 -18.400  1.00 20.00           C
ATOM    225  O   ILE B  24       9.769  22.472 -17.749  1.00 20.00           O
ATOM    226  CB  ILE B  24      11.526  20.442 -19.899  1.00 20.00           C
ATOM    227  CG1 ILE B  24      12.738  19.451 -19.962  1.00 20.00           C
ATOM    228  CG2 ILE B  24      11.966  21.865 -20.293  1.00 20.00           C
ATOM    229  CD1 ILE B  24      13.756  19.568 -21.111  1.00 20.00           C
ATOM    230  H   ILE B  24       9.876  18.462 -19.074  1.00  0.00           H
ATOM    231  HA  ILE B  24      11.535  20.702 -17.746  1.00  0.00           H
ATOM    232  HB  ILE B  24      10.810  20.127 -20.687  1.00  0.00           H
ATOM    233 1HG1 ILE B  24      12.330  18.429 -19.977  1.00  0.00           H
ATOM    234 2HG1 ILE B  24      13.278  19.452 -19.008  1.00  0.00           H
ATOM    235 1HG2 ILE B  24      12.385  21.868 -21.312  1.00  0.00           H
ATOM    236 2HG2 ILE B  24      11.137  22.596 -20.315  1.00  0.00           H
ATOM    237 3HG2 ILE B  24      12.726  22.236 -19.587  1.00  0.00           H
ATOM    238 1HD1 ILE B  24      14.395  18.673 -21.168  1.00  0.00           H
ATOM    239 2HD1 ILE B  24      13.269  19.667 -22.094  1.00  0.00           H
ATOM    240 3HD1 ILE B  24      14.421  20.442 -20.992  1.00  0.00           H
ATOM    241  N   SER B  25       8.510  21.435 -19.019  1.00 20.00           N
ATOM    242  CA  SER B  25       7.874  22.683 -18.628  1.00 20.00           C
ATOM    243  C   SER B  25       8.120  22.749 -17.084  1.00 20.00           C
```

```
ATOM    244  O   SER B  25       7.499  23.564 -16.387  1.00 20.00           O
ATOM    245  CB  SER B  25       6.392  22.619 -19.070  1.00 20.00           C
ATOM    246  OG  SER B  25       5.695  21.502 -18.513  1.00 20.00           O
ATOM    247  H   SER B  25       8.069  20.534 -19.238  1.00  0.00           H
ATOM    248  HA  SER B  25       8.311  23.573 -19.138  1.00  0.00           H
ATOM    249 1HB  SER B  25       6.332  22.584 -20.176  1.00  0.00           H
ATOM    250 2HB  SER B  25       5.880  23.552 -18.779  1.00  0.00           H
ATOM    251  HG  SER B  25       4.923  21.343 -19.065  1.00  0.00           H
ATOM    252  N   ASP B  26       9.025  21.766 -16.526  1.00 20.00           N
ATOM    253  CA  ASP B  26       9.543  21.883 -15.222  1.00 20.00           C
ATOM    254  C   ASP B  26      10.332  23.133 -15.032  1.00 20.00           C
ATOM    255  O   ASP B  26      10.650  23.621 -13.995  1.00 20.00           O
ATOM    256  CB  ASP B  26      10.315  20.683 -14.685  1.00 20.00           C
ATOM    257  CG  ASP B  26      10.831  20.474 -13.270  1.00 20.00           C
ATOM    258  OD1 ASP B  26      11.377  21.334 -12.591  1.00 20.00           O
ATOM    259  OD2 ASP B  26      10.732  19.168 -12.889  1.00 20.00           O
ATOM    260  H   ASP B  26       9.002  20.871 -17.022  1.00  0.00           H
ATOM    261  HA  ASP B  26       8.673  21.995 -14.547  1.00  0.00           H
ATOM    262 1HB  ASP B  26      11.260  20.693 -15.252  1.00  0.00           H
ATOM    263 2HB  ASP B  26       9.703  19.795 -14.921  1.00  0.00           H
ATOM    264  HD2 ASP B  26      11.192  19.048 -12.058  1.00  0.00           H
ATOM    265  N   GLU B  27      10.676  23.595 -16.313  1.00 20.00           N
ATOM    266  CA  GLU B  27      10.979  24.872 -16.843  1.00 20.00           C
ATOM    267  C   GLU B  27      12.457  25.146 -16.723  1.00 20.00           C
ATOM    268  O   GLU B  27      12.940  25.839 -15.845  1.00 20.00           O
ATOM    269  CB  GLU B  27      10.206  26.082 -16.188  1.00 20.00           C
ATOM    270  CG  GLU B  27       8.684  26.034 -16.015  1.00 20.00           C
ATOM    271  CD  GLU B  27       7.877  27.232 -15.535  1.00 20.00           C
ATOM    272  OE1 GLU B  27       8.110  28.394 -15.840  1.00 20.00           O
ATOM    273  OE2 GLU B  27       6.766  26.846 -14.844  1.00 20.00           O
ATOM    274  H   GLU B  27      10.168  22.932 -17.043  1.00  0.00           H
ATOM    275  HA  GLU B  27      10.682  24.869 -17.911  1.00  0.00           H
ATOM    276 1HB  GLU B  27      10.478  27.014 -16.720  1.00  0.00           H
ATOM    277 2HB  GLU B  27      10.600  26.182 -15.166  1.00  0.00           H
ATOM    278 1HG  GLU B  27       8.494  25.247 -15.267  1.00  0.00           H
ATOM    279 2HG  GLU B  27       8.246  25.716 -16.973  1.00  0.00           H
ATOM    280  HE2 GLU B  27       6.111  27.564 -14.861  1.00  0.00           H
ATOM    281  N   HIS B  28      13.173  24.815 -17.644  1.00 20.00           N
ATOM    282  CA  HIS B  28      14.477  25.353 -17.845  1.00 20.00           C
ATOM    283  C   HIS B  28      15.130  25.132 -19.137  1.00 20.00           C
ATOM    284  O   HIS B  28      16.054  25.682 -19.477  1.00 20.00           O
ATOM    285  CB  HIS B  28      15.382  24.433 -16.880  1.00 20.00           C
ATOM    286  CG  HIS B  28      15.257  22.879 -17.013  1.00 20.00           C
ATOM    287  ND1 HIS B  28      14.277  22.146 -16.346  1.00 20.00           N
ATOM    288  CD2 HIS B  28      15.839  22.107 -18.034  1.00 20.00           C
ATOM    289  CE1 HIS B  28      14.340  20.984 -17.057  1.00 20.00           C
ATOM    290  NE2 HIS B  28      15.234  20.869 -18.093  1.00 20.00           N
ATOM    291  H   HIS B  28      13.059  23.795 -17.700  1.00  0.00           H
ATOM    292  HA  HIS B  28      14.564  26.429 -17.582  1.00  0.00           H
ATOM    293 1HB  HIS B  28      15.117  24.644 -15.838  1.00  0.00           H
ATOM    294 2HB  HIS B  28      16.449  24.727 -16.929  1.00  0.00           H
ATOM    295  HD2 HIS B  28      16.562  22.479 -18.749  1.00  0.00           H
ATOM    296  HE1 HIS B  28      13.703  20.154 -16.777  1.00  0.00           H
ATOM    297  HE2 HIS B  28      15.342  20.112 -18.781  1.00  0.00           H
ATOM    298  N   GLY B  29      14.405  24.262 -19.730  1.00 20.00           N
ATOM    299  CA  GLY B  29      14.678  23.692 -20.978  1.00 20.00           C
ATOM    300  C   GLY B  29      15.439  24.657 -21.892  1.00 20.00           C
ATOM    301  O   GLY B  29      14.869  25.646 -22.384  1.00 20.00           O
ATOM    302  H   GLY B  29      13.489  24.219 -19.268  1.00  0.00           H
ATOM    303 1HA  GLY B  29      13.739  23.468 -21.505  1.00  0.00           H
ATOM    304 2HA  GLY B  29      15.225  22.736 -20.874  1.00  0.00           H
ATOM    305  HC  GLY B  29      16.514  24.432 -22.015  1.00  0.00           H
ATOM    306  N   SER B  35      11.672  31.987 -16.117  1.00 20.00           N
```

```
ATOM    307  CA  SER B  35      10.540  31.156 -16.015  1.00 20.00           C
ATOM    308  C   SER B  35      10.769  30.449 -14.744  1.00 20.00           C
ATOM    309  O   SER B  35      11.006  31.054 -13.733  1.00 20.00           O
ATOM    310  CB  SER B  35      10.306  30.429 -17.376  1.00 20.00           C
ATOM    311  OG  SER B  35      11.315  29.457 -17.661  1.00 20.00           O
ATOM    312 1H   SER B  35      12.536  31.435 -16.139  1.00  0.00           H
ATOM    313 2H   SER B  35      11.651  32.529 -16.988  1.00  0.00           H
ATOM    314  HA  SER B  35       9.663  31.807 -15.843  1.00  0.00           H
ATOM    315 1HB  SER B  35      10.233  31.155 -18.211  1.00  0.00           H
ATOM    316 2HB  SER B  35       9.322  29.927 -17.363  1.00  0.00           H
ATOM    317  HG  SER B  35      12.132  29.941 -17.815  1.00  0.00           H
ATOM    318  N   TYR B  36      10.770  29.221 -14.740  1.00 20.00           N
ATOM    319  CA  TYR B  36      10.873  28.327 -13.657  1.00 20.00           C
ATOM    320  C   TYR B  36      11.072  29.084 -12.383  1.00 20.00           C
ATOM    321  O   TYR B  36      11.146  28.417 -11.310  1.00 20.00           O
ATOM    322  CB  TYR B  36      12.352  27.799 -13.859  1.00 20.00           C
ATOM    323  CG  TYR B  36      13.674  28.654 -13.689  1.00 20.00           C
ATOM    324  CD1 TYR B  36      14.308  28.734 -12.440  1.00 20.00           C
ATOM    325  CD2 TYR B  36      14.248  29.314 -14.784  1.00 20.00           C
ATOM    326  CE1 TYR B  36      15.490  29.456 -12.292  1.00 20.00           C
ATOM    327  CE2 TYR B  36      15.432  30.032 -14.634  1.00 20.00           C
ATOM    328  CZ  TYR B  36      16.051  30.101 -13.390  1.00 20.00           C
ATOM    329  OH  TYR B  36      17.217  30.804 -13.252  1.00 20.00           O
ATOM    330  H   TYR B  36      10.596  28.874 -15.692  1.00  0.00           H
ATOM    331  HA  TYR B  36      10.077  27.562 -13.596  1.00  0.00           H
ATOM    332  HC  TYR B  36      11.849  29.862 -12.341  1.00  0.00           H
ATOM    333 1HB  TYR B  36      12.391  27.575 -14.910  1.00  0.00           H
ATOM    334 2HB  TYR B  36      12.465  26.825 -13.348  1.00  0.00           H
ATOM    335  HD1 TYR B  36      13.892  28.218 -11.586  1.00  0.00           H
ATOM    336  HD2 TYR B  36      13.781  29.260 -15.756  1.00  0.00           H
ATOM    337  HE1 TYR B  36      15.969  29.502 -11.326  1.00  0.00           H
ATOM    338  HE2 TYR B  36      15.874  30.535 -15.481  1.00  0.00           H
ATOM    339  HH  TYR B  36      17.472  30.801 -12.327  1.00  0.00           H
ATOM    340  N   ASP B  39       6.766  29.564 -10.458  1.00 20.00           N
ATOM    341  CA  ASP B  39       5.865  28.673 -11.126  1.00 20.00           C
ATOM    342  C   ASP B  39       5.089  29.250 -12.211  1.00 20.00           C
ATOM    343  O   ASP B  39       5.222  30.345 -12.635  1.00 20.00           O
ATOM    344  CB  ASP B  39       5.087  27.997  -9.925  1.00 20.00           C
ATOM    345  CG  ASP B  39       5.861  26.944  -9.123  1.00 20.00           C
ATOM    346  OD1 ASP B  39       6.101  27.031  -7.924  1.00 20.00           O
ATOM    347  OD2 ASP B  39       6.229  25.886  -9.895  1.00 20.00           O
ATOM    348 1H   ASP B  39       7.376  30.032 -11.139  1.00  0.00           H
ATOM    349 2H   ASP B  39       6.245  30.321 -10.001  1.00  0.00           H
ATOM    350  HA  ASP B  39       6.515  27.902 -11.594  1.00  0.00           H
ATOM    351 1HB  ASP B  39       4.184  27.471 -10.279  1.00  0.00           H
ATOM    352 2HB  ASP B  39       4.683  28.754  -9.225  1.00  0.00           H
ATOM    353  HD2 ASP B  39       6.698  25.240  -9.362  1.00  0.00           H
ATOM    354  N   SER B  40       4.320  28.432 -12.701  1.00 20.00           N
ATOM    355  CA  SER B  40       3.414  28.862 -13.590  1.00 20.00           C
ATOM    356  C   SER B  40       3.597  28.379 -14.983  1.00 20.00           C
ATOM    357  O   SER B  40       4.725  28.244 -15.463  1.00 20.00           O
ATOM    358  CB  SER B  40       2.648  30.257 -13.499  1.00 20.00           C
ATOM    359  OG  SER B  40       3.433  31.301 -14.069  1.00 20.00           O
ATOM    360  H   SER B  40       4.330  27.494 -12.285  1.00  0.00           H
ATOM    361  HA  SER B  40       2.596  28.251 -13.136  1.00  0.00           H
ATOM    362 1HB  SER B  40       2.416  30.506 -12.444  1.00  0.00           H
ATOM    363 2HB  SER B  40       1.666  30.228 -14.011  1.00  0.00           H
ATOM    364  HG  SER B  40       4.299  31.191 -13.630  1.00  0.00           H
ATOM    365  N   ASP B  41       2.496  28.040 -15.450  1.00 20.00           N
ATOM    366  CA  ASP B  41       2.171  27.935 -16.838  1.00 20.00           C
ATOM    367  C   ASP B  41       1.619  26.569 -17.167  1.00 20.00           C
ATOM    368  O   ASP B  41       0.707  26.127 -16.500  1.00 20.00           O
ATOM    369  CB  ASP B  41       2.941  28.889 -17.854  1.00 20.00           C
```

```
ATOM    370  CG  ASP B  41       2.915  30.387 -17.539  1.00 20.00           C
ATOM    371  OD1 ASP B  41       1.901  31.074 -17.591  1.00 20.00           O
ATOM    372  OD2 ASP B  41       4.138  30.868 -17.182  1.00 20.00           O
ATOM    373  H   ASP B  41       1.729  28.114 -14.774  1.00  0.00           H
ATOM    374  HA  ASP B  41       1.195  28.465 -16.853  1.00  0.00           H
ATOM    375 1HB  ASP B  41       2.501  28.798 -18.863  1.00  0.00           H
ATOM    376 2HB  ASP B  41       3.987  28.555 -17.956  1.00  0.00           H
ATOM    377  HD2 ASP B  41       4.039  31.781 -16.906  1.00  0.00           H
ATOM    378  N   LEU B  42       2.062  26.226 -18.304  1.00 20.00           N
ATOM    379  CA  LEU B  42       2.243  24.814 -18.624  1.00 20.00           C
ATOM    380  C   LEU B  42       1.778  24.530 -20.019  1.00 20.00           C
ATOM    381  O   LEU B  42       0.890  25.205 -20.556  1.00 20.00           O
ATOM    382  CB  LEU B  42       1.755  23.667 -17.620  1.00 20.00           C
ATOM    383  CG  LEU B  42       2.439  23.521 -16.226  1.00 20.00           C
ATOM    384  CD1 LEU B  42       1.677  22.491 -15.373  1.00 20.00           C
ATOM    385  CD2 LEU B  42       3.917  23.108 -16.292  1.00 20.00           C
ATOM    386  H   LEU B  42       2.672  26.931 -18.730  1.00  0.00           H
ATOM    387  HA  LEU B  42       3.353  24.748 -18.579  1.00  0.00           H
ATOM    388 1HB  LEU B  42       1.828  22.676 -18.108  1.00  0.00           H
ATOM    389 2HB  LEU B  42       0.665  23.800 -17.475  1.00  0.00           H
ATOM    390  HG  LEU B  42       2.392  24.483 -15.683  1.00  0.00           H
ATOM    391 1HD1 LEU B  42       2.111  22.392 -14.360  1.00  0.00           H
ATOM    392 2HD1 LEU B  42       0.619  22.783 -15.233  1.00  0.00           H
ATOM    393 3HD1 LEU B  42       1.681  21.483 -15.828  1.00  0.00           H
ATOM    394 1HD2 LEU B  42       4.366  23.043 -15.284  1.00  0.00           H
ATOM    395 2HD2 LEU B  42       4.048  22.117 -16.761  1.00  0.00           H
ATOM    396 3HD2 LEU B  42       4.534  23.833 -16.850  1.00  0.00           H
ATOM    397  N   GLN B  43       2.517  23.637 -20.497  1.00 20.00           N
ATOM    398  CA  GLN B  43       2.167  22.789 -21.619  1.00 20.00           C
ATOM    399  C   GLN B  43       3.242  22.844 -22.643  1.00 20.00           C
ATOM    400  O   GLN B  43       4.438  22.678 -22.315  1.00 20.00           O
ATOM    401  CB  GLN B  43       0.631  22.496 -21.919  1.00 20.00           C
ATOM    402  CG  GLN B  43      -0.178  21.837 -20.769  1.00 20.00           C
ATOM    403  CD  GLN B  43      -1.648  21.585 -21.107  1.00 20.00           C
ATOM    404  OE1 GLN B  43      -2.038  20.512 -21.553  1.00 20.00           O
ATOM    405  NE2 GLN B  43      -2.510  22.553 -20.907  1.00 20.00           N
ATOM    406  H   GLN B  43       3.281  23.363 -19.874  1.00  0.00           H
ATOM    407  HA  GLN B  43       2.433  21.790 -21.217  1.00  0.00           H
ATOM    408 1HB  GLN B  43       0.555  21.824 -22.797  1.00  0.00           H
ATOM    409 2HB  GLN B  43       0.138  23.437 -22.235  1.00  0.00           H
ATOM    410 1HG  GLN B  43      -0.113  22.440 -19.844  1.00  0.00           H
ATOM    411 2HG  GLN B  43       0.276  20.864 -20.505  1.00  0.00           H
ATOM    412 1HE2 GLN B  43      -2.130  23.454 -20.602  1.00  0.00           H
ATOM    413 2HE2 GLN B  43      -3.468  22.326 -21.187  1.00  0.00           H
ATOM    414  N   LEU B  44       2.723  23.162 -23.717  1.00 20.00           N
ATOM    415  CA  LEU B  44       3.497  23.213 -24.909  1.00 20.00           C
ATOM    416  C   LEU B  44       3.616  24.654 -25.280  1.00 20.00           C
ATOM    417  O   LEU B  44       3.428  24.979 -26.392  1.00 20.00           O
ATOM    418  CB  LEU B  44       2.813  22.271 -25.956  1.00 20.00           C
ATOM    419  CG  LEU B  44       3.659  21.889 -27.202  1.00 20.00           C
ATOM    420  CD1 LEU B  44       4.826  20.943 -26.859  1.00 20.00           C
ATOM    421  CD2 LEU B  44       2.768  21.218 -28.263  1.00 20.00           C
ATOM    422  H   LEU B  44       1.706  23.290 -23.703  1.00  0.00           H
ATOM    423  HA  LEU B  44       4.539  22.856 -24.765  1.00  0.00           H
ATOM    424 1HB  LEU B  44       1.869  22.747 -26.287  1.00  0.00           H
ATOM    425 2HB  LEU B  44       2.484  21.331 -25.475  1.00  0.00           H
ATOM    426  HG  LEU B  44       4.075  22.813 -27.653  1.00  0.00           H
ATOM    427 1HD1 LEU B  44       4.478  20.012 -26.375  1.00  0.00           H
ATOM    428 2HD1 LEU B  44       5.396  20.651 -27.761  1.00  0.00           H
ATOM    429 3HD1 LEU B  44       5.554  21.411 -26.172  1.00  0.00           H
ATOM    430 1HD2 LEU B  44       1.947  21.885 -28.585  1.00  0.00           H
ATOM    431 2HD2 LEU B  44       3.339  20.962 -29.175  1.00  0.00           H
ATOM    432 3HD2 LEU B  44       2.306  20.285 -27.892  1.00  0.00           H
```

```
ATOM    433  N   GLU B  47       3.551  25.573 -24.187  1.00 20.00           N
ATOM    434  CA  GLU B  47       3.785  26.990 -24.318  1.00 20.00           C
ATOM    435  C   GLU B  47       2.950  27.789 -23.342  1.00 20.00           C
ATOM    436  O   GLU B  47       1.989  27.354 -22.763  1.00 20.00           O
ATOM    437  CB  GLU B  47       3.981  27.659 -25.739  1.00 20.00           C
ATOM    438  CG  GLU B  47       5.360  27.407 -26.406  1.00 20.00           C
ATOM    439  CD  GLU B  47       5.500  28.057 -27.779  1.00 20.00           C
ATOM    440  OE1 GLU B  47       5.893  29.206 -27.953  1.00 20.00           O
ATOM    441  OE2 GLU B  47       5.142  27.219 -28.791  1.00 20.00           O
ATOM    442  H   GLU B  47       3.445  25.108 -23.278  1.00  0.00           H
ATOM    443  HA  GLU B  47       4.781  27.103 -23.856  1.00  0.00           H
ATOM    444 1HB  GLU B  47       3.878  28.759 -25.678  1.00  0.00           H
ATOM    445 2HB  GLU B  47       3.151  27.364 -26.409  1.00  0.00           H
ATOM    446 1HG  GLU B  47       5.565  26.326 -26.505  1.00  0.00           H
ATOM    447 2HG  GLU B  47       6.169  27.797 -25.761  1.00  0.00           H
ATOM    448  HE2 GLU B  47       5.243  27.683 -29.623  1.00  0.00           H
ATOM    449  N   ARG B  48       2.874  29.140 -23.382  1.00 20.00           N
ATOM    450  CA  ARG B  48       3.028  30.420 -22.705  1.00 20.00           C
ATOM    451  C   ARG B  48       2.591  31.544 -23.593  1.00 20.00           C
ATOM    452  O   ARG B  48       1.580  31.416 -24.308  1.00 20.00           O
ATOM    453  CB  ARG B  48       4.467  30.618 -22.151  1.00 20.00           C
ATOM    454  CG  ARG B  48       4.827  29.682 -20.972  1.00 20.00           C
ATOM    455  CD  ARG B  48       5.936  28.656 -21.279  1.00 20.00           C
ATOM    456  NE  ARG B  48       5.899  27.545 -20.273  1.00 20.00           N
ATOM    457  CZ  ARG B  48       6.285  27.487 -19.073  1.00 20.00           C
ATOM    458  NH1 ARG B  48       6.868  28.486 -18.470  1.00 20.00           N
ATOM    459  NH2 ARG B  48       6.054  26.396 -18.422  1.00 20.00           N
ATOM    460  H   ARG B  48       2.096  29.247 -24.044  1.00  0.00           H
ATOM    461  HA  ARG B  48       2.323  30.430 -21.850  1.00  0.00           H
ATOM    462  HC  ARG B  48       3.214  32.457 -23.563  1.00  0.00           H
ATOM    463 1HB  ARG B  48       4.580  31.656 -21.783  1.00  0.00           H
ATOM    464 2HB  ARG B  48       5.209  30.537 -22.971  1.00  0.00           H
ATOM    465 1HG  ARG B  48       3.918  29.142 -20.642  1.00  0.00           H
ATOM    466 2HG  ARG B  48       5.118  30.281 -20.087  1.00  0.00           H
ATOM    467 1HD  ARG B  48       6.934  29.136 -21.298  1.00  0.00           H
ATOM    468 2HD  ARG B  48       5.802  28.227 -22.286  1.00  0.00           H
ATOM    469 1HH1 ARG B  48       7.148  28.373 -17.489  1.00  0.00           H
ATOM    470 2HH1 ARG B  48       6.984  29.305 -19.068  1.00  0.00           H
ATOM    471 1HH2 ARG B  48       6.311  26.366 -17.433  1.00  0.00           H
ATOM    472 2HH2 ARG B  48       5.592  25.695 -19.000  1.00  0.00           H
ATOM    473  N   PHE B  83       1.262  15.881 -24.607  1.00 20.00           N
ATOM    474  CA  PHE B  83       2.001  17.004 -23.893  1.00 20.00           C
ATOM    475  C   PHE B  83       2.395  18.200 -24.738  1.00 20.00           C
ATOM    476  O   PHE B  83       2.770  19.264 -24.235  1.00 20.00           O
ATOM    477  CB  PHE B  83       3.118  16.479 -22.964  1.00 20.00           C
ATOM    478  CG  PHE B  83       3.374  17.372 -21.725  1.00 20.00           C
ATOM    479  CD1 PHE B  83       2.694  17.116 -20.529  1.00 20.00           C
ATOM    480  CD2 PHE B  83       4.357  18.370 -21.752  1.00 20.00           C
ATOM    481  CE1 PHE B  83       3.000  17.838 -19.377  1.00 20.00           C
ATOM    482  CE2 PHE B  83       4.664  19.088 -20.599  1.00 20.00           C
ATOM    483  CZ  PHE B  83       3.988  18.817 -19.412  1.00 20.00           C
ATOM    484 1H   PHE B  83       0.465  16.244 -25.143  1.00  0.00           H
ATOM    485 2H   PHE B  83       1.875  15.413 -25.285  1.00  0.00           H
ATOM    486  HA  PHE B  83       1.227  17.425 -23.220  1.00  0.00           H
ATOM    487  HC  PHE B  83       2.325  18.029 -25.828  1.00  0.00           H
ATOM    488 1HB  PHE B  83       4.052  16.326 -23.540  1.00  0.00           H
ATOM    489 2HB  PHE B  83       2.863  15.459 -22.613  1.00  0.00           H
ATOM    490  HD1 PHE B  83       1.943  16.340 -20.482  1.00  0.00           H
ATOM    491  HD2 PHE B  83       4.901  18.575 -22.663  1.00  0.00           H
ATOM    492  HE1 PHE B  83       2.483  17.624 -18.453  1.00  0.00           H
ATOM    493  HE2 PHE B  83       5.443  19.836 -20.630  1.00  0.00           H
ATOM    494  HZ  PHE B  83       4.236  19.350 -18.507  1.00  0.00           H
ATOM    495  N   LEU B 209      18.035  -0.588 -17.442  1.00 20.00           N
```

```
ATOM    496  CA  LEU B 209      17.039   0.374 -16.979  1.00 20.00           C
ATOM    497  C   LEU B 209      16.036  -0.299 -16.122  1.00 20.00           C
ATOM    498  O   LEU B 209      15.469   0.322 -15.241  1.00 20.00           O
ATOM    499  CB  LEU B 209      16.400   1.129 -18.183  1.00 20.00           C
ATOM    500  CG  LEU B 209      17.104   2.435 -18.641  1.00 20.00           C
ATOM    501  CD1 LEU B 209      18.499   2.207 -19.252  1.00 20.00           C
ATOM    502  CD2 LEU B 209      16.238   3.207 -19.653  1.00 20.00           C
ATOM    503 1H   LEU B 209      17.614  -1.253 -18.101  1.00  0.00           H
ATOM    504 2H   LEU B 209      18.760  -0.104 -17.985  1.00  0.00           H
ATOM    505  HA  LEU B 209      17.553   1.110 -16.329  1.00  0.00           H
ATOM    506  HC  LEU B 209      15.843  -1.364 -16.354  1.00  0.00           H
ATOM    507 1HB  LEU B 209      15.372   1.422 -17.897  1.00  0.00           H
ATOM    508 2HB  LEU B 209      16.250   0.449 -19.045  1.00  0.00           H
ATOM    509  HG  LEU B 209      17.210   3.087 -17.755  1.00  0.00           H
ATOM    510 1HD1 LEU B 209      18.974   3.158 -19.561  1.00  0.00           H
ATOM    511 2HD1 LEU B 209      19.196   1.743 -18.530  1.00  0.00           H
ATOM    512 3HD1 LEU B 209      18.463   1.553 -20.143  1.00  0.00           H
ATOM    513 1HD2 LEU B 209      16.706   4.166 -19.943  1.00  0.00           H
ATOM    514 2HD2 LEU B 209      16.070   2.632 -20.583  1.00  0.00           H
ATOM    515 3HD2 LEU B 209      15.244   3.460 -19.238  1.00  0.00           H
ATOM    516  N   ILE B 212      16.889  -0.953 -12.423  1.00 20.00           N
ATOM    517  CA  ILE B 212      16.587   0.279 -11.711  1.00 20.00           C
ATOM    518  C   ILE B 212      15.114   0.467 -11.449  1.00 20.00           C
ATOM    519  O   ILE B 212      14.707   0.759 -10.358  1.00 20.00           O
ATOM    520  CB  ILE B 212      17.502   1.459 -12.215  1.00 20.00           C
ATOM    521  CG1 ILE B 212      18.886   1.397 -11.490  1.00 20.00           C
ATOM    522  CG2 ILE B 212      16.895   2.865 -12.018  1.00 20.00           C
ATOM    523  CD1 ILE B 212      20.026   2.205 -12.118  1.00 20.00           C
ATOM    524 1H   ILE B 212      16.676  -0.847 -13.422  1.00  0.00           H
ATOM    525 2H   ILE B 212      17.896  -1.148 -12.384  1.00  0.00           H
ATOM    526  HA  ILE B 212      16.934   0.071 -10.680  1.00  0.00           H
ATOM    527  HB  ILE B 212      17.663   1.339 -13.306  1.00  0.00           H
ATOM    528 1HG1 ILE B 212      19.235   0.347 -11.437  1.00  0.00           H
ATOM    529 2HG1 ILE B 212      18.769   1.699 -10.430  1.00  0.00           H
ATOM    530 1HG2 ILE B 212      17.545   3.673 -12.400  1.00  0.00           H
ATOM    531 2HG2 ILE B 212      15.923   2.978 -12.523  1.00  0.00           H
ATOM    532 3HG2 ILE B 212      16.707   3.062 -10.951  1.00  0.00           H
ATOM    533 1HD1 ILE B 212      20.953   2.123 -11.520  1.00  0.00           H
ATOM    534 2HD1 ILE B 212      20.260   1.822 -13.125  1.00  0.00           H
ATOM    535 3HD1 ILE B 212      19.791   3.281 -12.204  1.00  0.00           H
ATOM    536  N   CYS B 213      14.322   0.307 -12.443  1.00 20.00           N
ATOM    537  CA  CYS B 213      12.899   0.530 -12.319  1.00 20.00           C
ATOM    538  C   CYS B 213      12.272  -0.616 -11.670  1.00 20.00           C
ATOM    539  O   CYS B 213      11.083  -0.856 -11.813  1.00 20.00           O
ATOM    540  CB  CYS B 213      12.371   0.813 -13.758  1.00 20.00           C
ATOM    541  SG  CYS B 213      11.581   2.450 -13.781  1.00 20.00           S
ATOM    542  H   CYS B 213      14.786   0.151 -13.350  1.00  0.00           H
ATOM    543  HA  CYS B 213      12.695   1.446 -11.743  1.00  0.00           H
ATOM    544  HC  CYS B 213      12.925  -1.224 -11.013  1.00  0.00           H
ATOM    545 1HB  CYS B 213      11.628   0.065 -14.097  1.00  0.00           H
ATOM    546 2HB  CYS B 213      13.142   0.811 -14.551  1.00  0.00           H
ATOM    547  HG  CYS B 213      11.209   2.447 -15.055  1.00  0.00           H
ATOM    548  N   THR B 216      15.553  -0.661  -7.257  1.00 20.00           N
ATOM    549  CA  THR B 216      15.416   0.629  -6.590  1.00 20.00           C
ATOM    550  C   THR B 216      13.989   1.019  -6.484  1.00 20.00           C
ATOM    551  O   THR B 216      13.526   1.419  -5.438  1.00 20.00           O
ATOM    552  CB  THR B 216      16.403   1.697  -7.137  1.00 20.00           C
ATOM    553  OG1 THR B 216      16.176   1.992  -8.514  1.00 20.00           O
ATOM    554  CG2 THR B 216      17.895   1.357  -6.971  1.00 20.00           C
ATOM    555 1H   THR B 216      15.571  -0.554  -8.277  1.00  0.00           H
ATOM    556 2H   THR B 216      16.460  -1.081  -7.024  1.00  0.00           H
ATOM    557  HA  THR B 216      15.725   0.453  -5.541  1.00  0.00           H
ATOM    558  HB  THR B 216      16.228   2.616  -6.548  1.00  0.00           H
```

```
ATOM    559  HG1 THR B 216      15.516   1.381  -8.871  1.00  0.00           H
ATOM    560 1HG2 THR B 216      18.153   1.128  -5.920  1.00  0.00           H
ATOM    561 2HG2 THR B 216      18.190   0.486  -7.584  1.00  0.00           H
ATOM    562 3HG2 THR B 216      18.538   2.201  -7.280  1.00  0.00           H
ATOM    563  N   LEU B 217      13.355   0.883  -7.557  1.00 20.00           N
ATOM    564  CA  LEU B 217      11.961   1.134  -7.652  1.00 20.00           C
ATOM    565  C   LEU B 217      11.294  -0.133  -7.434  1.00 20.00           C
ATOM    566  O   LEU B 217      11.893  -1.207  -7.546  1.00 20.00           O
ATOM    567  CB  LEU B 217      11.650   1.864  -8.995  1.00 20.00           C
ATOM    568  CG  LEU B 217      11.770   3.409  -8.955  1.00 20.00           C
ATOM    569  CD1 LEU B 217      11.926   3.992 -10.366  1.00 20.00           C
ATOM    570  CD2 LEU B 217      10.556   4.067  -8.272  1.00 20.00           C
ATOM    571  H   LEU B 217      13.820   0.223  -8.191  1.00  0.00           H
ATOM    572  HA  LEU B 217      11.651   1.842  -6.848  1.00  0.00           H
ATOM    573 1HB  LEU B 217      10.645   1.595  -9.371  1.00  0.00           H
ATOM    574 2HB  LEU B 217      12.326   1.460  -9.756  1.00  0.00           H
ATOM    575  HG  LEU B 217      12.686   3.674  -8.390  1.00  0.00           H
ATOM    576 1HD1 LEU B 217      12.010   5.095 -10.349  1.00  0.00           H
ATOM    577 2HD1 LEU B 217      12.848   3.616 -10.844  1.00  0.00           H
ATOM    578 3HD1 LEU B 217      11.076   3.734 -11.026  1.00  0.00           H
ATOM    579 1HD2 LEU B 217      10.689   5.161  -8.197  1.00  0.00           H
ATOM    580 2HD2 LEU B 217       9.614   3.891  -8.825  1.00  0.00           H
ATOM    581 3HD2 LEU B 217      10.404   3.706  -7.241  1.00  0.00           H
ATOM    582  N   LYS B 218      10.088   0.003  -7.128  1.00 20.00           N
ATOM    583  CA  LYS B 218       9.298  -1.191  -7.004  1.00 20.00           C
ATOM    584  C   LYS B 218       8.448  -1.430  -8.225  1.00 20.00           C
ATOM    585  O   LYS B 218       8.305  -2.587  -8.724  1.00 20.00           O
ATOM    586  CB  LYS B 218       8.452  -1.017  -5.705  1.00 20.00           C
ATOM    587  CG  LYS B 218       7.630  -2.257  -5.278  1.00 20.00           C
ATOM    588  CD  LYS B 218       6.839  -2.015  -3.978  1.00 20.00           C
ATOM    589  CE  LYS B 218       6.001  -3.238  -3.574  1.00 20.00           C
ATOM    590  NZ  LYS B 218       5.260  -2.951  -2.330  1.00 20.00           N
ATOM    591  H   LYS B 218       9.771   0.946  -6.885  1.00  0.00           H
ATOM    592  HA  LYS B 218       9.889  -2.121  -6.850  1.00  0.00           H
ATOM    593 1HB  LYS B 218       7.770  -0.149  -5.805  1.00  0.00           H
ATOM    594 2HB  LYS B 218       9.126  -0.757  -4.863  1.00  0.00           H
ATOM    595 1HG  LYS B 218       8.304  -3.127  -5.149  1.00  0.00           H
ATOM    596 2HG  LYS B 218       6.931  -2.543  -6.088  1.00  0.00           H
ATOM    597 1HD  LYS B 218       6.175  -1.137  -4.104  1.00  0.00           H
ATOM    598 2HD  LYS B 218       7.539  -1.748  -3.162  1.00  0.00           H
ATOM    599 1HE  LYS B 218       6.649  -4.126  -3.433  1.00  0.00           H
ATOM    600 2HE  LYS B 218       5.287  -3.501  -4.379  1.00  0.00           H
ATOM    601 1HZ  LYS B 218       4.724  -3.769  -2.017  1.00  0.00           H
ATOM    602 2HZ  LYS B 218       5.906  -2.734  -1.562  1.00  0.00           H
ATOM    603  N   LEU B 219       7.704  -0.297  -8.881  1.00 20.00           N
ATOM    604  CA  LEU B 219       6.813  -0.377 -10.142  1.00 20.00           C
ATOM    605  C   LEU B 219       6.267  -1.705 -10.183  1.00 20.00           C
ATOM    606  O   LEU B 219       6.936  -2.679 -10.172  1.00 20.00           O
ATOM    607  CB  LEU B 219       7.546   0.025 -11.446  1.00 20.00           C
ATOM    608  CG  LEU B 219       8.027   1.492 -11.563  1.00 20.00           C
ATOM    609  CD1 LEU B 219       8.689   1.677 -12.932  1.00 20.00           C
ATOM    610  CD2 LEU B 219       6.913   2.544 -11.403  1.00 20.00           C
ATOM    611  H   LEU B 219       7.927   0.607  -8.456  1.00  0.00           H
ATOM    612  HA  LEU B 219       5.972   0.326  -9.993  1.00  0.00           H
ATOM    613 1HB  LEU B 219       6.884  -0.197 -12.307  1.00  0.00           H
ATOM    614 2HB  LEU B 219       8.414  -0.652 -11.580  1.00  0.00           H
ATOM    615  HG  LEU B 219       8.794   1.674 -10.785  1.00  0.00           H
ATOM    616 1HD1 LEU B 219       9.125   2.686 -13.034  1.00  0.00           H
ATOM    617 2HD1 LEU B 219       9.510   0.953 -13.083  1.00  0.00           H
ATOM    618 3HD1 LEU B 219       7.976   1.541 -13.766  1.00  0.00           H
ATOM    619 1HD2 LEU B 219       7.303   3.570 -11.543  1.00  0.00           H
ATOM    620 2HD2 LEU B 219       6.096   2.399 -12.135  1.00  0.00           H
ATOM    621 3HD2 LEU B 219       6.463   2.523 -10.395  1.00  0.00           H
```

```
ATOM    622  N   THR B 220       5.097  -2.067 -10.215  1.00 20.00           N
ATOM    623  CA  THR B 220       5.087  -3.527 -10.126  1.00 20.00           C
ATOM    624  C   THR B 220       5.446  -4.241 -11.471  1.00 20.00           C
ATOM    625  O   THR B 220       6.064  -5.348 -11.440  1.00 20.00           O
ATOM    626  CB  THR B 220       3.613  -3.961  -9.760  1.00 20.00           C
ATOM    627  OG1 THR B 220       2.633  -3.458 -10.675  1.00 20.00           O
ATOM    628  CG2 THR B 220       3.140  -3.579  -8.344  1.00 20.00           C
ATOM    629  H   THR B 220       4.364  -1.437  -9.877  1.00  0.00           H
ATOM    630  HA  THR B 220       5.599  -4.021  -9.255  1.00  0.00           H
ATOM    631  HB  THR B 220       3.565  -5.070  -9.798  1.00  0.00           H
ATOM    632  HG1 THR B 220       2.898  -3.737 -11.558  1.00  0.00           H
ATOM    633 1HG2 THR B 220       2.128  -3.977  -8.142  1.00  0.00           H
ATOM    634 2HG2 THR B 220       3.811  -3.980  -7.562  1.00  0.00           H
ATOM    635 3HG2 THR B 220       3.087  -2.484  -8.207  1.00  0.00           H
ATOM    636  N   THR B 221       5.010  -3.504 -12.571  1.00 20.00           N
ATOM    637  CA  THR B 221       5.039  -3.827 -14.104  1.00 20.00           C
ATOM    638  C   THR B 221       5.545  -2.539 -14.789  1.00 20.00           C
ATOM    639  O   THR B 221       4.789  -1.588 -15.024  1.00 20.00           O
ATOM    640  CB  THR B 221       3.636  -4.248 -14.638  1.00 20.00           C
ATOM    641  OG1 THR B 221       2.676  -3.223 -14.391  1.00 20.00           O
ATOM    642  CG2 THR B 221       3.087  -5.563 -14.063  1.00 20.00           C
ATOM    643  H   THR B 221       4.700  -2.580 -12.246  1.00  0.00           H
ATOM    644  HA  THR B 221       5.719  -4.680 -14.276  1.00  0.00           H
ATOM    645  HB  THR B 221       3.715  -4.384 -15.736  1.00  0.00           H
ATOM    646  HG1 THR B 221       3.100  -2.401 -14.678  1.00  0.00           H
ATOM    647 1HG2 THR B 221       2.107  -5.813 -14.509  1.00  0.00           H
ATOM    648 2HG2 THR B 221       3.764  -6.414 -14.260  1.00  0.00           H
ATOM    649 3HG2 THR B 221       2.938  -5.507 -12.969  1.00  0.00           H
ATOM    650  N   PRO B 222       6.819  -2.397 -15.191  1.00 20.00           N
ATOM    651  CA  PRO B 222       7.323  -1.169 -15.718  1.00 20.00           C
ATOM    652  C   PRO B 222       6.695  -0.873 -16.949  1.00 20.00           C
ATOM    653  O   PRO B 222       5.648  -1.439 -17.289  1.00 20.00           O
ATOM    654  CB  PRO B 222       8.867  -1.379 -15.534  1.00 20.00           C
ATOM    655  CG  PRO B 222       9.098  -2.876 -15.669  1.00 20.00           C
ATOM    656  CD  PRO B 222       7.856  -3.445 -14.997  1.00 20.00           C
ATOM    657  HA  PRO B 222       7.037  -0.345 -15.030  1.00  0.00           H
ATOM    658 1HB  PRO B 222       9.171  -1.052 -14.519  1.00  0.00           H
ATOM    659 2HB  PRO B 222       9.499  -0.800 -16.234  1.00  0.00           H
ATOM    660 1HG  PRO B 222      10.038  -3.216 -15.194  1.00  0.00           H
ATOM    661 2HG  PRO B 222       9.134  -3.171 -16.736  1.00  0.00           H
ATOM    662 1HD  PRO B 222       7.580  -4.413 -15.459  1.00  0.00           H
ATOM    663 2HD  PRO B 222       8.035  -3.623 -13.917  1.00  0.00           H
ATOM    664  N   THR B 223       7.343  -0.088 -17.621  1.00 20.00           N
ATOM    665  CA  THR B 223       6.769   0.339 -18.786  1.00 20.00           C
ATOM    666  C   THR B 223       7.753   1.099 -19.511  1.00 20.00           C
ATOM    667  O   THR B 223       8.689   1.648 -18.930  1.00 20.00           O
ATOM    668  CB  THR B 223       5.419   1.223 -18.634  1.00 20.00           C
ATOM    669  OG1 THR B 223       4.647   0.937 -17.471  1.00 20.00           O
ATOM    670  CG2 THR B 223       4.408   1.030 -19.781  1.00 20.00           C
ATOM    671  H   THR B 223       8.199   0.306 -17.217  1.00  0.00           H
ATOM    672  HA  THR B 223       6.507  -0.576 -19.380  1.00  0.00           H
ATOM    673  HB  THR B 223       5.667   2.299 -18.564  1.00  0.00           H
ATOM    674  HG1 THR B 223       4.768  -0.016 -17.313  1.00  0.00           H
ATOM    675 1HG2 THR B 223       3.500   1.639 -19.614  1.00  0.00           H
ATOM    676 2HG2 THR B 223       4.802   1.317 -20.770  1.00  0.00           H
ATOM    677 3HG2 THR B 223       4.073  -0.022 -19.852  1.00  0.00           H
ATOM    678  N   TYR B 224       7.510   1.084 -20.758  1.00 20.00           N
ATOM    679  CA  TYR B 224       8.246   1.904 -21.594  1.00 20.00           C
ATOM    680  C   TYR B 224       7.786   3.322 -21.200  1.00 20.00           C
ATOM    681  O   TYR B 224       8.460   4.256 -21.106  1.00 20.00           O
ATOM    682  CB  TYR B 224       7.998   1.581 -23.094  1.00 20.00           C
ATOM    683  CG  TYR B 224       8.634   0.268 -23.588  1.00 20.00           C
ATOM    684  CD1 TYR B 224      10.000   0.213 -23.887  1.00 20.00           C
```

```
ATOM    685  CD2 TYR B 224       7.855  -0.886 -23.729  1.00 20.00           C
ATOM    686  CE1 TYR B 224      10.579  -0.980 -24.315  1.00 20.00           C
ATOM    687  CE2 TYR B 224       8.436  -2.078 -24.157  1.00 20.00           C
ATOM    688  CZ  TYR B 224       9.796  -2.124 -24.449  1.00 20.00           C
ATOM    689  OH  TYR B 224      10.358  -3.299 -24.870  1.00 20.00           O
ATOM    690  H   TYR B 224       6.759   0.467 -21.082  1.00  0.00           H
ATOM    691  HA  TYR B 224       9.338   1.830 -21.400  1.00  0.00           H
ATOM    692 1HB  TYR B 224       8.404   2.407 -23.709  1.00  0.00           H
ATOM    693 2HB  TYR B 224       6.914   1.599 -23.324  1.00  0.00           H
ATOM    694  HD1 TYR B 224      10.619   1.094 -23.783  1.00  0.00           H
ATOM    695  HD2 TYR B 224       6.798  -0.867 -23.505  1.00  0.00           H
ATOM    696  HE1 TYR B 224      11.635  -1.011 -24.541  1.00  0.00           H
ATOM    697  HE2 TYR B 224       7.835  -2.969 -24.264  1.00  0.00           H
ATOM    698  HH  TYR B 224      11.291  -3.157 -25.038  1.00  0.00           H
ATOM    699  N   GLY B 225       6.606   3.740 -20.847  1.00 20.00           N
ATOM    700  CA  GLY B 225       6.574   5.207 -20.510  1.00 20.00           C
ATOM    701  C   GLY B 225       7.283   5.461 -19.203  1.00 20.00           C
ATOM    702  O   GLY B 225       7.881   6.509 -19.054  1.00 20.00           O
ATOM    703  H   GLY B 225       5.809   3.109 -20.979  1.00  0.00           H
ATOM    704 1HA  GLY B 225       5.520   5.499 -20.359  1.00  0.00           H
ATOM    705 2HA  GLY B 225       6.908   5.891 -21.321  1.00  0.00           H
ATOM    706  N   ASP B 226       7.352   4.615 -18.320  1.00 20.00           N
ATOM    707  CA  ASP B 226       7.911   4.852 -17.047  1.00 20.00           C
ATOM    708  C   ASP B 226       9.410   4.927 -17.088  1.00 20.00           C
ATOM    709  O   ASP B 226      10.053   5.601 -16.316  1.00 20.00           O
ATOM    710  CB  ASP B 226       7.334   3.838 -16.016  1.00 20.00           C
ATOM    711  CG  ASP B 226       7.202   4.435 -14.609  1.00 20.00           C
ATOM    712  OD1 ASP B 226       8.145   4.860 -13.952  1.00 20.00           O
ATOM    713  OD2 ASP B 226       5.911   4.467 -14.177  1.00 20.00           O
ATOM    714  H   ASP B 226       6.941   3.719 -18.600  1.00  0.00           H
ATOM    715  HA  ASP B 226       7.579   5.855 -16.706  1.00  0.00           H
ATOM    716 1HB  ASP B 226       7.956   2.925 -15.964  1.00  0.00           H
ATOM    717 2HB  ASP B 226       6.331   3.473 -16.316  1.00  0.00           H
ATOM    718  HD2 ASP B 226       5.886   4.862 -13.304  1.00  0.00           H
ATOM    719  N   LEU B 227       9.936   4.229 -18.065  1.00 20.00           N
ATOM    720  CA  LEU B 227      11.354   4.291 -18.306  1.00 20.00           C
ATOM    721  C   LEU B 227      11.749   5.668 -18.727  1.00 20.00           C
ATOM    722  O   LEU B 227      12.917   6.031 -18.605  1.00 20.00           O
ATOM    723  CB  LEU B 227      11.767   3.176 -19.326  1.00 20.00           C
ATOM    724  CG  LEU B 227      12.461   1.924 -18.723  1.00 20.00           C
ATOM    725  CD1 LEU B 227      11.549   1.051 -17.843  1.00 20.00           C
ATOM    726  CD2 LEU B 227      13.042   1.040 -19.841  1.00 20.00           C
ATOM    727  H   LEU B 227       9.290   3.609 -18.574  1.00  0.00           H
ATOM    728  HA  LEU B 227      11.899   4.105 -17.356  1.00  0.00           H
ATOM    729 1HB  LEU B 227      12.475   3.610 -20.061  1.00  0.00           H
ATOM    730 2HB  LEU B 227      10.915   2.864 -19.960  1.00  0.00           H
ATOM    731  HG  LEU B 227      13.300   2.278 -18.093  1.00  0.00           H
ATOM    732 1HD1 LEU B 227      12.131   0.311 -17.262  1.00  0.00           H
ATOM    733 2HD1 LEU B 227      10.971   1.648 -17.118  1.00  0.00           H
ATOM    734 3HD1 LEU B 227      10.816   0.480 -18.442  1.00  0.00           H
ATOM    735 1HD2 LEU B 227      13.579   0.162 -19.437  1.00  0.00           H
ATOM    736 2HD2 LEU B 227      12.254   0.656 -20.518  1.00  0.00           H
ATOM    737 3HD2 LEU B 227      13.766   1.592 -20.469  1.00  0.00           H
ATOM    738  N   ASN B 228      10.772   6.420 -19.188  1.00 20.00           N
ATOM    739  CA  ASN B 228      10.987   7.782 -19.597  1.00 20.00           C
ATOM    740  C   ASN B 228      11.062   8.714 -18.350  1.00 20.00           C
ATOM    741  O   ASN B 228      11.707   9.754 -18.362  1.00 20.00           O
ATOM    742  CB  ASN B 228      10.264   8.024 -20.947  1.00 20.00           C
ATOM    743  CG  ASN B 228      10.745   7.209 -22.161  1.00 20.00           C
ATOM    744  OD1 ASN B 228      11.731   7.547 -22.807  1.00 20.00           O
ATOM    745  ND2 ASN B 228      10.092   6.139 -22.535  1.00 20.00           N
ATOM    746  H   ASN B 228       9.846   5.969 -19.182  1.00  0.00           H
ATOM    747  HA  ASN B 228      12.044   7.875 -19.930  1.00  0.00           H
```

```
ATOM    748 1HB  ASN B 228      10.502   9.040 -21.285  1.00  0.00           H
ATOM    749 2HB  ASN B 228       9.168   7.960 -20.834  1.00  0.00           H
ATOM    750 1HD2 ASN B 228       9.424   5.734 -21.865  1.00  0.00           H
ATOM    751 2HD2 ASN B 228      10.548   5.658 -23.314  1.00  0.00           H
ATOM    752  N   HIS B 229      10.350   8.392 -17.246  1.00 20.00           N
ATOM    753  CA  HIS B 229      10.717   9.020 -15.962  1.00 20.00           C
ATOM    754  C   HIS B 229      12.252   8.701 -15.921  1.00 20.00           C
ATOM    755  O   HIS B 229      13.088   9.463 -16.144  1.00 20.00           O
ATOM    756  CB  HIS B 229       9.786   8.550 -14.814  1.00 20.00           C
ATOM    757  CG  HIS B 229       8.362   9.123 -14.913  1.00 20.00           C
ATOM    758  ND1 HIS B 229       7.930  10.194 -14.150  1.00 20.00           N
ATOM    759  CD2 HIS B 229       7.391   8.797 -15.884  1.00 20.00           C
ATOM    760  CE1 HIS B 229       6.723  10.436 -14.751  1.00 20.00           C
ATOM    761  NE2 HIS B 229       6.301   9.641 -15.782  1.00 20.00           N
ATOM    762  H   HIS B 229       9.973   7.436 -17.287  1.00  0.00           H
ATOM    763  HA  HIS B 229      10.623  10.123 -16.045  1.00  0.00           H
ATOM    764 1HB  HIS B 229      10.230   8.869 -13.854  1.00  0.00           H
ATOM    765 2HB  HIS B 229       9.743   7.449 -14.744  1.00  0.00           H
ATOM    766  HD2 HIS B 229       7.539   8.088 -16.684  1.00  0.00           H
ATOM    767  HE1 HIS B 229       6.120  11.272 -14.418  1.00  0.00           H
ATOM    768  HE2 HIS B 229       5.507   9.773 -16.421  1.00  0.00           H
ATOM    769  N   LEU B 230      12.789   7.501 -15.745  1.00 20.00           N
ATOM    770  CA  LEU B 230      14.305   7.338 -15.562  1.00 20.00           C
ATOM    771  C   LEU B 230      15.245   8.344 -16.242  1.00 20.00           C
ATOM    772  O   LEU B 230      16.032   9.049 -15.605  1.00 20.00           O
ATOM    773  CB  LEU B 230      14.680   5.843 -15.824  1.00 20.00           C
ATOM    774  CG  LEU B 230      14.672   4.864 -14.626  1.00 20.00           C
ATOM    775  CD1 LEU B 230      13.419   4.951 -13.742  1.00 20.00           C
ATOM    776  CD2 LEU B 230      14.813   3.429 -15.165  1.00 20.00           C
ATOM    777  H   LEU B 230      12.118   6.729 -15.658  1.00  0.00           H
ATOM    778  HA  LEU B 230      14.498   7.524 -14.488  1.00  0.00           H
ATOM    779 1HB  LEU B 230      15.691   5.785 -16.272  1.00  0.00           H
ATOM    780 2HB  LEU B 230      14.037   5.439 -16.624  1.00  0.00           H
ATOM    781  HG  LEU B 230      15.551   5.087 -13.989  1.00  0.00           H
ATOM    782 1HD1 LEU B 230      13.431   4.179 -12.954  1.00  0.00           H
ATOM    783 2HD1 LEU B 230      13.344   5.923 -13.220  1.00  0.00           H
ATOM    784 3HD1 LEU B 230      12.489   4.825 -14.325  1.00  0.00           H
ATOM    785 1HD2 LEU B 230      14.799   2.676 -14.359  1.00  0.00           H
ATOM    786 2HD2 LEU B 230      13.992   3.156 -15.853  1.00  0.00           H
ATOM    787 3HD2 LEU B 230      15.761   3.284 -15.715  1.00  0.00           H
ATOM    788  N   VAL B 231      15.193   8.383 -17.523  1.00 20.00           N
ATOM    789  CA  VAL B 231      16.102   9.185 -18.298  1.00 20.00           C
ATOM    790  C   VAL B 231      15.992  10.655 -18.038  1.00 20.00           C
ATOM    791  O   VAL B 231      16.975  11.356 -17.997  1.00 20.00           O
ATOM    792  CB  VAL B 231      15.949   8.825 -19.833  1.00 20.00           C
ATOM    793  CG1 VAL B 231      16.956   9.563 -20.751  1.00 20.00           C
ATOM    794  CG2 VAL B 231      16.082   7.319 -20.188  1.00 20.00           C
ATOM    795  H   VAL B 231      14.470   7.779 -17.935  1.00  0.00           H
ATOM    796  HA  VAL B 231      17.136   8.900 -18.015  1.00  0.00           H
ATOM    797  HB  VAL B 231      14.932   9.136 -20.149  1.00  0.00           H
ATOM    798 1HG1 VAL B 231      16.821   9.303 -21.818  1.00  0.00           H
ATOM    799 2HG1 VAL B 231      16.844  10.662 -20.691  1.00  0.00           H
ATOM    800 3HG1 VAL B 231      18.006   9.332 -20.488  1.00  0.00           H
ATOM    801 1HG2 VAL B 231      15.922   7.130 -21.266  1.00  0.00           H
ATOM    802 2HG2 VAL B 231      17.077   6.916 -19.930  1.00  0.00           H
ATOM    803 3HG2 VAL B 231      15.335   6.697 -19.660  1.00  0.00           H
ATOM    804  N   SER B 232      14.822  11.162 -17.885  1.00 20.00           N
ATOM    805  CA  SER B 232      14.721  12.569 -17.652  1.00 20.00           C
ATOM    806  C   SER B 232      15.729  12.938 -16.591  1.00 20.00           C
ATOM    807  O   SER B 232      16.343  13.982 -16.629  1.00 20.00           O
ATOM    808  CB  SER B 232      13.252  12.862 -17.279  1.00 20.00           C
ATOM    809  OG  SER B 232      12.813  12.185 -16.090  1.00 20.00           O
ATOM    810  H   SER B 232      14.036  10.496 -17.889  1.00  0.00           H
```

```
ATOM    811  HA  SER B 232      14.970  13.124 -18.579  1.00  0.00           H
ATOM    812 1HB  SER B 232      12.581  12.595 -18.116  1.00  0.00           H
ATOM    813 2HB  SER B 232      13.132  13.951 -17.148  1.00  0.00           H
ATOM    814  HG  SER B 232      12.929  11.231 -16.234  1.00  0.00           H
ATOM    815  N   ALA B 233      15.869  12.048 -15.683  1.00 20.00           N
ATOM    816  CA  ALA B 233      16.776  12.208 -14.570  1.00 20.00           C
ATOM    817  C   ALA B 233      18.178  12.446 -15.024  1.00 20.00           C
ATOM    818  O   ALA B 233      18.726  13.513 -14.735  1.00 20.00           O
ATOM    819  CB  ALA B 233      16.404  11.057 -13.615  1.00 20.00           C
ATOM    820  H   ALA B 233      15.380  11.166 -15.881  1.00  0.00           H
ATOM    821  HA  ALA B 233      16.471  13.131 -14.032  1.00  0.00           H
ATOM    822 1HB  ALA B 233      16.322  11.435 -12.595  1.00  0.00           H
ATOM    823 2HB  ALA B 233      15.405  10.602 -13.773  1.00  0.00           H
ATOM    824 3HB  ALA B 233      17.136  10.232 -13.640  1.00  0.00           H
ATOM    825  N   THR B 234      18.644  11.552 -15.861  1.00 20.00           N
ATOM    826  CA  THR B 234      19.968  11.533 -16.398  1.00 20.00           C
ATOM    827  C   THR B 234      20.147  12.695 -17.277  1.00 20.00           C
ATOM    828  O   THR B 234      21.363  13.017 -17.339  1.00 20.00           O
ATOM    829  CB  THR B 234      20.222  10.139 -17.064  1.00 20.00           C
ATOM    830  OG1 THR B 234      20.014   9.092 -16.119  1.00 20.00           O
ATOM    831  CG2 THR B 234      21.648   9.908 -17.591  1.00 20.00           C
ATOM    832  H   THR B 234      17.958  10.822 -16.092  1.00  0.00           H
ATOM    833  HA  THR B 234      20.682  11.624 -15.552  1.00  0.00           H
ATOM    834  HB  THR B 234      19.513  10.004 -17.906  1.00  0.00           H
ATOM    835  HG1 THR B 234      20.492   8.332 -16.459  1.00  0.00           H
ATOM    836 1HG2 THR B 234      21.773   8.901 -18.030  1.00  0.00           H
ATOM    837 2HG2 THR B 234      21.912  10.632 -18.385  1.00  0.00           H
ATOM    838 3HG2 THR B 234      22.404  10.017 -16.790  1.00  0.00           H
ATOM    839  N   MET B 235      19.348  13.310 -17.913  1.00 20.00           N
ATOM    840  CA  MET B 235      19.501  14.454 -18.724  1.00 20.00           C
ATOM    841  C   MET B 235      19.355  15.738 -17.938  1.00 20.00           C
ATOM    842  O   MET B 235      20.116  16.692 -18.086  1.00 20.00           O
ATOM    843  CB  MET B 235      18.599  14.334 -19.979  1.00 20.00           C
ATOM    844  CG  MET B 235      19.003  13.239 -20.990  1.00 20.00           C
ATOM    845  SD  MET B 235      17.903  13.292 -22.415  1.00 20.00           S
ATOM    846  CE  MET B 235      18.649  12.004 -23.426  1.00 20.00           C
ATOM    847  H   MET B 235      18.426  12.856 -17.832  1.00  0.00           H
ATOM    848  HA  MET B 235      20.539  14.491 -19.118  1.00  0.00           H
ATOM    849 1HB  MET B 235      18.620  15.297 -20.524  1.00  0.00           H
ATOM    850 2HB  MET B 235      17.545  14.187 -19.677  1.00  0.00           H
ATOM    851 1HG  MET B 235      18.952  12.235 -20.528  1.00  0.00           H
ATOM    852 2HG  MET B 235      20.046  13.381 -21.330  1.00  0.00           H
ATOM    853 1HE  MET B 235      19.686  12.270 -23.698  1.00  0.00           H
ATOM    854 2HE  MET B 235      18.668  11.039 -22.888  1.00  0.00           H
ATOM    855 3HE  MET B 235      18.075  11.865 -24.360  1.00  0.00           H
ATOM    856  N   SER B 236      18.388  15.880 -17.087  1.00 20.00           N
ATOM    857  CA  SER B 236      18.152  17.136 -16.350  1.00 20.00           C
ATOM    858  C   SER B 236      19.395  17.550 -15.569  1.00 20.00           C
ATOM    859  O   SER B 236      19.707  18.721 -15.450  1.00 20.00           O
ATOM    860  CB  SER B 236      16.875  16.995 -15.481  1.00 20.00           C
ATOM    861  OG  SER B 236      16.958  15.922 -14.537  1.00 20.00           O
ATOM    862  H   SER B 236      17.749  15.071 -17.024  1.00  0.00           H
ATOM    863  HA  SER B 236      17.953  17.940 -17.085  1.00  0.00           H
ATOM    864 1HB  SER B 236      15.988  16.847 -16.128  1.00  0.00           H
ATOM    865 2HB  SER B 236      16.683  17.941 -14.940  1.00  0.00           H
ATOM    866  HG  SER B 236      17.064  15.106 -15.045  1.00  0.00           H
ATOM    867  N   GLY B 237      20.103  16.593 -15.036  1.00 20.00           N
ATOM    868  CA  GLY B 237      21.326  16.874 -14.290  1.00 20.00           C
ATOM    869  C   GLY B 237      22.346  17.446 -15.183  1.00 20.00           C
ATOM    870  O   GLY B 237      22.950  18.457 -14.874  1.00 20.00           O
ATOM    871  H   GLY B 237      19.671  15.662 -15.114  1.00  0.00           H
ATOM    872 1HA  GLY B 237      21.722  15.902 -13.961  1.00  0.00           H
ATOM    873 2HA  GLY B 237      21.209  17.376 -13.335  1.00  0.00           H
```

```
ATOM    874  N   VAL B 238      22.405  16.895 -16.350  1.00 20.00           N
ATOM    875  CA  VAL B 238      23.422  17.332 -17.237  1.00 20.00           C
ATOM    876  C   VAL B 238      22.978  18.644 -17.837  1.00 20.00           C
ATOM    877  O   VAL B 238      23.806  19.539 -17.984  1.00 20.00           O
ATOM    878  CB  VAL B 238      23.787  16.189 -18.264  1.00 20.00           C
ATOM    879  CG1 VAL B 238      24.827  16.622 -19.325  1.00 20.00           C
ATOM    880  CG2 VAL B 238      24.340  14.901 -17.603  1.00 20.00           C
ATOM    881  H   VAL B 238      21.698  16.177 -16.543  1.00  0.00           H
ATOM    882  HA  VAL B 238      24.368  17.543 -16.691  1.00  0.00           H
ATOM    883  HB  VAL B 238      22.864  15.907 -18.811  1.00  0.00           H
ATOM    884 1HG1 VAL B 238      25.052  15.812 -20.045  1.00  0.00           H
ATOM    885 2HG1 VAL B 238      24.469  17.479 -19.926  1.00  0.00           H
ATOM    886 3HG1 VAL B 238      25.786  16.930 -18.867  1.00  0.00           H
ATOM    887 1HG2 VAL B 238      24.558  14.111 -18.347  1.00  0.00           H
ATOM    888 2HG2 VAL B 238      25.272  15.089 -17.037  1.00  0.00           H
ATOM    889 3HG2 VAL B 238      23.615  14.459 -16.895  1.00  0.00           H
ATOM    890  N   THR B 239      21.710  18.535 -18.522  1.00 20.00           N
ATOM    891  CA  THR B 239      21.194  19.638 -19.295  1.00 20.00           C
ATOM    892  C   THR B 239      20.688  20.756 -18.399  1.00 20.00           C
ATOM    893  O   THR B 239      20.921  21.925 -18.767  1.00 20.00           O
ATOM    894  CB  THR B 239      20.145  19.150 -20.351  1.00 20.00           C
ATOM    895  OG1 THR B 239      19.068  18.455 -19.727  1.00 20.00           O
ATOM    896  CG2 THR B 239      20.704  18.229 -21.448  1.00 20.00           C
ATOM    897  H   THR B 239      21.149  17.700 -18.252  1.00  0.00           H
ATOM    898  HA  THR B 239      22.032  20.074 -19.875  1.00  0.00           H
ATOM    899  HB  THR B 239      19.725  20.043 -20.857  1.00  0.00           H
ATOM    900  HG1 THR B 239      19.480  17.744 -19.211  1.00  0.00           H
ATOM    901 1HG2 THR B 239      19.922  17.945 -22.175  1.00  0.00           H
ATOM    902 2HG2 THR B 239      21.516  18.718 -22.017  1.00  0.00           H
ATOM    903 3HG2 THR B 239      21.116  17.291 -21.031  1.00  0.00           H
ATOM    904  N   THR B 240      19.646  20.585 -17.595  1.00 20.00           N
ATOM    905  CA  THR B 240      19.240  21.576 -16.634  1.00 20.00           C
ATOM    906  C   THR B 240      20.356  21.847 -15.666  1.00 20.00           C
ATOM    907  O   THR B 240      20.574  23.022 -15.249  1.00 20.00           O
ATOM    908  CB  THR B 240      18.057  21.093 -15.671  1.00 20.00           C
ATOM    909  OG1 THR B 240      17.130  20.219 -16.278  1.00 20.00           O
ATOM    910  CG2 THR B 240      17.364  22.148 -14.796  1.00 20.00           C
ATOM    911  H   THR B 240      19.465  19.595 -17.398  1.00  0.00           H
ATOM    912  HA  THR B 240      18.950  22.513 -17.148  1.00  0.00           H
ATOM    913  HB  THR B 240      18.433  20.441 -14.871  1.00  0.00           H
ATOM    914  HG1 THR B 240      16.556  20.755 -16.847  1.00  0.00           H
ATOM    915 1HG2 THR B 240      16.371  21.816 -14.444  1.00  0.00           H
ATOM    916 2HG2 THR B 240      17.955  22.357 -13.884  1.00  0.00           H
ATOM    917 3HG2 THR B 240      17.248  23.116 -15.306  1.00  0.00           H
ATOM    918  N   CYS B 241      20.959  20.855 -15.074  1.00 20.00           N
ATOM    919  CA  CYS B 241      21.805  21.126 -13.931  1.00 20.00           C
ATOM    920  C   CYS B 241      23.078  21.787 -14.339  1.00 20.00           C
ATOM    921  O   CYS B 241      23.748  21.301 -15.205  1.00 20.00           O
ATOM    922  CB  CYS B 241      21.872  20.106 -12.793  1.00 20.00           C
ATOM    923  SG  CYS B 241      20.264  19.261 -12.721  1.00 20.00           S
ATOM    924  H   CYS B 241      20.576  19.911 -15.287  1.00  0.00           H
ATOM    925  HA  CYS B 241      21.301  21.931 -13.352  1.00  0.00           H
ATOM    926  HC  CYS B 241      23.309  22.737 -13.824  1.00  0.00           H
ATOM    927 1HB  CYS B 241      22.086  20.607 -11.832  1.00  0.00           H
ATOM    928 2HB  CYS B 241      22.694  19.381 -12.869  1.00  0.00           H
ATOM    929  HG  CYS B 241      19.477  20.296 -12.996  1.00  0.00           H
ATOM    930  N   PHE B 244      20.974  25.498 -14.954  1.00 20.00           N
ATOM    931  CA  PHE B 244      20.179  26.180 -14.130  1.00 20.00           C
ATOM    932  C   PHE B 244      21.144  26.663 -13.125  1.00 20.00           C
ATOM    933  O   PHE B 244      22.193  26.109 -12.909  1.00 20.00           O
ATOM    934  CB  PHE B 244      19.202  25.109 -13.562  1.00 20.00           C
ATOM    935  CG  PHE B 244      17.807  25.472 -13.080  1.00 20.00           C
ATOM    936  CD1 PHE B 244      16.946  26.134 -13.955  1.00 20.00           C
```

```
ATOM    937  CD2 PHE B 244      17.274  24.746 -12.011  1.00 20.00           C
ATOM    938  CE1 PHE B 244      15.574  26.035 -13.781  1.00 20.00           C
ATOM    939  CE2 PHE B 244      15.893  24.664 -11.837  1.00 20.00           C
ATOM    940  CZ  PHE B 244      15.043  25.300 -12.728  1.00 20.00           C
ATOM    941 1H   PHE B 244      21.896  25.417 -14.506  1.00  0.00           H
ATOM    942 2H   PHE B 244      20.657  24.519 -15.058  1.00  0.00           H
ATOM    943  HA  PHE B 244      19.677  27.005 -14.671  1.00  0.00           H
ATOM    944  HC  PHE B 244      20.809  27.569 -12.590  1.00  0.00           H
ATOM    945 1HB  PHE B 244      19.729  24.465 -12.826  1.00  0.00           H
ATOM    946 2HB  PHE B 244      18.933  24.392 -14.359  1.00  0.00           H
ATOM    947  HD1 PHE B 244      17.321  26.628 -14.840  1.00  0.00           H
ATOM    948  HD2 PHE B 244      17.921  24.160 -11.374  1.00  0.00           H
ATOM    949  HE1 PHE B 244      14.924  26.482 -14.512  1.00  0.00           H
ATOM    950  HE2 PHE B 244      15.475  24.064 -11.045  1.00  0.00           H
ATOM    951  HZ  PHE B 244      13.972  25.199 -12.621  1.00  0.00           H
ATOM    952  N   GLY B 271      23.751   7.696 -13.507  1.00 20.00           N
ATOM    953  CA  GLY B 271      22.776   7.315 -12.576  1.00 20.00           C
ATOM    954  C   GLY B 271      22.022   8.494 -11.964  1.00 20.00           C
ATOM    955  O   GLY B 271      22.569   9.593 -11.928  1.00 20.00           O
ATOM    956 1H   GLY B 271      24.345   8.439 -13.118  1.00  0.00           H
ATOM    957 2H   GLY B 271      24.384   6.918 -13.729  1.00  0.00           H
ATOM    958 1HA  GLY B 271      23.259   6.751 -11.755  1.00  0.00           H
ATOM    959 2HA  GLY B 271      22.091   6.600 -13.074  1.00  0.00           H
ATOM    960  N   PHE B 272      20.883   8.121 -11.481  1.00 20.00           N
ATOM    961  CA  PHE B 272      20.090   9.099 -10.736  1.00 20.00           C
ATOM    962  C   PHE B 272      19.751   8.505  -9.445  1.00 20.00           C
ATOM    963  O   PHE B 272      19.238   7.392  -9.582  1.00 20.00           O
ATOM    964  CB  PHE B 272      18.937   9.736 -11.559  1.00 20.00           C
ATOM    965  CG  PHE B 272      18.684  11.233 -11.243  1.00 20.00           C
ATOM    966  CD1 PHE B 272      17.584  11.623 -10.477  1.00 20.00           C
ATOM    967  CD2 PHE B 272      19.481  12.223 -11.830  1.00 20.00           C
ATOM    968  CE1 PHE B 272      17.274  12.972 -10.305  1.00 20.00           C
ATOM    969  CE2 PHE B 272      19.163  13.572 -11.669  1.00 20.00           C
ATOM    970  CZ  PHE B 272      18.062  13.944 -10.907  1.00 20.00           C
ATOM    971  H   PHE B 272      20.666   7.120 -11.503  1.00  0.00           H
ATOM    972  HA  PHE B 272      20.746   9.962 -10.502  1.00  0.00           H
ATOM    973 1HB  PHE B 272      18.013   9.135 -11.457  1.00  0.00           H
ATOM    974 2HB  PHE B 272      19.175   9.662 -12.639  1.00  0.00           H
ATOM    975  HD1 PHE B 272      16.895  10.877 -10.116  1.00  0.00           H
ATOM    976  HD2 PHE B 272      20.317  11.948 -12.457  1.00  0.00           H
ATOM    977  HE1 PHE B 272      16.396  13.260  -9.745  1.00  0.00           H
ATOM    978  HE2 PHE B 272      19.726  14.330 -12.190  1.00  0.00           H
ATOM    979  HZ  PHE B 272      17.803  14.989 -10.814  1.00  0.00           H
ATOM    980  N   ALA B 273      20.081   9.081  -8.354  1.00 20.00           N
ATOM    981  CA  ALA B 273      19.730   8.491  -7.122  1.00 20.00           C
ATOM    982  C   ALA B 273      18.767   9.413  -6.387  1.00 20.00           C
ATOM    983  O   ALA B 273      19.039  10.590  -6.202  1.00 20.00           O
ATOM    984  CB  ALA B 273      21.050   8.299  -6.352  1.00 20.00           C
ATOM    985  H   ALA B 273      20.567   9.983  -8.436  1.00  0.00           H
ATOM    986  HA  ALA B 273      19.286   7.473  -7.221  1.00  0.00           H
ATOM    987 1HB  ALA B 273      20.824   8.045  -5.303  1.00  0.00           H
ATOM    988 2HB  ALA B 273      21.659   7.481  -6.780  1.00  0.00           H
ATOM    989 3HB  ALA B 273      21.694   9.192  -6.314  1.00  0.00           H
ATOM    990  N   PRO B 274      17.927   8.962  -5.794  1.00 20.00           N
ATOM    991  CA  PRO B 274      16.599   9.444  -5.515  1.00 20.00           C
ATOM    992  C   PRO B 274      15.625   8.598  -6.226  1.00 20.00           C
ATOM    993  O   PRO B 274      14.513   9.039  -6.615  1.00 20.00           O
ATOM    994  CB  PRO B 274      16.314  10.890  -5.938  1.00 20.00           C
ATOM    995  CG  PRO B 274      16.584  10.975  -7.425  1.00 20.00           C
ATOM    996  CD  PRO B 274      17.389   9.645  -7.521  1.00 20.00           C
ATOM    997  HA  PRO B 274      16.415   9.349  -4.429  1.00  0.00           H
ATOM    998 1HB  PRO B 274      16.913  11.585  -5.321  1.00  0.00           H
ATOM    999 2HB  PRO B 274      15.260  11.086  -5.823  1.00  0.00           H
```

```
ATOM   1000 1HG  PRO B 274      17.197  11.862  -7.672  1.00  0.00           H
ATOM   1001 2HG  PRO B 274      15.668  10.965  -8.048  1.00  0.00           H
ATOM   1002 1HD  PRO B 274      16.925   8.894  -8.208  1.00  0.00           H
ATOM   1003 2HD  PRO B 274      17.993  10.066  -8.377  1.00  0.00           H
ATOM   1004  N   LEU B 275      16.035   7.352  -6.418  1.00 20.00           N
ATOM   1005  CA  LEU B 275      15.231   6.341  -7.082  1.00 20.00           C
ATOM   1006  C   LEU B 275      14.075   5.971  -6.229  1.00 20.00           C
ATOM   1007  O   LEU B 275      13.042   5.505  -6.703  1.00 20.00           O
ATOM   1008  CB  LEU B 275      16.094   5.174  -7.604  1.00 20.00           C
ATOM   1009  CG  LEU B 275      16.980   5.553  -8.811  1.00 20.00           C
ATOM   1010  CD1 LEU B 275      18.167   4.592  -8.983  1.00 20.00           C
ATOM   1011  CD2 LEU B 275      16.182   5.724 -10.119  1.00 20.00           C
ATOM   1012  H   LEU B 275      16.993   7.183  -6.079  1.00  0.00           H
ATOM   1013  HA  LEU B 275      14.756   6.807  -7.969  1.00  0.00           H
ATOM   1014 1HB  LEU B 275      15.440   4.331  -7.896  1.00  0.00           H
ATOM   1015 2HB  LEU B 275      16.716   4.789  -6.773  1.00  0.00           H
ATOM   1016  HG  LEU B 275      17.412   6.534  -8.567  1.00  0.00           H
ATOM   1017 1HD1 LEU B 275      18.814   4.592  -8.086  1.00  0.00           H
ATOM   1018 2HD1 LEU B 275      17.857   3.553  -9.156  1.00  0.00           H
ATOM   1019 3HD1 LEU B 275      18.810   4.881  -9.834  1.00  0.00           H
ATOM   1020 1HD2 LEU B 275      16.848   5.890 -10.986  1.00  0.00           H
ATOM   1021 2HD2 LEU B 275      15.549   4.847 -10.341  1.00  0.00           H
ATOM   1022 3HD2 LEU B 275      15.509   6.599 -10.079  1.00  0.00           H
ATOM   1023  N   THR B 276      13.588   5.684  -5.379  1.00 20.00           N
ATOM   1024  CA  THR B 276      13.275   6.043  -4.031  1.00 20.00           C
ATOM   1025  C   THR B 276      12.404   4.990  -3.460  1.00 20.00           C
ATOM   1026  O   THR B 276      12.517   4.841  -2.147  1.00 20.00           O
ATOM   1027  CB  THR B 276      12.685   7.496  -3.808  1.00 20.00           C
ATOM   1028  OG1 THR B 276      12.443   8.229  -5.013  1.00 20.00           O
ATOM   1029  CG2 THR B 276      13.567   8.387  -2.924  1.00 20.00           C
ATOM   1030  H   THR B 276      12.872   5.427  -6.095  1.00  0.00           H
ATOM   1031  HA  THR B 276      14.225   5.965  -3.464  1.00  0.00           H
ATOM   1032  HB  THR B 276      11.707   7.425  -3.288  1.00  0.00           H
ATOM   1033  HG1 THR B 276      13.297   8.429  -5.422  1.00  0.00           H
ATOM   1034 1HG2 THR B 276      13.127   9.395  -2.806  1.00  0.00           H
ATOM   1035 2HG2 THR B 276      13.678   7.965  -1.907  1.00  0.00           H
ATOM   1036 3HG2 THR B 276      14.580   8.515  -3.341  1.00  0.00           H
ATOM   1037  N   SER B 277      11.357   4.383  -4.126  1.00 20.00           N
ATOM   1038  CA  SER B 277      10.194   3.623  -3.828  1.00 20.00           C
ATOM   1039  C   SER B 277       9.075   4.519  -3.324  1.00 20.00           C
ATOM   1040  O   SER B 277       9.346   5.312  -2.400  1.00 20.00           O
ATOM   1041  CB  SER B 277      10.518   2.257  -3.188  1.00 20.00           C
ATOM   1042  OG  SER B 277      10.990   1.325  -4.169  1.00 20.00           O
ATOM   1043  H   SER B 277      11.454   4.681  -5.102  1.00  0.00           H
ATOM   1044  HA  SER B 277       9.871   3.309  -4.842  1.00  0.00           H
ATOM   1045 1HB  SER B 277       9.627   1.836  -2.684  1.00  0.00           H
ATOM   1046 2HB  SER B 277      11.297   2.361  -2.422  1.00  0.00           H
ATOM   1047  HG  SER B 277      11.905   1.559  -4.396  1.00  0.00           H
ATOM   1048  N   ARG B 278       7.948   4.488  -3.969  1.00 20.00           N
ATOM   1049  CA  ARG B 278       6.813   5.326  -3.630  1.00 20.00           C
ATOM   1050  C   ARG B 278       6.601   5.351  -2.180  1.00 20.00           C
ATOM   1051  O   ARG B 278       6.681   6.394  -1.519  1.00 20.00           O
ATOM   1052  CB  ARG B 278       5.611   4.947  -4.551  1.00 20.00           C
ATOM   1053  CG  ARG B 278       4.341   5.811  -4.371  1.00 20.00           C
ATOM   1054  CD  ARG B 278       3.202   5.411  -5.327  1.00 20.00           C
ATOM   1055  NE  ARG B 278       2.118   6.429  -5.297  1.00 20.00           N
ATOM   1056  CZ  ARG B 278       2.068   7.531  -6.049  1.00 20.00           C
ATOM   1057  NH1 ARG B 278       2.977   7.856  -6.928  1.00 20.00           N
ATOM   1058  NH2 ARG B 278       1.060   8.325  -5.888  1.00 20.00           N
ATOM   1059  H   ARG B 278       7.921   3.840  -4.762  1.00  0.00           H
ATOM   1060  HA  ARG B 278       7.113   6.349  -3.887  1.00  0.00           H
ATOM   1061 1HB  ARG B 278       5.342   3.882  -4.406  1.00  0.00           H
ATOM   1062 2HB  ARG B 278       5.934   5.020  -5.609  1.00  0.00           H
```

```
ATOM   1063 1HG  ARG B 278       4.589   6.878  -4.515  1.00  0.00           H
ATOM   1064 2HG  ARG B 278       3.969   5.750  -3.329  1.00  0.00           H
ATOM   1065 1HD  ARG B 278       2.779   4.435  -5.020  1.00  0.00           H
ATOM   1066 2HD  ARG B 278       3.568   5.244  -6.360  1.00  0.00           H
ATOM   1067 1HH1 ARG B 278       2.857   8.736  -7.444  1.00  0.00           H
ATOM   1068 2HH1 ARG B 278       3.729   7.171  -6.991  1.00  0.00           H
ATOM   1069 1HH2 ARG B 278       1.024   9.170  -6.459  1.00  0.00           H
ATOM   1070 2HH2 ARG B 278       0.406   7.989  -5.178  1.00  0.00           H
ATOM   1071  N   GLY B 279       6.421   4.075  -1.727  1.00 20.00           N
ATOM   1072  CA  GLY B 279       6.187   3.904  -0.342  1.00 20.00           C
ATOM   1073  C   GLY B 279       7.453   4.053   0.477  1.00 20.00           C
ATOM   1074  O   GLY B 279       7.498   4.854   1.401  1.00 20.00           O
ATOM   1075  H   GLY B 279       6.459   3.336  -2.436  1.00  0.00           H
ATOM   1076 1HA  GLY B 279       5.760   2.900  -0.158  1.00  0.00           H
ATOM   1077 2HA  GLY B 279       5.417   4.608   0.035  1.00  0.00           H
ATOM   1078  N   SER B 280       8.456   3.258   0.127  1.00 20.00           N
ATOM   1079  CA  SER B 280       9.717   3.343   0.828  1.00 20.00           C
ATOM   1080  C   SER B 280      10.155   4.772   0.968  1.00 20.00           C
ATOM   1081  O   SER B 280      11.147   5.091   1.567  1.00 20.00           O
ATOM   1082  CB  SER B 280      10.843   2.421   0.308  1.00 20.00           C
ATOM   1083  OG  SER B 280      10.373   1.134  -0.100  1.00 20.00           O
ATOM   1084  H   SER B 280       8.325   2.708  -0.726  1.00  0.00           H
ATOM   1085  HA  SER B 280       9.524   2.993   1.862  1.00  0.00           H
ATOM   1086 1HB  SER B 280      11.601   2.289   1.102  1.00  0.00           H
ATOM   1087 2HB  SER B 280      11.396   2.928  -0.500  1.00  0.00           H
ATOM   1088  HG  SER B 280      11.139   0.624  -0.384  1.00  0.00           H
ATOM   1089  N   GLN B 281       9.252   5.561   0.533  1.00 20.00           N
ATOM   1090  CA  GLN B 281       9.557   6.943   0.357  1.00 20.00           C
ATOM   1091  C   GLN B 281      10.331   7.502   1.512  1.00 20.00           C
ATOM   1092  O   GLN B 281      11.224   8.284   1.394  1.00 20.00           O
ATOM   1093  CB  GLN B 281       8.489   8.017  -0.007  1.00 20.00           C
ATOM   1094  CG  GLN B 281       7.226   8.127   0.891  1.00 20.00           C
ATOM   1095  CD  GLN B 281       6.214   9.183   0.443  1.00 20.00           C
ATOM   1096  OE1 GLN B 281       6.087  10.258   1.019  1.00 20.00           O
ATOM   1097  NE2 GLN B 281       5.452   8.902  -0.586  1.00 20.00           N
ATOM   1098  H   GLN B 281       8.307   5.251   0.968  1.00  0.00           H
ATOM   1099  HA  GLN B 281      10.266   6.980  -0.497  1.00  0.00           H
ATOM   1100 1HB  GLN B 281       8.240   7.911  -1.073  1.00  0.00           H
ATOM   1101 2HB  GLN B 281       8.968   9.019  -0.027  1.00  0.00           H
ATOM   1102 1HG  GLN B 281       7.534   8.368   1.924  1.00  0.00           H
ATOM   1103 2HG  GLN B 281       6.714   7.152   0.965  1.00  0.00           H
ATOM   1104 1HE2 GLN B 281       5.708   8.035  -1.080  1.00  0.00           H
ATOM   1105 2HE2 GLN B 281       4.864   9.677  -0.903  1.00  0.00           H
ATOM   1106  N   GLN B 282      10.384   6.881   2.618  1.00 20.00           N
ATOM   1107  CA  GLN B 282      10.631   7.299   3.955  1.00 20.00           C
ATOM   1108  C   GLN B 282      12.093   7.130   4.324  1.00 20.00           C
ATOM   1109  O   GLN B 282      12.487   7.553   5.442  1.00 20.00           O
ATOM   1110  CB  GLN B 282       9.684   6.521   4.921  1.00 20.00           C
ATOM   1111  CG  GLN B 282       8.154   6.753   4.763  1.00 20.00           C
ATOM   1112  CD  GLN B 282       7.639   8.177   5.030  1.00 20.00           C
ATOM   1113  OE1 GLN B 282       8.288   9.032   5.624  1.00 20.00           O
ATOM   1114  NE2 GLN B 282       6.436   8.477   4.606  1.00 20.00           N
ATOM   1115  H   GLN B 282      10.669   5.917   2.299  1.00  0.00           H
ATOM   1116  HA  GLN B 282      10.414   8.382   4.052  1.00  0.00           H
ATOM   1117 1HB  GLN B 282       9.956   6.772   5.966  1.00  0.00           H
ATOM   1118 2HB  GLN B 282       9.889   5.435   4.839  1.00  0.00           H
ATOM   1119 1HG  GLN B 282       7.620   6.073   5.452  1.00  0.00           H
ATOM   1120 2HG  GLN B 282       7.848   6.431   3.748  1.00  0.00           H
ATOM   1121 1HE2 GLN B 282       5.931   7.759   4.080  1.00  0.00           H
ATOM   1122 2HE2 GLN B 282       6.173   9.454   4.762  1.00  0.00           H
ATOM   1123  N   TYR B 283      12.904   6.499   3.548  1.00 20.00           N
ATOM   1124  CA  TYR B 283      14.312   6.278   3.881  1.00 20.00           C
ATOM   1125  C   TYR B 283      15.129   7.428   3.421  1.00 20.00           C
```

```
ATOM   1126  O   TYR B 283      14.898   7.896   2.356  1.00 20.00           O
ATOM   1127  CB  TYR B 283      14.772   4.977   3.140  1.00 20.00           C
ATOM   1128  CG  TYR B 283      14.390   3.650   3.829  1.00 20.00           C
ATOM   1129  CD1 TYR B 283      13.149   3.053   3.587  1.00 20.00           C
ATOM   1130  CD2 TYR B 283      15.281   3.035   4.717  1.00 20.00           C
ATOM   1131  CE1 TYR B 283      12.801   1.862   4.219  1.00 20.00           C
ATOM   1132  CE2 TYR B 283      14.933   1.843   5.349  1.00 20.00           C
ATOM   1133  CZ  TYR B 283      13.696   1.257   5.099  1.00 20.00           C
ATOM   1134  OH  TYR B 283      13.361   0.087   5.726  1.00 20.00           O
ATOM   1135  H   TYR B 283      12.518   6.323   2.612  1.00  0.00           H
ATOM   1136  HA  TYR B 283      14.419   5.995   4.961  1.00  0.00           H
ATOM   1137 1HB  TYR B 283      15.874   4.982   3.020  1.00  0.00           H
ATOM   1138 2HB  TYR B 283      14.415   4.975   2.089  1.00  0.00           H
ATOM   1139  HD1 TYR B 283      12.446   3.521   2.918  1.00  0.00           H
ATOM   1140  HD2 TYR B 283      16.244   3.481   4.923  1.00  0.00           H
ATOM   1141  HE1 TYR B 283      11.837   1.415   4.025  1.00  0.00           H
ATOM   1142  HE2 TYR B 283      15.621   1.370   6.035  1.00  0.00           H
ATOM   1143  HH  TYR B 283      12.479  -0.171   5.454  1.00  0.00           H
ATOM   1144  N   ARG B 284      15.063   8.189   4.527  1.00 20.00           N
ATOM   1145  CA  ARG B 284      14.774   9.629   4.646  1.00 20.00           C
ATOM   1146  C   ARG B 284      15.990  10.067   3.754  1.00 20.00           C
ATOM   1147  O   ARG B 284      16.607   9.647   2.762  1.00 20.00           O
ATOM   1148  CB  ARG B 284      14.555   9.929   6.178  1.00 20.00           C
ATOM   1149  CG  ARG B 284      15.521   9.405   7.282  1.00 20.00           C
ATOM   1150  CD  ARG B 284      16.965   9.940   7.265  1.00 20.00           C
ATOM   1151  NE  ARG B 284      17.720   9.433   8.440  1.00 20.00           N
ATOM   1152  CZ  ARG B 284      18.465   8.327   8.475  1.00 20.00           C
ATOM   1153  NH1 ARG B 284      18.631   7.511   7.465  1.00 20.00           N
ATOM   1154  NH2 ARG B 284      19.059   8.047   9.590  1.00 20.00           N
ATOM   1155  H   ARG B 284      14.809   7.624   5.343  1.00  0.00           H
ATOM   1156  HA  ARG B 284      13.845   9.868   4.090  1.00  0.00           H
ATOM   1157 1HB  ARG B 284      13.555   9.530   6.434  1.00  0.00           H
ATOM   1158 2HB  ARG B 284      14.402  11.006   6.323  1.00  0.00           H
ATOM   1159 1HG  ARG B 284      15.543   8.299   7.268  1.00  0.00           H
ATOM   1160 2HG  ARG B 284      15.076   9.646   8.268  1.00  0.00           H
ATOM   1161 1HD  ARG B 284      16.959  11.047   7.315  1.00  0.00           H
ATOM   1162 2HD  ARG B 284      17.488   9.686   6.324  1.00  0.00           H
ATOM   1163 1HH1 ARG B 284      19.230   6.699   7.617  1.00  0.00           H
ATOM   1164 2HH1 ARG B 284      18.132   7.792   6.619  1.00  0.00           H
ATOM   1165 1HH2 ARG B 284      19.632   7.204   9.630  1.00  0.00           H
ATOM   1166 2HH2 ARG B 284      18.867   8.741  10.316  1.00  0.00           H
ATOM   1167  N   ALA B 285      16.473  11.028   4.173  1.00 20.00           N
ATOM   1168  CA  ALA B 285      15.898  12.314   3.805  1.00 20.00           C
ATOM   1169  C   ALA B 285      16.719  12.905   2.736  1.00 20.00           C
ATOM   1170  O   ALA B 285      17.484  13.834   2.968  1.00 20.00           O
ATOM   1171  CB  ALA B 285      15.835  13.206   5.077  1.00 20.00           C
ATOM   1172  H   ALA B 285      16.623  10.905   5.178  1.00  0.00           H
ATOM   1173  HA  ALA B 285      14.848  12.253   3.433  1.00  0.00           H
ATOM   1174 1HB  ALA B 285      15.524  14.237   4.820  1.00  0.00           H
ATOM   1175 2HB  ALA B 285      15.109  12.868   5.830  1.00  0.00           H
ATOM   1176 3HB  ALA B 285      16.818  13.300   5.579  1.00  0.00           H
ATOM   1177  N   LEU B 286      16.623  12.302   1.563  1.00 20.00           N
ATOM   1178  CA  LEU B 286      17.376  12.730   0.447  1.00 20.00           C
ATOM   1179  C   LEU B 286      18.847  12.824   0.815  1.00 20.00           C
ATOM   1180  O   LEU B 286      19.401  13.909   0.872  1.00 20.00           O
ATOM   1181  CB  LEU B 286      16.649  14.010  -0.085  1.00 20.00           C
ATOM   1182  CG  LEU B 286      15.082  14.036   0.000  1.00 20.00           C
ATOM   1183  CD1 LEU B 286      14.574  15.457   0.018  1.00 20.00           C
ATOM   1184  CD2 LEU B 286      14.478  13.067  -1.015  1.00 20.00           C
ATOM   1185  H   LEU B 286      16.186  11.372   1.620  1.00  0.00           H
ATOM   1186  HA  LEU B 286      17.283  11.958  -0.341  1.00  0.00           H
ATOM   1187 1HB  LEU B 286      16.980  14.204  -1.122  1.00  0.00           H
ATOM   1188 2HB  LEU B 286      17.040  14.865   0.501  1.00  0.00           H
```

```
ATOM   1189  HG  LEU B 286      14.711  13.681   0.979  1.00  0.00           H
ATOM   1190 1HD1 LEU B 286      13.469  15.485  -0.014  1.00  0.00           H
ATOM   1191 2HD1 LEU B 286      14.893  15.999   0.928  1.00  0.00           H
ATOM   1192 3HD1 LEU B 286      14.967  16.014  -0.840  1.00  0.00           H
ATOM   1193 1HD2 LEU B 286      13.377  13.152  -1.081  1.00  0.00           H
ATOM   1194 2HD2 LEU B 286      14.904  13.265  -2.007  1.00  0.00           H
ATOM   1195 3HD2 LEU B 286      14.705  12.014  -0.770  1.00  0.00           H
ATOM   1196  N   THR B 287      19.513  11.749   1.141  1.00 20.00           N
ATOM   1197  CA  THR B 287      20.844  11.801   1.701  1.00 20.00           C
ATOM   1198  C   THR B 287      21.851  12.126   0.685  1.00 20.00           C
ATOM   1199  O   THR B 287      21.716  11.836  -0.453  1.00 20.00           O
ATOM   1200  CB  THR B 287      20.902  10.894   2.990  1.00 20.00           C
ATOM   1201  OG1 THR B 287      19.972  11.396   3.954  1.00 20.00           O
ATOM   1202  CG2 THR B 287      22.222  10.793   3.766  1.00 20.00           C
ATOM   1203  H   THR B 287      18.958  10.887   1.103  1.00  0.00           H
ATOM   1204  HA  THR B 287      20.888  12.766   2.254  1.00  0.00           H
ATOM   1205  HB  THR B 287      20.555   9.877   2.770  1.00  0.00           H
ATOM   1206  HG1 THR B 287      19.177  11.644   3.469  1.00  0.00           H
ATOM   1207 1HG2 THR B 287      22.108  10.140   4.652  1.00  0.00           H
ATOM   1208 2HG2 THR B 287      23.039  10.365   3.163  1.00  0.00           H
ATOM   1209 3HG2 THR B 287      22.555  11.777   4.142  1.00  0.00           H
ATOM   1210  N   VAL B 288      23.184  12.577   1.370  1.00 20.00           N
ATOM   1211  CA  VAL B 288      24.233  12.654   0.406  1.00 20.00           C
ATOM   1212  C   VAL B 288      24.912  11.294   0.221  1.00 20.00           C
ATOM   1213  O   VAL B 288      25.130  10.852  -0.892  1.00 20.00           O
ATOM   1214  CB  VAL B 288      25.279  13.753   0.833  1.00 20.00           C
ATOM   1215  CG1 VAL B 288      26.488  13.894  -0.130  1.00 20.00           C
ATOM   1216  CG2 VAL B 288      24.679  15.177   0.943  1.00 20.00           C
ATOM   1217  H   VAL B 288      23.190  12.877   2.350  1.00  0.00           H
ATOM   1218  HA  VAL B 288      23.859  13.025  -0.561  1.00  0.00           H
ATOM   1219  HC  VAL B 288      25.408  10.940   1.147  1.00  0.00           H
ATOM   1220  HB  VAL B 288      25.684  13.487   1.831  1.00  0.00           H
ATOM   1221 1HG1 VAL B 288      27.204  14.669   0.205  1.00  0.00           H
ATOM   1222 2HG1 VAL B 288      27.071  12.958  -0.211  1.00  0.00           H
ATOM   1223 3HG1 VAL B 288      26.173  14.163  -1.156  1.00  0.00           H
ATOM   1224 1HG2 VAL B 288      25.421  15.921   1.289  1.00  0.00           H
ATOM   1225 2HG2 VAL B 288      24.274  15.538  -0.022  1.00  0.00           H
ATOM   1226 3HG2 VAL B 288      23.848  15.207   1.668  1.00  0.00           H
ATOM   1227  N   GLU B 290      23.798   9.088   0.934  1.00 20.00           N
ATOM   1228  CA  GLU B 290      22.723   8.413   0.256  1.00 20.00           C
ATOM   1229  C   GLU B 290      22.821   8.555  -1.203  1.00 20.00           C
ATOM   1230  O   GLU B 290      22.800   7.655  -1.891  1.00 20.00           O
ATOM   1231  CB  GLU B 290      21.294   8.361   0.845  1.00 20.00           C
ATOM   1232  CG  GLU B 290      20.269   7.366   0.227  1.00 20.00           C
ATOM   1233  CD  GLU B 290      20.624   5.879   0.288  1.00 20.00           C
ATOM   1234  OE1 GLU B 290      20.850   5.189  -0.702  1.00 20.00           O
ATOM   1235  OE2 GLU B 290      20.645   5.402   1.563  1.00 20.00           O
ATOM   1236 1H   GLU B 290      24.565   9.231   0.263  1.00  0.00           H
ATOM   1237 2H   GLU B 290      23.492  10.029   1.204  1.00  0.00           H
ATOM   1238  HA  GLU B 290      23.037   7.360   0.402  1.00  0.00           H
ATOM   1239 1HB  GLU B 290      20.855   9.360   0.725  1.00  0.00           H
ATOM   1240 2HB  GLU B 290      21.375   8.148   1.927  1.00  0.00           H
ATOM   1241 1HG  GLU B 290      20.084   7.629  -0.831  1.00  0.00           H
ATOM   1242 2HG  GLU B 290      19.290   7.496   0.724  1.00  0.00           H
ATOM   1243  HE2 GLU B 290      20.871   4.471   1.537  1.00  0.00           H
ATOM   1244  N   LEU B 291      23.133   9.745  -1.350  1.00 20.00           N
ATOM   1245  CA  LEU B 291      23.173  10.049  -2.620  1.00 20.00           C
ATOM   1246  C   LEU B 291      24.464   9.605  -3.275  1.00 20.00           C
ATOM   1247  O   LEU B 291      24.443   9.400  -4.498  1.00 20.00           O
ATOM   1248  CB  LEU B 291      22.922  11.546  -3.004  1.00 20.00           C
ATOM   1249  CG  LEU B 291      21.458  12.094  -3.130  1.00 20.00           C
ATOM   1250  CD1 LEU B 291      21.453  13.628  -3.056  1.00 20.00           C
ATOM   1251  CD2 LEU B 291      20.602  11.607  -4.264  1.00 20.00           C
```

```
ATOM   1252  H   LEU B 291      22.795  10.411  -0.643  1.00  0.00           H
ATOM   1253  HA  LEU B 291      22.370   9.579  -3.250  1.00  0.00           H
ATOM   1254  HC  LEU B 291      25.340   9.408  -2.632  1.00  0.00           H
ATOM   1255 1HB  LEU B 291      23.431  11.766  -3.951  1.00  0.00           H
ATOM   1256 2HB  LEU B 291      23.503  12.184  -2.332  1.00  0.00           H
ATOM   1257  HG  LEU B 291      20.813  11.700  -2.339  1.00  0.00           H
ATOM   1258 1HD1 LEU B 291      20.458  14.048  -3.287  1.00  0.00           H
ATOM   1259 2HD1 LEU B 291      21.733  13.986  -2.049  1.00  0.00           H
ATOM   1260 3HD1 LEU B 291      22.164  14.078  -3.771  1.00  0.00           H
ATOM   1261 1HD2 LEU B 291      20.636  12.256  -5.146  1.00  0.00           H
ATOM   1262 2HD2 LEU B 291      20.860  10.579  -4.565  1.00  0.00           H
ATOM   1263 3HD2 LEU B 291      19.529  11.598  -3.986  1.00  0.00           H
ATOM   1264  N   GLN B 294      24.427   5.745  -3.793  1.00 20.00           N
ATOM   1265  CA  GLN B 294      23.616   5.182  -4.857  1.00 20.00           C
ATOM   1266  C   GLN B 294      24.181   5.505  -6.175  1.00 20.00           C
ATOM   1267  O   GLN B 294      23.737   4.994  -7.184  1.00 20.00           O
ATOM   1268  CB  GLN B 294      22.147   5.508  -4.492  1.00 20.00           C
ATOM   1269  CG  GLN B 294      21.047   4.814  -5.340  1.00 20.00           C
ATOM   1270  CD  GLN B 294      19.603   5.064  -4.876  1.00 20.00           C
ATOM   1271  OE1 GLN B 294      18.805   5.724  -5.532  1.00 20.00           O
ATOM   1272  NE2 GLN B 294      19.197   4.534  -3.746  1.00 20.00           N
ATOM   1273 1H   GLN B 294      24.283   6.761  -3.745  1.00  0.00           H
ATOM   1274 2H   GLN B 294      24.099   5.401  -2.883  1.00  0.00           H
ATOM   1275  HA  GLN B 294      23.717   4.082  -4.776  1.00  0.00           H
ATOM   1276  HC  GLN B 294      24.999   6.252  -6.180  1.00  0.00           H
ATOM   1277 1HB  GLN B 294      22.016   6.600  -4.473  1.00  0.00           H
ATOM   1278 2HB  GLN B 294      21.973   5.215  -3.435  1.00  0.00           H
ATOM   1279 1HG  GLN B 294      21.222   3.723  -5.373  1.00  0.00           H
ATOM   1280 2HG  GLN B 294      21.127   5.141  -6.394  1.00  0.00           H
ATOM   1281 1HE2 GLN B 294      19.926   4.142  -3.142  1.00  0.00           H
ATOM   1282 2HE2 GLN B 294      18.251   4.818  -3.479  1.00  0.00           H
ATOM   1283  N   MET B 302      22.249   3.365 -14.461  1.00 20.00           N
ATOM   1284  CA  MET B 302      21.185   3.289 -15.469  1.00 20.00           C
ATOM   1285  C   MET B 302      21.790   3.003 -16.815  1.00 20.00           C
ATOM   1286  O   MET B 302      21.478   3.673 -17.759  1.00 20.00           O
ATOM   1287  CB  MET B 302      20.371   4.610 -15.324  1.00 20.00           C
ATOM   1288  CG  MET B 302      18.999   4.604 -16.024  1.00 20.00           C
ATOM   1289  SD  MET B 302      18.471   6.294 -16.374  1.00 20.00           S
ATOM   1290  CE  MET B 302      19.252   6.530 -17.985  1.00 20.00           C
ATOM   1291 1H   MET B 302      22.839   4.187 -14.633  1.00  0.00           H
ATOM   1292 2H   MET B 302      21.846   3.509 -13.528  1.00  0.00           H
ATOM   1293  HA  MET B 302      20.526   2.435 -15.228  1.00  0.00           H
ATOM   1294  HC  MET B 302      22.510   2.165 -16.843  1.00  0.00           H
ATOM   1295 1HB  MET B 302      20.977   5.448 -15.719  1.00  0.00           H
ATOM   1296 2HB  MET B 302      20.196   4.867 -14.260  1.00  0.00           H
ATOM   1297 1HG  MET B 302      18.238   4.097 -15.402  1.00  0.00           H
ATOM   1298 2HG  MET B 302      19.043   4.047 -16.976  1.00  0.00           H
ATOM   1299 1HE  MET B 302      19.060   7.545 -18.374  1.00  0.00           H
ATOM   1300 2HE  MET B 302      20.346   6.382 -17.924  1.00  0.00           H
ATOM   1301 3HE  MET B 302      18.857   5.803 -18.718  1.00  0.00           H
ATOM   1302  N   ARG B 320      22.309  18.342  -6.951  1.00 20.00           N
ATOM   1303  CA  ARG B 320      21.581  19.593  -6.911  1.00 20.00           C
ATOM   1304  C   ARG B 320      20.461  19.561  -5.948  1.00 20.00           C
ATOM   1305  O   ARG B 320      19.269  19.816  -6.278  1.00 20.00           O
ATOM   1306  CB  ARG B 320      21.270  20.218  -8.317  1.00 20.00           C
ATOM   1307  CG  ARG B 320      20.122  19.614  -9.166  1.00 20.00           C
ATOM   1308  CD  ARG B 320      19.451  20.534 -10.190  1.00 20.00           C
ATOM   1309  NE  ARG B 320      18.304  19.769 -10.782  1.00 20.00           N
ATOM   1310  CZ  ARG B 320      17.164  20.260 -11.251  1.00 20.00           C
ATOM   1311  NH1 ARG B 320      16.769  21.482 -11.076  1.00 20.00           N
ATOM   1312  NH2 ARG B 320      16.407  19.462 -11.932  1.00 20.00           N
ATOM   1313 1H   ARG B 320      21.721  17.598  -7.347  1.00  0.00           H
ATOM   1314 2H   ARG B 320      23.112  18.416  -7.586  1.00  0.00           H
```

```
ATOM   1315  HA  ARG B 320      22.307  20.321  -6.493  1.00  0.00           H
ATOM   1316 1HB  ARG B 320      22.193  20.251  -8.928  1.00  0.00           H
ATOM   1317 2HB  ARG B 320      21.027  21.285  -8.143  1.00  0.00           H
ATOM   1318 1HG  ARG B 320      19.292  19.317  -8.510  1.00  0.00           H
ATOM   1319 2HG  ARG B 320      20.461  18.678  -9.651  1.00  0.00           H
ATOM   1320 1HD  ARG B 320      20.166  20.841 -10.955  1.00  0.00           H
ATOM   1321 2HD  ARG B 320      19.193  21.514  -9.776  1.00  0.00           H
ATOM   1322 1HH1 ARG B 320      15.851  21.733 -11.443  1.00  0.00           H
ATOM   1323 2HH1 ARG B 320      17.333  21.955 -10.363  1.00  0.00           H
ATOM   1324 1HH2 ARG B 320      15.563  19.851 -12.352  1.00  0.00           H
ATOM   1325 2HH2 ARG B 320      16.828  18.537 -12.050  1.00  0.00           H
ATOM   1326  N   GLY B 321      20.796  19.432  -4.693  1.00 20.00           N
ATOM   1327  CA  GLY B 321      19.776  19.437  -3.670  1.00 20.00           C
ATOM   1328  C   GLY B 321      19.782  20.627  -2.795  1.00 20.00           C
ATOM   1329  O   GLY B 321      19.039  20.753  -1.814  1.00 20.00           O
ATOM   1330  H   GLY B 321      21.762  19.110  -4.551  1.00  0.00           H
ATOM   1331 1HA  GLY B 321      19.960  18.579  -3.012  1.00  0.00           H
ATOM   1332 2HA  GLY B 321      18.775  19.290  -4.048  1.00  0.00           H
ATOM   1333  HC  GLY B 321      20.504  21.413  -3.092  1.00  0.00           H
ATOM   1334  N   MET B 323      22.260  21.160  -0.702  1.00 20.00           N
ATOM   1335  CA  MET B 323      23.111  20.730   0.379  1.00 20.00           C
ATOM   1336  C   MET B 323      24.443  21.390   0.258  1.00 20.00           C
ATOM   1337  O   MET B 323      24.806  22.066  -0.642  1.00 20.00           O
ATOM   1338  CB  MET B 323      23.157  19.190   0.500  1.00 20.00           C
ATOM   1339  CG  MET B 323      23.622  18.672   1.881  1.00 20.00           C
ATOM   1340  SD  MET B 323      22.553  17.321   2.417  1.00 20.00           S
ATOM   1341  CE  MET B 323      23.261  16.983   4.038  1.00 20.00           C
ATOM   1342 1H   MET B 323      22.222  22.186  -0.723  1.00  0.00           H
ATOM   1343 2H   MET B 323      22.697  20.898  -1.593  1.00  0.00           H
ATOM   1344  HA  MET B 323      22.646  21.129   1.302  1.00  0.00           H
ATOM   1345  HC  MET B 323      25.094  21.181   1.125  1.00  0.00           H
ATOM   1346 1HB  MET B 323      23.766  18.743  -0.310  1.00  0.00           H
ATOM   1347 2HB  MET B 323      22.143  18.788   0.321  1.00  0.00           H
ATOM   1348 1HG  MET B 323      23.577  19.457   2.660  1.00  0.00           H
ATOM   1349 2HG  MET B 323      24.673  18.329   1.846  1.00  0.00           H
ATOM   1350 1HE  MET B 323      22.706  16.169   4.537  1.00  0.00           H
ATOM   1351 2HE  MET B 323      24.319  16.674   3.952  1.00  0.00           H
ATOM   1352 3HE  MET B 323      23.211  17.876   4.686  1.00  0.00           H
ATOM   1353  N   ILE B 358      18.835  24.056  -7.329  1.00 20.00           N
ATOM   1354  CA  ILE B 358      17.416  23.836  -7.269  1.00 20.00           C
ATOM   1355  C   ILE B 358      17.145  22.351  -7.364  1.00 20.00           C
ATOM   1356  O   ILE B 358      17.607  21.728  -8.306  1.00 20.00           O
ATOM   1357  CB  ILE B 358      16.624  24.739  -8.287  1.00 20.00           C
ATOM   1358  CG1 ILE B 358      16.849  26.274  -8.073  1.00 20.00           C
ATOM   1359  CG2 ILE B 358      15.093  24.461  -8.263  1.00 20.00           C
ATOM   1360  CD1 ILE B 358      16.425  27.194  -9.233  1.00 20.00           C
ATOM   1361 1H   ILE B 358      19.312  23.490  -6.617  1.00  0.00           H
ATOM   1362 2H   ILE B 358      19.200  23.719  -8.227  1.00  0.00           H
ATOM   1363  HA  ILE B 358      17.152  24.285  -6.300  1.00  0.00           H
ATOM   1364  HB  ILE B 358      17.006  24.478  -9.287  1.00  0.00           H
ATOM   1365 1HG1 ILE B 358      17.923  26.470  -7.891  1.00  0.00           H
ATOM   1366 2HG1 ILE B 358      16.350  26.603  -7.141  1.00  0.00           H
ATOM   1367 1HG2 ILE B 358      14.545  25.050  -9.021  1.00  0.00           H
ATOM   1368 2HG2 ILE B 358      14.855  23.402  -8.476  1.00  0.00           H
ATOM   1369 3HG2 ILE B 358      14.640  24.702  -7.284  1.00  0.00           H
ATOM   1370 1HD1 ILE B 358      16.643  28.253  -9.002  1.00  0.00           H
ATOM   1371 2HD1 ILE B 358      16.963  26.952 -10.168  1.00  0.00           H
ATOM   1372 3HD1 ILE B 358      15.344  27.132  -9.451  1.00  0.00           H
ATOM   1373  N   PRO B 359      16.577  21.810  -6.385  1.00 20.00           N
ATOM   1374  CA  PRO B 359      16.368  20.384  -6.464  1.00 20.00           C
ATOM   1375  C   PRO B 359      15.041  20.034  -7.119  1.00 20.00           C
ATOM   1376  O   PRO B 359      14.059  20.757  -6.897  1.00 20.00           O
ATOM   1377  CB  PRO B 359      16.127  20.226  -5.014  1.00 20.00           C
```

```
ATOM   1378  CG  PRO B 359      15.438  21.408  -4.342  1.00 20.00           C
ATOM   1379  CD  PRO B 359      16.074  22.501  -5.147  1.00 20.00           C
ATOM   1380  HA  PRO B 359      17.279  19.890  -6.771  1.00  0.00           H
ATOM   1381 1HB  PRO B 359      17.084  20.073  -4.517  1.00  0.00           H
ATOM   1382 2HB  PRO B 359      15.524  19.312  -4.931  1.00  0.00           H
ATOM   1383 1HG  PRO B 359      15.645  21.475  -3.257  1.00  0.00           H
ATOM   1384 2HG  PRO B 359      14.341  21.379  -4.484  1.00  0.00           H
ATOM   1385 1HD  PRO B 359      15.336  23.297  -5.369  1.00  0.00           H
ATOM   1386 2HD  PRO B 359      16.910  22.948  -4.571  1.00  0.00           H
ATOM   1387  N   PRO B 360      15.535  19.068  -7.903  1.00 20.00           N
ATOM   1388  CA  PRO B 360      14.468  18.708  -8.821  1.00 20.00           C
ATOM   1389  C   PRO B 360      13.088  18.891  -8.237  1.00 20.00           C
ATOM   1390  O   PRO B 360      12.854  18.503  -7.128  1.00 20.00           O
ATOM   1391  CB  PRO B 360      14.674  17.288  -9.343  1.00 20.00           C
ATOM   1392  CG  PRO B 360      16.063  17.011  -8.866  1.00 20.00           C
ATOM   1393  CD  PRO B 360      16.124  17.763  -7.515  1.00 20.00           C
ATOM   1394  HA  PRO B 360      14.602  19.380  -9.697  1.00  0.00           H
ATOM   1395 1HB  PRO B 360      14.567  17.201 -10.441  1.00  0.00           H
ATOM   1396 2HB  PRO B 360      13.984  16.561  -8.878  1.00  0.00           H
ATOM   1397 1HG  PRO B 360      16.822  17.411  -9.571  1.00  0.00           H
ATOM   1398 2HG  PRO B 360      16.208  15.920  -8.829  1.00  0.00           H
ATOM   1399 1HD  PRO B 360      15.542  17.272  -6.711  1.00  0.00           H
ATOM   1400 2HD  PRO B 360      17.154  17.874  -7.145  1.00  0.00           H
ATOM   1401  N   ARG B 369      12.205  19.481  -9.015  1.00 20.00           N
ATOM   1402  CA  ARG B 369      10.833  19.718  -8.654  1.00 20.00           C
ATOM   1403  C   ARG B 369      10.259  18.496  -8.074  1.00 20.00           C
ATOM   1404  O   ARG B 369      10.023  17.494  -8.765  1.00 20.00           O
ATOM   1405  CB  ARG B 369      10.100  20.356  -9.857  1.00 20.00           C
ATOM   1406  CG  ARG B 369       8.757  21.093  -9.618  1.00 20.00           C
ATOM   1407  CD  ARG B 369       8.526  22.167 -10.705  1.00 20.00           C
ATOM   1408  NE  ARG B 369       7.104  22.582 -10.806  1.00 20.00           N
ATOM   1409  CZ  ARG B 369       6.599  23.323 -11.797  1.00 20.00           C
ATOM   1410  NH1 ARG B 369       7.310  23.861 -12.759  1.00 20.00           N
ATOM   1411  NH2 ARG B 369       5.320  23.514 -11.807  1.00 20.00           N
ATOM   1412  H   ARG B 369      12.606  19.860  -9.877  1.00  0.00           H
ATOM   1413  HA  ARG B 369      10.877  20.550  -7.914  1.00  0.00           H
ATOM   1414 1HB  ARG B 369       9.938  19.593 -10.636  1.00  0.00           H
ATOM   1415 2HB  ARG B 369      10.793  21.103 -10.293  1.00  0.00           H
ATOM   1416 1HG  ARG B 369       8.729  21.580  -8.624  1.00  0.00           H
ATOM   1417 2HG  ARG B 369       7.927  20.358  -9.609  1.00  0.00           H
ATOM   1418 1HD  ARG B 369       8.855  21.777 -11.688  1.00  0.00           H
ATOM   1419 2HD  ARG B 369       9.169  23.048 -10.510  1.00  0.00           H
ATOM   1420 1HH1 ARG B 369       6.812  24.410 -13.463  1.00  0.00           H
ATOM   1421 2HH1 ARG B 369       8.317  23.703 -12.678  1.00  0.00           H
ATOM   1422 1HH2 ARG B 369       4.929  24.068 -12.570  1.00  0.00           H
ATOM   1423 2HH2 ARG B 369       4.848  23.048 -11.029  1.00  0.00           H
ATOM   1424  N   GLY B 370      10.068  18.588  -6.813  1.00 20.00           N
ATOM   1425  CA  GLY B 370       9.526  17.518  -6.061  1.00 20.00           C
ATOM   1426  C   GLY B 370      10.394  16.328  -5.676  1.00 20.00           C
ATOM   1427  O   GLY B 370       9.891  15.314  -5.243  1.00 20.00           O
ATOM   1428  H   GLY B 370      10.569  19.373  -6.381  1.00  0.00           H
ATOM   1429 1HA  GLY B 370       8.620  17.114  -6.557  1.00  0.00           H
ATOM   1430 2HA  GLY B 370       9.137  17.929  -5.113  1.00  0.00           H
ATOM   1431  N   LEU B 371      11.711  16.039  -5.590  1.00 20.00           N
ATOM   1432  CA  LEU B 371      12.639  15.159  -4.904  1.00 20.00           C
ATOM   1433  C   LEU B 371      13.169  15.823  -3.665  1.00 20.00           C
ATOM   1434  O   LEU B 371      13.374  15.180  -2.571  1.00 20.00           O
ATOM   1435  CB  LEU B 371      13.647  14.780  -5.980  1.00 20.00           C
ATOM   1436  CG  LEU B 371      14.831  14.035  -5.379  1.00 20.00           C
ATOM   1437  CD1 LEU B 371      14.338  12.814  -4.562  1.00 20.00           C
ATOM   1438  CD2 LEU B 371      15.796  13.882  -6.541  1.00 20.00           C
ATOM   1439  H   LEU B 371      12.153  16.724  -6.221  1.00  0.00           H
ATOM   1440  HA  LEU B 371      12.078  14.261  -4.587  1.00  0.00           H
```

```
ATOM   1441 1HB  LEU B 371      14.003  15.686  -6.511  1.00  0.00           H
ATOM   1442 2HB  LEU B 371      13.151  14.157  -6.753  1.00  0.00           H
ATOM   1443  HG  LEU B 371      15.357  14.682  -4.664  1.00  0.00           H
ATOM   1444 1HD1 LEU B 371      15.162  12.271  -4.071  1.00  0.00           H
ATOM   1445 2HD1 LEU B 371      13.678  13.076  -3.723  1.00  0.00           H
ATOM   1446 3HD1 LEU B 371      13.703  12.133  -5.158  1.00  0.00           H
ATOM   1447 1HD2 LEU B 371      16.746  13.456  -6.206  1.00  0.00           H
ATOM   1448 2HD2 LEU B 371      15.375  13.284  -7.367  1.00  0.00           H
ATOM   1449 3HD2 LEU B 371      16.066  14.860  -6.958  1.00  0.00           H
ATOM   1450  N   LYS B 372      13.241  16.924  -3.692  1.00 20.00           N
ATOM   1451  CA  LYS B 372      13.897  17.782  -2.745  1.00 20.00           C
ATOM   1452  C   LYS B 372      15.388  17.778  -2.947  1.00 20.00           C
ATOM   1453  O   LYS B 372      15.994  18.810  -2.942  1.00 20.00           O
ATOM   1454  CB  LYS B 372      13.211  18.238  -1.416  1.00 20.00           C
ATOM   1455  CG  LYS B 372      11.663  18.299  -1.384  1.00 20.00           C
ATOM   1456  CD  LYS B 372      11.041  19.374  -2.300  1.00 20.00           C
ATOM   1457  CE  LYS B 372       9.507  19.393  -2.208  1.00 20.00           C
ATOM   1458  NZ  LYS B 372       8.960  20.467  -3.060  1.00 20.00           N
ATOM   1459  H   LYS B 372      12.797  17.293  -4.539  1.00  0.00           H
ATOM   1460  HA  LYS B 372      13.698  18.730  -3.286  1.00  0.00           H
ATOM   1461 1HB  LYS B 372      13.608  19.235  -1.139  1.00  0.00           H
ATOM   1462 2HB  LYS B 372      13.531  17.620  -0.576  1.00  0.00           H
ATOM   1463 1HG  LYS B 372      11.340  18.485  -0.341  1.00  0.00           H
ATOM   1464 2HG  LYS B 372      11.253  17.301  -1.636  1.00  0.00           H
ATOM   1465 1HD  LYS B 372      11.348  19.200  -3.349  1.00  0.00           H
ATOM   1466 2HD  LYS B 372      11.446  20.369  -2.030  1.00  0.00           H
ATOM   1467 1HE  LYS B 372       9.187  19.557  -1.159  1.00  0.00           H
ATOM   1468 2HE  LYS B 372       9.086  18.413  -2.508  1.00  0.00           H
ATOM   1469 1HZ  LYS B 372       9.213  20.331  -4.045  1.00  0.00           H
ATOM   1470 2HZ  LYS B 372       7.933  20.484  -3.031  1.00  0.00           H
ATOM   1471  N   MET B 373      16.108  16.628  -3.169  1.00 20.00           N
ATOM   1472  CA  MET B 373      17.542  16.681  -3.298  1.00 20.00           C
ATOM   1473  C   MET B 373      18.051  15.610  -4.233  1.00 20.00           C
ATOM   1474  O   MET B 373      17.899  14.417  -4.032  1.00 20.00           O
ATOM   1475  CB  MET B 373      18.147  16.817  -1.856  1.00 20.00           C
ATOM   1476  CG  MET B 373      19.550  16.280  -1.511  1.00 20.00           C
ATOM   1477  SD  MET B 373      20.012  16.568   0.225  1.00 20.00           S
ATOM   1478  CE  MET B 373      19.484  18.249   0.627  1.00 20.00           C
ATOM   1479  H   MET B 373      15.577  15.763  -3.006  1.00  0.00           H
ATOM   1480  HA  MET B 373      17.780  17.599  -3.844  1.00  0.00           H
ATOM   1481 1HB  MET B 373      17.467  16.393  -1.099  1.00  0.00           H
ATOM   1482 2HB  MET B 373      18.120  17.896  -1.617  1.00  0.00           H
ATOM   1483 1HG  MET B 373      20.342  16.665  -2.174  1.00  0.00           H
ATOM   1484 2HG  MET B 373      19.548  15.185  -1.646  1.00  0.00           H
ATOM   1485 1HE  MET B 373      19.893  18.558   1.605  1.00  0.00           H
ATOM   1486 2HE  MET B 373      19.833  18.969  -0.134  1.00  0.00           H
ATOM   1487 3HE  MET B 373      18.383  18.313   0.687  1.00  0.00           H
ATOM   1488  N   SER B 374      19.024  15.932  -5.190  1.00 20.00           N
ATOM   1489  CA  SER B 374      19.258  15.184  -6.387  1.00 20.00           C
ATOM   1490  C   SER B 374      20.708  14.742  -6.485  1.00 20.00           C
ATOM   1491  O   SER B 374      21.628  15.246  -5.893  1.00 20.00           O
ATOM   1492  CB  SER B 374      18.863  15.864  -7.678  1.00 20.00           C
ATOM   1493  OG  SER B 374      19.514  17.104  -7.866  1.00 20.00           O
ATOM   1494  H   SER B 374      19.480  16.837  -5.038  1.00  0.00           H
ATOM   1495  HA  SER B 374      18.681  14.242  -6.335  1.00  0.00           H
ATOM   1496 1HB  SER B 374      17.801  15.946  -7.590  1.00  0.00           H
ATOM   1497 2HB  SER B 374      19.027  15.224  -8.566  1.00  0.00           H
ATOM   1498  HG  SER B 374      19.282  17.681  -7.130  1.00  0.00           H
ATOM   1499  N   ALA B 375      20.968  13.822  -7.310  1.00 20.00           N
ATOM   1500  CA  ALA B 375      22.239  13.187  -7.590  1.00 20.00           C
ATOM   1501  C   ALA B 375      22.297  12.703  -8.994  1.00 20.00           C
ATOM   1502  O   ALA B 375      21.492  11.895  -9.439  1.00 20.00           O
ATOM   1503  CB  ALA B 375      22.698  12.085  -6.652  1.00 20.00           C
```

```
ATOM   1504  H   ALA B 375      20.126  13.439  -7.752  1.00  0.00           H
ATOM   1505  HA  ALA B 375      23.015  13.975  -7.459  1.00  0.00           H
ATOM   1506 1HB  ALA B 375      23.691  11.669  -6.910  1.00  0.00           H
ATOM   1507 2HB  ALA B 375      22.792  12.535  -5.660  1.00  0.00           H
ATOM   1508 3HB  ALA B 375      21.980  11.253  -6.614  1.00  0.00           H
ATOM   1509  N   THR B 376      23.191  13.233  -9.763  1.00 20.00           N
ATOM   1510  CA  THR B 376      23.403  12.743 -11.121  1.00 20.00           C
ATOM   1511  C   THR B 376      24.837  12.220 -11.199  1.00 20.00           C
ATOM   1512  O   THR B 376      25.726  12.699 -10.506  1.00 20.00           O
ATOM   1513  CB  THR B 376      23.252  13.891 -12.168  1.00 20.00           C
ATOM   1514  OG1 THR B 376      22.091  14.661 -11.895  1.00 20.00           O
ATOM   1515  CG2 THR B 376      23.125  13.394 -13.621  1.00 20.00           C
ATOM   1516  H   THR B 376      23.931  13.755  -9.280  1.00  0.00           H
ATOM   1517  HA  THR B 376      22.713  11.927 -11.409  1.00  0.00           H
ATOM   1518  HC  THR B 376      24.975  11.376 -11.900  1.00  0.00           H
ATOM   1519  HB  THR B 376      24.122  14.579 -12.101  1.00  0.00           H
ATOM   1520  HG1 THR B 376      21.957  14.572 -10.944  1.00  0.00           H
ATOM   1521 1HG2 THR B 376      23.117  14.232 -14.339  1.00  0.00           H
ATOM   1522 2HG2 THR B 376      23.966  12.742 -13.920  1.00  0.00           H
ATOM   1523 3HG2 THR B 376      22.191  12.824 -13.780  1.00  0.00           H
END
```

Appendix B: SB-T-2053 in β-Tubulin Binding Site (PDB File Format, Version 2.0)

```
REMARK   4
REMARK   4 COMPLIES WITH FORMAT V. 2.0, 10-JAN-2005
ATOM      1  CC  METH    1D      3.390   0.436  -3.807  0.00  0.00           C
ATOM      2  CC3 METH    1D      1.916   0.651  -4.114  1.00  0.00           C
ATOM      3 1O16 METH    1D     -1.318  -0.010  -2.411  0.00  0.00           O
ATOM      4 C161 METH    1D     -0.548   0.439  -3.558  1.00  0.00           C
ATOM      5 C161 METH    1D      0.924   0.163  -3.362  1.00  0.00           C
ATOM      6  H1  METH    1D      3.570   0.603  -2.731  1.00  0.00           H
ATOM      7  H2  METH    1D      3.935   1.286  -4.253  1.00  0.00           H
ATOM      8  H3  METH    1D      1.673   1.250  -4.994  1.00  0.00           H
ATOM      9  H4  METH    1D      1.177  -0.493  -2.534  1.00  0.00           H
ATOM     10  H5  METH    1D     -0.901  -0.105  -4.453  1.00  0.00           H
ATOM     11  H6  METH    1D     -0.733   1.505  -3.778  1.00  0.00           H
ATOM     12  O1  UNK     1      -3.361   1.580  -3.108  0.00  0.00           O
ATOM     13  O2  UNK     1      -4.454  -0.089  -1.109  0.00  0.00           O
ATOM     14  O3  UNK     1      -3.700  -0.769   1.469  0.00  0.00           O
ATOM     15  O4  UNK     1      -6.534  -0.165   2.650  0.00  0.00           O
ATOM     16  O5  UNK     1      -5.558   4.132   3.435  0.00  0.00           O
ATOM     17  O6  UNK     1      -4.988   5.374   1.000  0.00  0.00           O
ATOM     18  O7  UNK     1      -2.468   5.965   0.240  0.00  0.00           O
ATOM     19  O8  UNK     1      -0.032   0.533   0.252  0.00  0.00           O
ATOM     20  O9  UNK     1      -5.499   0.087  -3.143  0.00  0.00           O
ATOM     21  O10 UNK     1      -2.085   0.254   2.807  0.00  0.00           O
ATOM     22  O11 UNK     1       2.189   1.106  -0.084  0.00  0.00           O
ATOM     23  O12 UNK     1       1.036  -1.776   1.487  0.00  0.00           O
ATOM     24  O13 UNK     1       2.658  -3.480  -2.021  0.00  0.00           O
ATOM     25  N14 UNK     1       3.505  -1.538  -1.293  0.00  0.00           N
ATOM     26  C15 UNK     1      -3.019   1.828  -1.734  0.00  0.00           C
ATOM     27  C16 UNK     1      -4.291   1.354  -0.867  0.00  0.00           C
ATOM     28  C17 UNK     1      -4.327   1.596   0.734  0.00  0.00           C
ATOM     29  C18 UNK     1      -4.702   0.289   1.579  0.00  0.00           C
ATOM     30  C19 UNK     1      -5.270   0.401   3.024  0.00  0.00           C
ATOM     31  C20 UNK     1      -5.452   1.785   3.666  0.00  0.00           C
ATOM     32  C21 UNK     1      -4.895   2.987   2.886  0.00  0.00           C
ATOM     33  C22 UNK     1      -4.976   2.961   1.304  0.00  0.00           C
ATOM     34  C23 UNK     1      -4.282   4.356   0.953  0.00  0.00           C
ATOM     35  C24 UNK     1      -2.766   4.622   0.736  0.00  0.00           C
ATOM     36  C25 UNK     1      -2.083   3.612  -0.200  0.00  0.00           C
ATOM     37  C26 UNK     1      -1.049   2.833   0.246  0.00  0.00           C
ATOM     38  C27 UNK     1      -0.593   1.597  -0.569  0.00  0.00           C
ATOM     39  C28 UNK     1      -1.765   0.912  -1.357  0.00  0.00           C
ATOM     40  C29 UNK     1      -2.665   3.384  -1.645  0.00  0.00           C
ATOM     41  C30 UNK     1      -1.595   3.904  -2.668  0.00  0.00           C
ATOM     42  C31 UNK     1      -3.887   4.257  -2.106  0.00  0.00           C
ATOM     43  C32 UNK     1      -6.071  -0.374   1.314  0.00  0.00           C
ATOM     44  C33 UNK     1      -6.461   3.034   0.824  0.00  0.00           C
ATOM     45  C34 UNK     1      -0.290   3.063   1.553  0.00  0.00           C
ATOM     46  C35 UNK     1      -5.043  -0.630  -2.244  0.00  0.00           C
ATOM     47  C36 UNK     1      -2.533  -0.729   2.217  0.00  0.00           C
ATOM     48  C37 UNK     1      -1.887  -2.090   2.271  0.00  0.00           C
ATOM     49  C38 UNK     1       1.317   0.263   0.146  0.00  0.00           C
ATOM     50  C39 UNK     1       1.584  -1.251   0.275  0.00  0.00           C
ATOM     51  C40 UNK     1       3.071  -1.701   0.131  0.00  0.00           C
ATOM     52  C41 UNK     1       3.279  -2.439  -2.266  0.00  0.00           C
ATOM     53  C75 UNK     1      -2.191   6.982   1.144  0.00  0.00           C
ATOM     54  O76 UNK     1      -2.199   6.882   2.373  0.00  0.00           O
ATOM     55  C77 UNK     1      -1.844   8.277   0.437  0.00  0.00           C
```

```
ATOM     56  C81 UNK     1      -5.080  -2.130  -2.366  0.00  0.00           C
ATOM     57  C82 UNK     1      -4.477  -2.936  -1.384  0.00  0.00           C
ATOM     58  C83 UNK     1      -4.500  -4.323  -1.490  0.00  0.00           C
ATOM     59  C84 UNK     1      -5.127  -4.926  -2.576  0.00  0.00           C
ATOM     60  C85 UNK     1      -5.729  -4.145  -3.558  0.00  0.00           C
ATOM     61  C86 UNK     1      -5.705  -2.756  -3.456  0.00  0.00           C
ATOM     62  C92 UNK     1       4.007  -1.071   1.220  0.00  0.00           C
ATOM     63  C93 UNK     1       3.857  -1.487   2.551  0.00  0.00           C
ATOM     64  C94 UNK     1       4.693  -0.999   3.545  0.00  0.00           C
ATOM     65  C95 UNK     1       5.729  -0.130   3.223  0.00  0.00           C
ATOM     66  C96 UNK     1       5.912   0.273   1.906  0.00  0.00           C
ATOM     67  C97 UNK     1       5.028  -0.150   0.920  0.00  0.00           C
ATOM     68 C103 UNK     1       3.874  -2.164  -3.640  0.00  0.00           C
ATOM     69 C104 UNK     1       4.371  -3.311  -4.288  0.00  0.00           C
ATOM     70 C105 UNK     1       5.046  -3.216  -5.497  0.00  0.00           C
ATOM     71 C106 UNK     1       5.200  -1.985  -6.113  0.00  0.00           C
ATOM     72 C107 UNK     1       4.668  -0.843  -5.531  0.00  0.00           C
ATOM     73 C108 UNK     1       3.999  -0.907  -4.301  0.00  0.00           C
ATOM     74  H5  UNK     1      -5.464   4.843   2.787  1.00  0.00           H
ATOM     75  H12 UNK     1       0.895  -2.729   1.353  0.00  0.00           H
ATOM     76  H14 UNK     1       4.041  -0.717  -1.587  0.00  0.00           H
ATOM     77  H16 UNK     1      -5.179   1.852  -1.291  0.00  0.00           H
ATOM     78  H17 UNK     1      -3.274   1.682   1.030  0.00  0.00           H
ATOM     79  H19 UNK     1      -4.762  -0.284   3.731  0.00  0.00           H
ATOM     80 1H20 UNK     1      -5.000   1.785   4.676  0.00  0.00           H
ATOM     81 2H20 UNK     1      -6.518   1.934   3.869  0.00  0.00           H
ATOM     82  H21 UNK     1      -3.823   3.043   3.177  0.00  0.00           H
ATOM     83  H24 UNK     1      -2.369   4.511   1.761  0.00  0.00           H
ATOM     84  H27 UNK     1       0.153   1.961  -1.300  0.00  0.00           H
ATOM     85  H28 UNK     1      -2.143   0.200  -0.602  0.00  0.00           H
ATOM     86 1H30 UNK     1      -0.602   3.450  -2.554  0.00  0.00           H
ATOM     87 2H30 UNK     1      -1.888   3.719  -3.718  0.00  0.00           H
ATOM     88 3H30 UNK     1      -1.419   4.993  -2.565  0.00  0.00           H
ATOM     89 1H31 UNK     1      -4.824   4.033  -1.575  0.00  0.00           H
ATOM     90 2H31 UNK     1      -3.711   5.342  -1.973  0.00  0.00           H
ATOM     91 3H31 UNK     1      -4.133   4.105  -3.174  0.00  0.00           H
ATOM     92 1H32 UNK     1      -6.698   0.130   0.561  0.00  0.00           H
ATOM     93 2H32 UNK     1      -6.012  -1.452   1.070  0.00  0.00           H
ATOM     94 1H33 UNK     1      -6.570   3.130  -0.270  0.00  0.00           H
ATOM     95 2H33 UNK     1      -7.034   2.151   1.132  0.00  0.00           H
ATOM     96 3H33 UNK     1      -6.997   3.906   1.245  0.00  0.00           H
ATOM     97 1H34 UNK     1      -0.213   4.133   1.812  0.00  0.00           H
ATOM     98 2H34 UNK     1      -0.774   2.544   2.400  0.00  0.00           H
ATOM     99 3H34 UNK     1       0.754   2.707   1.503  0.00  0.00           H
ATOM    100 1H37 UNK     1      -1.024  -2.084   2.959  0.00  0.00           H
ATOM    101 2H37 UNK     1      -2.598  -2.856   2.625  0.00  0.00           H
ATOM    102 3H37 UNK     1      -1.534  -2.384   1.268  0.00  0.00           H
ATOM    103  H39 UNK     1       1.008  -1.716  -0.548  0.00  0.00           H
ATOM    104  H40 UNK     1       3.081  -2.790   0.344  0.00  0.00           H
ATOM    105  H1  UNK     1      -4.124   0.977  -3.111  0.00  0.00           H
ATOM    106 1H77 UNK     1      -2.723   8.681  -0.094  0.00  0.00           H
ATOM    107 2H77 UNK     1      -1.495   9.037   1.159  0.00  0.00           H
ATOM    108 3H77 UNK     1      -1.035   8.113  -0.297  0.00  0.00           H
ATOM    109  H84 UNK     1      -5.144  -6.003  -2.659  1.00  0.00           H
ATOM    110  H82 UNK     1      -3.973  -2.496  -0.536  0.00  0.00           H
ATOM    111  H83 UNK     1      -4.027  -4.931  -0.732  0.00  0.00           H
ATOM    112  H85 UNK     1      -6.213  -4.618  -4.402  0.00  0.00           H
ATOM    113  H86 UNK     1      -6.176  -2.168  -4.231  0.00  0.00           H
ATOM    114  H93 UNK     1       3.099  -2.205   2.827  0.00  0.00           H
ATOM    115  H94 UNK     1       4.535  -1.321   4.557  0.00  0.00           H
ATOM    116  H95 UNK     1       6.401   0.220   3.994  0.00  0.00           H
ATOM    117  H96 UNK     1       6.759   0.880   1.636  0.00  0.00           H
ATOM    118  H97 UNK     1       5.184   0.191  -0.091  0.00  0.00           H
```

```
ATOM    119 H104 UNK     1       4.288  -4.291  -3.834  0.00  0.00           H
ATOM    120 H105 UNK     1       5.459  -4.106  -5.953  0.00  0.00           H
ATOM    121 H106 UNK     1       5.722  -1.916  -7.057  0.00  0.00           H
ATOM    122 H107 UNK     1       4.763   0.092  -6.064  0.00  0.00           H
ATOM    123  N   ILE B  16       6.333 -15.273   4.338  1.00 20.00           N
ATOM    124  CA  ILE B  16       6.625 -13.911   4.728  1.00 20.00           C
ATOM    125  C   ILE B  16       7.567 -13.238   3.754  1.00 20.00           C
ATOM    126  O   ILE B  16       7.636 -12.084   3.584  1.00 20.00           O
ATOM    127  CB  ILE B  16       7.112 -13.829   6.230  1.00 20.00           C
ATOM    128  CG1 ILE B  16       6.252 -14.591   7.291  1.00 20.00           C
ATOM    129  CG2 ILE B  16       7.329 -12.375   6.736  1.00 20.00           C
ATOM    130  CD1 ILE B  16       4.767 -14.196   7.399  1.00 20.00           C
ATOM    131 1H   ILE B  16       5.775 -15.728   5.071  1.00  0.00           H
ATOM    132 2H   ILE B  16       5.738 -15.288   3.502  1.00  0.00           H
ATOM    133  HA  ILE B  16       5.675 -13.347   4.669  1.00  0.00           H
ATOM    134  HB  ILE B  16       8.109 -14.314   6.263  1.00  0.00           H
ATOM    135 1HG1 ILE B  16       6.720 -14.489   8.289  1.00  0.00           H
ATOM    136 2HG1 ILE B  16       6.309 -15.677   7.088  1.00  0.00           H
ATOM    137 1HG2 ILE B  16       7.682 -12.346   7.785  1.00  0.00           H
ATOM    138 2HG2 ILE B  16       8.091 -11.834   6.145  1.00  0.00           H
ATOM    139 3HG2 ILE B  16       6.401 -11.775   6.689  1.00  0.00           H
ATOM    140 1HD1 ILE B  16       4.253 -14.772   8.191  1.00  0.00           H
ATOM    141 2HD1 ILE B  16       4.634 -13.126   7.644  1.00  0.00           H
ATOM    142 3HD1 ILE B  16       4.219 -14.385   6.458  1.00  0.00           H
ATOM    143  N   GLY B  17       8.193 -14.226   3.031  1.00 20.00           N
ATOM    144  CA  GLY B  17       9.085 -13.731   2.010  1.00 20.00           C
ATOM    145  C   GLY B  17       8.404 -13.138   0.858  1.00 20.00           C
ATOM    146  O   GLY B  17       8.913 -12.188   0.241  1.00 20.00           O
ATOM    147  H   GLY B  17       8.002 -15.190   3.345  1.00  0.00           H
ATOM    148 1HA  GLY B  17       9.720 -14.561   1.646  1.00  0.00           H
ATOM    149 2HA  GLY B  17       9.811 -13.001   2.424  1.00  0.00           H
ATOM    150  N   ALA B  18       7.326 -13.755   0.641  1.00 20.00           N
ATOM    151  CA  ALA B  18       6.441 -13.382  -0.370  1.00 20.00           C
ATOM    152  C   ALA B  18       5.953 -11.993  -0.186  1.00 20.00           C
ATOM    153  O   ALA B  18       5.791 -11.265  -1.154  1.00 20.00           O
ATOM    154  CB  ALA B  18       5.309 -14.431  -0.426  1.00 20.00           C
ATOM    155  H   ALA B  18       7.132 -14.476   1.345  1.00  0.00           H
ATOM    156  HA  ALA B  18       6.966 -13.417  -1.348  1.00  0.00           H
ATOM    157 1HB  ALA B  18       4.597 -14.206  -1.243  1.00  0.00           H
ATOM    158 2HB  ALA B  18       5.695 -15.450  -0.623  1.00  0.00           H
ATOM    159 3HB  ALA B  18       4.718 -14.475   0.509  1.00  0.00           H
ATOM    160  N   LYS B  19       5.715 -11.595   1.049  1.00 20.00           N
ATOM    161  CA  LYS B  19       5.132 -10.302   1.245  1.00 20.00           C
ATOM    162  C   LYS B  19       6.111  -9.190   1.610  1.00 20.00           C
ATOM    163  O   LYS B  19       5.808  -8.035   1.526  1.00 20.00           O
ATOM    164  CB  LYS B  19       3.600  -9.982   1.111  1.00 20.00           C
ATOM    165  CG  LYS B  19       2.677 -11.049   0.474  1.00 20.00           C
ATOM    166  CD  LYS B  19       1.263 -10.499   0.193  1.00 20.00           C
ATOM    167  CE  LYS B  19       0.310 -11.567  -0.359  1.00 20.00           C
ATOM    168  NZ  LYS B  19      -1.012 -10.960  -0.608  1.00 20.00           N
ATOM    169  H   LYS B  19       5.930 -12.272   1.788  1.00  0.00           H
ATOM    170  HA  LYS B  19       5.226  -9.802   0.262  1.00  0.00           H
ATOM    171 1HB  LYS B  19       3.450  -9.059   0.502  1.00  0.00           H
ATOM    172 2HB  LYS B  19       3.215  -9.582   2.052  1.00  0.00           H
ATOM    173 1HG  LYS B  19       2.636 -11.948   1.116  1.00  0.00           H
ATOM    174 2HG  LYS B  19       3.117 -11.392  -0.482  1.00  0.00           H
ATOM    175 1HD  LYS B  19       1.338  -9.663  -0.532  1.00  0.00           H
ATOM    176 2HD  LYS B  19       0.839 -10.048   1.111  1.00  0.00           H
ATOM    177 1HE  LYS B  19       0.215 -12.412   0.351  1.00  0.00           H
ATOM    178 2HE  LYS B  19       0.709 -11.993  -1.301  1.00  0.00           H
ATOM    179 1HZ  LYS B  19      -1.705 -11.659  -0.903  1.00  0.00           H
ATOM    180 2HZ  LYS B  19      -1.380 -10.528   0.248  1.00  0.00           H
ATOM    181  N   PHE B  20       7.274  -9.496   2.008  1.00 20.00           N
```

```
ATOM    182  CA  PHE B  20       8.291  -8.469   2.297  1.00 20.00           C
ATOM    183  C   PHE B  20       8.816  -8.032   0.963  1.00 20.00           C
ATOM    184  O   PHE B  20       8.607  -6.925   0.489  1.00 20.00           O
ATOM    185  CB  PHE B  20       9.290  -8.957   3.404  1.00 20.00           C
ATOM    186  CG  PHE B  20      10.625  -8.182   3.508  1.00 20.00           C
ATOM    187  CD1 PHE B  20      11.836  -8.884   3.473  1.00 20.00           C
ATOM    188  CD2 PHE B  20      10.652  -6.781   3.547  1.00 20.00           C
ATOM    189  CE1 PHE B  20      13.049  -8.199   3.472  1.00 20.00           C
ATOM    190  CE2 PHE B  20      11.865  -6.098   3.542  1.00 20.00           C
ATOM    191  CZ  PHE B  20      13.062  -6.808   3.507  1.00 20.00           C
ATOM    192  H   PHE B  20       7.402 -10.497   2.209  1.00  0.00           H
ATOM    193  HA  PHE B  20       7.816  -7.566   2.735  1.00  0.00           H
ATOM    194 1HB  PHE B  20       9.501 -10.034   3.252  1.00  0.00           H
ATOM    195 2HB  PHE B  20       8.781  -8.926   4.387  1.00  0.00           H
ATOM    196  HD1 PHE B  20      11.845  -9.963   3.423  1.00  0.00           H
ATOM    197  HD2 PHE B  20       9.732  -6.214   3.556  1.00  0.00           H
ATOM    198  HE1 PHE B  20      13.979  -8.747   3.429  1.00  0.00           H
ATOM    199  HE2 PHE B  20      11.877  -5.018   3.560  1.00  0.00           H
ATOM    200  HZ  PHE B  20      14.002  -6.277   3.493  1.00  0.00           H
ATOM    201  N   TRP B  21       9.471  -8.940   0.424  1.00 20.00           N
ATOM    202  CA  TRP B  21       9.951  -8.783  -0.872  1.00 20.00           C
ATOM    203  C   TRP B  21       8.803  -8.409  -1.728  1.00 20.00           C
ATOM    204  O   TRP B  21       8.891  -7.862  -2.827  1.00 20.00           O
ATOM    205  CB  TRP B  21      10.725 -10.019  -1.411  1.00 20.00           C
ATOM    206  CG  TRP B  21      12.085 -10.263  -0.741  1.00 20.00           C
ATOM    207  CD1 TRP B  21      12.306 -11.002   0.441  1.00 20.00           C
ATOM    208  CD2 TRP B  21      13.322  -9.753  -1.098  1.00 20.00           C
ATOM    209  NE1 TRP B  21      13.655 -10.951   0.844  1.00 20.00           N
ATOM    210  CE2 TRP B  21      14.263 -10.162  -0.120  1.00 20.00           C
ATOM    211  CE3 TRP B  21      13.724  -8.922  -2.179  1.00 20.00           C
ATOM    212  CZ2 TRP B  21      15.607  -9.731  -0.205  1.00 20.00           C
ATOM    213  CZ3 TRP B  21      15.056  -8.511  -2.242  1.00 20.00           C
ATOM    214  CH2 TRP B  21      15.984  -8.908  -1.269  1.00 20.00           C
ATOM    215  H   TRP B  21       9.414  -9.852   0.890  1.00  0.00           H
ATOM    216  HA  TRP B  21      10.654  -7.937  -0.913  1.00  0.00           H
ATOM    217 1HB  TRP B  21      10.908  -9.886  -2.496  1.00  0.00           H
ATOM    218 2HB  TRP B  21      10.106 -10.930  -1.369  1.00  0.00           H
ATOM    219  HD1 TRP B  21      11.526 -11.510   0.991  1.00  0.00           H
ATOM    220  HE1 TRP B  21      14.096 -11.386   1.663  1.00  0.00           H
ATOM    221  HE3 TRP B  21      13.014  -8.597  -2.926  1.00  0.00           H
ATOM    222  HZ2 TRP B  21      16.328 -10.030   0.542  1.00  0.00           H
ATOM    223  HZ3 TRP B  21      15.379  -7.875  -3.054  1.00  0.00           H
ATOM    224  HH2 TRP B  21      17.009  -8.573  -1.345  1.00  0.00           H
ATOM    225  N   GLU B  22       7.541  -8.436  -1.695  1.00 20.00           N
ATOM    226  CA  GLU B  22       7.184  -7.892  -2.988  1.00 20.00           C
ATOM    227  C   GLU B  22       6.983  -6.420  -2.893  1.00 20.00           C
ATOM    228  O   GLU B  22       6.607  -5.684  -3.812  1.00 20.00           O
ATOM    229  CB  GLU B  22       5.649  -8.373  -3.011  1.00 20.00           C
ATOM    230  CG  GLU B  22       5.328  -9.766  -3.601  1.00 20.00           C
ATOM    231  CD  GLU B  22       3.921 -10.311  -3.339  1.00 20.00           C
ATOM    232  OE1 GLU B  22       2.993  -9.665  -2.860  1.00 20.00           O
ATOM    233  OE2 GLU B  22       3.806 -11.615  -3.712  1.00 20.00           O
ATOM    234  H   GLU B  22       7.107  -9.245  -1.235  1.00  0.00           H
ATOM    235  HA  GLU B  22       7.347  -8.345  -4.030  1.00  0.00           H
ATOM    236 1HB  GLU B  22       5.030  -7.702  -3.649  1.00  0.00           H
ATOM    237 2HB  GLU B  22       5.140  -8.263  -2.025  1.00  0.00           H
ATOM    238 1HG  GLU B  22       6.089 -10.512  -3.319  1.00  0.00           H
ATOM    239 2HG  GLU B  22       5.430  -9.689  -4.681  1.00  0.00           H
ATOM    240  HE2 GLU B  22       2.911 -11.901  -3.526  1.00  0.00           H
ATOM    241  N   VAL B  23       7.168  -6.005  -1.925  1.00 20.00           N
ATOM    242  CA  VAL B  23       7.022  -4.614  -1.601  1.00 20.00           C
ATOM    243  C   VAL B  23       8.262  -3.838  -1.977  1.00 20.00           C
ATOM    244  O   VAL B  23       8.414  -2.703  -1.746  1.00 20.00           O
```

```
ATOM    245  CB  VAL B  23       6.520  -4.508  -0.110  1.00 20.00           C
ATOM    246  CG1 VAL B  23       6.576  -3.088   0.477  1.00 20.00           C
ATOM    247  CG2 VAL B  23       5.071  -5.039   0.048  1.00 20.00           C
ATOM    248  H   VAL B  23       7.397  -6.739  -1.233  1.00  0.00           H
ATOM    249  HA  VAL B  23       6.215  -4.111  -2.179  1.00  0.00           H
ATOM    250  HB  VAL B  23       7.165  -5.113   0.547  1.00  0.00           H
ATOM    251 1HG1 VAL B  23       6.064  -2.998   1.452  1.00  0.00           H
ATOM    252 2HG1 VAL B  23       7.614  -2.752   0.650  1.00  0.00           H
ATOM    253 3HG1 VAL B  23       6.116  -2.361  -0.215  1.00  0.00           H
ATOM    254 1HG2 VAL B  23       4.652  -4.880   1.056  1.00  0.00           H
ATOM    255 2HG2 VAL B  23       4.377  -4.558  -0.659  1.00  0.00           H
ATOM    256 3HG2 VAL B  23       5.012  -6.126  -0.143  1.00  0.00           H
ATOM    257  N   ILE B  24       8.994  -4.635  -2.651  1.00 20.00           N
ATOM    258  CA  ILE B  24      10.293  -4.163  -3.043  1.00 20.00           C
ATOM    259  C   ILE B  24      10.394  -3.960  -4.547  1.00 20.00           C
ATOM    260  O   ILE B  24      10.863  -2.988  -5.078  1.00 20.00           O
ATOM    261  CB  ILE B  24      11.336  -5.218  -2.490  1.00 20.00           C
ATOM    262  CG1 ILE B  24      11.330  -5.295  -0.925  1.00 20.00           C
ATOM    263  CG2 ILE B  24      12.762  -4.979  -3.025  1.00 20.00           C
ATOM    264  CD1 ILE B  24      12.484  -5.993  -0.184  1.00 20.00           C
ATOM    265  H   ILE B  24       8.672  -5.613  -2.594  1.00  0.00           H
ATOM    266  HA  ILE B  24      10.580  -3.184  -2.603  1.00  0.00           H
ATOM    267  HB  ILE B  24      11.051  -6.223  -2.864  1.00  0.00           H
ATOM    268 1HG1 ILE B  24      10.393  -5.785  -0.618  1.00  0.00           H
ATOM    269 2HG1 ILE B  24      11.195  -4.293  -0.502  1.00  0.00           H
ATOM    270 1HG2 ILE B  24      13.438  -5.789  -2.702  1.00  0.00           H
ATOM    271 2HG2 ILE B  24      12.822  -4.968  -4.129  1.00  0.00           H
ATOM    272 3HG2 ILE B  24      13.149  -4.016  -2.657  1.00  0.00           H
ATOM    273 1HD1 ILE B  24      12.261  -6.086   0.889  1.00  0.00           H
ATOM    274 2HD1 ILE B  24      12.664  -7.013  -0.554  1.00  0.00           H
ATOM    275 3HD1 ILE B  24      13.435  -5.439  -0.273  1.00  0.00           H
ATOM    276  N   SER B  25      10.000  -4.822  -5.482  1.00 20.00           N
ATOM    277  CA  SER B  25      10.362  -4.177  -6.734  1.00 20.00           C
ATOM    278  C   SER B  25       9.859  -2.708  -6.545  1.00 20.00           C
ATOM    279  O   SER B  25       9.785  -1.943  -7.517  1.00 20.00           O
ATOM    280  CB  SER B  25       9.717  -4.968  -7.896  1.00 20.00           C
ATOM    281  OG  SER B  25       8.295  -5.056  -7.782  1.00 20.00           O
ATOM    282  H   SER B  25       9.226  -5.468  -5.292  1.00  0.00           H
ATOM    283  HA  SER B  25      11.459  -4.196  -6.929  1.00  0.00           H
ATOM    284 1HB  SER B  25      10.151  -5.988  -7.942  1.00  0.00           H
ATOM    285 2HB  SER B  25       9.986  -4.493  -8.858  1.00  0.00           H
ATOM    286  HG  SER B  25       8.008  -5.796  -8.325  1.00  0.00           H
ATOM    287  N   ASP B  26       9.412  -2.338  -5.218  1.00 20.00           N
ATOM    288  CA  ASP B  26       9.201  -0.996  -4.849  1.00 20.00           C
ATOM    289  C   ASP B  26      10.435  -0.170  -4.971  1.00 20.00           C
ATOM    290  O   ASP B  26      10.495   1.017  -4.991  1.00 20.00           O
ATOM    291  CB  ASP B  26       8.502  -0.767  -3.516  1.00 20.00           C
ATOM    292  CG  ASP B  26       7.969   0.552  -2.989  1.00 20.00           C
ATOM    293  OD1 ASP B  26       8.571   1.616  -3.039  1.00 20.00           O
ATOM    294  OD2 ASP B  26       6.787   0.387  -2.328  1.00 20.00           O
ATOM    295  H   ASP B  26       8.996  -3.116  -4.700  1.00  0.00           H
ATOM    296  HA  ASP B  26       8.508  -0.575  -5.603  1.00  0.00           H
ATOM    297 1HB  ASP B  26       9.270  -1.000  -2.763  1.00  0.00           H
ATOM    298 2HB  ASP B  26       7.656  -1.477  -3.477  1.00  0.00           H
ATOM    299  HD2 ASP B  26       6.558   1.211  -1.900  1.00  0.00           H
ATOM    300  N   GLU B  27      11.520  -1.062  -5.004  1.00 20.00           N
ATOM    301  CA  GLU B  27      12.825  -0.994  -5.545  1.00 20.00           C
ATOM    302  C   GLU B  27      13.778  -0.413  -4.531  1.00 20.00           C
ATOM    303  O   GLU B  27      14.144   0.749  -4.547  1.00 20.00           O
ATOM    304  CB  GLU B  27      12.971  -0.171  -6.883  1.00 20.00           C
ATOM    305  CG  GLU B  27      12.054  -0.452  -8.084  1.00 20.00           C
ATOM    306  CD  GLU B  27      12.304   0.181  -9.448  1.00 20.00           C
ATOM    307  OE1 GLU B  27      13.410   0.321  -9.956  1.00 20.00           O
```

```
ATOM    308  OE2 GLU B  27      11.135   0.467 -10.088  1.00 20.00           O
ATOM    309  H   GLU B  27      11.095  -2.086  -5.023  1.00  0.00           H
ATOM    310  HA  GLU B  27      13.133  -2.029  -5.798  1.00  0.00           H
ATOM    311 1HB  GLU B  27      14.026  -0.207  -7.219  1.00  0.00           H
ATOM    312 2HB  GLU B  27      12.784   0.880  -6.615  1.00  0.00           H
ATOM    313 1HG  GLU B  27      11.054  -0.101  -7.781  1.00  0.00           H
ATOM    314 2HG  GLU B  27      11.997  -1.541  -8.253  1.00  0.00           H
ATOM    315  HE2 GLU B  27      11.283   0.477 -11.050  1.00  0.00           H
ATOM    316  N   HIS B  28      14.345  -1.177  -3.781  1.00 20.00           N
ATOM    317  CA  HIS B  28      15.531  -0.832  -3.071  1.00 20.00           C
ATOM    318  C   HIS B  28      16.307  -1.905  -2.446  1.00 20.00           C
ATOM    319  O   HIS B  28      17.355  -1.775  -2.050  1.00 20.00           O
ATOM    320  CB  HIS B  28      14.958  -0.058  -1.781  1.00 20.00           C
ATOM    321  CG  HIS B  28      13.838  -0.762  -0.947  1.00 20.00           C
ATOM    322  ND1 HIS B  28      12.487  -0.662  -1.272  1.00 20.00           N
ATOM    323  CD2 HIS B  28      14.051  -1.822  -0.047  1.00 20.00           C
ATOM    324  CE1 HIS B  28      12.001  -1.709  -0.547  1.00 20.00           C
ATOM    325  NE2 HIS B  28      12.861  -2.468   0.209  1.00 20.00           N
ATOM    326  H   HIS B  28      13.584  -1.626  -3.255  1.00  0.00           H
ATOM    327  HA  HIS B  28      16.227  -0.190  -3.654  1.00  0.00           H
ATOM    328 1HB  HIS B  28      14.518   0.895  -2.103  1.00  0.00           H
ATOM    329 2HB  HIS B  28      15.777   0.266  -1.108  1.00  0.00           H
ATOM    330  HD2 HIS B  28      15.024  -2.159   0.285  1.00  0.00           H
ATOM    331  HE1 HIS B  28      10.938  -1.918  -0.558  1.00  0.00           H
ATOM    332  HE2 HIS B  28      12.681  -3.343   0.719  1.00  0.00           H
ATOM    333  N   GLY B  29      15.556  -2.936  -2.510  1.00 20.00           N
ATOM    334  CA  GLY B  29      15.856  -4.194  -1.974  1.00 20.00           C
ATOM    335  C   GLY B  29      17.363  -4.467  -1.971  1.00 20.00           C
ATOM    336  O   GLY B  29      17.968  -4.692  -3.033  1.00 20.00           O
ATOM    337  H   GLY B  29      14.817  -2.770  -3.203  1.00  0.00           H
ATOM    338 1HA  GLY B  29      15.409  -4.986  -2.595  1.00  0.00           H
ATOM    339 2HA  GLY B  29      15.437  -4.307  -0.957  1.00  0.00           H
ATOM    340  HC  GLY B  29      17.848  -4.388  -0.981  1.00  0.00           H
ATOM    341  N   TYR B  36      14.857   2.425  -8.295  1.00 20.00           N
ATOM    342  CA  TYR B  36      13.800   3.095  -7.650  1.00 20.00           C
ATOM    343  C   TYR B  36      13.881   4.564  -7.921  1.00 20.00           C
ATOM    344  O   TYR B  36      12.973   5.299  -7.437  1.00 20.00           O
ATOM    345  CB  TYR B  36      14.405   3.112  -6.189  1.00 20.00           C
ATOM    346  CG  TYR B  36      15.669   3.943  -5.715  1.00 20.00           C
ATOM    347  CD1 TYR B  36      15.515   5.251  -5.235  1.00 20.00           C
ATOM    348  CD2 TYR B  36      16.946   3.366  -5.713  1.00 20.00           C
ATOM    349  CE1 TYR B  36      16.613   5.963  -4.756  1.00 20.00           C
ATOM    350  CE2 TYR B  36      18.042   4.078  -5.232  1.00 20.00           C
ATOM    351  CZ  TYR B  36      17.874   5.374  -4.754  1.00 20.00           C
ATOM    352  OH  TYR B  36      18.954   6.065  -4.275  1.00 20.00           O
ATOM    353 1H   TYR B  36      14.724   2.410  -9.313  1.00  0.00           H
ATOM    354 2H   TYR B  36      15.753   2.893  -8.118  1.00  0.00           H
ATOM    355  HA  TYR B  36      12.798   2.651  -7.787  1.00  0.00           H
ATOM    356  HC  TYR B  36      14.735   4.930  -8.524  1.00  0.00           H
ATOM    357 1HB  TYR B  36      14.734   2.099  -5.999  1.00  0.00           H
ATOM    358 2HB  TYR B  36      13.576   3.267  -5.474  1.00  0.00           H
ATOM    359  HD1 TYR B  36      14.536   5.708  -5.209  1.00  0.00           H
ATOM    360  HD2 TYR B  36      17.087   2.354  -6.068  1.00  0.00           H
ATOM    361  HE1 TYR B  36      16.474   6.965  -4.378  1.00  0.00           H
ATOM    362  HE2 TYR B  36      19.023   3.626  -5.224  1.00  0.00           H
ATOM    363  HH  TYR B  36      18.672   6.946  -4.025  1.00  0.00           H
ATOM    364  N   ASP B  39      11.002   5.374 -11.600  1.00 20.00           N
ATOM    365  CA  ASP B  39      10.173   4.223 -11.793  1.00 20.00           C
ATOM    366  C   ASP B  39      10.636   3.265 -12.783  1.00 20.00           C
ATOM    367  O   ASP B  39      11.672   3.318 -13.348  1.00 20.00           O
ATOM    368  CB  ASP B  39       8.721   4.836 -11.937  1.00 20.00           C
ATOM    369  CG  ASP B  39       8.023   5.179 -10.617  1.00 20.00           C
ATOM    370  OD1 ASP B  39       7.690   6.313 -10.288  1.00 20.00           O
```

```
ATOM    371  OD2 ASP B  39       7.794   4.071  -9.859  1.00 20.00           O
ATOM    372 1H   ASP B  39      11.978   5.089 -11.460  1.00  0.00           H
ATOM    373 2H   ASP B  39      11.010   5.952 -12.448  1.00  0.00           H
ATOM    374  HA  ASP B  39      10.221   3.678 -10.825  1.00  0.00           H
ATOM    375 1HB  ASP B  39       8.036   4.138 -12.449  1.00  0.00           H
ATOM    376 2HB  ASP B  39       8.707   5.727 -12.595  1.00  0.00           H
ATOM    377  HD2 ASP B  39       7.341   4.318  -9.050  1.00  0.00           H
ATOM    378  N   SER B  40       9.851   2.332 -12.911  1.00 20.00           N
ATOM    379  CA  SER B  40      10.053   1.464 -13.912  1.00 20.00           C
ATOM    380  C   SER B  40      10.429   0.085 -13.504  1.00 20.00           C
ATOM    381  O   SER B  40      11.166  -0.109 -12.534  1.00 20.00           O
ATOM    382  CB  SER B  40      10.580   1.861 -15.364  1.00 20.00           C
ATOM    383  OG  SER B  40      12.002   1.928 -15.381  1.00 20.00           O
ATOM    384  H   SER B  40       9.024   2.346 -12.306  1.00  0.00           H
ATOM    385  HA  SER B  40       8.969   1.441 -14.184  1.00  0.00           H
ATOM    386 1HB  SER B  40      10.161   2.838 -15.675  1.00  0.00           H
ATOM    387 2HB  SER B  40      10.246   1.144 -16.139  1.00  0.00           H
ATOM    388  HG  SER B  40      12.207   2.500 -14.615  1.00  0.00           H
ATOM    389  N   ASP B  41       9.792  -0.735 -14.187  1.00 20.00           N
ATOM    390  CA  ASP B  41      10.154  -2.100 -14.412  1.00 20.00           C
ATOM    391  C   ASP B  41       9.030  -3.032 -14.033  1.00 20.00           C
ATOM    392  O   ASP B  41       7.920  -2.826 -14.478  1.00 20.00           O
ATOM    393  CB  ASP B  41      11.710  -2.468 -14.334  1.00 20.00           C
ATOM    394  CG  ASP B  41      12.643  -1.666 -15.247  1.00 20.00           C
ATOM    395  OD1 ASP B  41      12.613  -1.729 -16.471  1.00 20.00           O
ATOM    396  OD2 ASP B  41      13.501  -0.870 -14.552  1.00 20.00           O
ATOM    397  H   ASP B  41       9.121  -0.297 -14.825  1.00  0.00           H
ATOM    398  HA  ASP B  41      10.024  -2.172 -15.512  1.00  0.00           H
ATOM    399 1HB  ASP B  41      11.872  -3.522 -14.625  1.00  0.00           H
ATOM    400 2HB  ASP B  41      12.066  -2.399 -13.289  1.00  0.00           H
ATOM    401  HD2 ASP B  41      13.988  -0.329 -15.176  1.00  0.00           H
ATOM    402  N   LEU B  42       9.535  -4.064 -13.497  1.00 20.00           N
ATOM    403  CA  LEU B  42       8.776  -4.821 -12.506  1.00 20.00           C
ATOM    404  C   LEU B  42       8.939  -6.291 -12.735  1.00 20.00           C
ATOM    405  O   LEU B  42       9.167  -6.751 -13.862  1.00 20.00           O
ATOM    406  CB  LEU B  42       7.242  -4.477 -12.205  1.00 20.00           C
ATOM    407  CG  LEU B  42       6.879  -3.120 -11.527  1.00 20.00           C
ATOM    408  CD1 LEU B  42       5.359  -2.889 -11.593  1.00 20.00           C
ATOM    409  CD2 LEU B  42       7.329  -3.023 -10.061  1.00 20.00           C
ATOM    410  H   LEU B  42      10.557  -4.035 -13.450  1.00  0.00           H
ATOM    411  HA  LEU B  42       9.307  -4.519 -11.575  1.00  0.00           H
ATOM    412 1HB  LEU B  42       6.783  -5.268 -11.580  1.00  0.00           H
ATOM    413 2HB  LEU B  42       6.693  -4.564 -13.163  1.00  0.00           H
ATOM    414  HG  LEU B  42       7.357  -2.287 -12.075  1.00  0.00           H
ATOM    415 1HD1 LEU B  42       5.070  -1.916 -11.152  1.00  0.00           H
ATOM    416 2HD1 LEU B  42       4.996  -2.879 -12.638  1.00  0.00           H
ATOM    417 3HD1 LEU B  42       4.791  -3.672 -11.056  1.00  0.00           H
ATOM    418 1HD2 LEU B  42       7.057  -2.050  -9.611  1.00  0.00           H
ATOM    419 2HD2 LEU B  42       6.863  -3.804  -9.433  1.00  0.00           H
ATOM    420 3HD2 LEU B  42       8.424  -3.111  -9.952  1.00  0.00           H
ATOM    421  N   GLN B  43       8.924  -6.859 -11.617  1.00 20.00           N
ATOM    422  CA  GLN B  43       8.629  -8.262 -11.408  1.00 20.00           C
ATOM    423  C   GLN B  43       9.713  -8.887 -10.606  1.00 20.00           C
ATOM    424  O   GLN B  43      10.106  -8.352  -9.547  1.00 20.00           O
ATOM    425  CB  GLN B  43       7.711  -9.027 -12.460  1.00 20.00           C
ATOM    426  CG  GLN B  43       6.289  -8.442 -12.681  1.00 20.00           C
ATOM    427  CD  GLN B  43       5.447  -9.220 -13.693  1.00 20.00           C
ATOM    428  OE1 GLN B  43       4.674 -10.108 -13.351  1.00 20.00           O
ATOM    429  NE2 GLN B  43       5.561  -8.917 -14.965  1.00 20.00           N
ATOM    430  H   GLN B  43       8.885  -6.207 -10.829  1.00  0.00           H
ATOM    431  HA  GLN B  43       7.890  -8.200 -10.583  1.00  0.00           H
ATOM    432 1HB  GLN B  43       7.583 -10.078 -12.131  1.00  0.00           H
ATOM    433 2HB  GLN B  43       8.246  -9.093 -13.427  1.00  0.00           H
```

```
ATOM    434 1HG  GLN B  43       6.342  -7.381 -12.986  1.00  0.00           H
ATOM    435 2HG  GLN B  43       5.737  -8.434 -11.723  1.00  0.00           H
ATOM    436 1HE2 GLN B  43       6.268  -8.219 -15.212  1.00  0.00           H
ATOM    437 2HE2 GLN B  43       4.994  -9.499 -15.587  1.00  0.00           H
ATOM    438  N   LEU B  44      10.129  -9.866 -11.235  1.00 20.00           N
ATOM    439  CA  LEU B  44      11.120 -10.718 -10.675  1.00 20.00           C
ATOM    440  C   LEU B  44      12.370 -10.495 -11.458  1.00 20.00           C
ATOM    441  O   LEU B  44      12.990 -11.420 -11.828  1.00 20.00           O
ATOM    442  CB  LEU B  44      10.538 -12.173 -10.675  1.00 20.00           C
ATOM    443  CG  LEU B  44      11.283 -13.222  -9.805  1.00 20.00           C
ATOM    444  CD1 LEU B  44      11.119 -12.966  -8.294  1.00 20.00           C
ATOM    445  CD2 LEU B  44      10.771 -14.637 -10.129  1.00 20.00           C
ATOM    446  H   LEU B  44       9.651 -10.067 -12.119  1.00  0.00           H
ATOM    447  HA  LEU B  44      11.374 -10.458  -9.625  1.00  0.00           H
ATOM    448 1HB  LEU B  44      10.498 -12.531 -11.723  1.00  0.00           H
ATOM    449 2HB  LEU B  44       9.480 -12.165 -10.354  1.00  0.00           H
ATOM    450  HG  LEU B  44      12.364 -13.194 -10.051  1.00  0.00           H
ATOM    451 1HD1 LEU B  44      10.056 -12.948  -7.989  1.00  0.00           H
ATOM    452 2HD1 LEU B  44      11.620 -13.744  -7.689  1.00  0.00           H
ATOM    453 3HD1 LEU B  44      11.561 -12.002  -7.985  1.00  0.00           H
ATOM    454 1HD2 LEU B  44      11.307 -15.411  -9.549  1.00  0.00           H
ATOM    455 2HD2 LEU B  44       9.693 -14.752  -9.910  1.00  0.00           H
ATOM    456 3HD2 LEU B  44      10.916 -14.888 -11.196  1.00  0.00           H
ATOM    457  N   GLU B  47      12.500  -9.196 -12.042  1.00 20.00           N
ATOM    458  CA  GLU B  47      13.690  -8.737 -12.715  1.00 20.00           C
ATOM    459  C   GLU B  47      13.365  -7.783 -13.842  1.00 20.00           C
ATOM    460  O   GLU B  47      12.272  -7.666 -14.332  1.00 20.00           O
ATOM    461  CB  GLU B  47      14.902  -9.717 -12.993  1.00 20.00           C
ATOM    462  CG  GLU B  47      15.779 -10.055 -11.758  1.00 20.00           C
ATOM    463  CD  GLU B  47      16.928 -11.008 -12.070  1.00 20.00           C
ATOM    464  OE1 GLU B  47      18.029 -10.643 -12.471  1.00 20.00           O
ATOM    465  OE2 GLU B  47      16.598 -12.312 -11.854  1.00 20.00           O
ATOM    466  H   GLU B  47      11.705  -8.583 -11.832  1.00  0.00           H
ATOM    467  HA  GLU B  47      14.116  -8.020 -11.987  1.00  0.00           H
ATOM    468 1HB  GLU B  47      15.596  -9.288 -13.741  1.00  0.00           H
ATOM    469 2HB  GLU B  47      14.535 -10.637 -13.488  1.00  0.00           H
ATOM    470 1HG  GLU B  47      15.172 -10.488 -10.943  1.00  0.00           H
ATOM    471 2HG  GLU B  47      16.211  -9.129 -11.335  1.00  0.00           H
ATOM    472  HE2 GLU B  47      17.353 -12.859 -12.073  1.00  0.00           H
ATOM    473  N   ARG B  48      14.298  -7.344 -14.720  1.00 20.00           N
ATOM    474  CA  ARG B  48      14.988  -6.232 -15.356  1.00 20.00           C
ATOM    475  C   ARG B  48      15.938  -6.727 -16.402  1.00 20.00           C
ATOM    476  O   ARG B  48      15.609  -7.670 -17.145  1.00 20.00           O
ATOM    477  CB  ARG B  48      15.834  -5.462 -14.295  1.00 20.00           C
ATOM    478  CG  ARG B  48      15.123  -4.804 -13.091  1.00 20.00           C
ATOM    479  CD  ARG B  48      16.165  -4.266 -12.091  1.00 20.00           C
ATOM    480  NE  ARG B  48      15.517  -3.770 -10.839  1.00 20.00           N
ATOM    481  CZ  ARG B  48      15.003  -2.658 -10.536  1.00 20.00           C
ATOM    482  NH1 ARG B  48      14.903  -1.661 -11.371  1.00 20.00           N
ATOM    483  NH2 ARG B  48      14.561  -2.507  -9.332  1.00 20.00           N
ATOM    484  H   ARG B  48      14.238  -8.094 -15.420  1.00  0.00           H
ATOM    485  HA  ARG B  48      14.249  -5.556 -15.828  1.00  0.00           H
ATOM    486  HC  ARG B  48      16.907  -6.199 -16.486  1.00  0.00           H
ATOM    487 1HB  ARG B  48      16.410  -4.659 -14.799  1.00  0.00           H
ATOM    488 2HB  ARG B  48      16.604  -6.155 -13.895  1.00  0.00           H
ATOM    489 1HG  ARG B  48      14.475  -5.536 -12.575  1.00  0.00           H
ATOM    490 2HG  ARG B  48      14.451  -3.993 -13.429  1.00  0.00           H
ATOM    491 1HD  ARG B  48      16.784  -3.468 -12.546  1.00  0.00           H
ATOM    492 2HD  ARG B  48      16.880  -5.066 -11.815  1.00  0.00           H
ATOM    493 1HH1 ARG B  48      14.444  -0.813 -11.011  1.00  0.00           H
ATOM    494 2HH1 ARG B  48      15.254  -1.855 -12.309  1.00  0.00           H
ATOM    495 1HH2 ARG B  48      14.187  -1.583  -9.101  1.00  0.00           H
ATOM    496 2HH2 ARG B  48      14.713  -3.326  -8.742  1.00  0.00           H
```

```
ATOM    497  N   PHE B  83       4.566 -13.690  -8.018  1.00 20.00           N
ATOM    498  CA  PHE B  83       5.450 -12.454  -8.093  1.00 20.00           C
ATOM    499  C   PHE B  83       6.888 -12.675  -8.519  1.00 20.00           C
ATOM    500  O   PHE B  83       7.624 -11.740  -8.853  1.00 20.00           O
ATOM    501  CB  PHE B  83       5.284 -11.530  -6.865  1.00 20.00           C
ATOM    502  CG  PHE B  83       5.508 -10.027  -7.169  1.00 20.00           C
ATOM    503  CD1 PHE B  83       4.420  -9.212  -7.501  1.00 20.00           C
ATOM    504  CD2 PHE B  83       6.770  -9.443  -6.996  1.00 20.00           C
ATOM    505  CE1 PHE B  83       4.587  -7.836  -7.642  1.00 20.00           C
ATOM    506  CE2 PHE B  83       6.935  -8.067  -7.134  1.00 20.00           C
ATOM    507  CZ  PHE B  83       5.842  -7.264  -7.450  1.00 20.00           C
ATOM    508 1H   PHE B  83       3.598 -13.423  -7.802  1.00  0.00           H
ATOM    509 2H   PHE B  83       4.521 -14.160  -8.929  1.00  0.00           H
ATOM    510  HA  PHE B  83       5.026 -11.890  -8.948  1.00  0.00           H
ATOM    511  HC  PHE B  83       7.211 -13.732  -8.490  1.00  0.00           H
ATOM    512 1HB  PHE B  83       5.946 -11.868  -6.045  1.00  0.00           H
ATOM    513 2HB  PHE B  83       4.269 -11.652  -6.438  1.00  0.00           H
ATOM    514  HD1 PHE B  83       3.434  -9.639  -7.622  1.00  0.00           H
ATOM    515  HD2 PHE B  83       7.620 -10.052  -6.725  1.00  0.00           H
ATOM    516  HE1 PHE B  83       3.739  -7.210  -7.878  1.00  0.00           H
ATOM    517  HE2 PHE B  83       7.908  -7.627  -6.968  1.00  0.00           H
ATOM    518  HZ  PHE B  83       5.954  -6.193  -7.527  1.00  0.00           H
ATOM    519  N   LEU B 209      -1.064  -9.042  15.447  1.00 20.00           N
ATOM    520  CA  LEU B 209      -1.135  -8.527  14.081  1.00 20.00           C
ATOM    521  C   LEU B 209      -2.543  -8.259  13.708  1.00 20.00           C
ATOM    522  O   LEU B 209      -2.805  -7.386  12.900  1.00 20.00           O
ATOM    523  CB  LEU B 209      -0.421  -9.495  13.090  1.00 20.00           C
ATOM    524  CG  LEU B 209       1.101  -9.277  12.866  1.00 20.00           C
ATOM    525  CD1 LEU B 209       1.958  -9.575  14.110  1.00 20.00           C
ATOM    526  CD2 LEU B 209       1.618 -10.129  11.693  1.00 20.00           C
ATOM    527 1H   LEU B 209      -1.558  -8.426  16.103  1.00  0.00           H
ATOM    528 2H   LEU B 209      -1.511  -9.962  15.521  1.00  0.00           H
ATOM    529  HA  LEU B 209      -0.614  -7.549  14.058  1.00  0.00           H
ATOM    530  HC  LEU B 209      -3.300  -8.915  14.180  1.00  0.00           H
ATOM    531 1HB  LEU B 209      -0.894  -9.379  12.098  1.00  0.00           H
ATOM    532 2HB  LEU B 209      -0.619 -10.552  13.357  1.00  0.00           H
ATOM    533  HG  LEU B 209       1.252  -8.220  12.580  1.00  0.00           H
ATOM    534 1HD1 LEU B 209       3.036  -9.418  13.919  1.00  0.00           H
ATOM    535 2HD1 LEU B 209       1.697  -8.912  14.955  1.00  0.00           H
ATOM    536 3HD1 LEU B 209       1.833 -10.616  14.462  1.00  0.00           H
ATOM    537 1HD2 LEU B 209       2.690  -9.942  11.492  1.00  0.00           H
ATOM    538 2HD2 LEU B 209       1.509 -11.213  11.886  1.00  0.00           H
ATOM    539 3HD2 LEU B 209       1.083  -9.905  10.752  1.00  0.00           H
ATOM    540  N   ILE B 212      -4.178  -4.968  14.862  1.00 20.00           N
ATOM    541  CA  ILE B 212      -3.787  -3.957  13.892  1.00 20.00           C
ATOM    542  C   ILE B 212      -4.580  -4.025  12.611  1.00 20.00           C
ATOM    543  O   ILE B 212      -5.080  -3.045  12.134  1.00 20.00           O
ATOM    544  CB  ILE B 212      -2.227  -3.740  13.893  1.00 20.00           C
ATOM    545  CG1 ILE B 212      -1.836  -2.780  15.063  1.00 20.00           C
ATOM    546  CG2 ILE B 212      -1.667  -3.179  12.567  1.00 20.00           C
ATOM    547  CD1 ILE B 212      -0.353  -2.724  15.444  1.00 20.00           C
ATOM    548 1H   ILE B 212      -5.201  -5.049  14.913  1.00  0.00           H
ATOM    549 2H   ILE B 212      -3.836  -5.893  14.576  1.00  0.00           H
ATOM    550  HA  ILE B 212      -4.202  -3.022  14.319  1.00  0.00           H
ATOM    551  HB  ILE B 212      -1.735  -4.721  14.054  1.00  0.00           H
ATOM    552 1HG1 ILE B 212      -2.388  -3.071  15.979  1.00  0.00           H
ATOM    553 2HG1 ILE B 212      -2.191  -1.754  14.843  1.00  0.00           H
ATOM    554 1HG2 ILE B 212      -0.570  -3.046  12.583  1.00  0.00           H
ATOM    555 2HG2 ILE B 212      -1.892  -3.829  11.708  1.00  0.00           H
ATOM    556 3HG2 ILE B 212      -2.120  -2.202  12.337  1.00  0.00           H
ATOM    557 1HD1 ILE B 212      -0.174  -1.989  16.251  1.00  0.00           H
ATOM    558 2HD1 ILE B 212      -0.018  -3.703  15.823  1.00  0.00           H
ATOM    559 3HD1 ILE B 212       0.297  -2.439  14.597  1.00  0.00           H
```

```
ATOM    560  N   CYS B 213      -4.687  -5.174  12.055  1.00 20.00           N
ATOM    561  CA  CYS B 213      -5.366  -5.342  10.790  1.00 20.00           C
ATOM    562  C   CYS B 213      -6.810  -5.338  10.997  1.00 20.00           C
ATOM    563  O   CYS B 213      -7.569  -5.855  10.192  1.00 20.00           O
ATOM    564  CB  CYS B 213      -4.815  -6.663  10.168  1.00 20.00           C
ATOM    565  SG  CYS B 213      -4.035  -6.280   8.570  1.00 20.00           S
ATOM    566  H   CYS B 213      -4.115  -5.920  12.480  1.00  0.00           H
ATOM    567  HA  CYS B 213      -5.086  -4.543  10.086  1.00  0.00           H
ATOM    568  HC  CYS B 213      -7.173  -4.800  11.894  1.00  0.00           H
ATOM    569 1HB  CYS B 213      -5.607  -7.416   9.993  1.00  0.00           H
ATOM    570 2HB  CYS B 213      -4.065  -7.195  10.782  1.00  0.00           H
ATOM    571  HG  CYS B 213      -3.593  -7.500   8.292  1.00  0.00           H
ATOM    572  N   THR B 216      -6.997  -0.571  13.732  1.00 20.00           N
ATOM    573  CA  THR B 216      -6.454   0.463  12.857  1.00 20.00           C
ATOM    574  C   THR B 216      -7.009   0.340  11.487  1.00 20.00           C
ATOM    575  O   THR B 216      -7.445   1.305  10.899  1.00 20.00           O
ATOM    576  CB  THR B 216      -4.916   0.615  12.991  1.00 20.00           C
ATOM    577  OG1 THR B 216      -4.238  -0.563  12.567  1.00 20.00           O
ATOM    578  CG2 THR B 216      -4.408   0.977  14.398  1.00 20.00           C
ATOM    579 1H   THR B 216      -6.736  -0.383  14.707  1.00  0.00           H
ATOM    580 2H   THR B 216      -8.025  -0.556  13.715  1.00  0.00           H
ATOM    581  HA  THR B 216      -6.869   1.418  13.235  1.00  0.00           H
ATOM    582  HB  THR B 216      -4.620   1.448  12.327  1.00  0.00           H
ATOM    583  HG1 THR B 216      -4.847  -1.309  12.655  1.00  0.00           H
ATOM    584 1HG2 THR B 216      -4.901   1.883  14.795  1.00  0.00           H
ATOM    585 2HG2 THR B 216      -4.581   0.159  15.122  1.00  0.00           H
ATOM    586 3HG2 THR B 216      -3.323   1.180  14.397  1.00  0.00           H
ATOM    587  N   LEU B 217      -6.978  -0.832  11.042  1.00 20.00           N
ATOM    588  CA  LEU B 217      -7.524  -1.178   9.778  1.00 20.00           C
ATOM    589  C   LEU B 217      -8.884  -1.614  10.017  1.00 20.00           C
ATOM    590  O   LEU B 217      -9.266  -1.955  11.140  1.00 20.00           O
ATOM    591  CB  LEU B 217      -6.584  -2.192   9.055  1.00 20.00           C
ATOM    592  CG  LEU B 217      -5.442  -1.568   8.210  1.00 20.00           C
ATOM    593  CD1 LEU B 217      -4.336  -2.597   7.936  1.00 20.00           C
ATOM    594  CD2 LEU B 217      -5.946  -1.006   6.867  1.00 20.00           C
ATOM    595  H   LEU B 217      -6.791  -1.530  11.773  1.00  0.00           H
ATOM    596  HA  LEU B 217      -7.550  -0.277   9.121  1.00  0.00           H
ATOM    597 1HB  LEU B 217      -7.164  -2.880   8.412  1.00  0.00           H
ATOM    598 2HB  LEU B 217      -6.160  -2.851   9.820  1.00  0.00           H
ATOM    599  HG  LEU B 217      -4.984  -0.745   8.795  1.00  0.00           H
ATOM    600 1HD1 LEU B 217      -3.514  -2.169   7.333  1.00  0.00           H
ATOM    601 2HD1 LEU B 217      -3.882  -2.943   8.882  1.00  0.00           H
ATOM    602 3HD1 LEU B 217      -4.711  -3.489   7.399  1.00  0.00           H
ATOM    603 1HD2 LEU B 217      -5.124  -0.541   6.291  1.00  0.00           H
ATOM    604 2HD2 LEU B 217      -6.390  -1.790   6.224  1.00  0.00           H
ATOM    605 3HD2 LEU B 217      -6.709  -0.221   7.002  1.00  0.00           H
ATOM    606  N   LYS B 218      -9.585  -1.595   8.981  1.00 20.00           N
ATOM    607  CA  LYS B 218     -10.920  -2.120   9.075  1.00 20.00           C
ATOM    608  C   LYS B 218     -11.015  -3.516   8.517  1.00 20.00           C
ATOM    609  O   LYS B 218     -11.691  -4.422   9.092  1.00 20.00           O
ATOM    610  CB  LYS B 218     -11.838  -1.107   8.325  1.00 20.00           C
ATOM    611  CG  LYS B 218     -13.357  -1.384   8.429  1.00 20.00           C
ATOM    612  CD  LYS B 218     -14.198  -0.332   7.680  1.00 20.00           C
ATOM    613  CE  LYS B 218     -15.703  -0.628   7.761  1.00 20.00           C
ATOM    614  NZ  LYS B 218     -16.458   0.404   7.024  1.00 20.00           N
ATOM    615  H   LYS B 218      -9.199  -1.116   8.163  1.00  0.00           H
ATOM    616  HA  LYS B 218     -11.323  -2.172  10.111  1.00  0.00           H
ATOM    617 1HB  LYS B 218     -11.554  -1.052   7.255  1.00  0.00           H
ATOM    618 2HB  LYS B 218     -11.657  -0.086   8.722  1.00  0.00           H
ATOM    619 1HG  LYS B 218     -13.660  -1.416   9.494  1.00  0.00           H
ATOM    620 2HG  LYS B 218     -13.585  -2.392   8.028  1.00  0.00           H
ATOM    621 1HD  LYS B 218     -13.885  -0.293   6.618  1.00  0.00           H
ATOM    622 2HD  LYS B 218     -13.986   0.674   8.093  1.00  0.00           H
```

```
ATOM    623 1HE  LYS B 218     -16.038  -0.662   8.817  1.00  0.00           H
ATOM    624 2HE  LYS B 218     -15.924  -1.626   7.335  1.00  0.00           H
ATOM    625 1HZ  LYS B 218     -17.471   0.249   7.099  1.00  0.00           H
ATOM    626 2HZ  LYS B 218     -16.291   1.334   7.424  1.00  0.00           H
ATOM    627  N   LEU B 219     -10.329  -3.878   7.226  1.00 20.00           N
ATOM    628  CA  LEU B 219     -10.316  -5.262   6.538  1.00 20.00           C
ATOM    629  C   LEU B 219     -11.539  -5.922   6.904  1.00 20.00           C
ATOM    630  O   LEU B 219     -11.866  -6.099   8.026  1.00 20.00           O
ATOM    631  CB  LEU B 219      -9.042  -6.085   6.852  1.00 20.00           C
ATOM    632  CG  LEU B 219      -7.697  -5.514   6.339  1.00 20.00           C
ATOM    633  CD1 LEU B 219      -6.571  -6.467   6.751  1.00 20.00           C
ATOM    634  CD2 LEU B 219      -7.638  -5.300   4.815  1.00 20.00           C
ATOM    635  H   LEU B 219      -9.757  -3.111   6.865  1.00  0.00           H
ATOM    636  HA  LEU B 219     -10.348  -5.085   5.446  1.00  0.00           H
ATOM    637 1HB  LEU B 219      -9.169  -7.109   6.446  1.00  0.00           H
ATOM    638 2HB  LEU B 219      -8.982  -6.226   7.951  1.00  0.00           H
ATOM    639  HG  LEU B 219      -7.516  -4.540   6.834  1.00  0.00           H
ATOM    640 1HD1 LEU B 219      -5.580  -6.059   6.481  1.00  0.00           H
ATOM    641 2HD1 LEU B 219      -6.566  -6.631   7.844  1.00  0.00           H
ATOM    642 3HD1 LEU B 219      -6.662  -7.459   6.273  1.00  0.00           H
ATOM    643 1HD2 LEU B 219      -6.640  -4.946   4.495  1.00  0.00           H
ATOM    644 2HD2 LEU B 219      -7.856  -6.230   4.257  1.00  0.00           H
ATOM    645 3HD2 LEU B 219      -8.358  -4.534   4.475  1.00  0.00           H
ATOM    646  N   THR B 220     -12.423  -6.379   6.190  1.00 20.00           N
ATOM    647  CA  THR B 220     -13.502  -6.835   7.066  1.00 20.00           C
ATOM    648  C   THR B 220     -13.213  -8.209   7.755  1.00 20.00           C
ATOM    649  O   THR B 220     -13.672  -8.430   8.917  1.00 20.00           O
ATOM    650  CB  THR B 220     -14.781  -7.039   6.162  1.00 20.00           C
ATOM    651  OG1 THR B 220     -14.558  -7.922   5.059  1.00 20.00           O
ATOM    652  CG2 THR B 220     -15.399  -5.750   5.586  1.00 20.00           C
ATOM    653  H   THR B 220     -12.529  -6.033   5.232  1.00  0.00           H
ATOM    654  HA  THR B 220     -13.957  -6.105   7.792  1.00  0.00           H
ATOM    655  HB  THR B 220     -15.576  -7.489   6.794  1.00  0.00           H
ATOM    656  HG1 THR B 220     -14.216  -8.748   5.419  1.00  0.00           H
ATOM    657 1HG2 THR B 220     -16.326  -5.970   5.024  1.00  0.00           H
ATOM    658 2HG2 THR B 220     -15.662  -5.026   6.379  1.00  0.00           H
ATOM    659 3HG2 THR B 220     -14.714  -5.241   4.885  1.00  0.00           H
ATOM    660  N   THR B 221     -12.443  -9.036   6.939  1.00 20.00           N
ATOM    661  CA  THR B 221     -11.976 -10.521   7.124  1.00 20.00           C
ATOM    662  C   THR B 221     -10.482 -10.536   6.734  1.00 20.00           C
ATOM    663  O   THR B 221     -10.119 -10.590   5.553  1.00 20.00           O
ATOM    664  CB  THR B 221     -12.808 -11.508   6.250  1.00 20.00           C
ATOM    665  OG1 THR B 221     -12.718 -11.155   4.871  1.00 20.00           O
ATOM    666  CG2 THR B 221     -14.296 -11.611   6.618  1.00 20.00           C
ATOM    667  H   THR B 221     -12.103  -8.487   6.141  1.00  0.00           H
ATOM    668  HA  THR B 221     -12.130 -10.815   8.177  1.00  0.00           H
ATOM    669  HB  THR B 221     -12.374 -12.521   6.372  1.00  0.00           H
ATOM    670  HG1 THR B 221     -11.775 -11.008   4.706  1.00  0.00           H
ATOM    671 1HG2 THR B 221     -14.813 -12.350   5.980  1.00  0.00           H
ATOM    672 2HG2 THR B 221     -14.440 -11.926   7.668  1.00  0.00           H
ATOM    673 3HG2 THR B 221     -14.823 -10.648   6.489  1.00  0.00           H
ATOM    674  N   PRO B 222      -9.504 -10.522   7.655  1.00 20.00           N
ATOM    675  CA  PRO B 222      -8.124 -10.418   7.303  1.00 20.00           C
ATOM    676  C   PRO B 222      -7.713 -11.572   6.598  1.00 20.00           C
ATOM    677  O   PRO B 222      -8.538 -12.349   6.099  1.00 20.00           O
ATOM    678  CB  PRO B 222      -7.503  -9.933   8.660  1.00 20.00           C
ATOM    679  CG  PRO B 222      -8.380 -10.531   9.750  1.00 20.00           C
ATOM    680  CD  PRO B 222      -9.762 -10.456   9.117  1.00 20.00           C
ATOM    681  HA  PRO B 222      -8.003  -9.575   6.590  1.00  0.00           H
ATOM    682 1HB  PRO B 222      -7.551  -8.827   8.718  1.00  0.00           H
ATOM    683 2HB  PRO B 222      -6.438 -10.192   8.800  1.00  0.00           H
ATOM    684 1HG  PRO B 222      -8.315  -9.984  10.709  1.00  0.00           H
ATOM    685 2HG  PRO B 222      -8.097 -11.584   9.943  1.00  0.00           H
```

```
ATOM    686 1HD  PRO B 222     -10.396 -11.289   9.480  1.00  0.00           H
ATOM    687 2HD  PRO B 222     -10.268  -9.504   9.382  1.00  0.00           H
ATOM    688  N   THR B 223      -6.503 -11.723   6.625  1.00 20.00           N
ATOM    689  CA  THR B 223      -5.998 -12.756   5.885  1.00 20.00           C
ATOM    690  C   THR B 223      -4.598 -12.880   6.193  1.00 20.00           C
ATOM    691  O   THR B 223      -3.953 -11.922   6.620  1.00 20.00           O
ATOM    692  CB  THR B 223      -6.149 -12.744   4.298  1.00 20.00           C
ATOM    693  OG1 THR B 223      -7.384 -12.192   3.850  1.00 20.00           O
ATOM    694  CG2 THR B 223      -6.128 -14.149   3.669  1.00 20.00           C
ATOM    695  H   THR B 223      -5.926 -11.005   7.074  1.00  0.00           H
ATOM    696  HA  THR B 223      -6.442 -13.710   6.255  1.00  0.00           H
ATOM    697  HC  THR B 223      -4.183 -13.895   6.056  1.00  0.00           H
ATOM    698  HB  THR B 223      -5.355 -12.129   3.832  1.00  0.00           H
ATOM    699  HG1 THR B 223      -7.998 -12.284   4.605  1.00  0.00           H
ATOM    700 1HG2 THR B 223      -6.200 -14.091   2.567  1.00  0.00           H
ATOM    701 2HG2 THR B 223      -5.208 -14.713   3.902  1.00  0.00           H
ATOM    702 3HG2 THR B 223      -6.983 -14.762   4.012  1.00  0.00           H
ATOM    703  N   GLY B 225      -2.765 -13.403   3.656  1.00 20.00           N
ATOM    704  CA  GLY B 225      -1.893 -12.573   2.751  1.00 20.00           C
ATOM    705  C   GLY B 225      -1.904 -11.130   3.190  1.00 20.00           C
ATOM    706  O   GLY B 225      -0.900 -10.463   3.036  1.00 20.00           O
ATOM    707 1H   GLY B 225      -2.844 -14.360   3.290  1.00  0.00           H
ATOM    708 2H   GLY B 225      -2.311 -13.507   4.572  1.00  0.00           H
ATOM    709 1HA  GLY B 225      -2.257 -12.635   1.709  1.00  0.00           H
ATOM    710 2HA  GLY B 225      -0.858 -12.961   2.749  1.00  0.00           H
ATOM    711  N   ASP B 226      -2.857 -10.631   3.775  1.00 20.00           N
ATOM    712  CA  ASP B 226      -2.947  -9.262   4.104  1.00 20.00           C
ATOM    713  C   ASP B 226      -2.053  -8.892   5.252  1.00 20.00           C
ATOM    714  O   ASP B 226      -1.565  -7.792   5.373  1.00 20.00           O
ATOM    715  CB  ASP B 226      -4.440  -8.854   4.278  1.00 20.00           C
ATOM    716  CG  ASP B 226      -4.715  -7.399   3.877  1.00 20.00           C
ATOM    717  OD1 ASP B 226      -4.137  -6.430   4.359  1.00 20.00           O
ATOM    718  OD2 ASP B 226      -5.662  -7.300   2.904  1.00 20.00           O
ATOM    719  H   ASP B 226      -3.613 -11.307   3.924  1.00  0.00           H
ATOM    720  HA  ASP B 226      -2.564  -8.673   3.241  1.00  0.00           H
ATOM    721 1HB  ASP B 226      -4.777  -9.011   5.319  1.00  0.00           H
ATOM    722 2HB  ASP B 226      -5.108  -9.495   3.669  1.00  0.00           H
ATOM    723  HD2 ASP B 226      -5.787  -6.375   2.687  1.00  0.00           H
ATOM    724  N   LEU B 227      -1.824  -9.889   6.072  1.00 20.00           N
ATOM    725  CA  LEU B 227      -0.895  -9.724   7.159  1.00 20.00           C
ATOM    726  C   LEU B 227       0.484  -9.499   6.632  1.00 20.00           C
ATOM    727  O   LEU B 227       1.329  -8.962   7.346  1.00 20.00           O
ATOM    728  CB  LEU B 227      -0.992 -10.953   8.128  1.00 20.00           C
ATOM    729  CG  LEU B 227      -1.731 -10.705   9.471  1.00 20.00           C
ATOM    730  CD1 LEU B 227      -3.243 -10.466   9.326  1.00 20.00           C
ATOM    731  CD2 LEU B 227      -1.519 -11.892  10.428  1.00 20.00           C
ATOM    732  H   LEU B 227      -2.446 -10.704   5.965  1.00  0.00           H
ATOM    733  HA  LEU B 227      -1.150  -8.808   7.732  1.00  0.00           H
ATOM    734 1HB  LEU B 227       0.033 -11.287   8.386  1.00  0.00           H
ATOM    735 2HB  LEU B 227      -1.418 -11.844   7.625  1.00  0.00           H
ATOM    736  HG  LEU B 227      -1.286  -9.804   9.935  1.00  0.00           H
ATOM    737 1HD1 LEU B 227      -3.693 -10.116  10.274  1.00  0.00           H
ATOM    738 2HD1 LEU B 227      -3.474  -9.708   8.559  1.00  0.00           H
ATOM    739 3HD1 LEU B 227      -3.783 -11.387   9.037  1.00  0.00           H
ATOM    740 1HD2 LEU B 227      -1.993 -11.719  11.412  1.00  0.00           H
ATOM    741 2HD2 LEU B 227      -1.942 -12.832  10.025  1.00  0.00           H
ATOM    742 3HD2 LEU B 227      -0.447 -12.080  10.623  1.00  0.00           H
ATOM    743  N   ASN B 228       0.685  -9.884   5.390  1.00 20.00           N
ATOM    744  CA  ASN B 228       1.949  -9.699   4.729  1.00 20.00           C
ATOM    745  C   ASN B 228       2.097  -8.223   4.252  1.00 20.00           C
ATOM    746  O   ASN B 228       3.193  -7.690   4.138  1.00 20.00           O
ATOM    747  CB  ASN B 228       2.268 -10.975   3.908  1.00 20.00           C
ATOM    748  CG  ASN B 228       2.237 -12.345   4.612  1.00 20.00           C
```

```
ATOM    749  OD1 ASN B 228       2.507 -12.486   5.799  1.00 20.00           O
ATOM    750  ND2 ASN B 228       1.943 -13.404   3.898  1.00 20.00           N
ATOM    751  H   ASN B 228      -0.148 -10.269   4.921  1.00  0.00           H
ATOM    752  HA  ASN B 228       2.748  -9.742   5.500  1.00  0.00           H
ATOM    753 1HB  ASN B 228       3.314 -10.910   3.575  1.00  0.00           H
ATOM    754 2HB  ASN B 228       1.621 -10.994   3.016  1.00  0.00           H
ATOM    755 1HD2 ASN B 228       1.748 -13.261   2.904  1.00  0.00           H
ATOM    756 2HD2 ASN B 228       1.954 -14.279   4.428  1.00  0.00           H
ATOM    757  N   HIS B 229       0.988  -7.531   3.904  1.00 20.00           N
ATOM    758  CA  HIS B 229       1.064  -6.058   3.844  1.00 20.00           C
ATOM    759  C   HIS B 229       1.663  -5.750   5.261  1.00 20.00           C
ATOM    760  O   HIS B 229       2.762  -5.460   5.461  1.00 20.00           O
ATOM    761  CB  HIS B 229      -0.246  -5.353   3.420  1.00 20.00           C
ATOM    762  CG  HIS B 229      -0.424  -5.330   1.900  1.00 20.00           C
ATOM    763  ND1 HIS B 229       0.338  -4.523   1.057  1.00 20.00           N
ATOM    764  CD2 HIS B 229      -1.268  -6.170   1.154  1.00 20.00           C
ATOM    765  CE1 HIS B 229      -0.123  -4.973  -0.155  1.00 20.00           C
ATOM    766  NE2 HIS B 229      -1.095  -5.939  -0.200  1.00 20.00           N
ATOM    767  H   HIS B 229       0.118  -8.018   4.154  1.00  0.00           H
ATOM    768  HA  HIS B 229       1.857  -5.765   3.124  1.00  0.00           H
ATOM    769 1HB  HIS B 229      -0.222  -4.306   3.774  1.00  0.00           H
ATOM    770 2HB  HIS B 229      -1.127  -5.797   3.917  1.00  0.00           H
ATOM    771  HD2 HIS B 229      -1.913  -6.926   1.579  1.00  0.00           H
ATOM    772  HE1 HIS B 229       0.311  -4.586  -1.070  1.00  0.00           H
ATOM    773  HE2 HIS B 229      -1.458  -6.453  -1.011  1.00  0.00           H
ATOM    774  N   LEU B 230       1.030  -5.894   6.417  1.00 20.00           N
ATOM    775  CA  LEU B 230       1.667  -5.407   7.727  1.00 20.00           C
ATOM    776  C   LEU B 230       3.197  -5.411   7.853  1.00 20.00           C
ATOM    777  O   LEU B 230       3.846  -4.383   8.067  1.00 20.00           O
ATOM    778  CB  LEU B 230       0.932  -6.091   8.926  1.00 20.00           C
ATOM    779  CG  LEU B 230      -0.273  -5.363   9.568  1.00 20.00           C
ATOM    780  CD1 LEU B 230      -1.291  -4.809   8.559  1.00 20.00           C
ATOM    781  CD2 LEU B 230      -0.981  -6.342  10.523  1.00 20.00           C
ATOM    782  H   LEU B 230       0.081  -6.278   6.350  1.00  0.00           H
ATOM    783  HA  LEU B 230       1.429  -4.327   7.787  1.00  0.00           H
ATOM    784 1HB  LEU B 230       1.653  -6.282   9.745  1.00  0.00           H
ATOM    785 2HB  LEU B 230       0.625  -7.109   8.634  1.00  0.00           H
ATOM    786  HG  LEU B 230       0.109  -4.509  10.162  1.00  0.00           H
ATOM    787 1HD1 LEU B 230      -2.173  -4.387   9.070  1.00  0.00           H
ATOM    788 2HD1 LEU B 230      -0.868  -3.992   7.947  1.00  0.00           H
ATOM    789 3HD1 LEU B 230      -1.646  -5.587   7.858  1.00  0.00           H
ATOM    790 1HD2 LEU B 230      -1.863  -5.891  11.009  1.00  0.00           H
ATOM    791 2HD2 LEU B 230      -1.345  -7.247  10.003  1.00  0.00           H
ATOM    792 3HD2 LEU B 230      -0.314  -6.681  11.337  1.00  0.00           H
ATOM    793  N   VAL B 231       3.764  -6.558   7.760  1.00 20.00           N
ATOM    794  CA  VAL B 231       5.175  -6.729   7.983  1.00 20.00           C
ATOM    795  C   VAL B 231       6.041  -5.987   7.013  1.00 20.00           C
ATOM    796  O   VAL B 231       7.059  -5.447   7.373  1.00 20.00           O
ATOM    797  CB  VAL B 231       5.519  -8.273   8.055  1.00 20.00           C
ATOM    798  CG1 VAL B 231       7.002  -8.566   8.403  1.00 20.00           C
ATOM    799  CG2 VAL B 231       4.683  -9.104   9.066  1.00 20.00           C
ATOM    800  H   VAL B 231       3.121  -7.331   7.544  1.00  0.00           H
ATOM    801  HA  VAL B 231       5.415  -6.314   8.983  1.00  0.00           H
ATOM    802  HB  VAL B 231       5.328  -8.707   7.052  1.00  0.00           H
ATOM    803 1HG1 VAL B 231       7.222  -9.650   8.425  1.00  0.00           H
ATOM    804 2HG1 VAL B 231       7.696  -8.130   7.660  1.00  0.00           H
ATOM    805 3HG1 VAL B 231       7.287  -8.153   9.389  1.00  0.00           H
ATOM    806 1HG2 VAL B 231       4.943 -10.179   9.040  1.00  0.00           H
ATOM    807 2HG2 VAL B 231       4.824  -8.760  10.106  1.00  0.00           H
ATOM    808 3HG2 VAL B 231       3.598  -9.051   8.854  1.00  0.00           H
ATOM    809  N   SER B 232       5.689  -5.961   5.778  1.00 20.00           N
ATOM    810  CA  SER B 232       6.527  -5.265   4.852  1.00 20.00           C
ATOM    811  C   SER B 232       6.871  -3.924   5.455  1.00 20.00           C
```

```
ATOM    812  O   SER B 232       7.964  -3.421   5.312  1.00 20.00           O
ATOM    813  CB  SER B 232       5.760  -5.216   3.515  1.00 20.00           C
ATOM    814  OG  SER B 232       4.507  -4.520   3.594  1.00 20.00           O
ATOM    815  H   SER B 232       4.788  -6.408   5.554  1.00  0.00           H
ATOM    816  HA  SER B 232       7.469  -5.828   4.699  1.00  0.00           H
ATOM    817 1HB  SER B 232       5.580  -6.239   3.136  1.00  0.00           H
ATOM    818 2HB  SER B 232       6.404  -4.740   2.759  1.00  0.00           H
ATOM    819  HG  SER B 232       3.964  -4.962   4.269  1.00  0.00           H
ATOM    820  N   ALA B 233       5.915  -3.400   6.124  1.00 20.00           N
ATOM    821  CA  ALA B 233       6.032  -2.115   6.772  1.00 20.00           C
ATOM    822  C   ALA B 233       7.172  -2.080   7.735  1.00 20.00           C
ATOM    823  O   ALA B 233       8.101  -1.293   7.533  1.00 20.00           O
ATOM    824  CB  ALA B 233       4.595  -1.784   7.223  1.00 20.00           C
ATOM    825  H   ALA B 233       5.110  -4.024   6.263  1.00  0.00           H
ATOM    826  HA  ALA B 233       6.282  -1.366   5.994  1.00  0.00           H
ATOM    827 1HB  ALA B 233       4.356  -0.754   6.966  1.00  0.00           H
ATOM    828 2HB  ALA B 233       3.789  -2.341   6.704  1.00  0.00           H
ATOM    829 3HB  ALA B 233       4.441  -1.935   8.305  1.00  0.00           H
ATOM    830  N   THR B 234       7.166  -3.039   8.629  1.00 20.00           N
ATOM    831  CA  THR B 234       8.119  -3.191   9.684  1.00 20.00           C
ATOM    832  C   THR B 234       9.430  -3.510   9.105  1.00 20.00           C
ATOM    833  O   THR B 234      10.353  -3.140   9.878  1.00 20.00           O
ATOM    834  CB  THR B 234       7.567  -4.237  10.710  1.00 20.00           C
ATOM    835  OG1 THR B 234       6.285  -3.844  11.192  1.00 20.00           O
ATOM    836  CG2 THR B 234       8.419  -4.428  11.975  1.00 20.00           C
ATOM    837  H   THR B 234       6.386  -3.698   8.506  1.00  0.00           H
ATOM    838  HA  THR B 234       8.202  -2.220  10.214  1.00  0.00           H
ATOM    839  HB  THR B 234       7.463  -5.220  10.206  1.00  0.00           H
ATOM    840  HG1 THR B 234       6.450  -3.166  11.851  1.00  0.00           H
ATOM    841 1HG2 THR B 234       7.946  -5.139  12.679  1.00  0.00           H
ATOM    842 2HG2 THR B 234       9.418  -4.837  11.735  1.00  0.00           H
ATOM    843 3HG2 THR B 234       8.581  -3.479  12.520  1.00  0.00           H
ATOM    844  N   MET B 235       9.709  -4.057   8.084  1.00 20.00           N
ATOM    845  CA  MET B 235      10.962  -4.327   7.497  1.00 20.00           C
ATOM    846  C   MET B 235      11.443  -3.192   6.622  1.00 20.00           C
ATOM    847  O   MET B 235      12.602  -2.783   6.648  1.00 20.00           O
ATOM    848  CB  MET B 235      10.935  -5.725   6.827  1.00 20.00           C
ATOM    849  CG  MET B 235      10.813  -6.930   7.786  1.00 20.00           C
ATOM    850  SD  MET B 235      10.845  -8.464   6.842  1.00 20.00           S
ATOM    851  CE  MET B 235      10.761  -9.658   8.186  1.00 20.00           C
ATOM    852  H   MET B 235       8.846  -4.386   7.626  1.00  0.00           H
ATOM    853  HA  MET B 235      11.733  -4.405   8.293  1.00  0.00           H
ATOM    854 1HB  MET B 235      11.874  -5.862   6.259  1.00  0.00           H
ATOM    855 2HB  MET B 235      10.123  -5.769   6.077  1.00  0.00           H
ATOM    856 1HG  MET B 235       9.872  -6.881   8.366  1.00  0.00           H
ATOM    857 2HG  MET B 235      11.640  -6.936   8.521  1.00  0.00           H
ATOM    858 1HE  MET B 235      11.652  -9.582   8.834  1.00  0.00           H
ATOM    859 2HE  MET B 235       9.865  -9.491   8.810  1.00  0.00           H
ATOM    860 3HE  MET B 235      10.714 -10.687   7.786  1.00  0.00           H
ATOM    861  N   SER B 236      10.635  -2.621   5.784  1.00 20.00           N
ATOM    862  CA  SER B 236      11.068  -1.563   4.852  1.00 20.00           C
ATOM    863  C   SER B 236      11.697  -0.397   5.609  1.00 20.00           C
ATOM    864  O   SER B 236      12.645   0.216   5.153  1.00 20.00           O
ATOM    865  CB  SER B 236       9.891  -1.169   3.924  1.00 20.00           C
ATOM    866  OG  SER B 236       8.716  -0.787   4.644  1.00 20.00           O
ATOM    867  H   SER B 236       9.680  -3.014   5.777  1.00  0.00           H
ATOM    868  HA  SER B 236      11.860  -1.976   4.199  1.00  0.00           H
ATOM    869 1HB  SER B 236       9.644  -2.010   3.247  1.00  0.00           H
ATOM    870 2HB  SER B 236      10.196  -0.341   3.255  1.00  0.00           H
ATOM    871  HG  SER B 236       8.391  -1.584   5.088  1.00  0.00           H
ATOM    872  N   GLY B 237      11.172  -0.090   6.763  1.00 20.00           N
ATOM    873  CA  GLY B 237      11.711   0.990   7.583  1.00 20.00           C
ATOM    874  C   GLY B 237      13.073   0.658   8.031  1.00 20.00           C
```

```
ATOM    875  O   GLY B 237      13.983   1.456   7.907  1.00 20.00           O
ATOM    876  H   GLY B 237      10.303  -0.602   6.973  1.00  0.00           H
ATOM    877 1HA  GLY B 237      11.090   1.042   8.488  1.00  0.00           H
ATOM    878 2HA  GLY B 237      11.586   1.998   7.199  1.00  0.00           H
ATOM    879  N   VAL B 238      13.233  -0.574   8.385  1.00 20.00           N
ATOM    880  CA  VAL B 238      14.494  -0.952   8.912  1.00 20.00           C
ATOM    881  C   VAL B 238      15.446  -1.124   7.754  1.00 20.00           C
ATOM    882  O   VAL B 238      16.600  -0.719   7.868  1.00 20.00           O
ATOM    883  CB  VAL B 238      14.342  -2.195   9.875  1.00 20.00           C
ATOM    884  CG1 VAL B 238      15.691  -2.719  10.425  1.00 20.00           C
ATOM    885  CG2 VAL B 238      13.436  -1.933  11.106  1.00 20.00           C
ATOM    886  H   VAL B 238      12.421  -1.188   8.254  1.00  0.00           H
ATOM    887  HA  VAL B 238      14.921  -0.146   9.549  1.00  0.00           H
ATOM    888  HB  VAL B 238      13.882  -3.024   9.300  1.00  0.00           H
ATOM    889 1HG1 VAL B 238      15.562  -3.603  11.076  1.00  0.00           H
ATOM    890 2HG1 VAL B 238      16.373  -3.030   9.612  1.00  0.00           H
ATOM    891 3HG1 VAL B 238      16.225  -1.950  11.015  1.00  0.00           H
ATOM    892 1HG2 VAL B 238      13.326  -2.831  11.742  1.00  0.00           H
ATOM    893 2HG2 VAL B 238      13.827  -1.119  11.746  1.00  0.00           H
ATOM    894 3HG2 VAL B 238      12.411  -1.644  10.807  1.00  0.00           H
ATOM    895  N   THR B 239      14.976  -2.098   6.794  1.00 20.00           N
ATOM    896  CA  THR B 239      15.816  -2.518   5.701  1.00 20.00           C
ATOM    897  C   THR B 239      15.933  -1.435   4.641  1.00 20.00           C
ATOM    898  O   THR B 239      17.053  -1.279   4.113  1.00 20.00           O
ATOM    899  CB  THR B 239      15.367  -3.909   5.138  1.00 20.00           C
ATOM    900  OG1 THR B 239      14.006  -3.882   4.714  1.00 20.00           O
ATOM    901  CG2 THR B 239      15.512  -5.085   6.118  1.00 20.00           C
ATOM    902  H   THR B 239      13.957  -2.303   6.858  1.00  0.00           H
ATOM    903  HA  THR B 239      16.843  -2.665   6.092  1.00  0.00           H
ATOM    904  HB  THR B 239      15.994  -4.142   4.254  1.00  0.00           H
ATOM    905  HG1 THR B 239      13.500  -3.573   5.482  1.00  0.00           H
ATOM    906 1HG2 THR B 239      15.207  -6.040   5.652  1.00  0.00           H
ATOM    907 2HG2 THR B 239      16.557  -5.207   6.458  1.00  0.00           H
ATOM    908 3HG2 THR B 239      14.887  -4.951   7.021  1.00  0.00           H
ATOM    909  N   THR B 240      14.883  -1.041   3.932  1.00 20.00           N
ATOM    910  CA  THR B 240      14.936   0.080   3.030  1.00 20.00           C
ATOM    911  C   THR B 240      15.311   1.328   3.776  1.00 20.00           C
ATOM    912  O   THR B 240      16.078   2.185   3.249  1.00 20.00           O
ATOM    913  CB  THR B 240      13.516   0.468   2.402  1.00 20.00           C
ATOM    914  OG1 THR B 240      12.657  -0.629   2.177  1.00 20.00           O
ATOM    915  CG2 THR B 240      13.495   1.468   1.236  1.00 20.00           C
ATOM    916  H   THR B 240      13.995  -1.272   4.390  1.00  0.00           H
ATOM    917  HA  THR B 240      15.667  -0.112   2.221  1.00  0.00           H
ATOM    918  HB  THR B 240      12.906   1.040   3.113  1.00  0.00           H
ATOM    919  HG1 THR B 240      12.966  -1.081   1.377  1.00  0.00           H
ATOM    920 1HG2 THR B 240      12.555   1.417   0.656  1.00  0.00           H
ATOM    921 2HG2 THR B 240      13.567   2.509   1.604  1.00  0.00           H
ATOM    922 3HG2 THR B 240      14.340   1.336   0.544  1.00  0.00           H
ATOM    923  N   CYS B 241      14.677   1.649   4.868  1.00 20.00           N
ATOM    924  CA  CYS B 241      14.826   2.986   5.403  1.00 20.00           C
ATOM    925  C   CYS B 241      16.175   3.184   6.009  1.00 20.00           C
ATOM    926  O   CYS B 241      16.582   2.399   6.817  1.00 20.00           O
ATOM    927  CB  CYS B 241      13.636   3.650   6.097  1.00 20.00           C
ATOM    928  SG  CYS B 241      12.120   3.009   5.324  1.00 20.00           S
ATOM    929  H   CYS B 241      13.892   1.016   5.129  1.00  0.00           H
ATOM    930  HA  CYS B 241      14.862   3.671   4.527  1.00  0.00           H
ATOM    931  HC  CYS B 241      16.746   4.049   5.628  1.00  0.00           H
ATOM    932 1HB  CYS B 241      13.684   4.749   5.989  1.00  0.00           H
ATOM    933 2HB  CYS B 241      13.604   3.522   7.186  1.00  0.00           H
ATOM    934  HG  CYS B 241      12.546   2.933   4.068  1.00  0.00           H
ATOM    935  N   PHE B 244      17.920   3.455   2.077  1.00 20.00           N
ATOM    936  CA  PHE B 244      17.601   4.242   1.050  1.00 20.00           C
ATOM    937  C   PHE B 244      18.027   5.562   1.548  1.00 20.00           C
```

```
ATOM    938  O   PHE B 244      18.115   5.819   2.723  1.00 20.00           O
ATOM    939  CB  PHE B 244      16.058   4.103   0.912  1.00 20.00           C
ATOM    940  CG  PHE B 244      15.357   4.316  -0.421  1.00 20.00           C
ATOM    941  CD1 PHE B 244      15.768   3.577  -1.532  1.00 20.00           C
ATOM    942  CD2 PHE B 244      14.074   4.869  -0.401  1.00 20.00           C
ATOM    943  CE1 PHE B 244      14.891   3.369  -2.587  1.00 20.00           C
ATOM    944  CE2 PHE B 244      13.203   4.660  -1.468  1.00 20.00           C
ATOM    945  CZ  PHE B 244      13.608   3.902  -2.556  1.00 20.00           C
ATOM    946 1H   PHE B 244      18.157   4.061   2.874  1.00  0.00           H
ATOM    947 2H   PHE B 244      17.101   2.914   2.406  1.00  0.00           H
ATOM    948  HA  PHE B 244      18.158   3.933   0.145  1.00  0.00           H
ATOM    949  HC  PHE B 244      18.247   6.288   0.745  1.00  0.00           H
ATOM    950 1HB  PHE B 244      15.553   4.659   1.729  1.00  0.00           H
ATOM    951 2HB  PHE B 244      15.760   3.057   1.110  1.00  0.00           H
ATOM    952  HD1 PHE B 244      16.718   3.063  -1.540  1.00  0.00           H
ATOM    953  HD2 PHE B 244      13.714   5.377   0.482  1.00  0.00           H
ATOM    954  HE1 PHE B 244      15.193   2.727  -3.396  1.00  0.00           H
ATOM    955  HE2 PHE B 244      12.194   5.038  -1.431  1.00  0.00           H
ATOM    956  HZ  PHE B 244      12.913   3.700  -3.358  1.00  0.00           H
ATOM    957  N   GLY B 271       6.197  -1.045  15.077  1.00 20.00           N
ATOM    958  CA  GLY B 271       4.978  -0.597  14.551  1.00 20.00           C
ATOM    959  C   GLY B 271       5.128   0.191  13.251  1.00 20.00           C
ATOM    960  O   GLY B 271       6.189   0.763  13.023  1.00 20.00           O
ATOM    961 1H   GLY B 271       6.064  -1.700  15.858  1.00  0.00           H
ATOM    962 2H   GLY B 271       6.765  -1.539  14.379  1.00  0.00           H
ATOM    963 1HA  GLY B 271       4.480   0.049  15.299  1.00  0.00           H
ATOM    964 2HA  GLY B 271       4.315  -1.477  14.422  1.00  0.00           H
ATOM    965  N   PHE B 272       4.023   0.200  12.579  1.00 20.00           N
ATOM    966  CA  PHE B 272       3.950   1.023  11.373  1.00 20.00           C
ATOM    967  C   PHE B 272       2.770   1.877  11.490  1.00 20.00           C
ATOM    968  O   PHE B 272       1.761   1.218  11.751  1.00 20.00           O
ATOM    969  CB  PHE B 272       4.131   0.235  10.047  1.00 20.00           C
ATOM    970  CG  PHE B 272       4.906   1.006   8.946  1.00 20.00           C
ATOM    971  CD1 PHE B 272       4.236   1.545   7.844  1.00 20.00           C
ATOM    972  CD2 PHE B 272       6.304   1.050   8.970  1.00 20.00           C
ATOM    973  CE1 PHE B 272       4.943   2.104   6.781  1.00 20.00           C
ATOM    974  CE2 PHE B 272       7.012   1.602   7.903  1.00 20.00           C
ATOM    975  CZ  PHE B 272       6.332   2.128   6.811  1.00 20.00           C
ATOM    976  H   PHE B 272       3.199  -0.217  13.024  1.00  0.00           H
ATOM    977  HA  PHE B 272       4.817   1.714  11.379  1.00  0.00           H
ATOM    978 1HB  PHE B 272       3.152  -0.129   9.679  1.00  0.00           H
ATOM    979 2HB  PHE B 272       4.691  -0.699  10.254  1.00  0.00           H
ATOM    980  HD1 PHE B 272       3.170   1.417   7.755  1.00  0.00           H
ATOM    981  HD2 PHE B 272       6.847   0.611   9.794  1.00  0.00           H
ATOM    982  HE1 PHE B 272       4.417   2.473   5.912  1.00  0.00           H
ATOM    983  HE2 PHE B 272       8.090   1.565   7.888  1.00  0.00           H
ATOM    984  HZ  PHE B 272       6.887   2.524   5.972  1.00  0.00           H
ATOM    985  N   ALA B 273       2.875   3.149  11.428  1.00 20.00           N
ATOM    986  CA  ALA B 273       1.718   3.948  11.531  1.00 20.00           C
ATOM    987  C   ALA B 273       1.516   4.700  10.223  1.00 20.00           C
ATOM    988  O   ALA B 273       2.417   5.364   9.732  1.00 20.00           O
ATOM    989  CB  ALA B 273       1.968   4.901  12.715  1.00 20.00           C
ATOM    990  H   ALA B 273       3.818   3.527  11.270  1.00  0.00           H
ATOM    991  HA  ALA B 273       0.798   3.376  11.792  1.00  0.00           H
ATOM    992 1HB  ALA B 273       1.203   5.695  12.710  1.00  0.00           H
ATOM    993 2HB  ALA B 273       1.910   4.374  13.685  1.00  0.00           H
ATOM    994 3HB  ALA B 273       2.939   5.420  12.692  1.00  0.00           H
ATOM    995  N   PRO B 274       0.473   4.854   9.839  1.00 20.00           N
ATOM    996  CA  PRO B 274      -0.040   4.944   8.496  1.00 20.00           C
ATOM    997  C   PRO B 274      -0.858   3.752   8.216  1.00 20.00           C
ATOM    998  O   PRO B 274      -0.984   3.283   7.056  1.00 20.00           O
ATOM    999  CB  PRO B 274       1.008   5.031   7.385  1.00 20.00           C
ATOM   1000  CG  PRO B 274       1.885   3.803   7.512  1.00 20.00           C
```

```
ATOM   1001  CD  PRO B 274       1.429   3.424   8.955  1.00 20.00           C
ATOM   1002  HA  PRO B 274      -0.693   5.833   8.434  1.00  0.00           H
ATOM   1003 1HB  PRO B 274       1.539   5.996   7.472  1.00  0.00           H
ATOM   1004 2HB  PRO B 274       0.520   4.945   6.428  1.00  0.00           H
ATOM   1005 1HG  PRO B 274       2.957   4.068   7.459  1.00  0.00           H
ATOM   1006 2HG  PRO B 274       1.656   3.013   6.770  1.00  0.00           H
ATOM   1007 1HD  PRO B 274       0.949   2.416   9.020  1.00  0.00           H
ATOM   1008 2HD  PRO B 274       2.440   2.964   9.164  1.00  0.00           H
ATOM   1009  N   LEU B 275      -1.430   3.228   9.291  1.00 20.00           N
ATOM   1010  CA  LEU B 275      -2.292   2.061   9.248  1.00 20.00           C
ATOM   1011  C   LEU B 275      -3.569   2.398   8.569  1.00 20.00           C
ATOM   1012  O   LEU B 275      -4.255   1.542   8.018  1.00 20.00           O
ATOM   1013  CB  LEU B 275      -2.420   1.400  10.637  1.00 20.00           C
ATOM   1014  CG  LEU B 275      -1.126   0.706  11.116  1.00 20.00           C
ATOM   1015  CD1 LEU B 275      -1.097   0.508  12.640  1.00 20.00           C
ATOM   1016  CD2 LEU B 275      -0.827  -0.604  10.361  1.00 20.00           C
ATOM   1017  H   LEU B 275      -1.176   3.714  10.164  1.00  0.00           H
ATOM   1018  HA  LEU B 275      -1.829   1.311   8.577  1.00  0.00           H
ATOM   1019 1HB  LEU B 275      -3.236   0.653  10.617  1.00  0.00           H
ATOM   1020 2HB  LEU B 275      -2.739   2.166  11.369  1.00  0.00           H
ATOM   1021  HG  LEU B 275      -0.313   1.407  10.884  1.00  0.00           H
ATOM   1022 1HD1 LEU B 275      -1.169   1.476  13.171  1.00  0.00           H
ATOM   1023 2HD1 LEU B 275      -1.917  -0.124  13.007  1.00  0.00           H
ATOM   1024 3HD1 LEU B 275      -0.155   0.038  12.977  1.00  0.00           H
ATOM   1025 1HD2 LEU B 275       0.041  -1.137  10.792  1.00  0.00           H
ATOM   1026 2HD2 LEU B 275      -1.687  -1.296  10.368  1.00  0.00           H
ATOM   1027 3HD2 LEU B 275      -0.577  -0.420   9.301  1.00  0.00           H
ATOM   1028  N   THR B 276      -4.416   2.932   8.373  1.00 20.00           N
ATOM   1029  CA  THR B 276      -4.932   4.191   7.936  1.00 20.00           C
ATOM   1030  C   THR B 276      -6.409   4.097   7.890  1.00 20.00           C
ATOM   1031  O   THR B 276      -7.035   5.248   8.099  1.00 20.00           O
ATOM   1032  CB  THR B 276      -4.340   4.751   6.575  1.00 20.00           C
ATOM   1033  OG1 THR B 276      -3.438   3.863   5.908  1.00 20.00           O
ATOM   1034  CG2 THR B 276      -3.601   6.086   6.735  1.00 20.00           C
ATOM   1035  H   THR B 276      -4.673   2.014   7.943  1.00  0.00           H
ATOM   1036  HA  THR B 276      -4.710   4.918   8.742  1.00  0.00           H
ATOM   1037  HB  THR B 276      -5.164   4.945   5.857  1.00  0.00           H
ATOM   1038  HG1 THR B 276      -2.638   3.789   6.448  1.00  0.00           H
ATOM   1039 1HG2 THR B 276      -3.193   6.438   5.768  1.00  0.00           H
ATOM   1040 2HG2 THR B 276      -4.275   6.880   7.107  1.00  0.00           H
ATOM   1041 3HG2 THR B 276      -2.757   6.012   7.441  1.00  0.00           H
ATOM   1042  N   SER B 277      -7.119   3.014   7.409  1.00 20.00           N
ATOM   1043  CA  SER B 277      -8.428   2.710   6.948  1.00 20.00           C
ATOM   1044  C   SER B 277      -8.632   3.206   5.526  1.00 20.00           C
ATOM   1045  O   SER B 277      -8.331   4.391   5.283  1.00 20.00           O
ATOM   1046  CB  SER B 277      -9.501   2.868   8.045  1.00 20.00           C
ATOM   1047  OG  SER B 277      -9.466   1.770   8.965  1.00 20.00           O
ATOM   1048  H   SER B 277      -6.420   2.276   7.280  1.00  0.00           H
ATOM   1049  HA  SER B 277      -8.379   1.605   6.859  1.00  0.00           H
ATOM   1050 1HB  SER B 277     -10.512   2.940   7.602  1.00  0.00           H
ATOM   1051 2HB  SER B 277      -9.339   3.790   8.618  1.00  0.00           H
ATOM   1052  HG  SER B 277      -8.693   1.882   9.543  1.00  0.00           H
ATOM   1053  N   ARG B 278      -8.987   2.332   4.634  1.00 20.00           N
ATOM   1054  CA  ARG B 278      -9.166   2.654   3.231  1.00 20.00           C
ATOM   1055  C   ARG B 278      -9.908   3.909   3.078  1.00 20.00           C
ATOM   1056  O   ARG B 278      -9.419   4.902   2.525  1.00 20.00           O
ATOM   1057  CB  ARG B 278      -9.697   1.391   2.478  1.00 20.00           C
ATOM   1058  CG  ARG B 278      -9.994   1.579   0.969  1.00 20.00           C
ATOM   1059  CD  ARG B 278     -10.319   0.257   0.249  1.00 20.00           C
ATOM   1060  NE  ARG B 278     -10.529   0.486  -1.205  1.00 20.00           N
ATOM   1061  CZ  ARG B 278      -9.575   0.515  -2.138  1.00 20.00           C
ATOM   1062  NH1 ARG B 278      -8.304   0.355  -1.889  1.00 20.00           N
ATOM   1063  NH2 ARG B 278      -9.938   0.720  -3.362  1.00 20.00           N
```

```
ATOM   1064  H   ARG B 278      -9.103   1.376   4.984  1.00  0.00           H
ATOM   1065  HA  ARG B 278      -8.166   2.872   2.833  1.00  0.00           H
ATOM   1066 1HB  ARG B 278     -10.616   1.012   2.967  1.00  0.00           H
ATOM   1067 2HB  ARG B 278      -8.959   0.575   2.598  1.00  0.00           H
ATOM   1068 1HG  ARG B 278      -9.144   2.072   0.465  1.00  0.00           H
ATOM   1069 2HG  ARG B 278     -10.841   2.280   0.833  1.00  0.00           H
ATOM   1070 1HD  ARG B 278     -11.247  -0.179   0.669  1.00  0.00           H
ATOM   1071 2HD  ARG B 278      -9.541  -0.511   0.429  1.00  0.00           H
ATOM   1072 1HH1 ARG B 278      -7.646   0.389  -2.673  1.00  0.00           H
ATOM   1073 2HH1 ARG B 278      -8.115   0.198  -0.900  1.00  0.00           H
ATOM   1074 1HH2 ARG B 278      -9.210   0.746  -4.077  1.00  0.00           H
ATOM   1075 2HH2 ARG B 278     -10.950   0.835  -3.456  1.00  0.00           H
ATOM   1076  N   GLY B 279     -11.112   3.803   3.715  1.00 20.00           N
ATOM   1077  CA  GLY B 279     -11.976   4.922   3.661  1.00 20.00           C
ATOM   1078  C   GLY B 279     -11.538   6.030   4.597  1.00 20.00           C
ATOM   1079  O   GLY B 279     -11.357   7.162   4.169  1.00 20.00           O
ATOM   1080  H   GLY B 279     -11.303   2.905   4.170  1.00  0.00           H
ATOM   1081 1HA  GLY B 279     -13.003   4.613   3.932  1.00  0.00           H
ATOM   1082 2HA  GLY B 279     -12.068   5.322   2.631  1.00  0.00           H
ATOM   1083  N   SER B 280     -11.396   5.680   5.869  1.00 20.00           N
ATOM   1084  CA  SER B 280     -10.953   6.658   6.837  1.00 20.00           C
ATOM   1085  C   SER B 280      -9.764   7.417   6.325  1.00 20.00           C
ATOM   1086  O   SER B 280      -9.259   8.321   6.936  1.00 20.00           O
ATOM   1087  CB  SER B 280     -10.759   6.142   8.280  1.00 20.00           C
ATOM   1088  OG  SER B 280     -11.747   5.186   8.675  1.00 20.00           O
ATOM   1089  H   SER B 280     -11.476   4.682   6.078  1.00  0.00           H
ATOM   1090  HA  SER B 280     -11.766   7.408   6.916  1.00  0.00           H
ATOM   1091 1HB  SER B 280     -10.790   6.997   8.981  1.00  0.00           H
ATOM   1092 2HB  SER B 280      -9.737   5.744   8.400  1.00  0.00           H
ATOM   1093  HG  SER B 280     -11.562   4.939   9.587  1.00  0.00           H
ATOM   1094  N   GLN B 281      -9.508   7.086   5.120  1.00 20.00           N
ATOM   1095  CA  GLN B 281      -8.283   7.511   4.524  1.00 20.00           C
ATOM   1096  C   GLN B 281      -7.974   8.945   4.828  1.00 20.00           C
ATOM   1097  O   GLN B 281      -6.878   9.351   5.064  1.00 20.00           O
ATOM   1098  CB  GLN B 281      -7.949   7.308   3.016  1.00 20.00           C
ATOM   1099  CG  GLN B 281      -8.965   7.835   1.965  1.00 20.00           C
ATOM   1100  CD  GLN B 281      -8.577   7.563   0.510  1.00 20.00           C
ATOM   1101  OE1 GLN B 281      -8.130   8.436  -0.225  1.00 20.00           O
ATOM   1102  NE2 GLN B 281      -8.753   6.350   0.047  1.00 20.00           N
ATOM   1103  H   GLN B 281     -10.439   7.124   4.565  1.00  0.00           H
ATOM   1104  HA  GLN B 281      -7.488   6.938   5.047  1.00  0.00           H
ATOM   1105 1HB  GLN B 281      -7.689   6.252   2.857  1.00  0.00           H
ATOM   1106 2HB  GLN B 281      -6.969   7.778   2.790  1.00  0.00           H
ATOM   1107 1HG  GLN B 281      -9.082   8.926   2.087  1.00  0.00           H
ATOM   1108 2HG  GLN B 281      -9.969   7.417   2.150  1.00  0.00           H
ATOM   1109 1HE2 GLN B 281      -9.015   5.657   0.763  1.00  0.00           H
ATOM   1110 2HE2 GLN B 281      -8.387   6.199  -0.896  1.00  0.00           H
ATOM   1111  N   GLN B 282      -8.876   9.723   5.268  1.00 20.00           N
ATOM   1112  CA  GLN B 282      -9.038  11.136   5.241  1.00 20.00           C
ATOM   1113  C   GLN B 282      -8.518  11.775   6.516  1.00 20.00           C
ATOM   1114  O   GLN B 282      -8.498  13.030   6.598  1.00 20.00           O
ATOM   1115  CB  GLN B 282     -10.537  11.478   4.979  1.00 20.00           C
ATOM   1116  CG  GLN B 282     -11.143  11.034   3.616  1.00 20.00           C
ATOM   1117  CD  GLN B 282     -10.537  11.664   2.352  1.00 20.00           C
ATOM   1118  OE1 GLN B 282      -9.838  12.673   2.365  1.00 20.00           O
ATOM   1119  NE2 GLN B 282     -10.799  11.092   1.202  1.00 20.00           N
ATOM   1120  H   GLN B 282      -9.260   9.157   6.072  1.00  0.00           H
ATOM   1121  HA  GLN B 282      -8.433  11.563   4.416  1.00  0.00           H
ATOM   1122 1HB  GLN B 282     -10.674  12.574   5.066  1.00  0.00           H
ATOM   1123 2HB  GLN B 282     -11.157  11.059   5.796  1.00  0.00           H
ATOM   1124 1HG  GLN B 282     -12.224  11.268   3.617  1.00  0.00           H
ATOM   1125 2HG  GLN B 282     -11.089   9.930   3.545  1.00  0.00           H
ATOM   1126 1HE2 GLN B 282     -11.352  10.232   1.222  1.00  0.00           H
```

```
ATOM   1127 2HE2 GLN B 282     -10.322  11.523   0.406  1.00  0.00           H
ATOM   1128  N   TYR B 283      -8.175  11.054   7.526  1.00 20.00           N
ATOM   1129  CA  TYR B 283      -7.706  11.628   8.789  1.00 20.00           C
ATOM   1130  C   TYR B 283      -6.238  11.842   8.735  1.00 20.00           C
ATOM   1131  O   TYR B 283      -5.562  11.000   8.245  1.00 20.00           O
ATOM   1132  CB  TYR B 283      -8.048  10.607   9.927  1.00 20.00           C
ATOM   1133  CG  TYR B 283      -9.504  10.645  10.437  1.00 20.00           C
ATOM   1134  CD1 TYR B 283     -10.499   9.894   9.804  1.00 20.00           C
ATOM   1135  CD2 TYR B 283      -9.845  11.445  11.533  1.00 20.00           C
ATOM   1136  CE1 TYR B 283     -11.815   9.939  10.259  1.00 20.00           C
ATOM   1137  CE2 TYR B 283     -11.162  11.488  11.989  1.00 20.00           C
ATOM   1138  CZ  TYR B 283     -12.144  10.736  11.352  1.00 20.00           C
ATOM   1139  OH  TYR B 283     -13.435  10.787  11.804  1.00 20.00           O
ATOM   1140  H   TYR B 283      -8.096  10.053   7.305  1.00  0.00           H
ATOM   1141  HA  TYR B 283      -8.323  12.522   9.066  1.00  0.00           H
ATOM   1142 1HB  TYR B 283      -7.387  10.782  10.799  1.00  0.00           H
ATOM   1143 2HB  TYR B 283      -7.778   9.574   9.623  1.00  0.00           H
ATOM   1144  HD1 TYR B 283     -10.256   9.286   8.949  1.00  0.00           H
ATOM   1145  HD2 TYR B 283      -9.094  12.037  12.035  1.00  0.00           H
ATOM   1146  HE1 TYR B 283     -12.574   9.357   9.757  1.00  0.00           H
ATOM   1147  HE2 TYR B 283     -11.425  12.106  12.835  1.00  0.00           H
ATOM   1148  HH  TYR B 283     -13.982  10.225  11.252  1.00  0.00           H
ATOM   1149  N   ARG B 284      -6.221  13.091   8.237  1.00 20.00           N
ATOM   1150  CA  ARG B 284      -5.416  13.643   7.130  1.00 20.00           C
ATOM   1151  C   ARG B 284      -4.041  13.305   7.806  1.00 20.00           C
ATOM   1152  O   ARG B 284      -3.542  12.378   8.464  1.00 20.00           O
ATOM   1153  CB  ARG B 284      -6.001  15.067   6.792  1.00 20.00           C
ATOM   1154  CG  ARG B 284      -6.338  16.119   7.890  1.00 20.00           C
ATOM   1155  CD  ARG B 284      -5.165  16.666   8.726  1.00 20.00           C
ATOM   1156  NE  ARG B 284      -5.637  17.728   9.651  1.00 20.00           N
ATOM   1157  CZ  ARG B 284      -6.059  17.546  10.903  1.00 20.00           C
ATOM   1158  NH1 ARG B 284      -6.130  16.384  11.500  1.00 20.00           N
ATOM   1159  NH2 ARG B 284      -6.424  18.596  11.564  1.00 20.00           N
ATOM   1160  H   ARG B 284      -7.121  13.554   8.392  1.00  0.00           H
ATOM   1161  HA  ARG B 284      -5.516  12.990   6.240  1.00  0.00           H
ATOM   1162 1HB  ARG B 284      -6.944  14.893   6.241  1.00  0.00           H
ATOM   1163 2HB  ARG B 284      -5.386  15.543   6.018  1.00  0.00           H
ATOM   1164 1HG  ARG B 284      -7.112  15.716   8.570  1.00  0.00           H
ATOM   1165 2HG  ARG B 284      -6.840  16.977   7.400  1.00  0.00           H
ATOM   1166 1HD  ARG B 284      -4.399  17.108   8.060  1.00  0.00           H
ATOM   1167 2HD  ARG B 284      -4.648  15.863   9.286  1.00  0.00           H
ATOM   1168 1HH1 ARG B 284      -6.467  16.376  12.463  1.00  0.00           H
ATOM   1169 2HH1 ARG B 284      -5.828  15.601  10.919  1.00  0.00           H
ATOM   1170 1HH2 ARG B 284      -6.749  18.472  12.523  1.00  0.00           H
ATOM   1171 2HH2 ARG B 284      -6.332  19.453  11.013  1.00  0.00           H
ATOM   1172  N   ALA B 285      -3.284  14.170   7.646  1.00 20.00           N
ATOM   1173  CA  ALA B 285      -2.527  14.165   6.403  1.00 20.00           C
ATOM   1174  C   ALA B 285      -1.184  13.630   6.677  1.00 20.00           C
ATOM   1175  O   ALA B 285      -0.208  14.370   6.729  1.00 20.00           O
ATOM   1176  CB  ALA B 285      -2.488  15.620   5.853  1.00 20.00           C
ATOM   1177  H   ALA B 285      -3.753  15.057   7.850  1.00  0.00           H
ATOM   1178  HA  ALA B 285      -2.977  13.550   5.588  1.00  0.00           H
ATOM   1179 1HB  ALA B 285      -1.815  15.692   4.977  1.00  0.00           H
ATOM   1180 2HB  ALA B 285      -3.458  15.997   5.500  1.00  0.00           H
ATOM   1181 3HB  ALA B 285      -2.100  16.343   6.596  1.00  0.00           H
ATOM   1182  N   LEU B 286      -1.142  12.335   6.939  1.00 20.00           N
ATOM   1183  CA  LEU B 286       0.069  11.682   7.257  1.00 20.00           C
ATOM   1184  C   LEU B 286       0.781  12.417   8.380  1.00 20.00           C
ATOM   1185  O   LEU B 286       1.828  13.005   8.166  1.00 20.00           O
ATOM   1186  CB  LEU B 286       0.825  11.504   5.891  1.00 20.00           C
ATOM   1187  CG  LEU B 286      -0.029  11.293   4.591  1.00 20.00           C
ATOM   1188  CD1 LEU B 286       0.742  11.698   3.356  1.00 20.00           C
ATOM   1189  CD2 LEU B 286      -0.698   9.917   4.597  1.00 20.00           C
```

```
ATOM   1190  H   LEU B 286      -2.066  11.950   7.184  1.00  0.00           H
ATOM   1191  HA  LEU B 286      -0.177  10.667   7.625  1.00  0.00           H
ATOM   1192 1HB  LEU B 286       1.570  10.693   5.996  1.00  0.00           H
ATOM   1193 2HB  LEU B 286       1.428  12.422   5.745  1.00  0.00           H
ATOM   1194  HG  LEU B 286      -0.868  12.009   4.536  1.00  0.00           H
ATOM   1195 1HD1 LEU B 286       0.132  11.540   2.449  1.00  0.00           H
ATOM   1196 2HD1 LEU B 286       1.028  12.766   3.376  1.00  0.00           H
ATOM   1197 3HD1 LEU B 286       1.666  11.119   3.276  1.00  0.00           H
ATOM   1198 1HD2 LEU B 286      -1.187   9.677   3.635  1.00  0.00           H
ATOM   1199 2HD2 LEU B 286       0.046   9.138   4.812  1.00  0.00           H
ATOM   1200 3HD2 LEU B 286      -1.474   9.838   5.380  1.00  0.00           H
ATOM   1201  N   THR B 287       0.240  12.486   9.567  1.00 20.00           N
ATOM   1202  CA  THR B 287       0.760  13.343  10.607  1.00 20.00           C
ATOM   1203  C   THR B 287       1.994  12.807  11.190  1.00 20.00           C
ATOM   1204  O   THR B 287       2.220  11.646  11.234  1.00 20.00           O
ATOM   1205  CB  THR B 287      -0.422  14.183  11.229  1.00 20.00           C
ATOM   1206  OG1 THR B 287      -1.006  14.993  10.206  1.00 20.00           O
ATOM   1207  CG2 THR B 287      -0.111  15.177  12.356  1.00 20.00           C
ATOM   1208  H   THR B 287      -0.655  11.992   9.646  1.00  0.00           H
ATOM   1209  HA  THR B 287       1.222  14.202  10.071  1.00  0.00           H
ATOM   1210  HB  THR B 287      -1.234  13.527  11.565  1.00  0.00           H
ATOM   1211  HG1 THR B 287      -1.044  14.449   9.410  1.00  0.00           H
ATOM   1212 1HG2 THR B 287      -1.028  15.705  12.679  1.00  0.00           H
ATOM   1213 2HG2 THR B 287       0.304  14.689  13.253  1.00  0.00           H
ATOM   1214 3HG2 THR B 287       0.602  15.957  12.032  1.00  0.00           H
ATOM   1215  N   VAL B 288       2.742  13.921  11.994  1.00 20.00           N
ATOM   1216  CA  VAL B 288       3.800  13.352  12.763  1.00 20.00           C
ATOM   1217  C   VAL B 288       3.292  12.861  14.122  1.00 20.00           C
ATOM   1218  O   VAL B 288       3.593  11.758  14.538  1.00 20.00           O
ATOM   1219  CB  VAL B 288       4.964  14.399  12.943  1.00 20.00           C
ATOM   1220  CG1 VAL B 288       6.156  13.890  13.797  1.00 20.00           C
ATOM   1221  CG2 VAL B 288       5.592  14.870  11.609  1.00 20.00           C
ATOM   1222  H   VAL B 288       2.518  14.911  11.843  1.00  0.00           H
ATOM   1223  HA  VAL B 288       4.287  12.526  12.220  1.00  0.00           H
ATOM   1224  HC  VAL B 288       2.902  13.687  14.750  1.00  0.00           H
ATOM   1225  HB  VAL B 288       4.556  15.296  13.452  1.00  0.00           H
ATOM   1226 1HG1 VAL B 288       6.951  14.653  13.907  1.00  0.00           H
ATOM   1227 2HG1 VAL B 288       5.851  13.620  14.825  1.00  0.00           H
ATOM   1228 3HG1 VAL B 288       6.628  12.990  13.358  1.00  0.00           H
ATOM   1229 1HG2 VAL B 288       6.375  15.637  11.758  1.00  0.00           H
ATOM   1230 2HG2 VAL B 288       6.049  14.036  11.041  1.00  0.00           H
ATOM   1231 3HG2 VAL B 288       4.834  15.325  10.949  1.00  0.00           H
ATOM   1232  N   GLU B 290       0.802  12.412  14.583  1.00 20.00           N
ATOM   1233  CA  GLU B 290       0.034  11.287  14.120  1.00 20.00           C
ATOM   1234  C   GLU B 290       0.835  10.056  14.081  1.00 20.00           C
ATOM   1235  O   GLU B 290       0.491   9.106  14.593  1.00 20.00           O
ATOM   1236  CB  GLU B 290      -1.049  11.433  13.025  1.00 20.00           C
ATOM   1237  CG  GLU B 290      -2.039  10.255  12.794  1.00 20.00           C
ATOM   1238  CD  GLU B 290      -2.920   9.846  13.975  1.00 20.00           C
ATOM   1239  OE1 GLU B 290      -2.851   8.755  14.536  1.00 20.00           O
ATOM   1240  OE2 GLU B 290      -3.804  10.821  14.327  1.00 20.00           O
ATOM   1241 1H   GLU B 290       1.618  12.058  15.098  1.00  0.00           H
ATOM   1242 2H   GLU B 290       1.185  12.916  13.776  1.00  0.00           H
ATOM   1243  HA  GLU B 290      -0.605  11.112  15.009  1.00  0.00           H
ATOM   1244 1HB  GLU B 290      -0.529  11.582  12.070  1.00  0.00           H
ATOM   1245 2HB  GLU B 290      -1.638  12.343  13.243  1.00  0.00           H
ATOM   1246 1HG  GLU B 290      -1.483   9.360  12.459  1.00  0.00           H
ATOM   1247 2HG  GLU B 290      -2.708  10.502  11.949  1.00  0.00           H
ATOM   1248  HE2 GLU B 290      -4.325  10.508  15.067  1.00  0.00           H
ATOM   1249  N   LEU B 291       1.914  10.438  13.607  1.00 20.00           N
ATOM   1250  CA  LEU B 291       2.715   9.421  13.429  1.00 20.00           C
ATOM   1251  C   LEU B 291       3.401   8.999  14.710  1.00 20.00           C
ATOM   1252  O   LEU B 291       3.786   7.823  14.792  1.00 20.00           O
```

```
ATOM   1253  CB  LEU B 291       3.811   9.562  12.318  1.00 20.00           C
ATOM   1254  CG  LEU B 291       3.461   9.279  10.815  1.00 20.00           C
ATOM   1255  CD1 LEU B 291       4.526   9.896   9.897  1.00 20.00           C
ATOM   1256  CD2 LEU B 291       3.139   7.870  10.404  1.00 20.00           C
ATOM   1257  H   LEU B 291       1.886  11.228  12.950  1.00  0.00           H
ATOM   1258  HA  LEU B 291       2.222   8.482  13.058  1.00  0.00           H
ATOM   1259  HC  LEU B 291       3.458   9.724  15.541  1.00  0.00           H
ATOM   1260 1HB  LEU B 291       4.668   8.926  12.573  1.00  0.00           H
ATOM   1261 2HB  LEU B 291       4.281  10.545  12.411  1.00  0.00           H
ATOM   1262  HG  LEU B 291       2.485   9.689  10.543  1.00  0.00           H
ATOM   1263 1HD1 LEU B 291       4.394   9.586   8.846  1.00  0.00           H
ATOM   1264 2HD1 LEU B 291       4.489  11.001   9.920  1.00  0.00           H
ATOM   1265 3HD1 LEU B 291       5.548   9.599  10.193  1.00  0.00           H
ATOM   1266 1HD2 LEU B 291       4.003   7.322  10.011  1.00  0.00           H
ATOM   1267 2HD2 LEU B 291       2.690   7.290  11.226  1.00  0.00           H
ATOM   1268 3HD2 LEU B 291       2.413   7.848   9.566  1.00  0.00           H
ATOM   1269  N   GLN B 294       0.876   7.116  17.003  1.00 20.00           N
ATOM   1270  CA  GLN B 294       0.504   5.752  16.674  1.00 20.00           C
ATOM   1271  C   GLN B 294       1.628   4.832  16.900  1.00 20.00           C
ATOM   1272  O   GLN B 294       1.470   3.629  16.835  1.00 20.00           O
ATOM   1273  CB  GLN B 294      -0.228   5.835  15.312  1.00 20.00           C
ATOM   1274  CG  GLN B 294      -0.954   4.550  14.828  1.00 20.00           C
ATOM   1275  CD  GLN B 294      -1.767   4.702  13.532  1.00 20.00           C
ATOM   1276  OE1 GLN B 294      -1.452   4.143  12.488  1.00 20.00           O
ATOM   1277  NE2 GLN B 294      -2.852   5.441  13.543  1.00 20.00           N
ATOM   1278 1H   GLN B 294       1.487   7.498  16.270  1.00  0.00           H
ATOM   1279 2H   GLN B 294       0.047   7.721  16.982  1.00  0.00           H
ATOM   1280  HA  GLN B 294      -0.257   5.448  17.419  1.00  0.00           H
ATOM   1281  HC  GLN B 294       2.609   5.307  17.100  1.00  0.00           H
ATOM   1282 1HB  GLN B 294       0.469   6.217  14.553  1.00  0.00           H
ATOM   1283 2HB  GLN B 294      -0.996   6.634  15.373  1.00  0.00           H
ATOM   1284 1HG  GLN B 294      -1.625   4.169  15.620  1.00  0.00           H
ATOM   1285 2HG  GLN B 294      -0.216   3.741  14.675  1.00  0.00           H
ATOM   1286 1HE2 GLN B 294      -2.987   6.034  14.367  1.00  0.00           H
ATOM   1287 2HE2 GLN B 294      -3.278   5.550  12.619  1.00  0.00           H
ATOM   1288  N   MET B 302       2.727  -3.861  16.477  1.00 20.00           N
ATOM   1289  CA  MET B 302       2.536  -5.062  15.654  1.00 20.00           C
ATOM   1290  C   MET B 302       3.263  -6.219  16.280  1.00 20.00           C
ATOM   1291  O   MET B 302       3.985  -6.899  15.606  1.00 20.00           O
ATOM   1292  CB  MET B 302       2.946  -4.658  14.207  1.00 20.00           C
ATOM   1293  CG  MET B 302       2.497  -5.647  13.115  1.00 20.00           C
ATOM   1294  SD  MET B 302       3.542  -5.480  11.654  1.00 20.00           S
ATOM   1295  CE  MET B 302       4.869  -6.621  12.096  1.00 20.00           C
ATOM   1296 1H   MET B 302       3.712  -3.571  16.454  1.00  0.00           H
ATOM   1297 2H   MET B 302       2.201  -3.073  16.085  1.00  0.00           H
ATOM   1298  HA  MET B 302       1.463  -5.326  15.657  1.00  0.00           H
ATOM   1299  HC  MET B 302       3.075  -6.370  17.359  1.00  0.00           H
ATOM   1300 1HB  MET B 302       4.047  -4.543  14.163  1.00  0.00           H
ATOM   1301 2HB  MET B 302       2.546  -3.662  13.934  1.00  0.00           H
ATOM   1302 1HG  MET B 302       1.440  -5.481  12.838  1.00  0.00           H
ATOM   1303 2HG  MET B 302       2.564  -6.689  13.474  1.00  0.00           H
ATOM   1304 1HE  MET B 302       5.641  -6.647  11.309  1.00  0.00           H
ATOM   1305 2HE  MET B 302       5.357  -6.309  13.037  1.00  0.00           H
ATOM   1306 3HE  MET B 302       4.480  -7.645  12.237  1.00  0.00           H
ATOM   1307  N   VAL B 318      11.629   5.351  13.514  1.00 20.00           N
ATOM   1308  CA  VAL B 318      12.037   5.823  12.187  1.00 20.00           C
ATOM   1309  C   VAL B 318      10.880   6.331  11.353  1.00 20.00           C
ATOM   1310  O   VAL B 318       9.887   5.625  11.185  1.00 20.00           O
ATOM   1311  CB  VAL B 318      12.972   4.779  11.470  1.00 20.00           C
ATOM   1312  CG1 VAL B 318      13.339   5.110  10.001  1.00 20.00           C
ATOM   1313  CG2 VAL B 318      14.312   4.546  12.211  1.00 20.00           C
ATOM   1314 1H   VAL B 318      11.229   6.122  14.060  1.00  0.00           H
ATOM   1315 2H   VAL B 318      10.851   4.673  13.434  1.00  0.00           H
```

```
ATOM   1316  HA  VAL B 318      12.669   6.715  12.364  1.00  0.00           H
ATOM   1317  HC  VAL B 318      11.015   7.339  10.919  1.00  0.00           H
ATOM   1318  HB  VAL B 318      12.446   3.809  11.455  1.00  0.00           H
ATOM   1319 1HG1 VAL B 318      13.984   4.331   9.551  1.00  0.00           H
ATOM   1320 2HG1 VAL B 318      12.444   5.168   9.353  1.00  0.00           H
ATOM   1321 3HG1 VAL B 318      13.876   6.072   9.908  1.00  0.00           H
ATOM   1322 1HG2 VAL B 318      14.923   3.759  11.729  1.00  0.00           H
ATOM   1323 2HG2 VAL B 318      14.931   5.462  12.255  1.00  0.00           H
ATOM   1324 3HG2 VAL B 318      14.150   4.216  13.254  1.00  0.00           H
ATOM   1325  N   ARG B 320      10.035   8.351   7.636  1.00 20.00           N
ATOM   1326  CA  ARG B 320      10.503   8.659   6.301  1.00 20.00           C
ATOM   1327  C   ARG B 320       9.439   9.226   5.448  1.00 20.00           C
ATOM   1328  O   ARG B 320       9.111   8.722   4.338  1.00 20.00           O
ATOM   1329  CB  ARG B 320      11.409   7.555   5.648  1.00 20.00           C
ATOM   1330  CG  ARG B 320      10.737   6.282   5.070  1.00 20.00           C
ATOM   1331  CD  ARG B 320      11.480   5.540   3.954  1.00 20.00           C
ATOM   1332  NE  ARG B 320      10.571   4.446   3.479  1.00 20.00           N
ATOM   1333  CZ  ARG B 320      10.510   3.919   2.262  1.00 20.00           C
ATOM   1334  NH1 ARG B 320      11.100   4.416   1.221  1.00 20.00           N
ATOM   1335  NH2 ARG B 320       9.820   2.834   2.119  1.00 20.00           N
ATOM   1336 1H   ARG B 320       9.421   9.086   8.003  1.00  0.00           H
ATOM   1337 2H   ARG B 320       9.451   7.504   7.615  1.00  0.00           H
ATOM   1338  HA  ARG B 320      11.230   9.484   6.450  1.00  0.00           H
ATOM   1339 1HB  ARG B 320      12.203   7.254   6.357  1.00  0.00           H
ATOM   1340 2HB  ARG B 320      11.958   8.044   4.818  1.00  0.00           H
ATOM   1341 1HG  ARG B 320       9.781   6.551   4.599  1.00  0.00           H
ATOM   1342 2HG  ARG B 320      10.473   5.587   5.891  1.00  0.00           H
ATOM   1343 1HD  ARG B 320      12.430   5.143   4.321  1.00  0.00           H
ATOM   1344 2HD  ARG B 320      11.849   6.214   3.173  1.00  0.00           H
ATOM   1345 1HH1 ARG B 320      10.940   3.952   0.327  1.00  0.00           H
ATOM   1346 2HH1 ARG B 320      11.438   5.366   1.407  1.00  0.00           H
ATOM   1347 1HH2 ARG B 320       9.828   2.385   1.203  1.00  0.00           H
ATOM   1348 2HH2 ARG B 320       9.437   2.503   3.007  1.00  0.00           H
ATOM   1349  N   GLY B 321       8.974  10.388   5.821  1.00 20.00           N
ATOM   1350  CA  GLY B 321       7.964  11.049   5.027  1.00 20.00           C
ATOM   1351  C   GLY B 321       8.422  12.269   4.331  1.00 20.00           C
ATOM   1352  O   GLY B 321       7.668  13.006   3.684  1.00 20.00           O
ATOM   1353  H   GLY B 321       9.294  10.718   6.739  1.00  0.00           H
ATOM   1354 1HA  GLY B 321       7.165  11.370   5.706  1.00  0.00           H
ATOM   1355 2HA  GLY B 321       7.478  10.403   4.309  1.00  0.00           H
ATOM   1356  HC  GLY B 321       9.506  12.474   4.429  1.00  0.00           H
ATOM   1357  N   MET B 323       9.231  14.966   6.028  1.00 20.00           N
ATOM   1358  CA  MET B 323       8.915  15.992   6.988  1.00 20.00           C
ATOM   1359  C   MET B 323      10.168  16.461   7.648  1.00 20.00           C
ATOM   1360  O   MET B 323      11.244  15.994   7.509  1.00 20.00           O
ATOM   1361  CB  MET B 323       7.787  15.556   7.951  1.00 20.00           C
ATOM   1362  CG  MET B 323       7.065  16.727   8.658  1.00 20.00           C
ATOM   1363  SD  MET B 323       5.286  16.429   8.666  1.00 20.00           S
ATOM   1364  CE  MET B 323       4.718  17.941   9.463  1.00 20.00           C
ATOM   1365 1H   MET B 323       8.452  14.833   5.372  1.00  0.00           H
ATOM   1366 2H   MET B 323      10.035  15.256   5.458  1.00  0.00           H
ATOM   1367  HA  MET B 323       8.543  16.851   6.397  1.00  0.00           H
ATOM   1368  HC  MET B 323       9.992  17.325   8.314  1.00  0.00           H
ATOM   1369 1HB  MET B 323       8.159  14.822   8.692  1.00  0.00           H
ATOM   1370 2HB  MET B 323       7.027  14.994   7.381  1.00  0.00           H
ATOM   1371 1HG  MET B 323       7.234  17.694   8.146  1.00  0.00           H
ATOM   1372 2HG  MET B 323       7.431  16.856   9.694  1.00  0.00           H
ATOM   1373 1HE  MET B 323       3.617  17.934   9.560  1.00  0.00           H
ATOM   1374 2HE  MET B 323       5.151  18.043  10.474  1.00  0.00           H
ATOM   1375 3HE  MET B 323       5.001  18.830   8.871  1.00  0.00           H
ATOM   1376  N   ILE B 358      12.341   9.219   1.408  1.00 20.00           N
ATOM   1377  CA  ILE B 358      11.380   8.834   0.412  1.00 20.00           C
ATOM   1378  C   ILE B 358      10.221   8.138   1.091  1.00 20.00           C
```

```
ATOM   1379  O   ILE B 358      10.452   7.183   1.816  1.00 20.00           O
ATOM   1380  CB  ILE B 358      12.039   8.050  -0.785  1.00 20.00           C
ATOM   1381  CG1 ILE B 358      13.151   8.860  -1.533  1.00 20.00           C
ATOM   1382  CG2 ILE B 358      10.989   7.580  -1.834  1.00 20.00           C
ATOM   1383  CD1 ILE B 358      14.081   8.054  -2.460  1.00 20.00           C
ATOM   1384 1H   ILE B 358      13.083   9.794   0.993  1.00  0.00           H
ATOM   1385 2H   ILE B 358      11.900   9.803   2.129  1.00  0.00           H
ATOM   1386  HA  ILE B 358      11.121   9.798  -0.051  1.00  0.00           H
ATOM   1387  HB  ILE B 358      12.507   7.155  -0.344  1.00  0.00           H
ATOM   1388 1HG1 ILE B 358      13.807   9.362  -0.797  1.00  0.00           H
ATOM   1389 2HG1 ILE B 358      12.693   9.690  -2.105  1.00  0.00           H
ATOM   1390 1HG2 ILE B 358      11.439   6.978  -2.644  1.00  0.00           H
ATOM   1391 2HG2 ILE B 358      10.205   6.941  -1.386  1.00  0.00           H
ATOM   1392 3HG2 ILE B 358      10.473   8.430  -2.318  1.00  0.00           H
ATOM   1393 1HD1 ILE B 358      14.841   8.706  -2.929  1.00  0.00           H
ATOM   1394 2HD1 ILE B 358      14.630   7.267  -1.910  1.00  0.00           H
ATOM   1395 3HD1 ILE B 358      13.535   7.559  -3.284  1.00  0.00           H
ATOM   1396  N   PRO B 359       9.091   8.674   0.987  1.00 20.00           N
ATOM   1397  CA  PRO B 359       8.003   8.029   1.681  1.00 20.00           C
ATOM   1398  C   PRO B 359       7.316   6.979   0.821  1.00 20.00           C
ATOM   1399  O   PRO B 359       7.190   7.194  -0.393  1.00 20.00           O
ATOM   1400  CB  PRO B 359       7.115   9.211   1.611  1.00 20.00           C
ATOM   1401  CG  PRO B 359       7.278  10.070   0.363  1.00 20.00           C
ATOM   1402  CD  PRO B 359       8.758   9.909   0.196  1.00 20.00           C
ATOM   1403  HA  PRO B 359       8.276   7.803   2.704  1.00  0.00           H
ATOM   1404 1HB  PRO B 359       7.308   9.842   2.477  1.00  0.00           H
ATOM   1405 2HB  PRO B 359       6.098   8.802   1.677  1.00  0.00           H
ATOM   1406 1HG  PRO B 359       6.958  11.119   0.511  1.00  0.00           H
ATOM   1407 2HG  PRO B 359       6.721   9.653  -0.497  1.00  0.00           H
ATOM   1408 1HD  PRO B 359       9.017   9.815  -0.877  1.00  0.00           H
ATOM   1409 2HD  PRO B 359       9.277  10.799   0.607  1.00  0.00           H
ATOM   1410  N   PRO B 360       7.251   6.048   1.782  1.00 20.00           N
ATOM   1411  CA  PRO B 360       6.818   4.825   1.130  1.00 20.00           C
ATOM   1412  C   PRO B 360       5.930   5.066  -0.067  1.00 20.00           C
ATOM   1413  O   PRO B 360       5.035   5.859   0.005  1.00 20.00           O
ATOM   1414  CB  PRO B 360       6.176   3.866   2.129  1.00 20.00           C
ATOM   1415  CG  PRO B 360       6.348   4.614   3.407  1.00 20.00           C
ATOM   1416  CD  PRO B 360       6.382   6.096   2.989  1.00 20.00           C
ATOM   1417  HA  PRO B 360       7.758   4.332   0.800  1.00  0.00           H
ATOM   1418 1HB  PRO B 360       6.710   2.907   2.177  1.00  0.00           H
ATOM   1419 2HB  PRO B 360       5.106   3.650   1.927  1.00  0.00           H
ATOM   1420 1HG  PRO B 360       7.307   4.334   3.891  1.00  0.00           H
ATOM   1421 2HG  PRO B 360       5.542   4.328   4.102  1.00  0.00           H
ATOM   1422 1HD  PRO B 360       5.378   6.500   2.752  1.00  0.00           H
ATOM   1423 2HD  PRO B 360       6.803   6.748   3.770  1.00  0.00           H
ATOM   1424  N   ARG B 369       6.208   4.361  -1.143  1.00 20.00           N
ATOM   1425  CA  ARG B 369       5.462   4.424  -2.372  1.00 20.00           C
ATOM   1426  C   ARG B 369       4.025   4.353  -2.078  1.00 20.00           C
ATOM   1427  O   ARG B 369       3.492   3.307  -1.675  1.00 20.00           O
ATOM   1428  CB  ARG B 369       6.017   3.407  -3.389  1.00 20.00           C
ATOM   1429  CG  ARG B 369       5.630   3.568  -4.878  1.00 20.00           C
ATOM   1430  CD  ARG B 369       6.473   2.611  -5.746  1.00 20.00           C
ATOM   1431  NE  ARG B 369       5.928   2.488  -7.120  1.00 20.00           N
ATOM   1432  CZ  ARG B 369       6.434   1.697  -8.068  1.00 20.00           C
ATOM   1433  NH1 ARG B 369       7.528   0.989  -7.936  1.00 20.00           N
ATOM   1434  NH2 ARG B 369       5.795   1.631  -9.191  1.00 20.00           N
ATOM   1435  H   ARG B 369       7.073   3.819  -1.069  1.00  0.00           H
ATOM   1436  HA  ARG B 369       5.747   5.404  -2.819  1.00  0.00           H
ATOM   1437 1HB  ARG B 369       5.729   2.395  -3.065  1.00  0.00           H
ATOM   1438 2HB  ARG B 369       7.122   3.460  -3.344  1.00  0.00           H
ATOM   1439 1HG  ARG B 369       5.789   4.608  -5.224  1.00  0.00           H
ATOM   1440 2HG  ARG B 369       4.548   3.374  -5.017  1.00  0.00           H
ATOM   1441 1HD  ARG B 369       6.501   1.606  -5.281  1.00  0.00           H
```

```
ATOM   1442 2HD  ARG B 369       7.527   2.958  -5.773  1.00  0.00           H
ATOM   1443 1HH1 ARG B 369       7.835   0.434  -8.737  1.00  0.00           H
ATOM   1444 2HH1 ARG B 369       8.005   1.129  -7.044  1.00  0.00           H
ATOM   1445 1HH2 ARG B 369       6.171   1.021  -9.917  1.00  0.00           H
ATOM   1446 2HH2 ARG B 369       4.948   2.203  -9.195  1.00  0.00           H
ATOM   1447  N   GLY B 370       3.425   5.468  -2.259  1.00 20.00           N
ATOM   1448  CA  GLY B 370       2.036   5.613  -2.028  1.00 20.00           C
ATOM   1449  C   GLY B 370       1.499   5.744  -0.610  1.00 20.00           C
ATOM   1450  O   GLY B 370       0.313   5.634  -0.388  1.00 20.00           O
ATOM   1451  H   GLY B 370       4.057   6.269  -2.370  1.00  0.00           H
ATOM   1452 1HA  GLY B 370       1.475   4.791  -2.516  1.00  0.00           H
ATOM   1453 2HA  GLY B 370       1.693   6.514  -2.568  1.00  0.00           H
ATOM   1454  N   LEU B 371       1.980   6.048   0.616  1.00 20.00           N
ATOM   1455  CA  LEU B 371       1.562   6.576   1.902  1.00 20.00           C
ATOM   1456  C   LEU B 371       1.774   8.063   1.949  1.00 20.00           C
ATOM   1457  O   LEU B 371       0.945   8.860   2.524  1.00 20.00           O
ATOM   1458  CB  LEU B 371       2.296   5.742   2.941  1.00 20.00           C
ATOM   1459  CG  LEU B 371       2.134   6.342   4.334  1.00 20.00           C
ATOM   1460  CD1 LEU B 371       0.634   6.498   4.689  1.00 20.00           C
ATOM   1461  CD2 LEU B 371       3.107   5.555   5.191  1.00 20.00           C
ATOM   1462  H   LEU B 371       2.983   5.823   0.546  1.00  0.00           H
ATOM   1463  HA  LEU B 371       0.474   6.404   1.997  1.00  0.00           H
ATOM   1464 1HB  LEU B 371       3.369   5.664   2.676  1.00  0.00           H
ATOM   1465 2HB  LEU B 371       1.918   4.700   2.924  1.00  0.00           H
ATOM   1466  HG  LEU B 371       2.537   7.363   4.357  1.00  0.00           H
ATOM   1467 1HD1 LEU B 371       0.477   6.948   5.684  1.00  0.00           H
ATOM   1468 2HD1 LEU B 371       0.088   7.173   4.015  1.00  0.00           H
ATOM   1469 3HD1 LEU B 371       0.071   5.552   4.584  1.00  0.00           H
ATOM   1470 1HD2 LEU B 371       3.132   5.934   6.215  1.00  0.00           H
ATOM   1471 2HD2 LEU B 371       2.910   4.468   5.188  1.00  0.00           H
ATOM   1472 3HD2 LEU B 371       4.131   5.709   4.834  1.00  0.00           H
ATOM   1473  N   LYS B 372       2.605   8.459   1.340  1.00 20.00           N
ATOM   1474  CA  LYS B 372       3.153   9.786   1.364  1.00 20.00           C
ATOM   1475  C   LYS B 372       4.058   9.981   2.550  1.00 20.00           C
ATOM   1476  O   LYS B 372       5.119  10.515   2.409  1.00 20.00           O
ATOM   1477  CB  LYS B 372       2.357  10.950   0.692  1.00 20.00           C
ATOM   1478  CG  LYS B 372       2.574  11.176  -0.824  1.00 20.00           C
ATOM   1479  CD  LYS B 372       3.925  11.837  -1.171  1.00 20.00           C
ATOM   1480  CE  LYS B 372       4.095  12.053  -2.682  1.00 20.00           C
ATOM   1481  NZ  LYS B 372       5.398  12.690  -2.954  1.00 20.00           N
ATOM   1482  H   LYS B 372       3.003   7.719   0.751  1.00  0.00           H
ATOM   1483  HA  LYS B 372       3.950   9.637   0.611  1.00  0.00           H
ATOM   1484 1HB  LYS B 372       2.551  11.900   1.225  1.00  0.00           H
ATOM   1485 2HB  LYS B 372       1.279  10.755   0.826  1.00  0.00           H
ATOM   1486 1HG  LYS B 372       1.756  11.818  -1.205  1.00  0.00           H
ATOM   1487 2HG  LYS B 372       2.461  10.216  -1.365  1.00  0.00           H
ATOM   1488 1HD  LYS B 372       4.758  11.220  -0.785  1.00  0.00           H
ATOM   1489 2HD  LYS B 372       4.008  12.807  -0.642  1.00  0.00           H
ATOM   1490 1HE  LYS B 372       3.280  12.693  -3.075  1.00  0.00           H
ATOM   1491 2HE  LYS B 372       4.022  11.090  -3.225  1.00  0.00           H
ATOM   1492 1HZ  LYS B 372       6.171  12.104  -2.618  1.00  0.00           H
ATOM   1493 2HZ  LYS B 372       5.555  12.807  -3.963  1.00  0.00           H
ATOM   1494  N   MET B 373       3.738   9.544   3.814  1.00 20.00           N
ATOM   1495  CA  MET B 373       4.620   9.810   4.921  1.00 20.00           C
ATOM   1496  C   MET B 373       4.556   8.711   5.954  1.00 20.00           C
ATOM   1497  O   MET B 373       3.539   8.417   6.558  1.00 20.00           O
ATOM   1498  CB  MET B 373       4.412  11.304   5.356  1.00 20.00           C
ATOM   1499  CG  MET B 373       4.650  11.762   6.809  1.00 20.00           C
ATOM   1500  SD  MET B 373       4.345  13.538   7.056  1.00 20.00           S
ATOM   1501  CE  MET B 373       5.038  14.386   5.620  1.00 20.00           C
ATOM   1502  H   MET B 373       2.761   9.242   3.918  1.00  0.00           H
ATOM   1503  HA  MET B 373       5.643   9.717   4.544  1.00  0.00           H
ATOM   1504 1HB  MET B 373       3.403  11.656   5.087  1.00  0.00           H
```

```
ATOM   1505 2HB  MET B 373       5.055  11.907   4.690  1.00  0.00           H
ATOM   1506 1HG  MET B 373       5.651  11.501   7.191  1.00  0.00           H
ATOM   1507 2HG  MET B 373       3.932  11.237   7.463  1.00  0.00           H
ATOM   1508 1HE  MET B 373       5.060  15.477   5.788  1.00  0.00           H
ATOM   1509 2HE  MET B 373       6.069  14.047   5.418  1.00  0.00           H
ATOM   1510 3HE  MET B 373       4.427  14.196   4.719  1.00  0.00           H
ATOM   1511  N   SER B 374       5.743   8.217   6.513  1.00 20.00           N
ATOM   1512  CA  SER B 374       5.872   6.931   7.127  1.00 20.00           C
ATOM   1513  C   SER B 374       6.400   7.049   8.547  1.00 20.00           C
ATOM   1514  O   SER B 374       7.000   7.996   8.987  1.00 20.00           O
ATOM   1515  CB  SER B 374       6.744   5.938   6.377  1.00 20.00           C
ATOM   1516  OG  SER B 374       8.044   6.430   6.119  1.00 20.00           O
ATOM   1517  H   SER B 374       6.571   8.784   6.310  1.00  0.00           H
ATOM   1518  HA  SER B 374       4.872   6.473   7.229  1.00  0.00           H
ATOM   1519 1HB  SER B 374       6.192   5.724   5.489  1.00  0.00           H
ATOM   1520 2HB  SER B 374       6.821   4.962   6.894  1.00  0.00           H
ATOM   1521  HG  SER B 374       7.975   7.172   5.508  1.00  0.00           H
ATOM   1522  N   ALA B 375       6.256   6.039   9.291  1.00 20.00           N
ATOM   1523  CA  ALA B 375       6.629   5.877  10.681  1.00 20.00           C
ATOM   1524  C   ALA B 375       6.941   4.458  10.990  1.00 20.00           C
ATOM   1525  O   ALA B 375       6.124   3.561  10.828  1.00 20.00           O
ATOM   1526  CB  ALA B 375       5.673   6.418  11.730  1.00 20.00           C
ATOM   1527  H   ALA B 375       5.725   5.286   8.842  1.00  0.00           H
ATOM   1528  HA  ALA B 375       7.548   6.486  10.835  1.00  0.00           H
ATOM   1529 1HB  ALA B 375       6.031   6.276  12.768  1.00  0.00           H
ATOM   1530 2HB  ALA B 375       5.599   7.496  11.565  1.00  0.00           H
ATOM   1531 3HB  ALA B 375       4.676   5.962  11.646  1.00  0.00           H
ATOM   1532  N   THR B 376       8.149   4.189  11.366  1.00 20.00           N
ATOM   1533  CA  THR B 376       8.521   2.847  11.801  1.00 20.00           C
ATOM   1534  C   THR B 376       8.972   2.948  13.258  1.00 20.00           C
ATOM   1535  O   THR B 376       9.493   3.969  13.692  1.00 20.00           O
ATOM   1536  CB  THR B 376       9.689   2.272  10.929  1.00 20.00           C
ATOM   1537  OG1 THR B 376       9.506   2.582   9.556  1.00 20.00           O
ATOM   1538  CG2 THR B 376       9.867   0.743  11.028  1.00 20.00           C
ATOM   1539  H   THR B 376       8.886   4.953  11.322  1.00  0.00           H
ATOM   1540  HA  THR B 376       7.682   2.128  11.720  1.00  0.00           H
ATOM   1541  HB  THR B 376      10.635   2.747  11.243  1.00  0.00           H
ATOM   1542  HG1 THR B 376       9.040   3.426   9.560  1.00  0.00           H
ATOM   1543 1HG2 THR B 376      10.783   0.403  10.518  1.00  0.00           H
ATOM   1544 2HG2 THR B 376       9.962   0.392  12.071  1.00  0.00           H
ATOM   1545 3HG2 THR B 376       9.020   0.199  10.572  1.00  0.00           H
ATOM   1546  N   PHE B 377       8.772   1.896  14.007  1.00 20.00           N
ATOM   1547  CA  PHE B 377       9.109   1.894  15.437  1.00 20.00           C
ATOM   1548  C   PHE B 377       9.757   0.619  15.855  1.00 20.00           C
ATOM   1549  O   PHE B 377       9.409  -0.450  15.371  1.00 20.00           O
ATOM   1550  CB  PHE B 377       7.811   2.211  16.239  1.00 20.00           C
ATOM   1551  CG  PHE B 377       8.002   2.502  17.738  1.00 20.00           C
ATOM   1552  CD1 PHE B 377       7.747   1.507  18.688  1.00 20.00           C
ATOM   1553  CD2 PHE B 377       8.431   3.764  18.162  1.00 20.00           C
ATOM   1554  CE1 PHE B 377       7.924   1.771  20.045  1.00 20.00           C
ATOM   1555  CE2 PHE B 377       8.607   4.026  19.519  1.00 20.00           C
ATOM   1556  CZ  PHE B 377       8.354   3.030  20.459  1.00 20.00           C
ATOM   1557  H   PHE B 377       8.135   1.192  13.608  1.00  0.00           H
ATOM   1558  HA  PHE B 377       9.851   2.688  15.667  1.00  0.00           H
ATOM   1559  HC  PHE B 377      10.540   0.729  16.627  1.00  0.00           H
ATOM   1560 1HB  PHE B 377       7.076   1.396  16.096  1.00  0.00           H
ATOM   1561 2HB  PHE B 377       7.307   3.090  15.789  1.00  0.00           H
ATOM   1562  HD1 PHE B 377       7.415   0.527  18.377  1.00  0.00           H
ATOM   1563  HD2 PHE B 377       8.630   4.544  17.440  1.00  0.00           H
ATOM   1564  HE1 PHE B 377       7.727   1.000  20.775  1.00  0.00           H
ATOM   1565  HE2 PHE B 377       8.939   5.002  19.842  1.00  0.00           H
ATOM   1566  HZ  PHE B 377       8.490   3.234  21.511  1.00  0.00           H
END
```